

Development and Application of
an Advanced Green Roof Model

Dmitrii Konkov

A Thesis

in the

Building Science Graduate Program

Presented in Partial Fulfillment of the Requirements for

the degree of Master of Applied Science in Building Engineering/Building Science

at the

British Columbia Institute of Technology

Burnaby, British Columbia, Canada

May 2018

© Dmitrii Konkov, 2018

ABSTRACT

Green roofs are becoming a common application in order to improve building energy performance, runoff water control with several additional environmental benefits. Models are essential in the building science due to a necessity of prediction how different structures perform. This knowledge helps to choose right materials and material dimensions. A green roof structure is a complex system of different layers, including growing media and plants. Those two layers make the green roof modelling entirely different from ordinary modelling. Nowadays, several green roof models cover different phenomena and use different physical principles. However, a green roof model is still can be improved. Therefore, this study develops a green roof model- HAMFit-GR that better covers heat and moisture movement sources. The model is based on Heat-Air-Moisture model called HAMFit and Fast All-Season Soil Strength models from US Army Corps of engineers. A combined model is proposed to be more accurate than the most comprehensive green roof models. The result is achieved by adding uncovered components, such as coupling heat and moisture transport in growing media and runoff water flow. Green roof parameters that are required for accurate modelling are measured through laboratory and field experiments. The benchmark data is obtained from the field experiment that is being performed at Whole Building Performance Research Laboratory (WBPRL) of Building Science Centre of Excellence at British Columbia Institute of Technology (BCIT), Burnaby. A case study is prepared with the validated model. The case study includes analysis of green roof parameters impact on roof hydrothermal performance.

This thesis is dedicated to the memory of my brother, Roman Konkov.

ACKNOWLEDGEMENTS

I would first like to thank my thesis supervisor Dr. Fitusm Tariku of the Building Science department, at British Columbia Institute of Technology. The door to his office was always open whenever I had a question regarding my research or writing. I would also like to thank Doug Horn, who was involved in the validation of this research project.

I must express my very profound gratitude to my wife – Irina and my grandfather – Yurii for providing me with unfailing support and continuous encouragement throughout my years of study and through the process of researching and writing this thesis. This accomplishment would not have been possible without them. Thank you.

TABLE OF CONTENT

ABSTRACT	ii
ACKNOWLEDGEMENTS.....	iv
TABLE OF CONTENT.....	v
LIST OF FIGURES	x
LIST OF TABLES.....	xvii
1 INTRODUCTION.....	1
2 BACKGROUND.....	3
2.1 Green roof systems	3
2.2 Green roof benefits	7
2.2.1 Buildings energy use.....	7
2.2.2 Urban heat island	9
2.2.3 Rainwater retention.....	10
2.2.4 Acoustics and air quality.....	10
2.3 Heat and moisture transfer in green roof	11
2.3.1 Vegetative model	11
2.3.2 Heat and Moisture model.....	14
2.4 Review of Current Green roof models.....	16
3 PROBLEM STATEMENT	20

4	RESEARCH APPROACH.....	24
4.1	Objectives	24
4.2	Scope.....	25
4.3	Methodology.....	25
5	MODEL DEVELOPMENT.....	26
5.1	Vegetative model	28
5.1.1	Radiation	28
5.1.2	Sensible heat	30
5.1.3	Latent heat.....	35
5.1.4	Water movement.....	37
5.1.5	Final energy balance equations	41
5.2	Coupled Heat and Moisture model	42
5.2.1	Moisture governing equation	43
5.2.2	Energy governing equation	44
5.2.3	Model modifications	45
5.3	Model inputs	47
6	CHARACTERIZATION OF GROWING MEDIA AND VEGETATION PROPERTIES	
	50	
6.1	Growing media characterization.....	50
6.1.1	Density and porosity	50

6.1.2	Sorption Isotherm and Moisture Storage capacity	54
6.1.3	Hydraulic properties.....	55
6.1.4	Conductivity and heat capacity	56
6.1.5	Growing media hydrothermal property summary.....	59
6.2	Vegetation parameters visualization.....	63
6.2.1	Coverage ratio	63
6.2.2	Leaf area index.....	67
6.3	Input parameters from literature	71
7	VALIDATION.....	72
7.1	Field experiment	72
7.2	HAMFit-GR Model Validation: A case with No Vegetation.....	75
7.2.1	Bare growing media in the dry period	75
7.2.2	Bare soil in the rainy period.....	81
7.3	Vegetative Model Validation.....	86
7.3.1	Leaves temperature	86
7.4	HAMFit-GR Model Validation: A case with Vegetation.....	87
7.4.1	Vegetated roof in the dry period	87
7.4.2	Vegetated roof in the rainy period	93
7.5	Sensitivity analysis	98
7.5.1	Coverage ratio.....	98

7.5.2	Leaf Area Index	100
7.5.3	Coverage ratio and leaf area index.....	102
7.5.4	Root depth and root fraction.	106
7.5.5	Minimal stomatal resistance.....	107
7.5.6	Plants height.....	110
7.5.7	Density and heat capacity	111
7.5.8	Moisture content	113
7.5.9	Runoff convection.....	115
8	MODEL APPLICATION	117
8.1	Comparison of conventional and green roof systems (Energy).....	117
8.1.1	Green roof performance in mild temperature and wet climate: Vancouver.....	117
8.1.2	Green roof performance in cold and hot summer climates: Toronto.....	121
8.1.3	Green roof performance in non-insulated and high-insulated roofs	123
8.1.4	Green Roof performance in light weight roof system: wood-frame roof	126
8.1.5	Comparison of conventional and green roof systems summary	128
8.2	Impact of growing media thickness in green roof performance	131
8.3	Impact of Green roof parameters on membrane and plywood temperatures.....	139
8.4	Impact of green roofs on rainwater retention.....	142
8.5	Green roof recommendations.....	144
	CONCLUSIONS	145

FUTURE WORK.....	147
REFERENCES	148
Appendix A. Heat flux on ceiling.....	155
Appendix B. MEMBRANE AND PLYWOOD TEMPERATURES	166
Appendix C. DRAINAGE	170
Appendix D. Vegetation parameters visualization matlab scripts.....	173

LIST OF FIGURES

Figure 1. Intensive Green Roof	4
Figure 2. Extensive green roof.....	4
Figure 3. Green roof structure.	5
Figure 4. Radiative heat exchange in a green roof.	11
Figure 5. Heat and moisture transport interdependence	21
Figure 6. Green roof model discretization.....	22
Figure 7. Methodology flowchart	25
Figure 8. Heat and moisture sources in the green roof.	26
Figure 9. Green roof model.	27
Figure 10. Solar and infrared radiation in a green roof.	29
Figure 11. Temperature distribution.	31
Figure 12. Water movement.	38
Figure 13. HAMFit model workspace.	42
Figure 14. Heat and Moisture model via COMSOL Multiphysics differential equations.....	45
Figure 15. Soil specimens in the oven.	51
Figure 16. Density and Porosity measurement.	52
Figure 17. Measure sorption isotherm.	54
Figure 18. Sorption isotherm test.....	55

Figure 19. Liquid permeability test.	56
Figure 20. Thermal conductivity measurement.	57
Figure 21. Conductivity and heat capacity graphs based on the test data.	59
Figure 22. Sorption isotherm. Top – region 0-0.93; bottom – region 0.96-0.99.	60
Figure 23. Sorption isotherm. Region – 0.99-1.	61
Figure 24. Liquid diffusivity curve.....	62
Figure 25. The coverage ratio of the single leaf.	64
Figure 26. The area covered by vegetation after several weeks of plants grow.....	65
Figure 27. Green roof coverage ratio in June 2017..	66
Figure 28. Green roof coverage ratio in July 2017.	67
Figure 29. LAI estimation samples.....	68
Figure 30. LAI image visualization using Matlab.	69
Figure 31. Sensors installed in the test green roof tray.....	73
Figure 32. Additional sensors..	74
Figure 33. Case 1- Relative Humidity – ½” below the upper surface.	76
Figure 34. Case 1- Relative Humidity – ½” above the soil bottom.....	77
Figure 35. Case 1- Ground temperature – ½” below the upper surface.	77
Figure 36. Case 1- Ground temperature in the middle of the soil layer.	78
Figure 37. Case 1- Ground temperature – ½” above the soil bottom.	78
Figure 38. Case 1- Correlation of measured and calculated values.....	79

Figure 39. Case 1 - Heat Flux - growing media bottom.	80
Figure 40. Case 1 - Heat Flux - Ceiling.....	80
Figure 41. Case 2 - Relative Humidity – ½” below the upper surface.	81
Figure 42. Case 2- Relative Humidity – ½” above the bottom surface.	82
Figure 43. Case 2 – Temperature – ½” below the upper surface.....	82
Figure 44. Case 2 -Temperature –in the middle of the growing media layer.	83
Figure 45. Case 2 - Temperature – ½” above the bottom surface.	83
Figure 46. Case 2- Correlation of measured and calculated values.....	84
Figure 47. Case 2 - Heat Flux - growing media bottom.	84
Figure 48. Case 2 - Heat Flux - Ceiling.....	85
Figure 49. Measured and Modeled Temperatures.	86
Figure 50. Case 3- Correlation of measured and calculated values.....	87
Figure 51. Relative Humidity – ½” below the upper surface.	88
Figure 52. Relative Humidity – ½” above the bottom surface.	89
Figure 53. Case 4 – Foliage Temperatures.	89
Figure 54. Case 4 – Temperature – Soil Surface.	90
Figure 55. Case 4 – Temperature – in the middle of the soil layer.....	90
Figure 56. Case 4- Temperature– ½” above the bottom surface.	91
Figure 57. Case 4 – Correlation of measured and calculated values.	91
Figure 58. Case 4 - Heat Flux - Growing media.....	92

Figure 59. Case 4 - Heat Flux - Ceiling.....	92
Figure 60. Case 5- Relative Humidity – ½” above the bottom surface.	94
Figure 61. Case 5- Relative Humidity – ½” above the bottom surface.	94
Figure 62. Case 5 – Foliage Temperature.....	95
Figure 63. Case 5 – Soil Surface Temperature.	95
Figure 64. Case 5 – Soil Middle Point Temperature.	96
Figure 65. Case 5 – Soil Bottom Point Temperature.....	96
Figure 66. Case 5 – Temperature values distribution.	97
Figure 67. Case 5 – Heat Flux model vs measured.	97
Figure 68. Case 6 – Heat Flux model vs measured.	98
Figure 69. Coverage ratio impact on the growing media temperature.	99
Figure 70. Coverage ratio impact on heat flux.	100
Figure 71. Leaf Area Index impact on the growing media temperature.....	101
Figure 72. Leaf Area Index impact on heat flux.....	101
Figure 73. Heat flux through Low, Normal, and High covered green roofs in February in Vancouver.....	103
Figure 74. Overall heat losses through Low, Normal, and High covered green roofs in February Vancouver.....	104
Figure 75. Heat flux through Low, Normal, and High covered green roofs in August in Vancouver.....	105

Figure 76. Overall heat losses through Low, Normal, and High covered green roofs in August in Vancouver.....	105
Figure 77. Root distribution impact on the growing media temperature.....	106
Figure 78. Root distribution impact on heat flux.....	107
Figure 79. Minimal stomatal resistance impact on the growing media temperature.....	108
Figure 80. Minimal stomatal resistance impact on heat flux.....	108
Figure 81. Heat flux through 200 and 700 minimum stomatal resistance sedums planted green roofs in summer in Vancouver.	109
Figure 82. Plants height impact on the growing media temperature.	110
Figure 83. Plant height impact on heat flux.....	111
Figure 84. Thermal mass impact on the growing media temperature.	112
Figure 85. Thermal mass impact on heat flux.	112
Figure 86. Moisture content impact on the growing media temperature.....	114
Figure 87. Moisture content impact on heat flux.....	114
Figure 88. Convective heat flow impact on the growing media temperature.....	115
Figure 89. Runoff convection impact on heat flux.	116
Figure 90. Heat flux through R33 insulated roof in Vancouver.	118
Figure 91. Heat flux through R33 insulated roof in Vancouver in February.	119
Figure 92. Energy consumption in Vancouver in February – R33-insulated concrete roof.	119
Figure 93. Heat flux through building code insulated roof in Vancouver in August.	120

Figure 94. Energy consumption in Vancouver in August– R33-insulated concrete roof.....	121
Figure 95. Heat flux through R33 insulated roof in Toronto.....	122
Figure 96. Energy consumption in Toronto – R33 insulated concrete roof.	122
Figure 97. Heat flux through the non-insulated roof in Vancouver in 2016.	124
Figure 98. Energy consumption in Vancouver – non-insulated concrete roof.	124
Figure 99. Heat flux through the R60-insulated roof in Vancouver.....	125
Figure 100. Energy consumption in Vancouver – R60-insulated concrete roof.	125
Figure 101. Heat flux through R33 insulated roof in Vancouver.	126
Figure 102. Energy consumption in Vancouver – R33-insulated wood frame roof.....	127
Figure 103. Heat flux through R33 insulated roof in Winnipeg.....	127
Figure 104. Energy consumption in Winnipeg in 2016.....	128
Figure 105. Heat flux through 10, 15, 20 cm green roofs in Vancouver in 2016.....	131
Figure 106. Heat flux through 10, 15, 20 cm green roofs in Vancouver in February.	132
Figure 107. Overall heat left through 10, 15, 20 cm green roofs in Vancouver in February.	133
Figure 108. Heat flux through 10, 15, 20 cm green roofs in Vancouver in May.	134
Figure 109. Heat flux through 10, 15, 20 cm green roofs in Vancouver in July.	135
Figure 110. Overall heat through 10, 15, 20 cm green roofs in Vancouver in July.	135
Figure 111. Heat flux through 10, 15, 20 cm green roofs in Winnipeg.....	137
Figure 112. Overall heat through 10, 15, 20 cm green roofs in Winnipeg.....	137

Figure 113. Heat flux through 10, 15, 20 cm green roofs in Toronto.	138
Figure 114. Overall heat through 10, 15, 20 cm green roofs in Toronto.....	138
Figure 115. Membrane temperature under 10, 15, 20 cm green roof in Vancouver.	140
Figure 116. Membrane temperature under 10, 15, 20 cm green roof in Toronto.	140
Figure 117. Plywood temperature under 10, 15, 20 cm green roof in Winnipeg.	141
Figure 118. Drainage via 10, 15, 20 cm soil in Vancouver.	142
Figure 119. Drainage via low, standard, high dense covered green roof in Vancouver.	143
Figure 120. Drainage via low and high minimum stomatal resistance green roof in Vancouver.	144

LIST OF TABLES

Table 1. Growing media parameters.....	47
Table 2. Vegetation parameters.	48
Table 3. Soil density and porosity test ASTM D7263 - Volumetric method - B	53
Table 4. Thermal conductivity measurement.	58
Table 5. Parameters are taken from literature.....	71
Table 6. Parameters and sensors used in the benchmark experiment.....	73
Table 7. Energy consumption summary – concrete frame.	129
Table 8. Energy consumption summary – wooden frame.	130

1 INTRODUCTION

The idea of sustainability appeared in the late sixties of the last century and was first discussed at the United Nations Conference on the Human Environment in Stockholm in 1972 (Report of the IUCN Renowned Thinkers Meeting, 2006). The sustainability concept can be described as a possibility to reach an economic and industrial development without environmental damage (Report of the IUCN Renowned Thinkers Meeting, 2006). Energy efficiency or in other words, reducing energy consumption becomes a crucial part of sustainability. By reducing energy usage, we can cut energy bills as well as scale down greenhouse gas emissions. Buildings are the most significant energy consumers. According to Getter et al. (2011), buildings consumption in the USA is almost 40% of the total energy usage and more than 70% of the electrical use. Moreover, heating and cooling part forms half of the overall building's consumption (Intermediate Energy Infobook, 2016). Following the sustainability concept, the building society introduced high-performance buildings. A high-performance structure is a combination of low energy usage and low emission (Terms and Definitions for High-Performance Building, 2011). To improve building energy performance, designers apply high-efficient heating, cooling and ventilation equipment; modern lighting systems and building envelope improvements (Intermediate Energy Infobook, 2016). One of the newest technologies that are currently being applied is green roofs.

A green roof is a roof that has soil or soil-based material and vegetation layers above the construction layer. Green roofs attract more and more attention from the building society because of its environmental benefits. Green roofs might reduce heat gain by 90-160% during summer (Djedjig et al., 2012). The lower heat gain and the green roof cooling effect due to evapotranspiration as well as the shading effect results in more moderate surface temperature (Yang & Wang, 2014). Green roof growing media serve as an additional layer of insulation, which lead to lower heating consumption

during winter as well as lower noise coming through a roof. Several publications described green roofs as a possible solution to urban heat island phenomena that is a local increase in temperature (Ouldboukhitine et al., 2011). Studies also show that green roof assemblies have an ability to control runoff water, by being porous water storage (Stovin et al., 2013). Besides, green roof coverage is a natural vegetation layer and as plants convert carbon dioxide in the atmosphere to oxygen. Green roofs absorb polluting air particles and compounds not only through the plants but also by deposition in the growing medium. As reported by the European Federation of Green Roof Associations (EFB), green roofs improve urban biodiversity by creating living space for spiders and beetles. The EFB noticed the positive effect of green roofs on human mental and physical health.

Computer software became common in the construction industry in recent years. Engineers use various computer programs from drafting tools to databases, but in term of energy savings, models and modelling software play an essential role. Those tools help designers estimate a future building consumption or evaluate the energy performance of a building without high-cost equipment usage. The most important characteristic of a modelling tool is its accuracy. Green roof as relatively new technology is poorly presented in building energy modelling programs. Green roofs are complex engineered structures that are influenced by many factors. From the energy savings point of view, green roof behaves differently in different climates. Green roof savings vary with designed parameters such as growing media type and thicknesses, coverage ratio and leaf area index (LAI) as well as plant selection (Sailor, 2012). Moreover, green roof performance strongly depends on insulation presence and its property (Moody and Sailor, 2013). Therefore, it is necessary to have an accurate tool that can estimate the building energy performance in the case of a green roof. This tool can help designers choose the optimal design for every situation in every climate.

2 BACKGROUND

2.1 Green roof systems

A green roof is a roof that has soil or soil-based material and the vegetation layer above the construction layer. Green roofs, currently, attract more and more attention from the building society because of its environmental benefits and potential energy savings. Green roofs can be classified as extensive, intensive and semi-intensive based on their parameters and purposes. Green roofs might be built with different growing media thickness and plant types depending on weather conditions and green roof function.

An intensive green roof is a green roof system that requires regular maintenance; it usually has a thick growing media layer and might be equipped with an irrigation system. Intensive green roofs are often called roof garden. The typical intensive green roof structure is illustrated in Figure 1. This type of green roof has massive structure due to a thick layer of soil and requires suitable structure below to load roof garden weight. Typically, green roofs are called intensive if the growing media layer exceeds 200 mm in depth. Intensive green roofs have a wide variety of plants and can be built in combination with other garden accessories, e.g. benches, tables, streetlights. (Bianchini & Hewage, 2012; Yang & Wang, 2014; Green Roof Handbook).

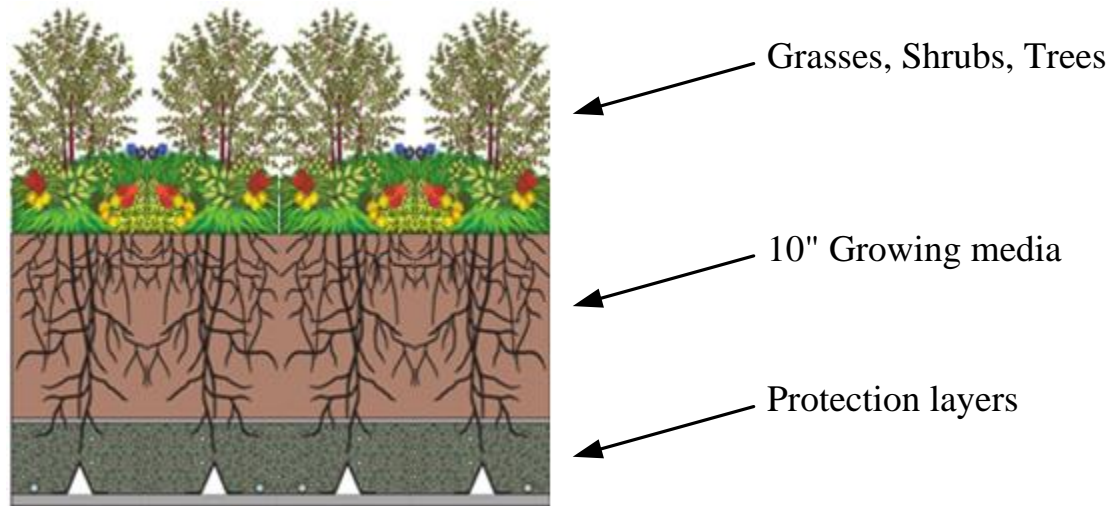


Figure 1. Intensive Green Roof

An extensive green roof is a type of green roof systems that is characterized by its drought-resistant vegetation, ranging from sedums to small grasses, herbs and flowering. The schematic structure of an extensive green roof is shown in Figure 2. The principal feature of the extensive green roof system is no necessity for regular maintenance or permanent irrigation. Usually, the thickness of growing media is less than 200 mm and the growing media in this type of green roofs are designed to be lightweight and self-maintained (Yang & Wang, 2014; Bianchini & Hewage, 2012, Green Roof Handbook, 2008).

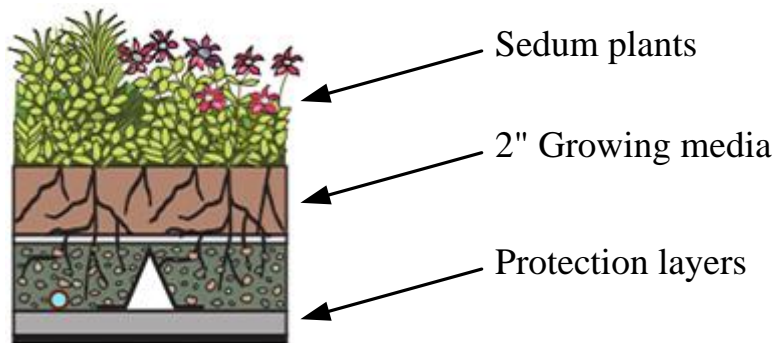


Figure 2. Extensive green roof

The third type of green roof called a semi-intensive green roof that is a combination of extensive and intensive, but the extensive type must be 25% or less of the total green roof's area (Bianchini & Hewage, 2012).

To build a green roof, several additional engineering products are required. Figure 3 illustrates typical green roof layers. Green roof growing media and vegetation layers represent a mixture of natural and building materials. Special membranes are used to protect the building structure from the negative impact of wet soil or plant roof.

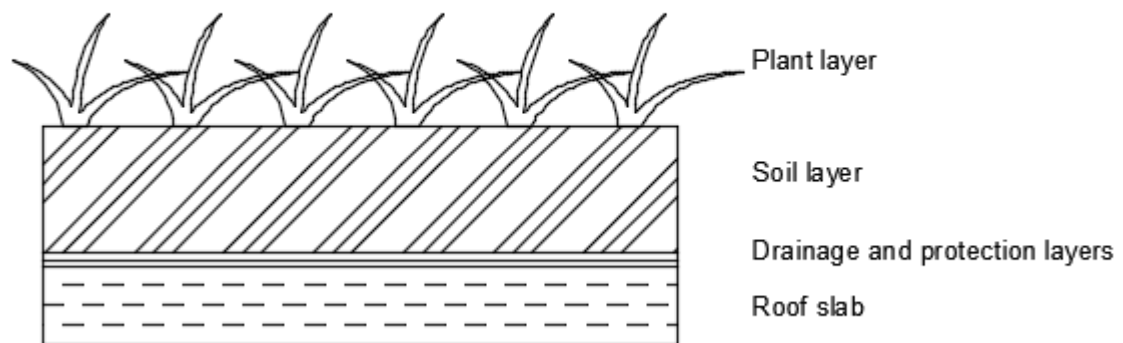


Figure 3. Green roof structure.

Designers divide the green roof system into the following layers (from bottom to top) (Sailor, 2008; Tabares-Velasco & Srebric, 2012; Bianchini & Hewage, 2012):

Roof slab – structural element;

Waterproofing membrane – a membrane is designed to protect the building components from the water leakage. Those membranes are required for all roof types;

Root barrier layer - a membrane designed to protect the underlying layers from the root microorganisms penetration. A root-barrier failure can cause structural damage to the waterproof membrane or the slab;

Drainage layer – a material specially designed to carry the excess water to the roof drains, and eventually off the roof;

Growing medium layer - an inorganic and organic component mixture. A blend is designed to meet the green roof requirements, such as being lightweight, chemically inert, and physically stable. Moreover, the substrate should retain adequate amounts of water and minerals for plant growth, and at the same time it should provide enough drainage ability (Kotsiris et al., 2012);

Vegetation layer – plants that are chosen based on green roof type (i.e., extensive or intensive) and the ambient climate. Rayner et al. (2016) underlined that plant selection is especially important in hot, dry climates with conditions of severe water deficit, lack of artificial irrigation, or where winter freezing happens.

The described structure is not unique. Green roof designers apply different strategies depending on a green roof purpose, type of green roof, local climate or an architect's view (Green Roof Handbook, 2008). In some cases, the filter layer and the water retention layer can be used to achieve better water movement control (Bianchini, 2012).

2.2 Green roof benefits

2.2.1 Buildings energy use

Green roofs are known as an environmentally friendly building option due to economic and environmental benefits. Potential budgetary savings associated with green roof installation are coming with possible cooling and heating demand reduction. In the time periods, when internal building temperatures exceed designed level, and there is a necessity to cool down a building, a green roof works as an additional cooling source by transferring excess heat through the slab, membrane, media, and plants where it is cooled through evaporation, conduction, and convection.

Several papers have appeared in recent years documenting main factors affecting building energy use, and hence, the potential energy impacts of a green roof. Nevertheless, green roof models and experimental works show the green roof positive influence on cooling energy use. According to a study of green roofs by Sailor (2012), the baseline green roof showed cooling energy cost savings for both the office and lodging buildings in comparison to the conventional roof in four of these climate zones: Houston, Texas; Phoenix, Arizona; Portland, Oregon, and New York City. Yaghoobian (2015) obtained similar results in mixed-humid climate and hot-to mixed-dry climate. Djedjig et al. (2012) and Getter et al. (2011) have also discussed the green roof cooling power. They stated that using a green roof; the solar heat gain could be reduced by 70-90% in the summertime and reduced heat flux through the building envelope by an average 167% during summer. Recently, several authors Gagliano et al. (2011), Kotsiris et al. (2012), Heidarinejad and Esmaili (2015) and Gargari et al. (2016) have proved the statement that green roofs can reach a significant effect on reducing the energy consumption required for cooling a building under different circumstances. The green roof cooling effect can be explained by the ability of the green roof to release heat into the environment (He & Jim, 2010). Gagliano et al. (2011) explained that the cooling process in green roof

systems occurs due to the following processes: about 50% by evapotranspiration and about 30 % by the long-wave radiative thermal flux. The evapotranspiration is a combination of plants transpiration and evaporation. Ouldboukhitine et al. (2014) defined evaporation as the movement of thermal energy from a water surface to the atmosphere involving the change in phase from liquid water to vapour and transpiration as the physiological process of transforming water into vapour at the plants. The second-factor influences the cooling green roof performance are plants and growing media radiation properties. Plants radiative parameters have a significant effect on the net radiation exchange, as it becomes an exterior layer. Plants reflect almost 30% of incoming solar radiation while 60% is absorbed by plants, and 13 % is transmitted to the growing media (Ayata et al. 2011; Zhao et al., 2014).

Positive effect on energy consumption is observed not only during the summertime due to reduced cooling load, but the green roofs have an impact on the building thermal performance during winter. Sailor (2008) explained this effect by soil working as an additional insulator. His simulation showed the impact of energy saving was strongly affected by the thickness of the growing media layer. Several modelling and experimenting examples are presented in the works done by Getter et al. (2011), Djedjig et al. (2012), Kotsiris et al. (2012), Coutts et al. (2013), Berardi (2016), Tang & Qu (2016). Ouldboukhitine et al. (2011, 2012) compared insulation role of a green roof with rock wool, and frozen green roofs with conventional roofs under snow the layer. They found that the green roof substrate shows similar properties as rock wool in the substrate dry state and same as snow when the green roof substrate is saturated and frozen. Berardi (2016) explained that the most significant contributor to the energy saving was the heating reduction on the top floor. However, green roofs in certain climates can be a reason for excessive heat losses due to evapotranspirative processes and higher soil conductivity (Moody & Sailor, 2013).

The green roof thermal performance is unstable and might be affected by solar radiation, ambient outside temperature a relative humidity, water content and its quality (Ouldboukhitime et al., 2014, Getter et al., 2011). Water in growing media has the impact on substrate thermal conductivity and specific heat capacity, as well as on vapour and air transport properties.

2.2.2 Urban heat island

Several publications described green roofs as a possible solution to urban heat island phenomena. The urban heat island effect is the temperature difference between urban areas and the surrounding countryside. According to the European Federation of Green Roof Associations (EFB), in some large cities, the gap can be up to a 5°C between the city and the rural areas. Significant regions of high-absorbing surfaces can explain this effect. These surfaces absorb solar radiation and reflect it back into the surrounding atmosphere. Any possible reduction can have a vital positive effect city environment. To reduce the urban heat island effect, many researchers have proposed green roofs. The surface of a conventional rooftop can exceed the ambient air temperature up to 50°C, while the green roof, rooftop can be colder than the surrounding air (Reducing Urban Heat Islands: Compendium of Strategies, 2008). Considering the urban heat effect island, green roofs work by shading roof surfaces and through evapotranspiration. For example, a modelling study for Toronto predicted that adding green roofs to 50 percent of the available rooftops downtown would cool the entire city by 0.4 to 0.7°C (Berardi, 2016). Gargari et al. (2016) compared the roof temperature between an insulated pitched roof and green roof. Results showed the maximum surface temperature difference over 25°C in June and an average 18°C for July-September. Ouldboukhitime et al. (2011), Djedjig & Bozonnet (2013) Ambrosini et al. (2014), Heidarinejad & Esmaili (2015), Yaghoobian et al. (2015) reported the positive effect in urban areas by urban heat island mitigation.

2.2.3 Rainwater retention

Green roofs can store rainwater in the plants and growing mediums and then release water into the atmosphere. The amount of water that can be stored on a green roof structure back depends on the growing medium and its dimensions. As it reported by the European Federation of Green Roof Associations (EFB) during summer green roofs can retain 70-80% of rainfall and 25-40% in winter. Green roofs also able to delay runoff during times of heavy precipitation (Ayata, 2011) helping a sewer system to deal with water.

2.2.4 Acoustics and air quality

In addition, green roofs are useful to improve air quality. According to Connelly and Hodgson, green roofs have high sound-absorptive characteristics, and it is a function of substrate depth, plants, and moisture content of the substrate. Vegetation removes air pollutants and greenhouse gas emissions from the air and releases oxygen (Ouldboukhitine et al. 2011, Reducing Urban Heat Islands: Compendium of Strategies, 2008).

2.3 Heat and moisture transfer in green roof

2.3.1 Vegetative model

The vegetative model describes physical phenomena that occur above the growing media. Those aspects make green roof modelling complicated and different from building energy modelling. In general, vegetative model defines an outside boundary condition for heat and moisture model. Due to complexity, there are various approaches to estimate each phenomenon.

The roof is affected by shortwave solar radiation, incoming and outgoing long-wave radiation and multiplied reflection between leaves and growing media. Figure 4 represents radiation on the green rooftop surface. According to Lazzarin et al. (2005), the portion of the radiation entering the system depends on plant coverage ratio that is described by a proportion of covered area and corresponding leaf area index (LAI). By the end, the short-wave radiation energy balance at the top of the growing media layer consists of the sum of the direct sun radiation and the radiation that is transmitted by the canopy leaves.

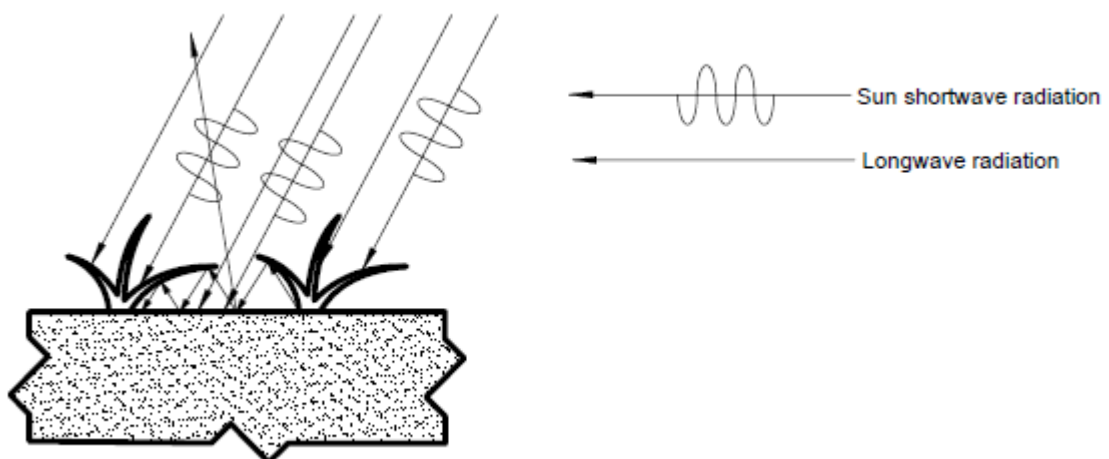


Figure 4. Radiative heat exchange in a green roof.

The long-wave radiation balance is the sum of sky thermal radiation exchange and the radiation emitted by the plant and growing media layers (Ambrosini et al., 2014; Yaghoobian et al., 2015). Green roof radiation properties and shading effects are strongly correlated with vegetation structure and plants transmittance and reflectance. Absolutely covered green roof receives 80% less shortwave radiation than a roof with bare soil (Yaghoobian et al., 2015; He & Jim, 2010). According to Tabares-Velasco et al. (2014), green roofs absorb radiation until noon and then after the pick at noon, net radiation decreases due to less solar intensity radiation. During the night, green roofs reradiate to the environment. Gargari et al. (2016) stated that very dense canopy (high coverage ratio and leaf area index) could limit outgoing radiation from the growing media to the sky.

Air moving across the green roof structure is a factor influencing the overall thermal performance. As it reported by Sun (2013), convective heat transfer is an essential part of overall energy performance. In order, to calculate the convection heat flux, scientists use formulas based on Nusselt, Grashof and Reynolds numbers (Tabares-Velasco & Srebric, 2012). Convection is affected by plants structure and the volumetric water content in comparison with rectangular smooth or rough roofs (Ayata et al., 2011).

Evaporation is the energy movement from a water state in the soil or on its surface to the atmosphere, including a phase change phenomenon from water to vapour. Transpiration – the biological process of water loss through plants. Stomatal resistance determines transpiration. It is a resistance to the diffusion of water vapour from these spaces into the atmosphere (Sailor, 2008; Ouldboukhitine et al., 2014). Evapotranspiration depends on the following factors (Ouldboukhitine et al., 2011, 2014):

- Canopy characteristics (height, leaf area, leaf density);

- Weather factors (wind speed, temperature, pressure, solar radiation);
- Amount of water in the root area.

Much research on green roofs has been shown that evapotranspiration is the primary sources of green roof cooling. Yang & Wang (2014) reported that higher green roof fraction resulted in higher evaporative cooling effect. They also found that the relation between maximum latent heat and green roof fractions are nearly linear. The study of “Crop evapotranspiration estimation with FAO56: Past and future” indicates that weather conditions determine the rate of evapotranspiration. The major drivers of evapotranspiration are solar radiation, wind speed and vapour pressure differences (Pereira et al., 2015).

Due to the difficulty of direct measuring and complex physics of the evapotranspiration process, several models have been developed with different approaches and assumptions (Zhao et al., 2013). The most common way to estimate the evapotranspiration rate that modellers use is vapour pressure deficit method (Jim and Tsang, 2011; Tabares-Velasco and Srebric, 2012). These models (Penman, 1948; Penman–Monteith, 1965; Priestley–Taylor, 1972 and Hargreaves and Allen, 2003) predict the maximum or potential evapotranspiration rate (PET) and are referred as PET models. The Hargreaves and Priestley–Taylor models use a composite of energy and temperature data when the Penman and Penman-Monteith models are based on wind and humidity data to calculate advective evapotranspiration (Marasco et al., 2015). For higher accuracy in green roof modelling, it is necessary to estimate actual evapotranspiration (AET). Actual evapotranspiration is a function of moisture availability in the soil. Actual evapotranspiration is equal to potential evapotranspiration when the soil is saturated with water; the actual evapotranspiration decreases with water availability reduction.

There is another way to estimate evapotranspiration that was implemented by Djedjig et al. (2012) estimated evapotranspiration as the sum of water evaporation from the soil and the transpired water from plants. In this method, evaporation and transpiration calculate from pressure difference, resistance to mass transfer and thermal properties of foliage and soil.

2.3.2 Heat and Moisture model

A green roof as a part of the outside building envelope is a subject of weather influence. In addition to common weather factors influencing a building such as short and long wave radiation exchange, ambient temperature, wind and precipitation loads, the green roof is impacted by plants. All of these loads result in heat and moisture transport in the growing media. The vegetative model that is described above calculates leaf energy balance and provides boundary conditions for the HM model. The HM model is desired to deal with physics occurring in the growing media.

Jim & He (2010) stated that moisture in the green roof system has the most significant impact on the green roof thermal performance. Precipitation is a major source of water in the green roof system. Usually, precipitation is represented by rain events, rarely – snow. Concerning water balance, it is possible to divide into three stages: unsaturated, saturated and oversaturated. When the incoming water (rain) excess the amount of water that growing media of the green roof cannot absorb after reaching full saturation, runoff water flow occurs. Runoff water can result in transport of heat through the growing media. Regardless the stage, moisture affects the heat flow, as well as temperature, affects moisture flow. As water balance changes, the green roof thermal performance changes; therefore, the HM model estimates water and heat balances as well as their influence on each other. How it was mentioned above, precipitation is the source of water replenishment in the system. The green roof growing media dries due to evaporation, transpiration and liquid water flow via drainage.

Moister transport depends on the temperature that reflects heat transfer. Firstly, the temperature is a crucial factor influencing saturated vapour pressure. Secondly, moisture transport material properties and moisture storage capacity are also temperature-dependent (Tariku, 2008).

The presence of moisture in the growing media makes the HM model more complicated than 1D heat flux through the solid material. The rate of heat transfer through a material by conduction depends on its thermal conductivity. Conduction heat transfer in porous media (soil or substrate layer) differs from that of non-porous materials. Alexandri and Jones (2007) described green roof materials as capillary-porous bodies. Firstly, moisture changes conductivity properties of the growing media. As Ayata et al. (2011) reported, “The thermal conductivity is decreased, and the heat flux through the roof is reduced with soil density decreases.” To describe the amount of water in the soil, researchers have proposed the term – volumetric water content (VWC). Sailor (2008), as well as Kotsiris (2012), has found that soil thermal transmittances varies linearly with volumetric water content. The volumetric water content in the substrate layer can be described by the sum of precipitation, irrigation, evapotranspiration, and runoff water. In general rule, if the substrate is wet, the conduction rate is high (Yaghoobian et al., 2015; Ouldboukhite, 2015). Secondly, moisture in the substrate layer results in the soil reflectivity variation from 0.10 in wet soil to 0.35 for dry soil, but emissivity stays between 0.90-0.98. Thirdly, water in growing media changes growing media heat capacity of the soil (Tariku, 2008; Ouldboukhite, 2015).

In addition to conductivity change with wetness, moisture in the growing media causes enthalpy transfer. According to Tariku (2008), as moisture transports by convection, diffusion or both through porous materials, it can transport heat along with it. Although moisture can exist in all three states of matter (gas, liquid and solid), moisture transport in a growing media is possible in vapour and liquid forms through vapour diffusion, capillary suction and gravity flow. Liquid water movement

in a porous material requires pores be nearly filled with water (Tariku, 2008). The growing media is located outside from control and protect membranes and exposed to outside conditions (rain, snow, solar radiation, etc.); therefore, liquid water movement, as well as vapour flow, occurs in a green roof growing media layer. In other words, when water goes through the media, leaving water temperature differs from incoming water temperature; therefore, some amount of energy is stored or taken away from the growing media depending on the media temperature and the incoming water temperature.

2.4 Review of Current Green roof models

Green roof models exist to estimate green roof thermal performance accurately. Adequate understanding of heat and moisture flow through a roof allows creating a better design with suitable materials. Green roof models have been widely researched; however, most of the previous studies do not take into account some heat or moisture flow source.

Lazzarin et al. published the earliest green roof model in 2005 in Italy. The model deals with fundamental physics, such as evapotranspiration, convection, conduction and incoming shortwave radiation. Thermal conductivity in the soil in this model depends on the water content of each layer. They used an empirical version of the Penman model and a reduction factor based on relative humidity to predict evapotranspiration. The portion of the incident radiation is estimated by the leaf area index (LAI).

Another model published in 2007 by Alexandria & Jones in the USA. Conductive heat transfer through the soil layer is considered as heat flux through homogenous the soil–water–air mixture. The convective heat exchange was found from the Reynolds, Prandtl, Grashof and Nusselt numbers (analytical method). Shortwave and longwave portions of the radiative heat transfers were calculated from leaf area index (LAI). Evapotranspiration was determined by the FAO56 method (Penman-

Monteith). This model ignores longwave radiation exchange between leaves and soil. It also doesn't take into account water going through the growing media and energy associated with them.

The model published in China in 2013 by Sun et al. The authors included Richards' equation-based hydrologic module that is consisted of infiltration, hydraulic diffusion and runoff generation processes. The thermal processes of the green roof were experimentally measured and added to the model. Although the model considers the runoff water, it does not take into account energy associated with the leaving water, water transport and long-wave radiation between foliage and soil.

Tabares-Velasco & Srebric published their model in 2012 in the USA. They built a laboratory setup – cold plate apparatus to validate the model and get extra data on green roofs. The conductive heat transfer in the model is estimated using linear function based on cold plate apparatus data. The convective heat flux is calculated using Nusselt, Grashof and Reynolds numbers. The sky temperature to calculate long wave heat exchange measured from the pyrgeometer in the laboratory. Incoming shortwave radiation is distributed between plants and soil by leaf area index (LAI). In the model, the radiation between soil and plant layers is considered as the radiation between two infinite parallel plates. The model ignores water movement in the system.

The model published by Tang and Qu in the USA in 2016 and is dedicated to phase change phenomena during cold periods. The model and the experiment proved the phase change effect. The authors stated that frequent phase changes in the soil layer of the green roof system could have a significant impact on the green roof performance.

The model by Sailor (2008) became a base model for many green roof models. The method based on (FASST) model developed by Frankenstein and Koenig for the US Army Corps of Engineers. The Fast All-season Soil STrength (FASST) model was designed with the purpose to

predict the state of soil including energy balance, water and ice content, and soil strength. The principles implemented in the FASST are now used in the majority of green roof models; however, now all phenomena have been transferred from the FASST model to the green roof simulating tools. EnergyPlus from the US Department of Energy, Sailor (2008), Ouldboukhitine et al. (2011) models are notable examples of FASST implementation. The models include the following heat exchange mechanisms: long wave and short wave radiative exchange within the plant canopy; plant canopy effects on convective heat transfer; evapotranspiration; and heat conduction in the soil layer. The models ignore phase change phenomena, precipitation and runoff water. It is also questionable how moisture-dependent soil properties, mass and heat transfer within the growing media were estimated.

The model was written by Djedjig & Ouldboukhitine in 2012. Was based on the previous Ouldboukhitine et al. (2011) model, but several improvements were made. This model is included in the popular simulation software – TRANSYS as a green roof model tool. The model considers the coupled heat and mass transfer through the green roof. The vegetative part (Long and shortwave radiation and evapotranspiration) is calculated from the coverage ratio and the leaf area index. The long-wave radiative heat exchange between foliage and soil is considered as long-wave radiation between two infinite parallel surfaces. The soil layer is a porous medium characterized by water content. Water content and evapotranspiration depend on water balance, which is estimated as a sum of the rainfall, the drainage and evapotranspiration. The water transfer module used Richard's equation. The model does not consider vapour flow when the soil layer is not fully saturated. This model also doesn't take into account the energy loss/gain associated with runoff water, phase change phenomena as well as enthalpy transfer.

Another widespread model with green roof simulation option is WUFI. WUFI is used to simulate buildings performance regarding heat and moisture movement and storage. WUFI is designed to consider building's materials as layers including air gaps and vegetation layers. Stockl et al. (2014) described how WUFI model could be used regarding green roof simulation. In this work, validation exercise included temperature comparison between measured and modelled results under the growing media, not within it or vegetation. The model showed good correlation in moisture content values and temperature under the growing media. WUFI principle of simulation is to estimate virtual thermal mass and moisture holding capacity as well as resistance to heat and moisture flow of the vegetation and apply it as a layer in the model.

3 PROBLEM STATEMENT

Many previous papers have stated that modern urban cities face environmental problems, such as the urban heat island effect, noise or contaminant air pollution. Green roofs have been gaining attention from urban designers over the last years as a solution to those problems. The first positive impact of a green roof is an energy savings possibility. Secondly, green roofs can reduce the urban heat island effect. Thirdly, green roofs have some water storage and can reduce the load on a city drainage system. However, the listed benefits might be achieved if a green roof is appropriately designed and located in the appropriate climate. Due to plants and soil presence, a green roof is affected by combined heat and moisture transfer.

Since 2007, several green roof models have been published. The latest models consider heat and moisture parameters but do not take into account the coupled heat and moisture transfer phenomena in the growing media, the different level of saturation levels and the associated heat and moisture transfer processes, convective heat transfer associated with runoff water.

Coupling heat and moisture transfer in green roof modelling increases model accuracy. Figure 5 illustrates the relationship between moisture and heat transport. Heat transport depends on the moisture balance by thermal storage, heat capacity, thermal conductivity and phase change effect. On the other hand, temperature determines saturated vapour pressure, vapour permeability and moisture transfer coefficients.

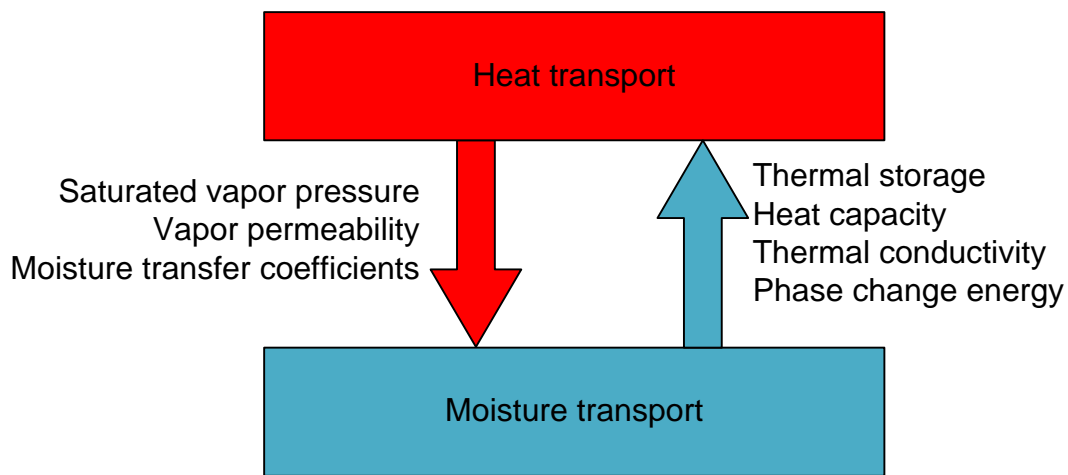


Figure 5. Heat and moisture transport interdependence

Although the best available model is called coupled, it is the only one-way relationship between moisture and heat transfer. The model considers such moisture effect on heat transfer as heat capacity and conductivity changes and phase change energy associated with vaporization. The most comprehensive model ignores vapour permeability, moisture transfer coefficient changes due to temperature change. Moreover, the well-developed model should judge the growing media layer as multi-level material, where each layer has its moisture content and temperature values. Figure 6 compares fully discretized and current green roof models. The current model estimates only lumped moisture content in the growing media, while temperatures are discretized.

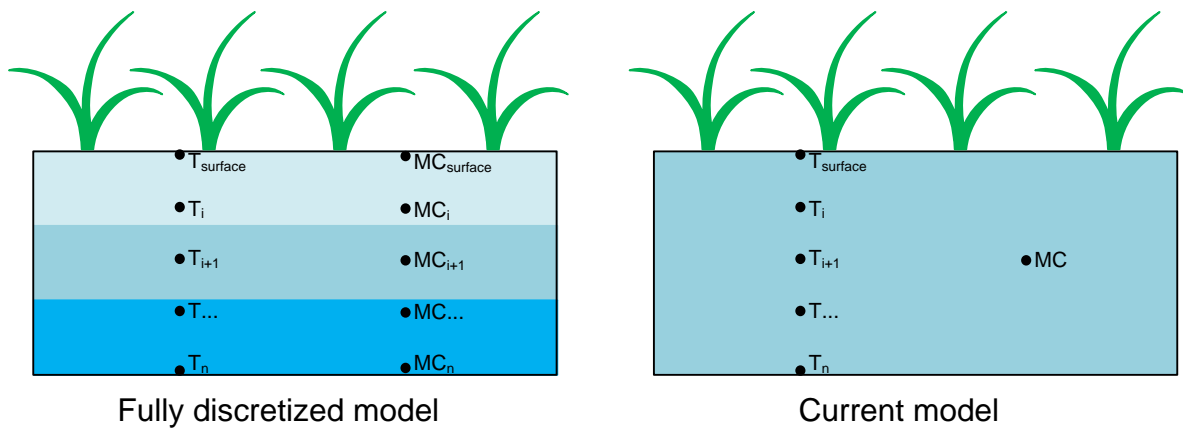


Figure 6. Green roof model discretization.

As it was mentioned before, moisture in the growing media layer plays a significant role in green roof energy performance. Thus, water balance requires extra attention. During wetting and drying, the growing media layer can be in three stages:

- Unsaturated – when pores within the growing media are not filled with water
- Saturated – when 100% growing media pores are filled with water
- Oversaturated – when 100% growing media pores are filled with water, and the roof substrate cannot absorb water anymore.

A critical limitation of the best available model is the absence of vapour flow in an unsaturated stage. In a case when the substrate is saturated, the whole amount of porous is filled with water and there is no space for vapour to move. However, in real life, a green roof can have an unsaturated section whereby vapour can move through the growing media. As discussed in the literature review section, enthalpy transfer is one of the phenomena that occur in a green roof growing media layer, but it is not covered by current models. To develop an accurate coupled heat and moisture model, it is

essential to include in the model an energy exchange that occurs when water or vapour goes through the growing media.

Most of the previous studies do not take into account energy that leaves the system by convection with runoff water. Runoff water has an influence on overall water balance; moreover, liquid water flow leads to energy transfer by convection. A model that covers this phenomenon might show better accuracy. Concerning vegetative model, they are almost entirely developed.

Green roof energy saving benefits were proved by numerous authors; nevertheless, there are no consciences in their performance during a winter season. In addition to climate, roof design itself can have an impact on the overall green roof energy performance. It is essential to assess and identify the optimal green roof design and roof insulation layer thickness for specific climate and seasons. The modelling tool should cover as many physical processes as possible, be reliable and accurate. The tool has to be able to deal with different climates, green roof design as well as building conditions. Another feature that is necessary for designers to include is model flexibility. There are several green roof models can be downloaded or purchased, but a designer could not change the vast number of parameters; therefore, to estimate green roof performance within various circumstances, the model has to be developed.

4 RESEARCH APPROACH

4.1 Objectives

The aim of this research project is to develop a comprehensive green roof model that accurately predicts the heat and moisture movement phenomena that occur in an extensive green roof system.

Accordingly, the objectives of the research project are:

- i) to develop an advanced green roof model that fully couple heat and moisture transfer in the growing media and takes into account the additional heat and moisture driving forces discussed in the problem statement section
 - a. Create a two-way coupled green roof model, which simultaneously deals with energy and water retention performance of green roof.
 - b. Implement discretization for moisture content in the growing media as well as temperature instead of uniform moisture content assumption.
 - c. Accurately model evapotranspiration and outdoor radiation.
 - d. Take into account water and vapour flow in the growing media and energy associated with it.
- ii) to evaluate the impacts of green roof components and designs on the energy performance of the systems in different climates and seasons.
 - a. Model and compare green roof systems for new buildings with various insulation and growing media thicknesses for different climate zones that yield an optimized energy performance.
 - b. Develop green roof systems for integration in existing or old buildings.

4.2 Scope

This research project is limited to extensive green roof type. The model does not include irrigation as a moisture source. Due to time constraint, the developed model is not integrated with other energy simulation tools, but rather is used as a model component.

4.3 Methodology

Based on principles described in the FASST and HAMFit models, a green roof model that takes into account the heat and moisture properties of green roof materials, coupled vapour and liquid moisture transfers, phase change phenomenon, and runoff is developed. Fig. PP shows a flowchart of the development process. The newly developed green roof model has been benchmarked against the concurrently running field experimental study at BCIT. Once the model has been validated, it was used to study the impact of the various green roof system components on the overall energy and water balance of the system. Moreover, the model was run to identify the optimal green roof system design for different buildings, roof design and climate zones. The model was run comparing green roof behaviour with various insulation and growing media thicknesses as well as different plants properties in different climates and seasons.



Figure 7. Methodology flowchart

5 MODEL DEVELOPMENT

Green roof models deal with combined heat and moisture transfer through the roof, taking simultaneously into account the effects of shading of the leaves, insulation, evapotranspiration, thermal mass, convection, short- and longwave radiation, conduction within layers and water flow to and within a green roof with associated heat. The physical phenomena that occur in a green roof system are shown schematically in Figure 8. Factors such as plant growth, substrate thermal properties, solar radiation intensity, precipitation and volumetric water content must be included in a model. The presence of the growing media and vegetation layers makes the heat and moisture flows and the green roof thermal response complex when compared to a conventional roof system. To understand the overall thermal system of a green roof, each of the listed driving sources of heat and moisture transfer needs to be considered.

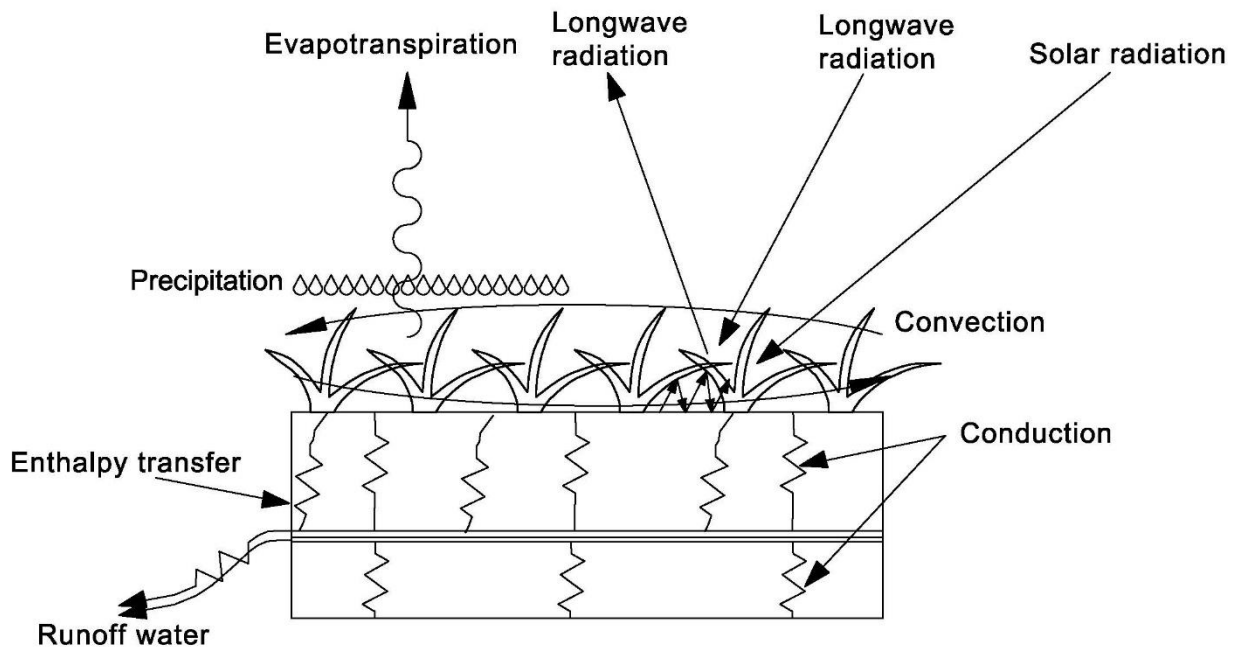


Figure 8. Heat and moisture sources in the green roof.

To build a comprehensive and detailed green roof model, the heat and moisture transport phenomena in the system are handled with two coupled models: Vegetative model and HM (heat and moisture) model. The newly developed green roof model, which is referred hereafter as HAMFit-GR. The model scheme is shown in Figure 9. The coupling interface for the two models is the top surface of the growing media; thus, the vegetative model describes the heat and moisture transfer phenomena above the growing media, while the heat and moisture model covers phenomena in the growing media and roof structure. Therefore, the main purpose of the vegetative model is to determine foliage temperature (T_f) and calculate boundary conditions to heat and moisture model, which is responsible for heat and moisture movement within the green roof structure including ground temperature (T_g) that is included in the vegetative model.

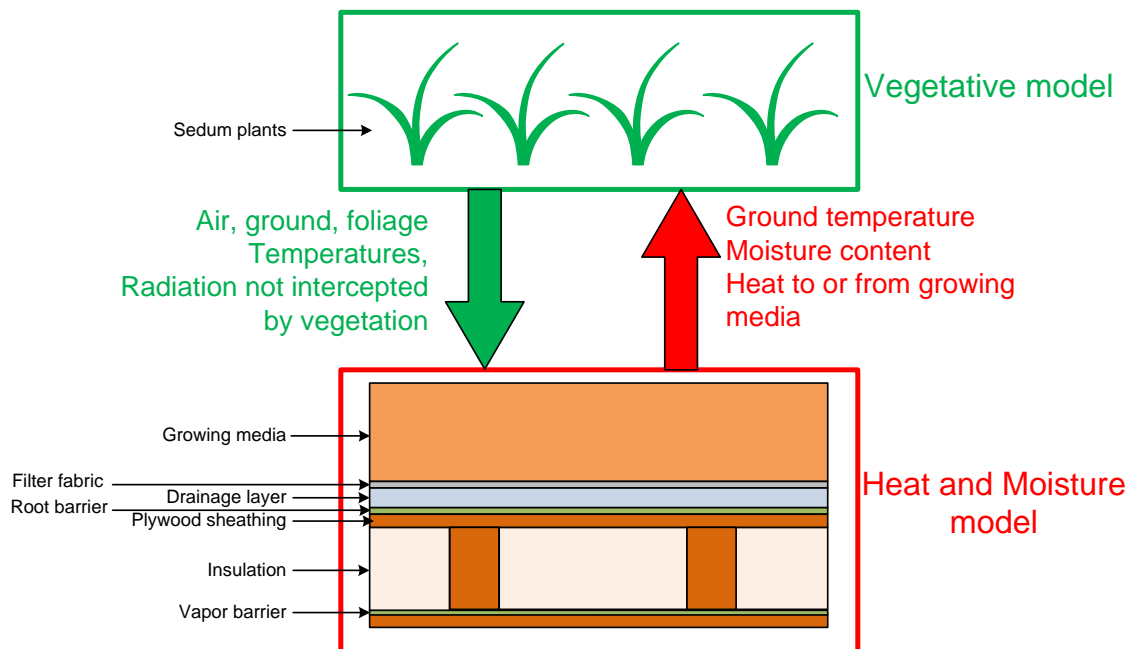


Figure 9. Green roof model.

The green roof model is developed using COMSOL Multiphysics software. COMSOL Multiphysics was chosen as the primary programming environment as it was a programming environment for the hygrothermal base model, HAMFit (Tariku, 2008). COMSOL Multiphysics allows implementation of user-developed governing equations in PDE (Partial Differential Equation) mode and solve coupled one-, two- and three-dimensional phenomena in a steady-state or transient time domain.

5.1 Vegetative model

Much research on green roof modelling has been done based on the Fast All-Season Soil Strength (FASST) model. FASST is developed by Frankenstein and Koenig (2012) for the US Army Corps of Engineers to estimate soil strength. For HAMFit-GR model, FASST model is adopted. The energy balance is done for the leaf foliage layer and the growing media top surface by assuming steady-state heat exchange between them. In this model, energy transfer due to convection, solar radiation gain, longwave radiation exchange with sky and between leaf and growing media, latent and sensible heat transfer associated with precipitation and evapotranspiration are considered.

5.1.1 Radiation

In the HAMFit-GR model radiation heat fluxes are calculated using two semi-infinite plane parallel method. In this method, plants are assumed to be single, homogeneous layer. Figure 10 illustrates how radiation is calculated in HAMFit-GR. The model assumes that ground surface is partially covered by vegetation, and the area that is covered by the plants and prevents radiation from reaching the growing media surface is expressed by fractional coverage ratio (σ_f). The fractional coverage ratio is calculated based on seasons and plants properties (Dickinson, 1998; Ramirez and Senarath, 2000). Incoming solar on foliage and growing media surfaces can be written as in Equations [1] and [2] respectively. The incoming solar heat radiation (I_s) is taken from a meteorological input

file, and the reflective properties of vegetation and growing media are expressed by the respective albedo (α) values.

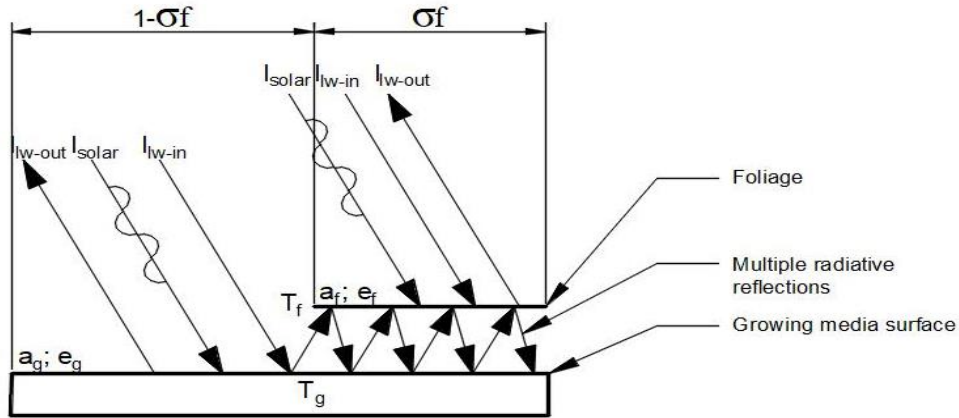


Figure 10. Solar and infrared radiation in a green roof.

$$I_f^s = \sigma_f(1 - a_f)I_s \quad [1]$$

$$I_g^s = (1 - \sigma_f)(1 - a_g)I_s \quad [2]$$

Similarly to solar radiation, total longwave radiation (I_{irr}) or sky temperature can be available from the meteorological station or can be estimated empirically (ISO 15927, 2003). The longwave radiation from the sky to the foliage and growing media surface are given in Equations [3] and [4]. In consistent to gray body radiation assumption, the foliage and ground longwave absorptivity are equal to their corresponding longwave emissivities (ε) values.

$$I_f^{irr} = \sigma_f \varepsilon_f I_{irr} \quad [3]$$

$$I_g^{irr} = (1 - \sigma_f)\varepsilon_g I_{irr} \quad [4]$$

Based on infinite parallel plates assumptions, the radiative heat exchange between plants and the growing media is given by Equation [5].

$$I_{fg} = \frac{\sigma_f \varepsilon_f \varepsilon_g \sigma}{\varepsilon_f + \varepsilon_g - \varepsilon_f \varepsilon_g} (T_g^4 - T_f^4) \quad [5]$$

Where σ_f is leaf coverage ratio, σ - Stefan-Boltzmann constant, T_g and T_f are ground and foliage temperatures respectively, ε_f and ε_g – foliage and ground emissivity.

5.1.2 Sensible heat

The vegetative part of the HAMFit-GR model determines convective (sensible) heat flux separately for ground and plants surfaces. The sensible heat fluxes are calculated using foliage temperature, ground temperature, the temperature of the air above and the below the foliage, and the corresponding effective convective heat transfer coefficients. Figure 11 shows the representation of this temperature in HAMFit-GR, where the subscripts f, g, a, af stand for foliage, ground, air and air-foliage respectively.

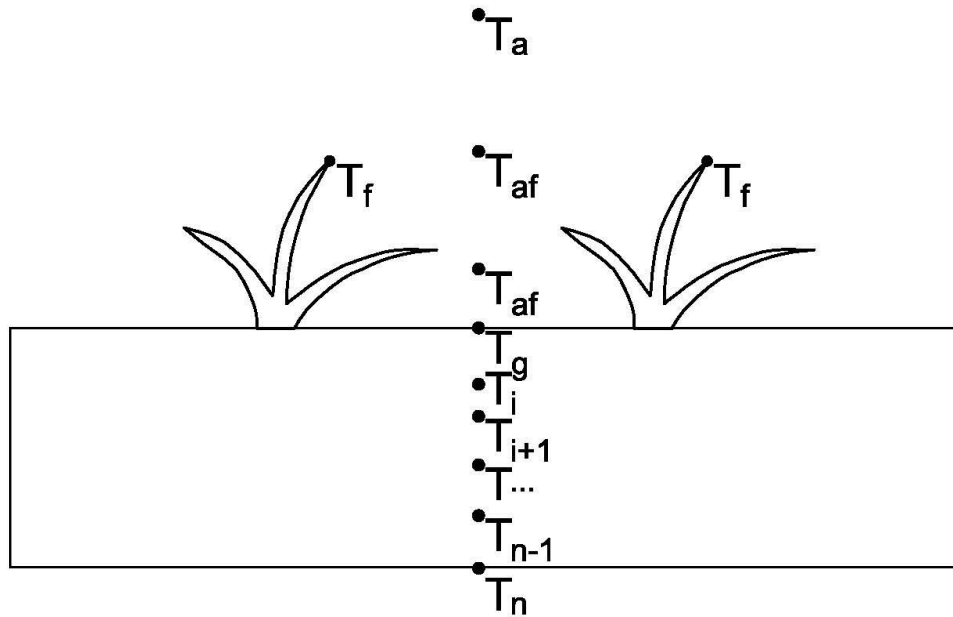


Figure 11. Temperature distribution.

The sensible heat fluxes from the foliage and the ground surfaces are calculated using Equations. [6] and [7], respectively.

$$H_f = hf(T_{af} - T_f) \quad [6]$$

$$H_g = hg(T_{af} - T_g) \quad [7]$$

The effective air temperature surrounding the foliage (above and below), which is referred here as the air-foilage temperature is determined from surrounding air, ground surface and foliage temperatures. In this model, the empirical relation that has been put forward to estimate air-foilage temperature by Dearforff (1978) and commonly used in green roof modelling, Equation [8], is used.

As can be seen in the equation, the air-foliage temperature depends on plant cover ratio. When there is no plant, $T_{af}=T_a$, and during fully coverage T_{af} is determined mainly by the foliage temperature.

$$T_{af} = (1 - \sigma_f)T_a + \sigma_f(0.3T_a + 0.6T_f + 0.1T_g) \quad [8]$$

The sensible heat flux transfer coefficient, h_f and h_g can be estimated using Equations [9] and [10] by considering the air mass blowing through the green roof canopy. Area Index represents an area of plants which is exposed to the air movement and associated heat exchange (Leaf area index is discussed in the vegetation characterization section). $c_{p,a}$ is heat capacity of air and e_0 – windless sensible heat transfer coefficient to reflect natural convection due to the temperature gradient (equal to $2 \text{ W/m}^2\text{K}$). ρ - air density near foliage or ground surface that is calculated by the Ideal Gas Law, W_{af} is wind speed within the foliage and C_h and C_h^g are bulk transfer coefficients.

$$h_f = (e_0 + 1.1LAI\rho_{af}c_{p,a}C_fW_{af}) \quad [9]$$

$$h_g = (e_0 + \rho_{ag}c_{p,a}C_h^gW_{af}) \quad [10]$$

Bulk transfer coefficient, which is a resistance of plants to wind flow, is determined based on roughness length (z_0). – a mathematical representation of the surface roughness. In the vegetation presence case roughness length is shifted upward by a value called zero displacement height (Z_d). Those values are defined in Equations [11] and [12] (Frankenstein and Koenig, 2004). Z_f – is plants height in meters and is one of the model inputs.

$$Z_d = 0.701Z_f^{0.975} \quad [11]$$

$$Z_0 = 0.131Z_f^{0.997} \quad [12]$$

Then, using the logarithmic wind profile semi-empirical method, the bulk transfer coefficient at the foliage top surface is equal to Equation [13]:

$$C_{hn}^f = \left[\frac{k}{\ln\left(\frac{Z_a - Z_d}{z_0}\right)} \right]^2 \quad [13]$$

Where, k is Von Karman constant (0.4), Z_a is temperature sensor height, that equals 2 m by default.

According to Deardorff (1978), in the case of vegetation, wind speed within the plant's layer is roughly equal to 0.3 of the wind speed above the plants and can be calculated using Equation [14] where W is the wind speed from the weather file and limited to be greater than 2 m/s. The wind speed within the foliage is highly interconnected with foliage density (coverage ratio) and become equal to ambient wind speed in a case of plants absence. The coefficient of 0.83 is an empirical number for relative dense canopies like green roof vegetation.

$$W_{af} = 0.83\sigma_f \sqrt{C_{hn}^f} W + (1 - \sigma_f) * W \quad [14]$$

Finally, the bulk transfer coefficient for wind flow within foliage is given by Equation [15]. The value 0.01 is multiplication factor for forced convection within the plants and 0.3 is free convection enhancement.

$$C_f = 0.01 \left(1 + \frac{0.3}{W_{af}} \right) \quad [15]$$

The bulk transfer coefficient near the ground surface is determined as Equation [16], where r_{ch} is Schmidt number (0.63) and z_0 is growing media roughness length equals to 0.001 m.

$$C_{hn}^g = \frac{\left[\frac{k}{\ln \left(\frac{Z_a - Z_d}{z_0} \right)} \right]^2}{r_{ch}} \quad [16]$$

Sensible heat exchange stability correction factor [17] and Richardson number [18] and [19] (Louis, 1979) are used for determination of bulk transfer coefficient for the growing media sensible heat flux [17] (Frankenstein and Koenig, 2004).

$$C_h^g = \gamma \left((1 - \sigma_f) * C_{hn}^g + \sigma_f C_{hn}^f \right) \quad [17]$$

$$R_{ib} = \frac{2gZ_a(T_{af} - T_g)}{W_{af}^2(T_{af} + T_g)} \quad [18]$$

$$\gamma = \begin{cases} 1 - \frac{9.4R_{ib}}{\sqrt{\left(1 + 7.4C_{hn}^g 9.4 \sqrt{\frac{Z_a}{z_0}} |R_{ib}| \right)}} & R_{ib} < 0 \\ 1 & R_{ib} = 0 \\ \frac{1}{(1 + 4.7R_{ib})^2} & R_{ib} > 0 \end{cases} \quad [19]$$

5.1.3 Latent heat

In the green roof system, heat associated with phase change requires explicit attention due to the relatively large amount of moisture in the growing media and its transfer to or from the surroundings. In green roof modelling, the process of water evaporation or sublimation is complicated by plants and its transpiration. Mixing ratio, which is the mass of water vapour per unit of dry mass, is used as driving potential in the latent heat calculation. The model calculates mixing ratios of ambient air (q_a) and the foliage (q_f) and ground (q_g) interfaces using Equation [20].

$$q = \frac{0.622P_v}{P_a - P_v} \quad [20]$$

Where P_a is air pressure and P_v is vapour pressure.

In the calculation, foliage is assumed to be always saturated. The mixing ratio of the air between the ground surface and plants is estimated using Equation [21] (Deardorff, 1978, Frankenstein and Koenig, 2004).

$$q_{af} = \frac{(1 - \sigma_f)q_a + \sigma_f(0.3q_a + 0.6q_{f,sat}r_t + 0.1q_{g,sat}M_g)}{1 - \sigma_f(0.6(1 - r_t) + 0.1(1 - M_g))} \quad [21]$$

Where M_g is a ground moisture factor that equals to 1, when rain falls, otherwise it equals to the moisture content of soil near the top surface (taken from the heat and moisture model—model coupling parameter). r_t is foliage surface wetness and is calculated from atmospheric (r_a) and plants resistance to vapour diffusion (r_s), which is referred as stomatal resistance, using Equations [22] and [23]

$$r_t = \frac{r_a}{r_a + r_s} \quad [22]$$

$$r_a = \frac{1}{C_f W_{af}} \quad [23]$$

Where, W_{af} – wind speed within the foliage and C_f – foliage bulk transfer coefficient.

The stomatal resistance (Equation [24]) is a function of plants properties, minimal stomatal resistance and leaf area index, solar radiation and moisture availability at the plant root (Equations [25] and [26]). Moisture content within the root zone is obtained from the heat and moisture model (—model coupling parameter), and minimum and maximum moisture content are the input parameters of the growing media (Chen et al. 1996, Frankenstein and Koenig, 2004).

$$r_s = \frac{r_{s,min}}{LAI} f_{sun} f_{mc} \quad [24]$$

$$f_{sun} = \min\left(1, \frac{0.004I_s + 0.005}{0.81(0.004I_s + 1)}\right) \quad [25]$$

$$f_{mc} = \frac{MC_{root} - MC_{min}}{MC_{mac} - MC_{min}} \quad [26]$$

Following the work of Frankenstein and Koenig (2012), the latent heat flux from the foliage and ground surfaces are given by Equations [27] and [28]. l – is either latent heat of sublimation or evaporation.

$$L_f = LAI \rho_{af} C_f l W_{af} r_t (q_{af} - q_{fsat}) \quad [27]$$

$$L_g = C_e^g l W_{af} \rho_{ag} (q_{af} - q_g) \quad [28]$$

5.1.4 Water movement

Precipitation in the green roof modelling plays a significant role due to plants dependence on moisture availability and the ability of green roofs to retain water in its structure. In the HAMFit-GR model, the effect of rain in both energy and moisture transfer is considered. During rain events, part of the rainwater is intercepted by leaves and then evaporates back to the atmosphere or drip to the soil, and the rest will pass the leaves and directly touches and saturates the growing media. If the amount of water is not significant, the water stays on the foliage and evaporates back to the surrounding environment or absorbed by the plant and finally transpired to the atmosphere. In the other extreme case, where the rainfall exceeds the moisture storage capacity of the growing media, any excess water goes through the soil and leaves the system by drainage. Figure 12 schematically shows water movement through a green roof.

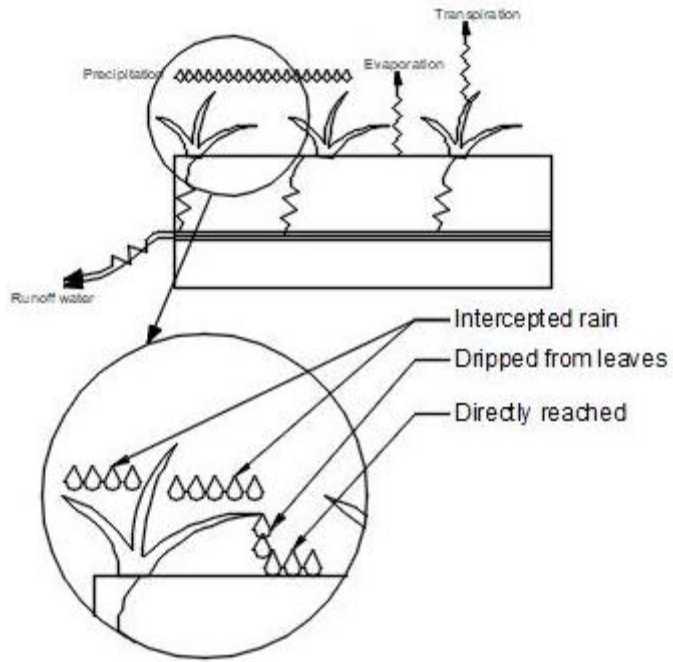


Figure 12. Water movement.

The model takes the amount of incoming rain from a weather file and then calculates the portions of rain amount that are intercepted by leaves (Equation [29]) (Frankenstein and Koenig, 2004), and the balance is assumed to saturate the growing media.

$$Intp = 1 - \exp(-0.5(LAI + SAI))\sigma_f Prc \quad [29]$$

Where, Prc is a rain fall rate and SAI is stem area index, represents additional plants covered not green areas.

The maximum leaf storage capacity is given by Ramirez and Senarath (2000) in Equation [30].

$$Sc_{max} = 0.2(LAI + SAI) \quad [30]$$

Where,

SAI – is a steam area index, which is relatively low in the case of green roofs and can be within the range of 0.5 to 2.

Then the dripped amount can be estimated as Equation [31], where Δt is a time step.

$$D = Intp - \frac{Sc_{max}}{\Delta t} \quad [31]$$

Heat fluxes due to precipitation on ground and leaf surfaces respectively can be calculated using Equations [32] and [33]. γ_p is water density, c_p is water heat capacity and T_p is rainwater temperature, that is assumed to be at air temperature.

$$P_g = -\gamma_p c_p T_p (Prc - Intp + D) \quad [32]$$

$$P_f = -\gamma_p c_p T_p Intp \quad [33]$$

Regarding water balance within the growing media, plants transpire water to the atmosphere causing mass flow from the growing media. This flow is calculated using Equation [34] (Frankenstein and Koenig, 2004). Transpiration occurs at the minimum rate of what plants root can uptake or what plants can transport to the surroundings based on the conditions. The amount of water that leaves the system by evaporation is estimated by the heat and moisture model using vapour pressure based on air-foliage mixing ratio provided by the vegetation model.

$$E_{tr} = \min \left(1.5 * 10^{-7} \sigma_f f f M C_{root}, r_d L A I \rho_a C_f W_{af} (q_{af} - q_{f,sat}) \right) \quad [34]$$

Where,

ff is a freezing factor that is 0 if soil temperature below zero, MC_{root} moisture content in the root zone and r_d is a root distribution factor.

In the green roof structure, water causes heat transfer not only when it touches the surfaces of plants and soil, but also when water flows through the growing media to the drainage outlet. The model compares the incoming water flow on the top ground surface with the growing media water holding capacity at that moment, and the difference is assumed to be a drainage amount (Equation [35]). t is time step and z is coordinate along roof height.

$$Drg = 1000(Prc - Intp + D) * t - \int MCdz \quad [35]$$

Heat associated with runoff water is given by Equation [36] and is a subject to add into governing energy equation under the heat and moisture model.

$$H_{drg} = DrgC_lT \quad [36]$$

5.1.5 Final energy balance equations

Finally, the general governing equations for heat balance at the foliage layer and top growing media surface can be written as Equations [37] and [38]:

$$\begin{aligned} \sigma_f [I_s(1 - \alpha_f) + \varepsilon_f I_{lw} - \varepsilon_f \sigma T_f^4 + \gamma_p c_p T_p Intp] + \frac{\sigma_f \varepsilon_f \varepsilon_g \sigma}{\varepsilon_1} (T_g^4 - T_f^4) \\ + (e_0 + 1.1LAI\rho_{af}c_{p,a}C_f W_{af})(T_{af} - T_f) + LAI\rho_{af}C_f lW_{af} r_t (q_{af} \\ - q_{fsat}) = 0 \end{aligned} \quad [37]$$

$$\begin{aligned} (1 - \sigma_f) [I_s(1 - \alpha_g) + \varepsilon_g I_{lw} - \varepsilon_g \sigma T_g^4] - \frac{\sigma_f \varepsilon_f \varepsilon_g \sigma}{\varepsilon_1} (T_g^4 - T_f^4) + (e_0 \\ + \rho_{ag}c_{p,a}C_h^g W_{af})(T_{af} - T_g) + C_e^g lW_{af} \rho_{ag} (q_{af} - q_g) + \gamma_p c_p T_p (PrC \\ - Intp + D) + k \frac{\partial T_g}{\partial z} - \vartheta c_p T_g = 0 \end{aligned} \quad [38]$$

5.2 Coupled Heat and Moisture model

The heat and Moisture model has adopted from the HAMFit model. HAM is an abbreviation for Heat, Air and Moisture. The HAMFit model can be used to estimate coupled mass and energy transfer through the building envelope that can be presented as 1-D, 2-D or 3-D structure. HAMFit model is validated through the series of the benchmarks, including comparison with other models and experimental results (Tariku, 2008). Figure 13 shows the main HAMFit workspace in the COMSOL Multiphysics environment. Under model section in the model builder, indoor and outdoor boundary conditions, a number of designed layers and its properties could be defined.

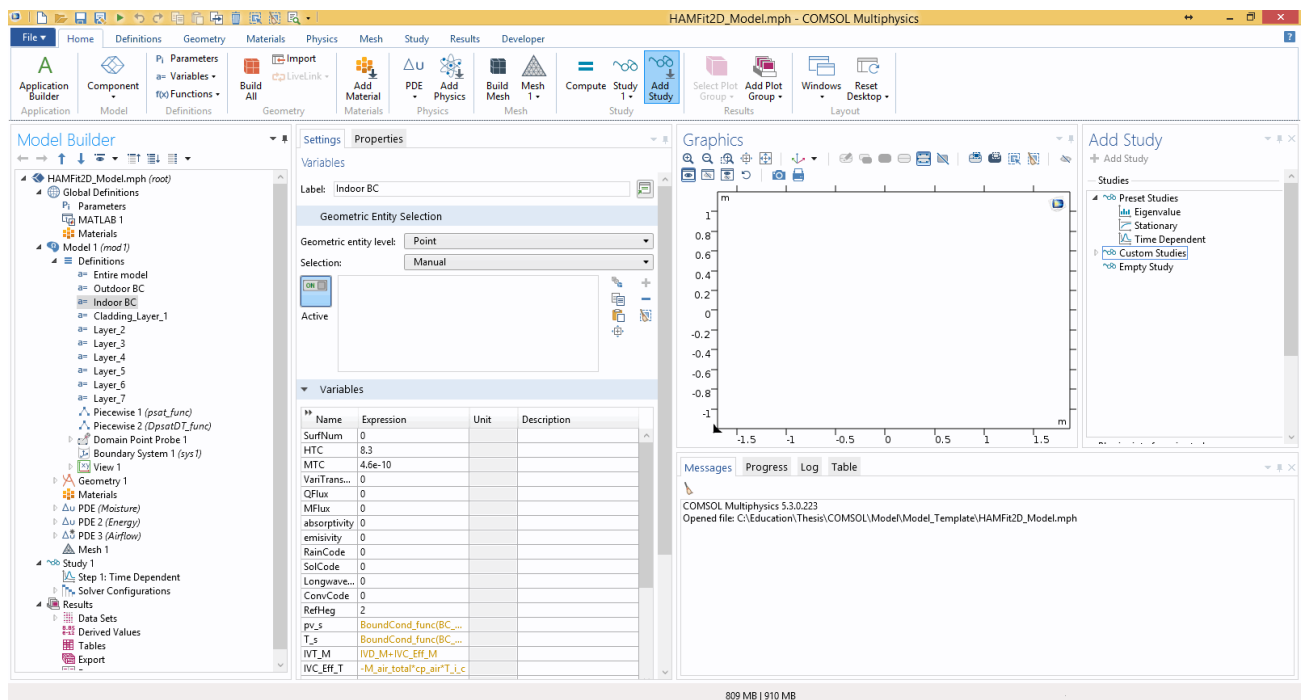


Figure 13. HAMFit model workspace.

The model is based on three Partial Differential Equations: PDE (Moisture), PDE (Energy), PDE (Airflow) for moisture, heat and air flows respectively with strong interconnection between them. Although the original HAM model deals with air movement and the associated energy and moisture

transport, it is reasonable to exclude air part within solid layers in this thesis. The effect of wind and corresponding convection within foliage is a part of energy calculation under the vegetative model.

5.2.1 Moisture governing equation

Moisture transport can be written as the following Equation [39]:

$$\frac{\partial w}{\partial t} + \text{div} \left(-\delta_v \frac{\partial P_v}{\partial x_i} \right) + \text{div} \left(D_l \left(\frac{\partial P_s}{\partial x_i} + \rho_v g \right) \right) = 0 \quad [39]$$

The driving sources are vapour pressure (P_v) and suction pressure (P_s), while the moisture content (w) serves as a variable. To build a model, it was decided to transform the formula to a single driving potential, relative humidity. Relative humidity is chosen, because it is continuous within the whole building structure, while moisture content could be discontinuous at a location where two different materials are contacted (Tariku, 2008).

Therefore, the moisture balance equation might be presented as Equations [40] and [41]:

$$\Theta \frac{\partial RH}{\partial t} = \frac{\partial}{\partial x_i} \left(D_{RH} \frac{\partial RH}{\partial x_i} + D_T \frac{\partial T}{\partial x_i} \right) - \frac{\partial}{\partial x_i} D_l \rho_w g \quad [40]$$

And

$$D_{RH} = \left(\delta_v P_s + D_l \frac{\rho_w R T}{M RH} \right) \quad D_T = \left(\delta_v RH \frac{\partial P_{sat}}{\partial T} + D_l \frac{\rho_w R}{M} \ln(RH) \right) \quad [41]$$

Where

θ - is sorption capacity; D_{RH} and D_T are moisture and temperature conduction coefficients; D_l – is liquid conductivity; δ_v – vapor permeability; P_{sat} – saturated vapor pressure; R – universal gas constant; M - molecular mass of a water molecule.

5.2.2 Energy governing equation

The heat balance is expressed by Equations [42] and [43].

$$\begin{aligned} \rho_m C p_{eff} \frac{\partial T}{\partial t} + \text{div} \left(-\lambda_{eff} \text{grad}(T) \right) & \quad [42] \\ & = \text{div} \left(\delta_v \frac{\partial P_v}{\partial x_i} \right) h_{fg} + \text{div} \left(\delta_v \frac{\partial P_v}{\partial x_i} \right) T (C p_v - C p_l) + Q_s \end{aligned}$$

And

$$C p_{eff} = C v_m + Y_l C p_l \quad [43]$$

Where ρ_m – is material density, λ_{eff} - effective thermal conductivity, δ_v - vapor permeability, P_v - vapor pressure, h_{fg} - latent heat of evaporation/ condensation. $C v_m$, $C p_v$ and $C p_l$ - specific capacity of the solid matrix, water vapour and water respectively, Q_s - heat source, Y_l - mass fraction of liquid water.

As it can be seen from the formulas, water content interacts with heat balance as well as the temperature influences moisture balance. Therefore, this interdependence makes the model coupled. Figure 14 shows the COMCOL Multiphysics interface with equations are implemented.

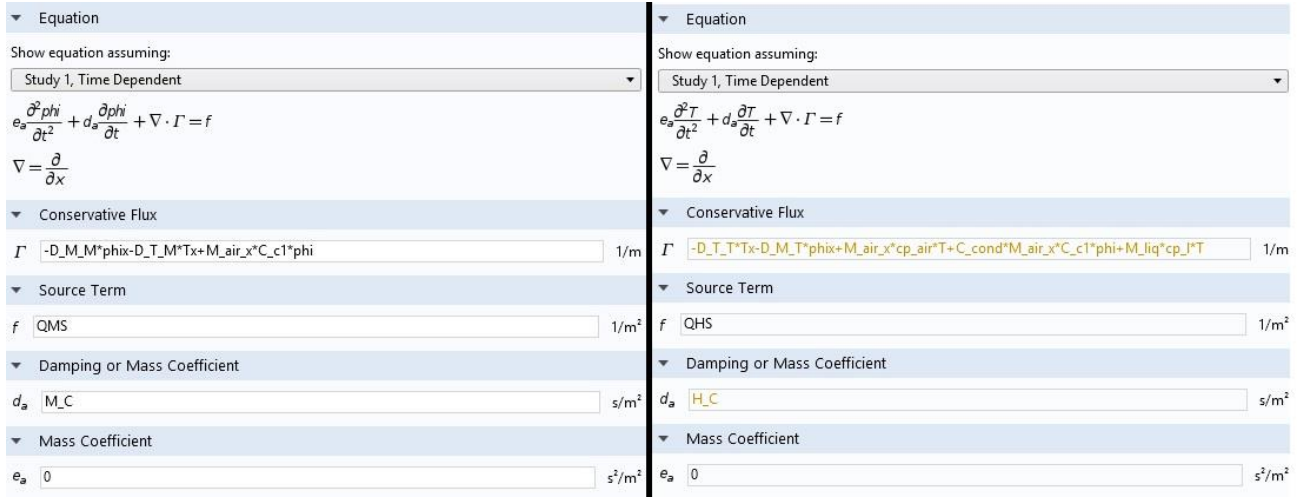


Figure 14. Heat and Moisture model via COMSOL Multiphysics differential equations.

5.2.3 Model modifications

To couple vegetative model with HAMFit, some modifications are required. First, the vegetative model calculates radiative, sensible, latent and precipitation heat fluxes due to plants presence on the top surface of growing media. Thus, those terms are added to the HAMFit energy equation on the top surface. Energy balance on the top surface can be written as Equation 44.

$$\rho_m c_{p_{eff}} \frac{\partial T}{\partial t} + \text{div} \left(-\lambda_{eff} \text{grad}(T) \right) \quad [44]$$

$$= \text{div} \left(\delta_v \frac{\partial P_v}{\partial x_i} \right) h_{fg} + \text{div} \left(\delta_v \frac{\partial P_v}{\partial x_i} \right) T (C_{p_v} - C_{p_l})$$

$$+ (1 - \sigma_f) [I_s (1 - \alpha_g) + \varepsilon_g I_{lw} - \varepsilon_g \sigma T_g^4] - \frac{\sigma_f \varepsilon_f \varepsilon_g \sigma}{\varepsilon_1} (T_g^4 - T_f^4) + (e_0$$

$$+ \rho_{ag} c_{p,a} C_h^g W_{af}) (T_{af} - T_g) + C_e^g l W_{af} \rho_{ag} (q_{af} - q_g) + \gamma_p c_p T_p (Prc - Intp + D)$$

Second, water that penetrates to the growing media results in convective heat flow; thus, the governing energy equation within the soil needs to be modified as well (Equation [45]).

$$\rho_m C p_{eff} \frac{\partial T}{\partial t} + \text{div} \left(-\lambda_{eff} \text{grad}(T) \right) \quad [45]$$

$$= \text{div} \left(\delta_v \frac{\partial P_v}{\partial x_i} \right) h_{fg} + \text{div} \left(\delta_v \frac{\partial P_v}{\partial x_i} \right) T (C p_v - C p_l) + \boxed{\text{Drg} C p_l T} + Q_s$$

Thirdly, regarding moisture balance, outdoor flow due to rains is restricted by vegetation model and equals to the amount of rain that is not intercepted by leaves plus dripped water from leaves and can be written as Equation [46].

$$M = Prc - Intp + D - E_{tr} \quad [46]$$

Finally, although evaporation process is covered by the HAMFit model, it is an exchange with outdoor air. In the green roof model, there is a need to include the additional evaporation process due to plants. Thus, the mixing ratio of the air within foliage is converted and applied as outside vapour pressure.

5.3 Model inputs

In order to properly model heat and moisture movement within the green roof structure, adequate input data is required. Model input parameters include outdoor and indoor conditions data, soil and other materials properties, and vegetation characteristics.

Boundary conditions consist of inside and outside temperatures (room set and air temperatures respectively), relative humidities in the form of vapour pressure, incoming sun and longwave radiation, wind speed and amount of rain coming on the modelled roof.

A number of physical properties describe each layer in the model. Typical widely distributed in the construction industry materials are already included in the HAMFit model based on the information available from ASHRAE. Unfortunately, growing media properties are not unique and should be characterized separately. Table 1 summarizes growing media variables to include in the mode. Main soil properties to be described are radiative parameters (albedo and emissivity); density and heat capacity; thermal, liquid and vapour conductivity (or diffusivity); moisture content (sorption) and moisture storage capacity.

Table 1. Growing media parameters.

#	Symbol	Name	Unit
1	a_g	albedo groud	-
2	e_g	Emissivity	-
3	Density	Soil Density	kg/m ³
4	H_C	Heat Capacity	J/kgK
5	Sorption	Moisture content in soil	kg/m ³
6	Conductivity	Conductivity	W/m ² K
7	VperPermeability	Vapour Permeability	kg/Pam
8	Diffusivity	Water diffusivity	m ² /s
9	M_C	Moisture storage capacity	kg/m ³

Such parameters as density, heat capacity, thermal and liquid conductivity are moisture-dependent defined based on moisture content (Sorption), which in its term is a function of relative humidity, following the sorption isotherm of the material.

The vegetation layer is different from the rest of layers because plants only partly cover the growing media surface. The heat capacity of plants is assumed to be negligible and temperature to be uniform within the whole layer. Table 2 lists vegetative-connected inputs.

Table 2. Vegetation parameters.

#	Name	Definition	Unit
1	CV_min	Minimum coverage ratio	m ² /m ²
2	CV_max	Maximum coverage ratio	m ² /m ²
3	Z _{root}	Root depth	mm
4	a _f	Foliage albedo	-
5	e _f	Foliage emissivity	-
6	a _{root}	Root fraction parameter a	m ⁻¹
7	b _{root}	Root fraction parameter b	m ⁻¹
8	LAI_min	Minimum Leaf Area Index	m ⁻² /m ⁻²
9	LAI_max	Maximum Leaf Area Index	m ⁻² /m ⁻²
10	rsmin	Minimal stomatal resistance	s/m
11	SAI	Stem Area Index	m ² /m ²
12	z _{0fm}	Roughness length	m
13	Z _{fmin}	Minimum plants Height	m
14	Z _{fmax}	Maximum plants Height	m

Coverage ratio (CV_min, CV_max) and Leaf Area Index (LAI_min, LAI_max), parameters that changes with seasons, are main parameters that influence the overall green roof performance. Another important variable in the green roof simulation process is stomatal resistance, that can be

defined as an ability of plants to transfer water through it. All the specific numbers listed above variables are defined through experiments.

6 CHARACTERIZATION OF GROWING MEDIA AND VEGETATION PROPERTIES

With the aim to validate the correctness of the physics within the developed green roof model, it was essential to determine the growing media, drainage mat and vegetation characteristics in the field experiment that will be used for validation purpose. In the case of drainage mat, SOPRADRAIN ECO-VENT is used. All the necessary data is available from the manufacture website. The properties of the growing media are experimentally measured in the lab.

6.1 Growing media characterization

6.1.1 Density and porosity

Density and Porosity have been measured according to ASTM D7263 – 09 (Standard Test Methods for Laboratory Determination of Density (Unit Weight) of Soil Specimens). There only pieces of equipment that are required for the test are a balance and a drying oven. Empty cylinders were prepared marked and measured. Three samples of the growing media being used in the field experiment were prepared and dried. Figure 15 shows specimens in the oven at the beginning of the test. During the drying, specimen mass had been checked every two hours after 16 hours of oven-drying until the daily mass change is within 0.1%.



Figure 15. Soil specimens in the oven.

Since the soil specimens were dried and contained no moisture in it, containers with growing media have been weighted. The whole process is shown in Figure 16 and Table 3. Water was added to the cylinder with dry growing media mass until the water began to pour out. The measurement showed that density of the soil specimen is $740 \text{ kg/m}^3 \pm 10 \text{ kg/m}^3$ and porosity is 0.56 ± 0.12 .

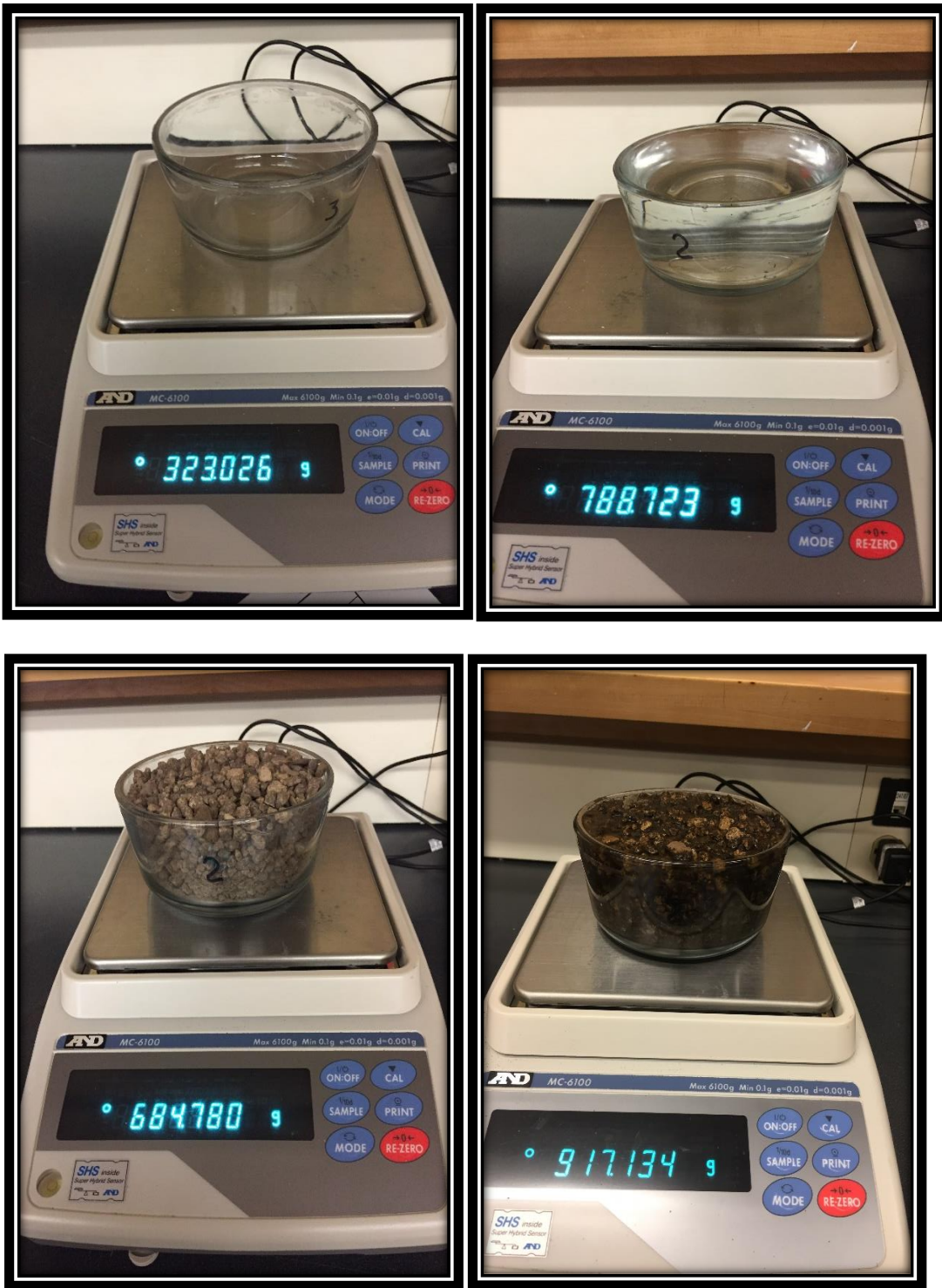


Figure 16. Density and Porosity measurement. Top left – empty cylinder; top right – cylinder filled with water; bottom left – dry growing media specimen; bottom right – wet growing media specimen.

Table 3. Soil density and porosity test ASTM D7263 - Volumetric method - B

Name <u>Soil test 1</u>		Date <u>15-May-17</u>	Job # <u>Thesis</u>	
Location <u>Lab</u>				
Description				
Sample #		1	2	3
Mass in grams	Tare plus not-dried soil	669.3	684.77	NA
	Tare	362.42	362.42	96.38
	Not-dried soil	306.88	322.35	NA
	Tare plus dry soil	667.3	682.6	2680.86
	Dry Soil	304.88	320.18	2584.48
Tare				
Water + tare in grams		778.48	788.72	3560.36
Water in grams		416.06	426.3	3463.98
Volume in ml		416.06	426.3	3463.98
Volume in cm3		416.06	426.3	3463.98
Density of not-dried soil in g/cm3		0.738	0.756	NA
Density of dry soil in g/cm3		0.733	0.751	0.746
Additional water				
Total mass, in g		904.05	917.13	4628.63
Water mass, in g		236.75	234.53	1947.77
Water volume in cm3		236.75	234.53	1947.77
Cylinder volume in cm3		416.06	426.3	3463.98

Porosity	0.5690	0.5502	0.5623
-----------------	---------------	---------------	---------------

6.1.2 Sorption Isotherm and Moisture Storage capacity

As it was mentioned before, the main variable for the moisture governing equation is relative humidity; therefore, a function connecting relative humidity and moisture content is needed. To determine the sorption property and storage capacity of the growing media as a function of relative humidity, firstly, three samples had been prepared, dried in an oven and then their dry weight is determined. Then they are placed in an environmental chamber, Figure 18, to determine their equilibrium moisture contents under various test conditions. The available environmental chambers can reach relative humidity up to 95%; thus, the equilibrium moisture contents of the specimens were determined at 0%, 50%; 80%; and 95% RH and temperature of 21°C. As part of the measurement procedure, the specimens' are kept in the chamber, and their moisture gains are recorded periodically until a mass change in successive five measurements is less than 0.1%. The results of sorption measurements are plotted in Figure 17.

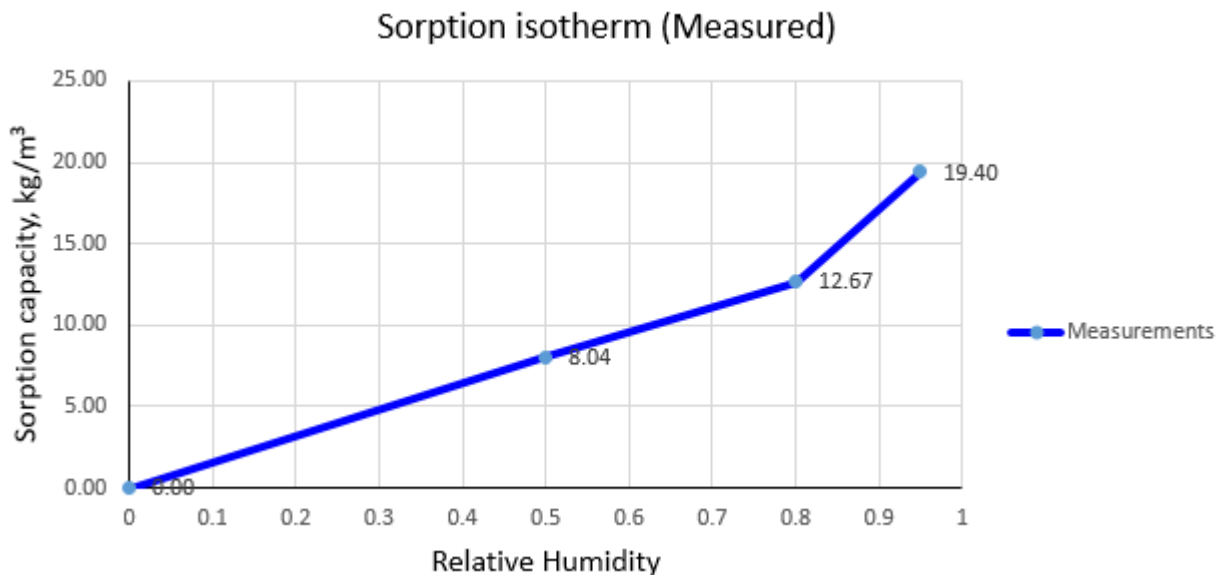


Figure 17. Measure sorption isotherm.

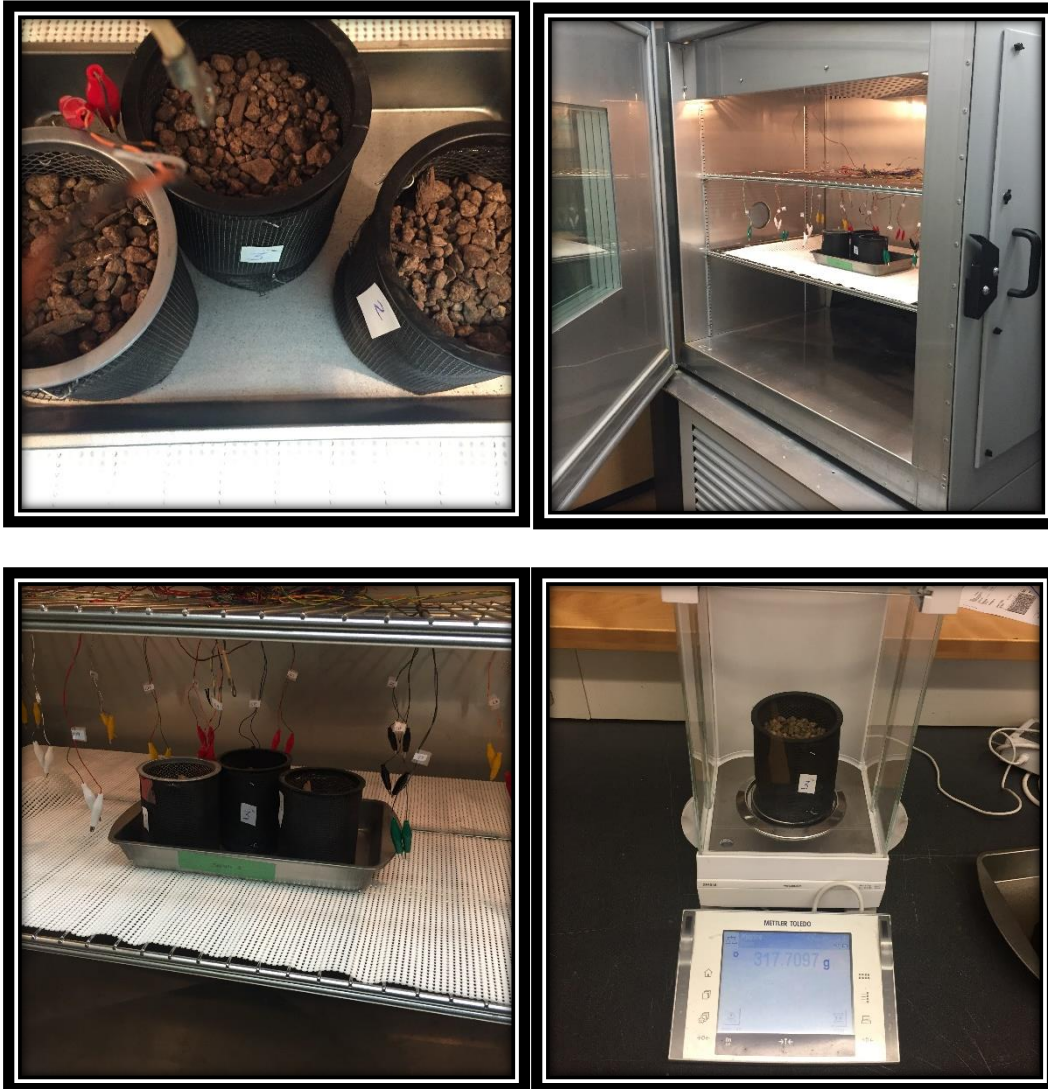


Figure 18. Sorption isotherm test. Top left – three growing media specimen; top right environmental chamber; bottom left – growing media specimen in the chamber; bottom right – specimen weight measurement.

6.1.3 Hydraulic properties

One of the important growing media property that is essential for green roof modelling is soil saturated hydraulic conductivity, which is the resistance to water flow. In this thesis, Dualhead

Infiltrometer is used to characterize the soil saturated hydraulic conductivity. Figure 19 shows a field test using the infiltrometer. As it follows from the device name, the hydraulic diffusivity of the soil obtained from the test is only for the saturated stage. The measured saturated hydraulic conductivity of the growing media is 0.036 cm/s.



Figure 19. Liquid permeability test.

6.1.4 Conductivity and heat capacity

Conductivity and specific heat capacity measurement were conducted according to ASTM D5334 – 14 Standard. The primary two tools to be used in the test are a laboratory balance and a thermal properties analyzer. The device called “KD2-Pro” was used. According to the manufacturer manual, KD2 – Pro is “a device that creates a linear heat source and incorporates a thermocouple or thermistor to measure the variation of temperature at a point along the line.” Figure 20 illustrates the

measurement process. The process involves six thermal conductivity measurements at points from thoroughly dried to fully saturated growing media stage. At each stage, some amount of water was added to reach the certain saturation level. The results are shown in Table 4.

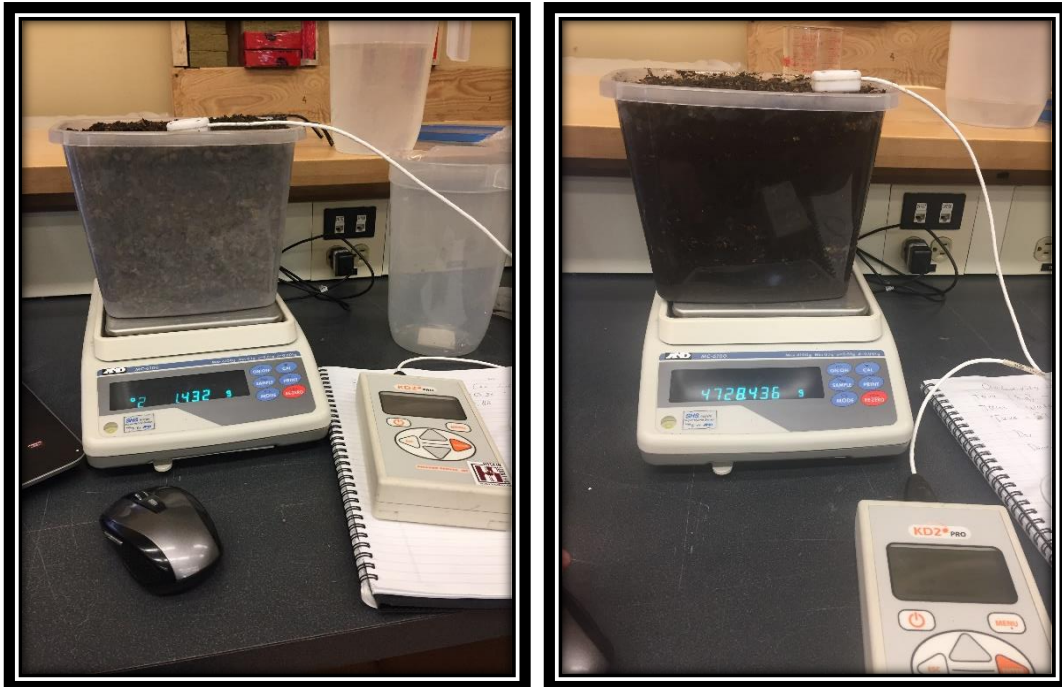


Figure 20. Thermal conductivity measurement. Left – dry growing media specimen; right – wet growing media specimen.

Table 4. Thermal conductivity measurement.

Saturation level	Weight			Conductivity (W/mK)			Heat Capacity (mJ/m ³ K)
	Water added	Water + jug	Total	Left	Middle	Right	
0	0	0	2680.86	0.076	0.084	0.081	0.869
10	362.24	458.98	3043.10	0.199	0.149	0.16	1.14
20	724.49	458.98	3405.35	0.23	0.271	0.327	1.223
30	1086.73	458.98	3767.59	0.527	0.521	0.398	1.278
45	1448.98	458.98	4129.84	0.79	0.738	0.776	NA
55 Sat	1811.22	458.98	4492.08	0.833	0.754	0.83	NA

It is clear from the table that thermal conductivity raises with higher moisture content level, and at the fully saturated stage it is ten times higher than fully dried soil. Figure 21 illustrates the rise of thermal parameters with moisture level. Unfortunately, the device is designed to measure heat capacity of soils, sands etc. below saturation level and measurement of highly saturated growing media was out of range of the device. In the model effective heat capacity of the growing media above 30% moisture content is calculated using the growing media porosity (\emptyset), the heat capacities of the dry soil ($c_{p,soil}$), water ($c_{p,l}$) and air ($c_{p,a}$), and their volume proportion in the growing media $(\frac{MC}{MC_{max}})$ (Eq. 45).

$$c_{p,eff} = c_{p,soil} + (1 - \emptyset) \left[\frac{MC}{MC_{max}} c_{p,l} + \left(1 - \frac{MC}{MC_{max}} \right) c_{p,a} \right] \quad [45]$$

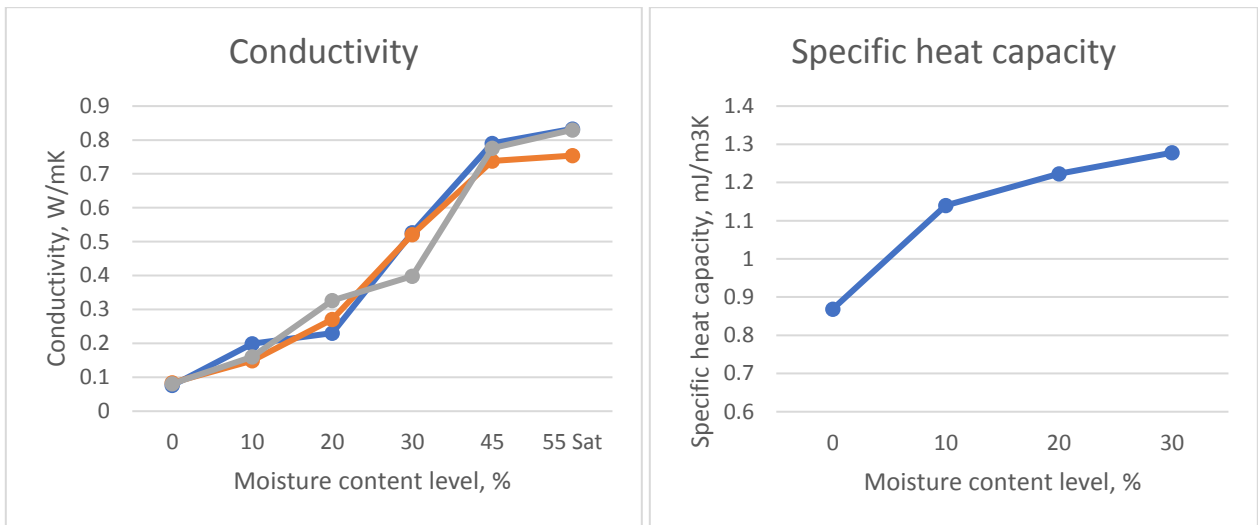


Figure 21. Conductivity and heat capacity graphs based on the test data.

6.1.5 Growing media hydrothermal property summary

Although the growing media sample from the field validation experiment is analyzed through the lab test, some of the required parameters are still unknown or measured in a limited framework. Therefore, the most similar growing media substrate is chosen from the WUFI database based on known properties (porosity, density, conductivity, heat capacity, measured moisture content points, saturated hydraulic conductivity).

First, the sorption isotherm is adopted from the chosen WUFI growing media isotherm and plotted against WUFI isotherm in Figures 22-23. The graph is divided into three parts to show unsaturated and near-saturated zones clearly.

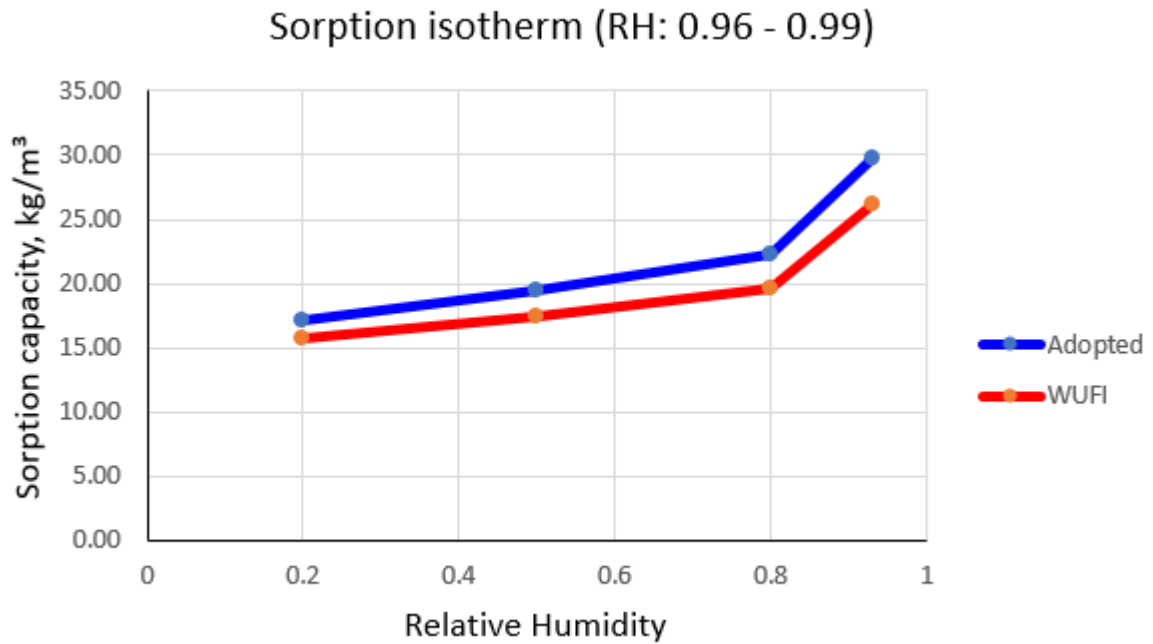
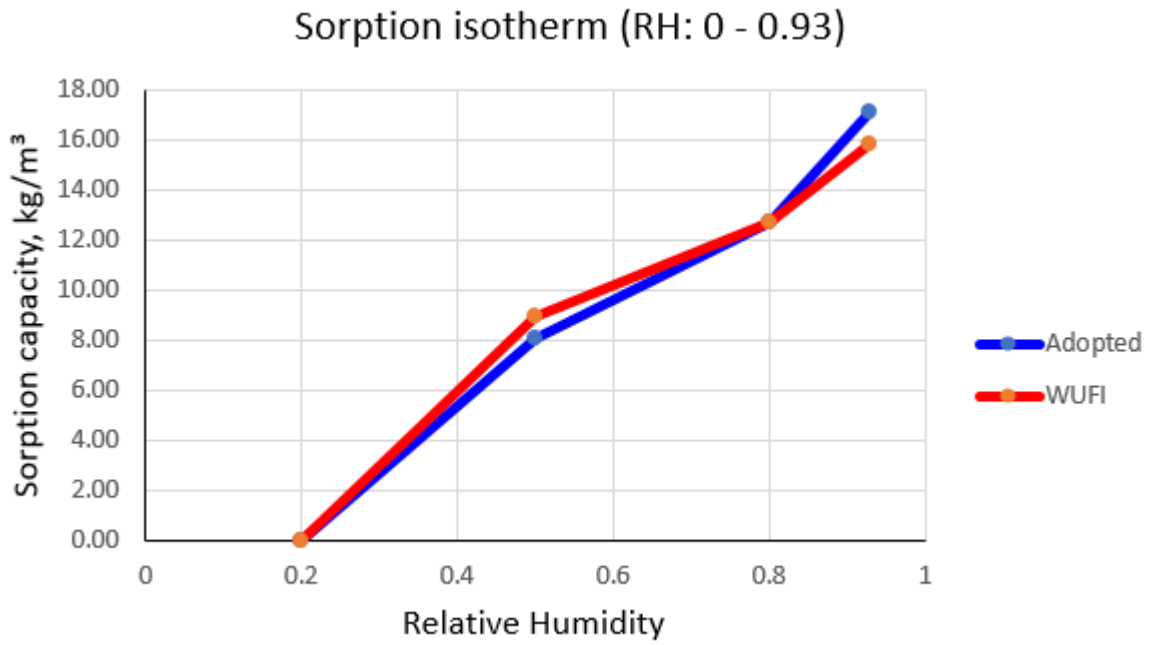


Figure 22. Sorption isotherm. Top – region 0-0.93; bottom – region 0.96-0.99.

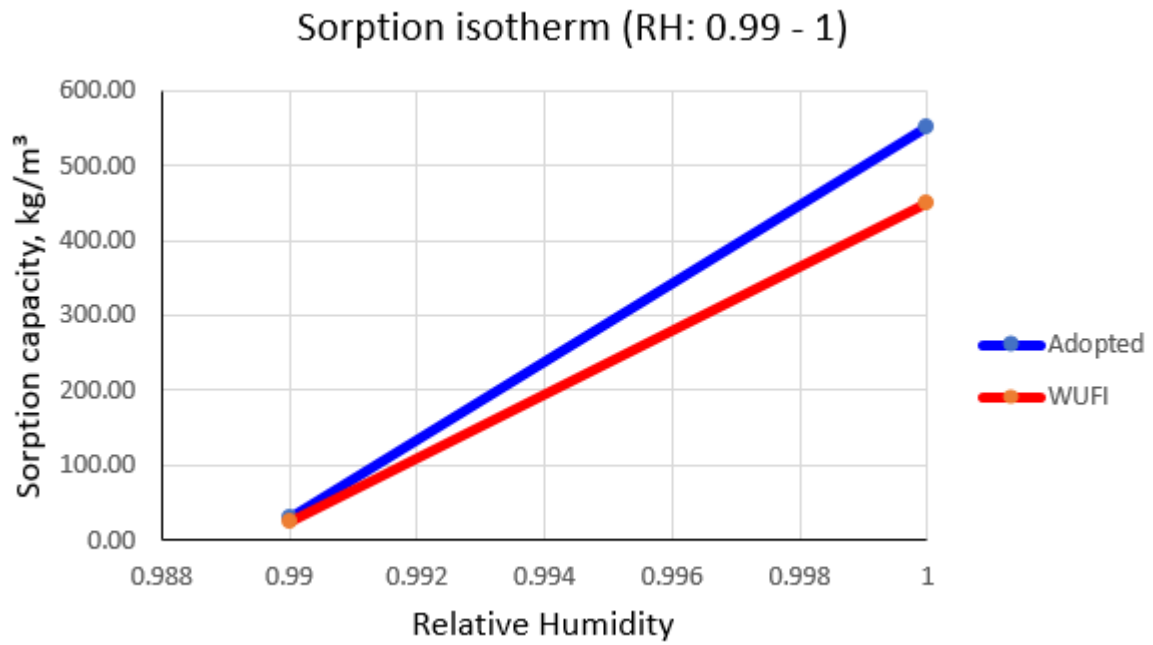


Figure 23. Sorption isotherm. Region – 0.99-1.

Second, similar to the sorption isotherm, the liquid permeability graph is taken from the WUFI database with regards to saturated liquid conductivity measured in the section 7.1.3. The graph showing liquid conductivity dependence is plotted in Figure 24.

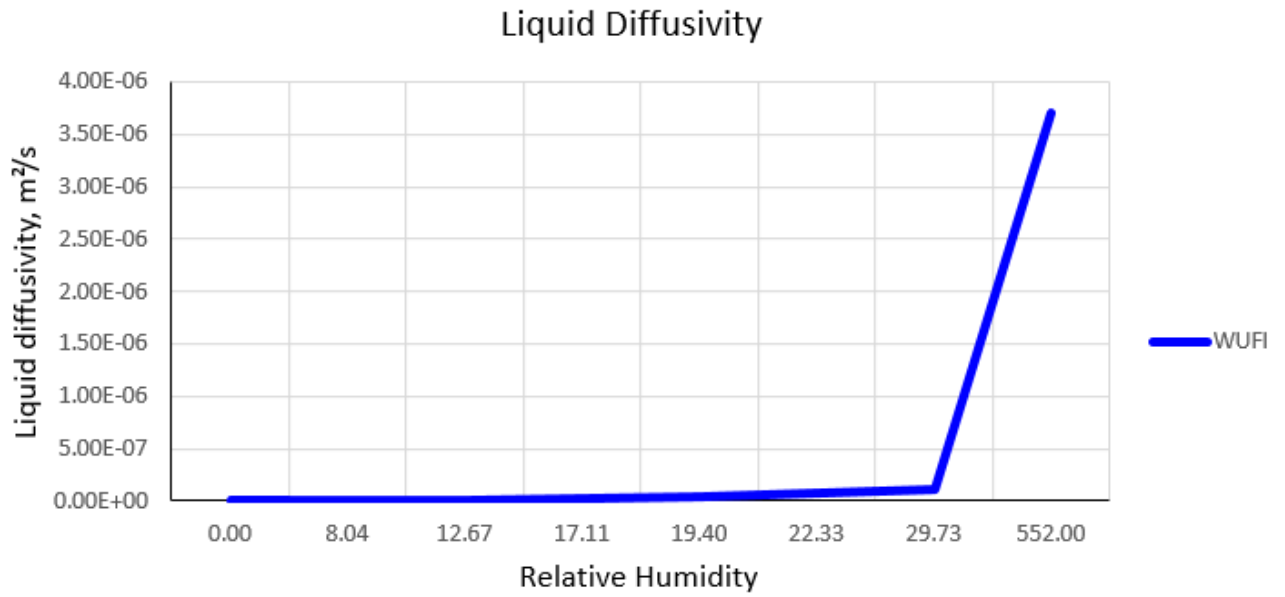


Figure 24. Liquid diffusivity curve.

Third, the growing media vapour permeability value is converted from the μ – value (3.3) given in the WUFI database.

$$\delta_v = \frac{129}{3.3} = 39.09 \text{ Perm} - \text{inch} = 5.70336E - 11 \frac{\text{kg}}{\text{msPa}}$$

6.2 Vegetation parameters visualization

A coverage ratio and a corresponding leaf area index are the critical parameters in the green roof modelling. During the validation process, the image visualization technique applied to get actual parameters of the tested green roof. The coverage ratio is the percentage of area covered by plants leaves and stems per unit area. Leaf area index that is the ratio of the plants one-sided green surface to the projected soil area. In this thesis, these parameters are quantified through visualization of the test green roofs images. This is achieved by taking pictures of the plants at different times and using custom made Matlab scripts, which are developed based on the definition of the two parameters. The Matlab code for the two values is provided in Appendix D.

6.2.1 Coverage ratio

The Coverage Ratio script separates green and close to green colours from the rest of other colours in an image; and then determines the ratio of the green area to the total area. Figure 25 shows the script implementation on a leaf.



Figure 25. The coverage ratio of the single leaf (left original side picture with the area covered by the leaf – 0.342 (manually measured); the right side – script output image with the area covered by the leaf – 0.3493 (Image visualization using Matlab).

Several pictures during the plants' development had been taken and analyzed by the script. Figure 26 illustrates original and computed images of one of the green roof test beds taken a few weeks after sedum species have been planted. In this case, the calculated plant coverage ratio is 0.5060.

Figure 26 shows coverage ratio of 0.83, 13 months after plantation, and Figure 27 shows green roof images in June 2017. During the experimental period, the green roof coverage ratio varies from 0.5 to 0.9.



Figure 26. The area covered by vegetation after several weeks of plants grow.

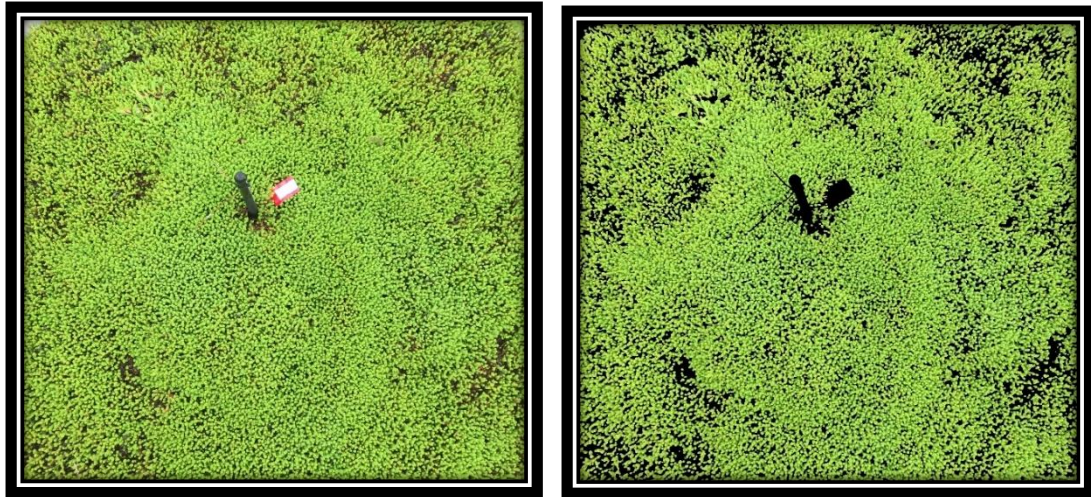


Figure 27. Green roof coverage ratio in June 2017. Left – original picture, right – non-green points are blacked.

The same script is applied to pictures taken in the summer season when green roof sample was covered by green plants with yellow blossoms. Figure 28 shows the original shot and separated yellow and green dots pictures. In this figure separated yellow zone is 0.519 and green is 0.453, and the final coverage ratio equals to 0.9722 that means almost full coverage of the roof.

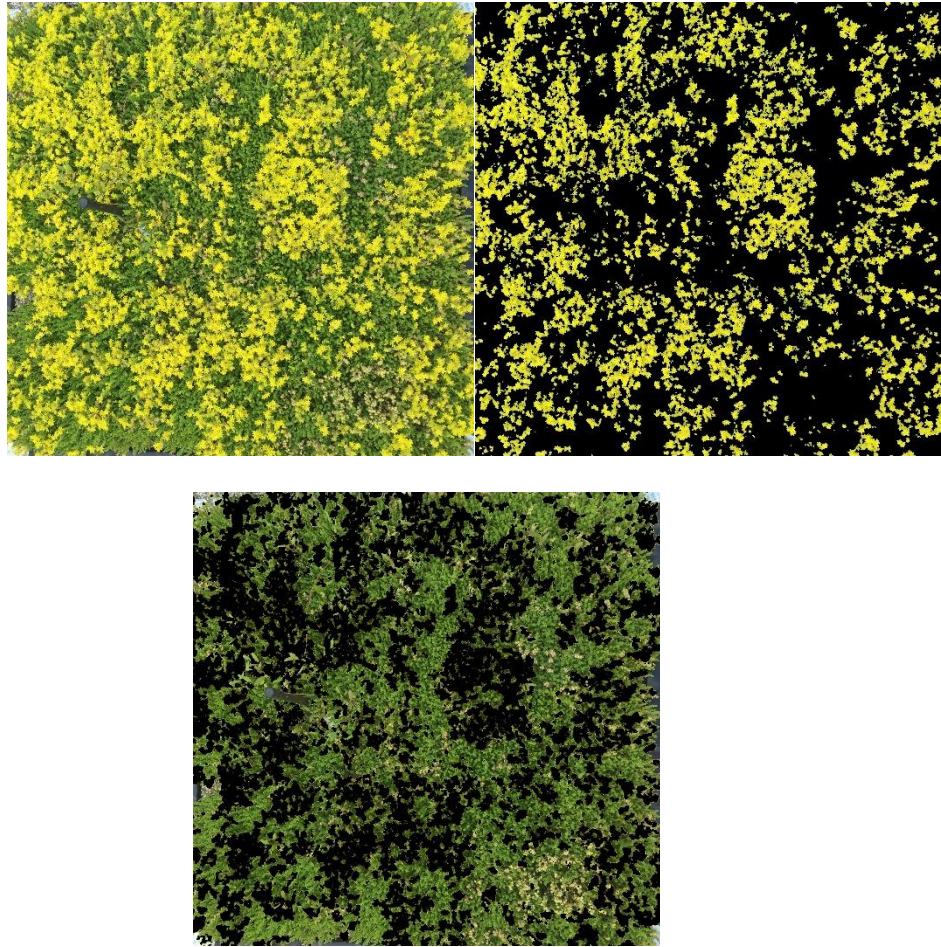
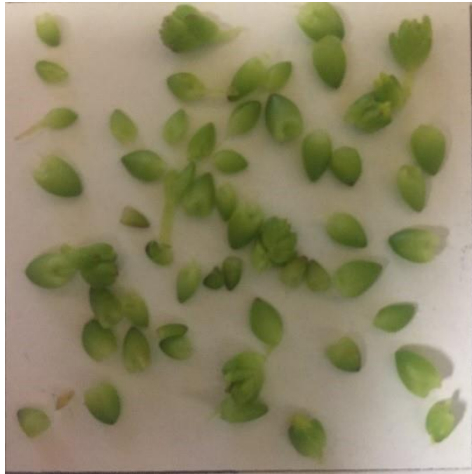


Figure 28. Green roof coverage ratio in July 2017. Top left – original picture; top right – non-yellow points are blacked, bottom – non-green locations are blacked.

6.2.2 Leaf area index

Additionally to the coverage ratio value, leaf area index is needed to be determined. Leaf Area Index (LAI) is defined as the one-sided green leaf area per unit ground surface area. In order to estimate LAI, a hundred of sedum sprouts were picked up from the test green roof. Manual counting showed that area of 12.7 by 12.7 cm contains 100 sprouts. Following the definition, several sprouts were cut, and leaves were separated from stems (Figure 29 shows four cut sprouts). Then, each sprout was placed on pieces of paper with known dimensions.

Sample 1.



Sample 2.



Sample 3.



Sample 4.



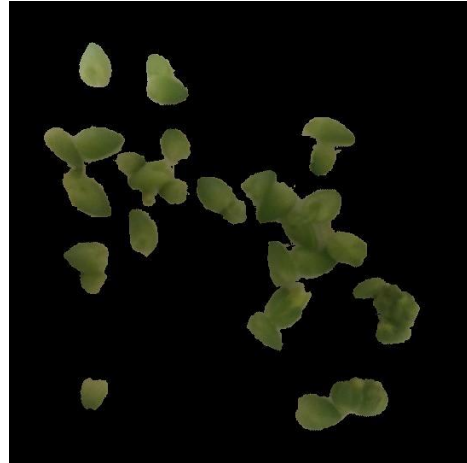
Figure 29. LAI estimation samples

Then, image visualization technique applied to get a proportion of green areas per known paper squares. Figure 30 illustrates images of Matlab script outputs.

Sample 1. Area = 0.2822



Sample 2. Area = 0.1988



Sample 3. Area = 0.3004



Sample 4. Area = 0.2855

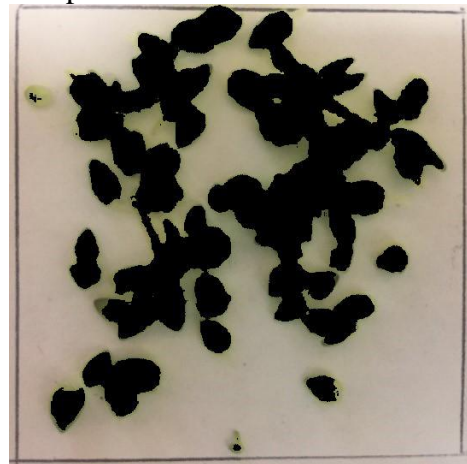


Figure 30. LAI image visualization using Matlab.

Based on the image analysis, the average green surface ratio is 0.2677. The actual leaf area index value for the tested green roof is determined using Equation. [47], which is derived from the LAI definition and calculated from the average green surface ratio (CR_g), the area of the paper square box (S_1) and the area (S_2) of the green roof with 100 (n) sprouts.

$$LAI = \frac{CR_g S_1 n}{S_2} \quad [47]$$

$$LAI = \frac{0.2677 * 2500 \text{ mm}^2 * 100}{16129 \text{ mm}^2} = 4.15$$

Therefore, Leaf Area Index equals 4.15. The numbers obtained from the vegetation tests are within the range of typical values for coverage ratio and leaf area index in the literature. However, approximate values of those parameters can be found in the previous studies; the exact values are essential within the validation process.

6.3 Input parameters from literature

Some of the listed values, such as root fraction numbers and roughness length are common for the low type of vegetation (Frankenstein and Koenig (2004), and there is no need to measure them. For the rest of variables, several field and laboratory tests have been conducted. Table 5 provides a summary of reasonable values for an extensive green roof simulation. Sources: Tabares-Velasco et al. (2011, 2012,2013); Berghage et al. (2012); Gagliano et al. (2014); Olivieri et al. (2013); Yaghoobian et al. (2015); Berardi et al. (2016); Allen et al. (1998); Gargari et al. (2016); Deardorff, J. W. (1978); Ouldboukhitine et al. (2013); WUFI (2017).

Table 5. Parameters are taken from literature

#	Name	Definition	Unit	Min value	Max value
1	zroot	Root depth	mm	5	30
2	a _{root}	Root fraction parameter a	m ⁻¹	5.558	10.739
3	b _{root}	Root fraction parameter b	m ⁻¹	1.627	2.614
4	rsmin	Minimal stomatal resistance	s/m	120	900
5	SAI	Stem Area Index	m ² /m ²	0.5	6
6	z _{0fm}	Roughness length	m	0.02	0.02
7	Sorption	Moisture content in soil	kg/m ³	400	600
8	Conductivity	Conductivity	W/m ² K	0.4	1.2
9	V _{per} Permeability	Vapour Permeability	kg/Pam	5.70E-11	
10	Diffusivity	Water diffusivity	m ² /s	3.6E-09	3.71E-06

7 VALIDATION

In parallel with this work, Hagos (2018) conducted an experimental field study on green roofs using the Whole Building Performance Research Laboratory (WBPR). The primary objective of this work was to investigate thermal performance and water retention capacity of an extensive green roof in marine climates, and the effects of the plants, moisture, drainage layers and growing media type in the green roof performance. The experimental field study has more than 15 months of data from eight 4' by 4' square test beds covering all the seasons. The WBPR comprises two identical 250 ft² air-conditioned buildings, located in Burnaby, BC, Canada with a latitude of 49.24°N and longitude of 123.00° W. During the experimental period, the weather was mild with warm summer and rainy winter, and with two weeks of snow in December. The indoor temperature is kept at 21 °C during the whole experiment period.

7.1 Field experiment

With regards to model validation, the data from sensors are essential. The sensors and the measured parameters used in the original field experimental are described in Table 6 and shown in Figure 31. The roof used for the validation is a flat wood constructed roof with 12 inches of fibreglass insulation (R 38) with the interior air barrier. There are also green roof protection layers, such as root barrier, filter fabric and SOPRADRAIN ECO-VENT drainage mat. The growing media layer is 4-inch height and planted by sedum plants.

For the validation exercise, the readings from the temperature and moisture content sensors in the growing media and the heat flux sensors at the bottom of the growing media and in the inside are used for comparison with HAMFit-GR simulation results.

Table 6. Parameters and sensors used in the benchmark experiment.

#	Parameter	Sensor
1	Temperature	Thermocouples
2	Relative Humidity	Relative Humidity Transducer
3	Moisture Content	Dragon Device GS1
4	Solar reflection	Pyranometer
5	Heat Flux	Heat Flux Transducer
6	Precipitation, wind speed	Weather station

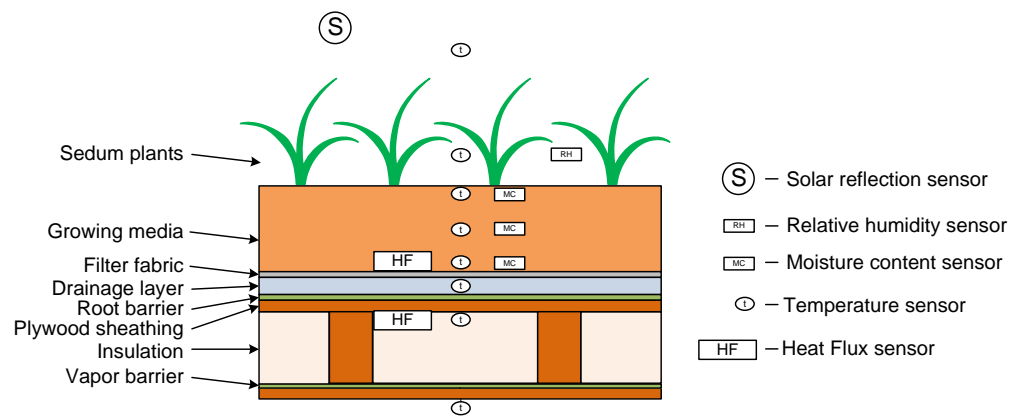


Figure 31. Sensors installed in the test green roof tray.

The data available from the field experiment is valuable, but not sufficient for the comprehensive validation. Therefore, new sensors have been installed as shown in Figure 32. The additional sensors include: 1) two long-wave radiation sensors – pyrgeometers were installed, one facing the sky, another facing the surface of the green roof, to measure longwave radiations from the sky to the roof and vice versa; 2) additional thermocouple and relative humidity sensors within plants and the soil surface; 3) additional thermocouples intended to measure foliage, ground surface and air within foliage temperatures are added.



Figure 32. Additional sensors. Top and bottom left – a view of installed sensors; top right – the pyrgometer before installation; bottom right – RH sensor installation.

The validation process consists of the comparison between modelled and measured values. In addition to the field experiment data, the green roof cases were modelled in WUFI software. Both HAMFit-GR model and WUFI model used weather data from the test field weather station and the same parameters for materials as well as heat and moisture surface transfer coefficients. Weather data consist of ambient air temperature, relative humidity, wind speed, rain amount and incoming

longwave and shortwave radiation. HAMFit-GR validation is done in steps with four experimental test cases, starting from relatively simple to complex validation cases. In the first test case, the model's capability was tested for a green roof system with dry growing media and no vegetation. In the second validation case, wet growing media is considered. In the third and fourth test cases, a full green roof system with vegetation is considered in a dry (case 3), and wet (case 4) seasons. The accuracy of the model is analyzed by Mean Bias Error (MBE) as the difference between measured and model value and Root Mean Square Error (RMSE) as the square root of squared errors.

7.2 HAMFit-GR Model Validation: A case with No Vegetation

7.2.1 Bare growing media in the dry period

A period of two weeks with no precipitation in June 2017 is selected to represent dry and warm weather conditions that a green roof is expected to be exposed in Vancouver. The first validation case is focused on soil properties and heat and moisture movement with no liquid water flow due to rain. The outdoor air temperature during the day varies between 20-32°C and in the night 11- 17°C. The roof is also exposed to solar radiation every day with a maximum solar gain of 900 W/m² at noon times. The test building indoor temperature and relative humidity are kept constant at 23°C, and 45, respectively, during the experimental period. Using the measured soil parameters, indoor and weather data, the temperature distribution across the thickness of the green roof with no plant (a bare growing media roof) is simulated, and the temperature profiles at the top, middle and bottom of the growing media are presented in Figures 35-37. Temperature lines in all three plots show the same trend. However, at the top position in the early afternoon, some temperature differences between measured and simulated results are observed. This discrepancy is caused by a shadow that measurement devices cast on sensors at noon times (circled on the graph). Figure 38 represents the correlation between the modelled and measured temperature values. Most of the data points lie on or near the 45° line, except

some noon top surface measurements. Mean bias error for temperatures was 2.06°C, and RMSE was 2.71°C.

Besides temperature, HAMFit-GR model soil moisture content prediction is compared with the experimental data. The soil moisture content at the top and bottom, expressed in relative humidity, are plotted against measured data in Figures 33 and 34, respectively. The results are in the good agreement in the dry summer period, MBE is 0.044 and RMSE is 0.047. As it can be seen from the graphs, the developed model can predict drying process and moisture movement within the growing media. The next case includes modelling the same roof, but a simulation period was chosen to have continuous precipitation events.

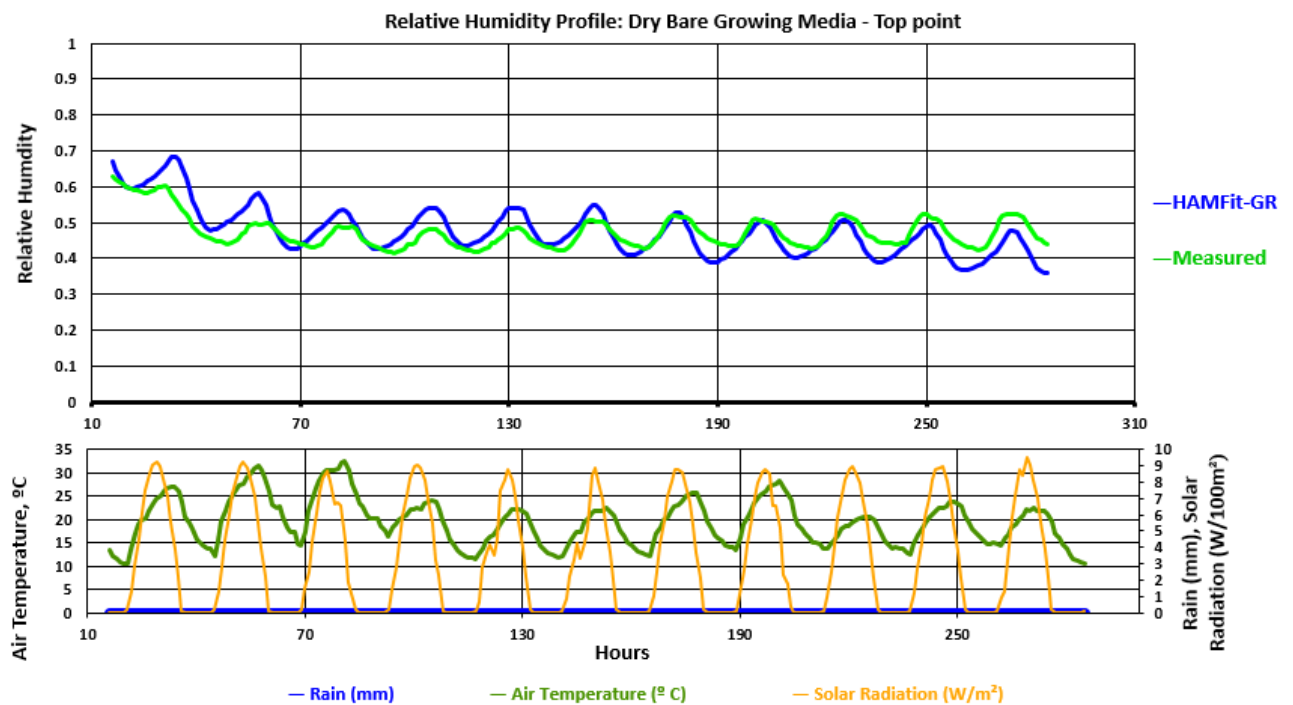


Figure 33. Case 1- Relative Humidity – 1/2” below the upper surface.

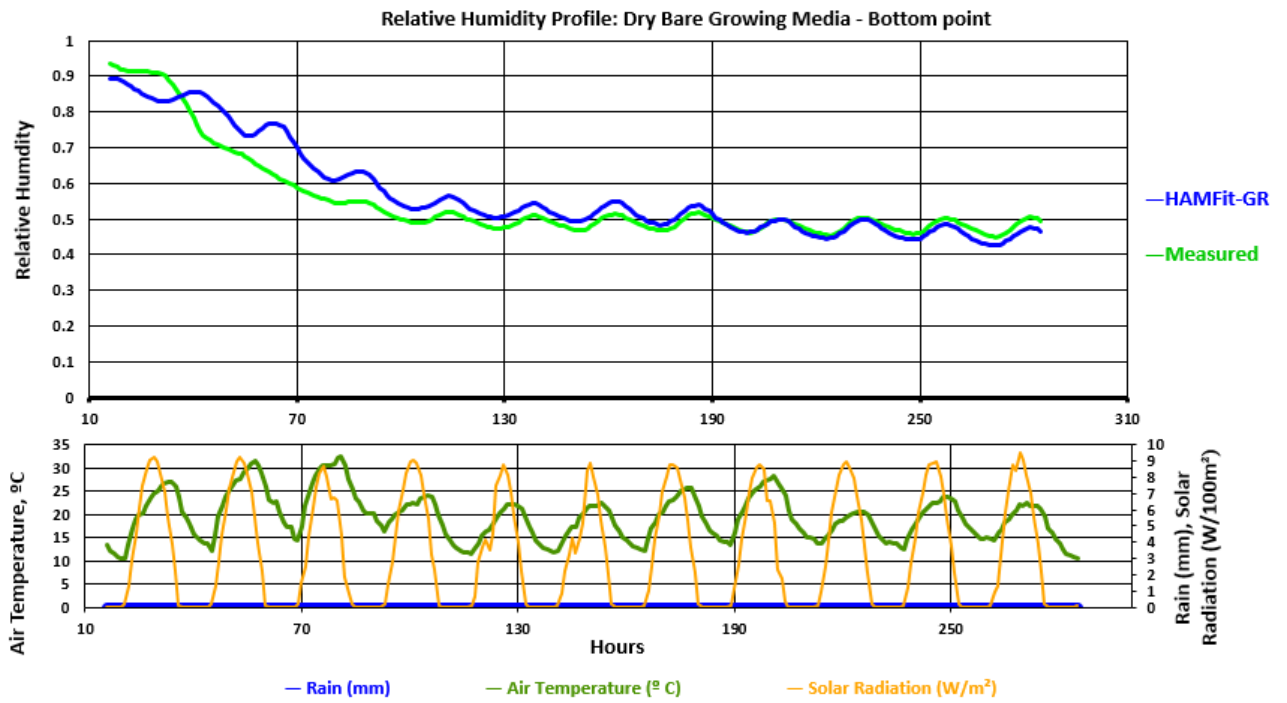


Figure 34. Case 1- Relative Humidity – ½” above the soil bottom.

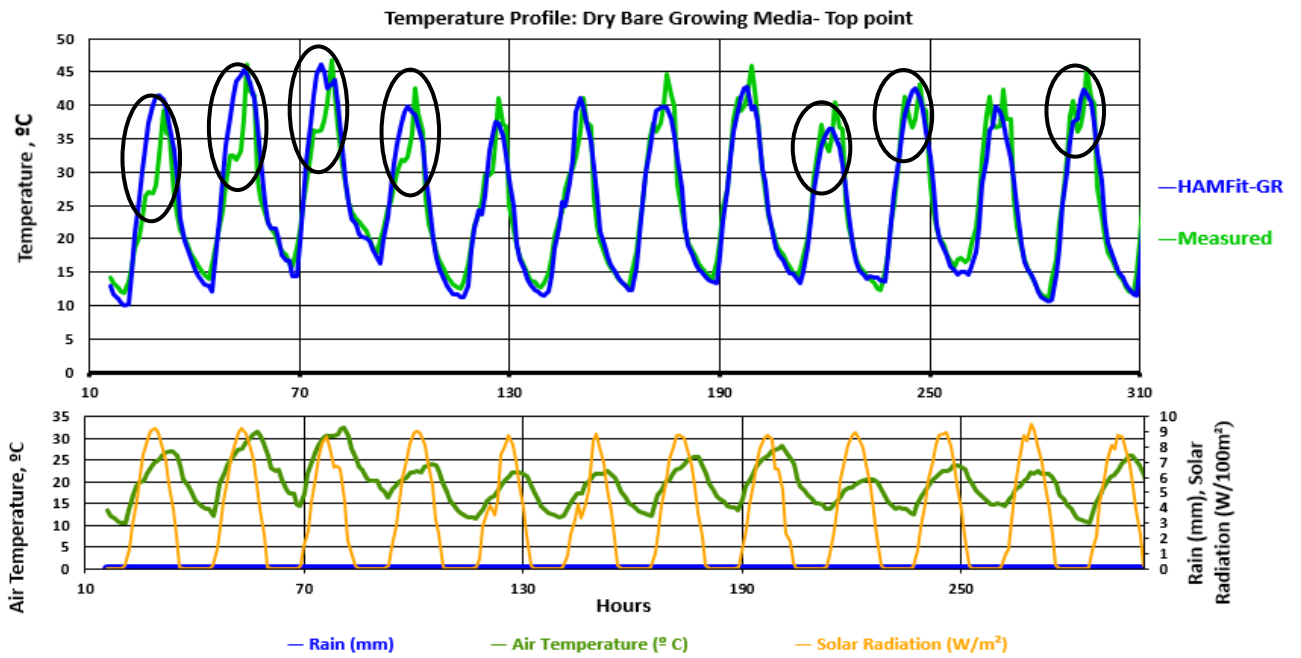


Figure 35. Case 1- Ground temperature – ½” below the upper surface.

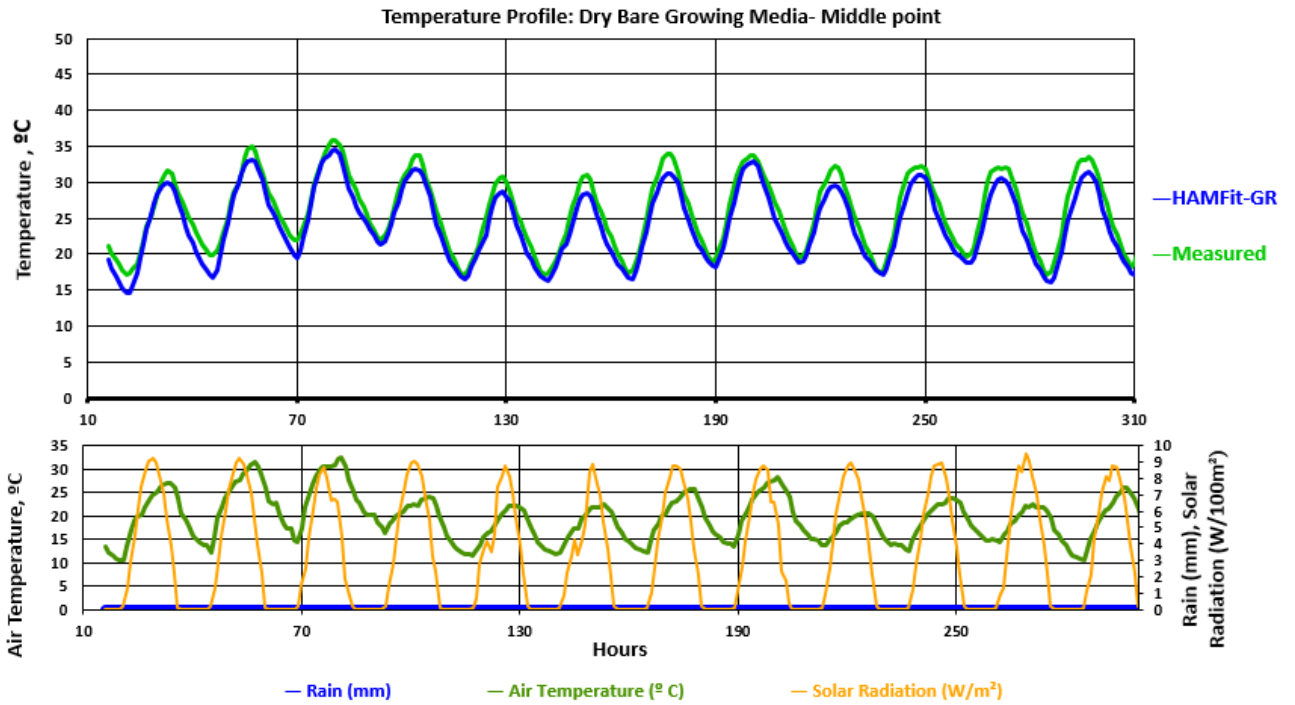


Figure 36. Case 1- Ground temperature in the middle of the soil layer.

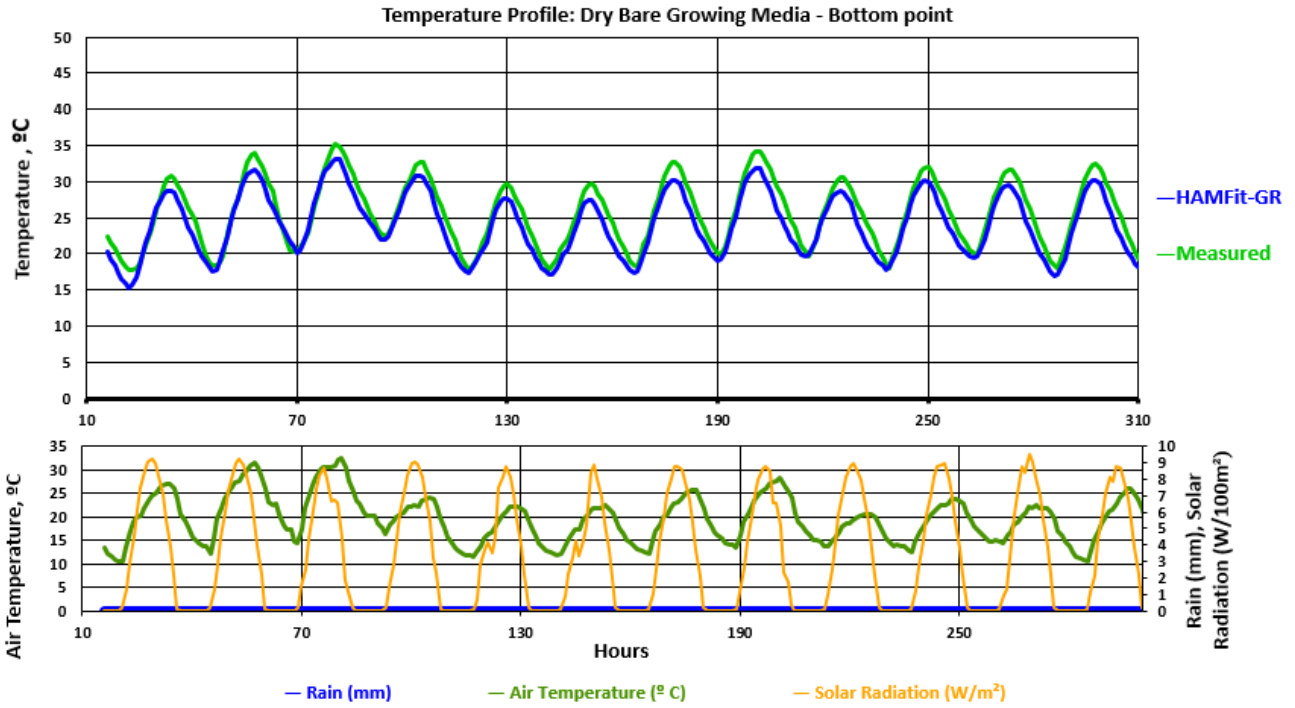


Figure 37. Case 1- Ground temperature – ½” above the soil bottom.

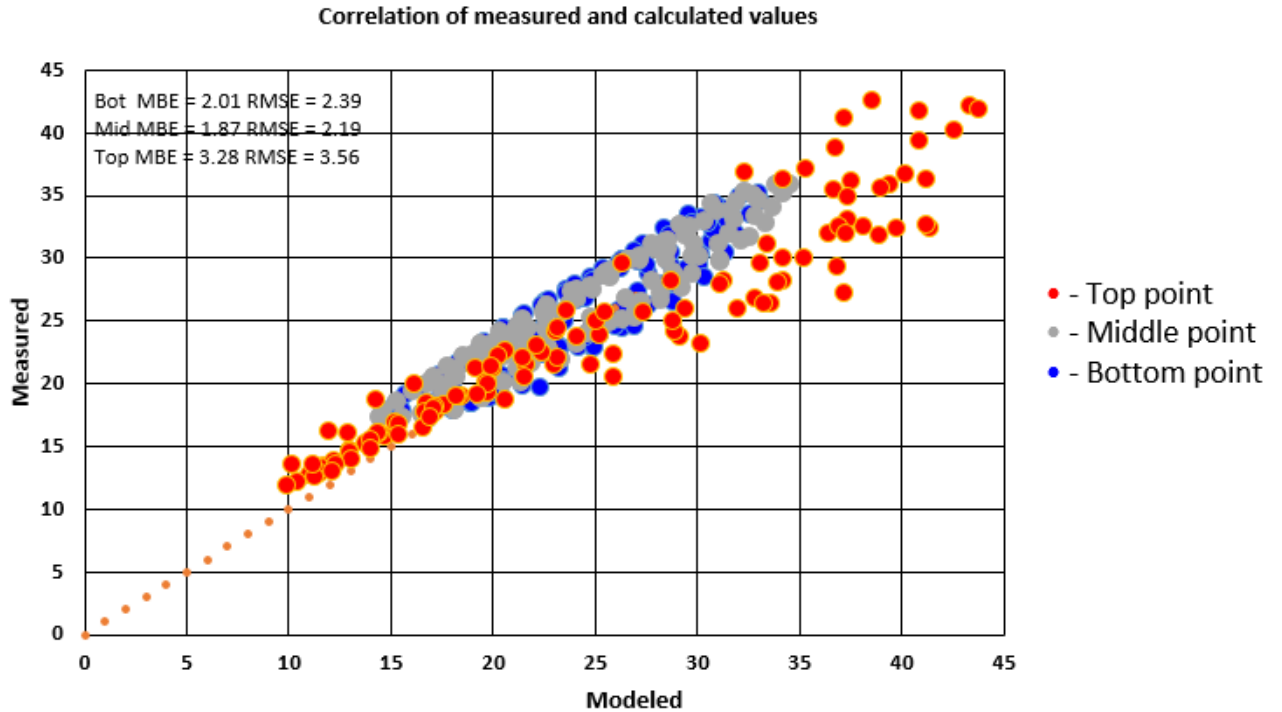


Figure 38. Case 1- Correlation of measured and calculated values

The test hut buildings are also equipped with heat flux sensor: the first sensor is located under the growing media and the second sensor is located above inside drywall. HAMFit-GR is able to export heat flux value at any point thought the simulated assembly; thus, the heat flux is a subject of the validation procedure. Figures 39 and 40 present heat flux profiles. Under the growing media without plants heat flux can reach 20-25 W/m² in the daytime with a sharp drop and rises in the measured values; however, HAMFit-GR can accurately predict the heat flux trends. Heat flux that is taken from the inside ceiling pointy stays in the range of ± 1 W/m² with good agreement between HAMFit-GR and experimental values.

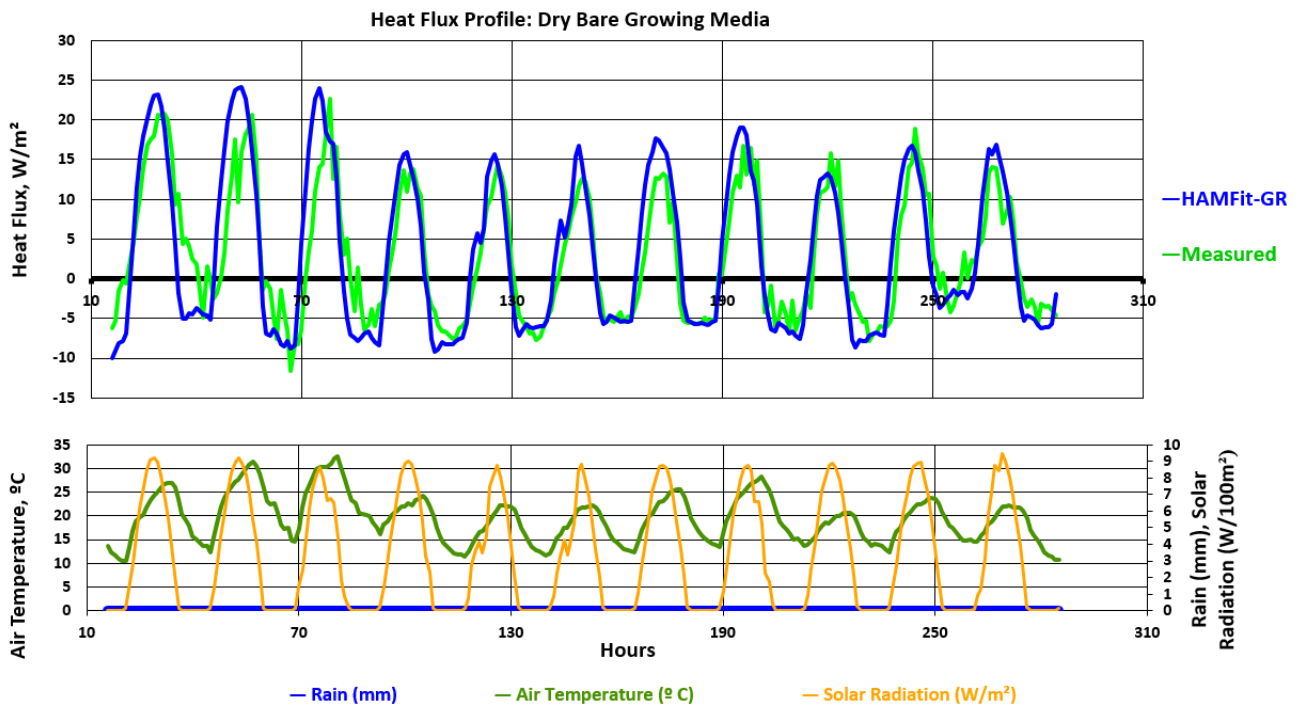


Figure 39. Case 1 - Heat Flux - growing media bottom.

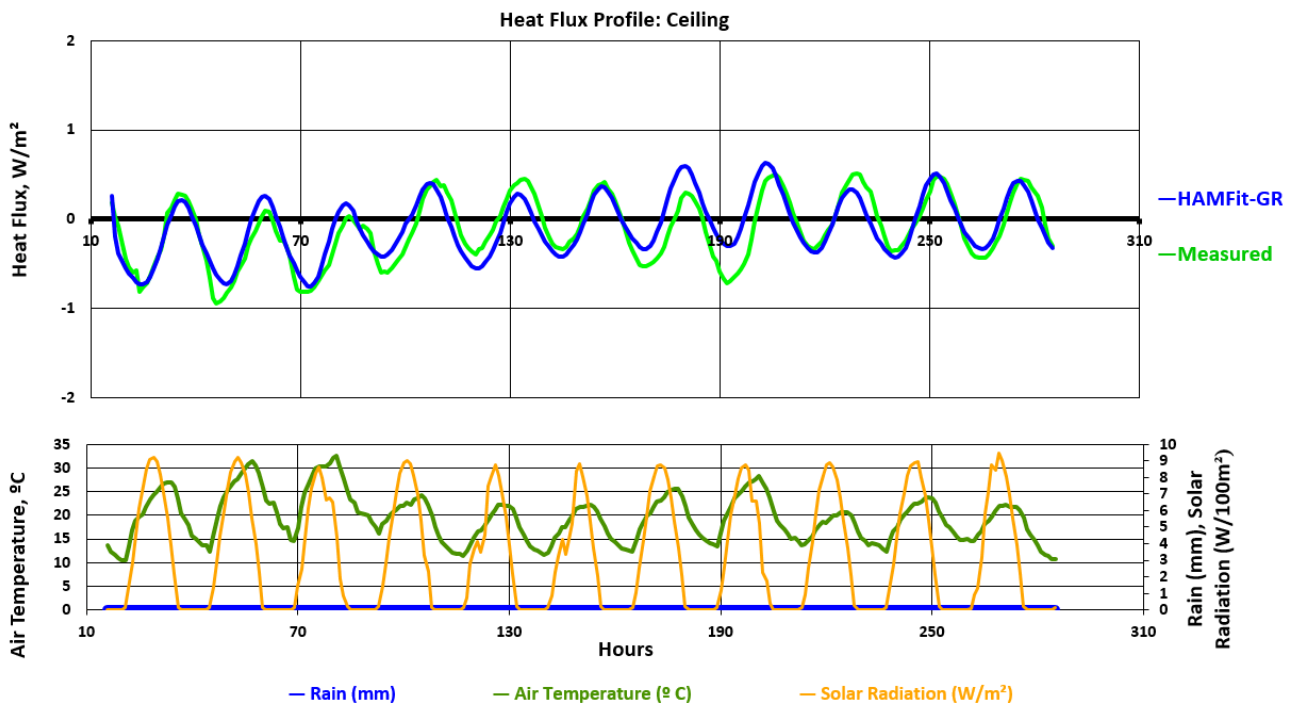


Figure 40. Case 1 - Heat Flux - Ceiling.

7.2.2 Bare soil in the rainy period

The second case was simulated using the same roof as previous, but the timeframe was selected to represent rainy period. Two weeks of May 2017 with rain events in the beginning and during the second week; temperature between 10 to 20°C; various solar activity and relatively moist air. As in the first case, temperatures and relative humidity were plotted against corresponding measured values. Figures from 41 to 46 illustrate this comparison. In that case, MBE is 1.07, and RMSE is 1.3° for soil temperatures and MBE is 0.0053, and RMSE is 0.0059 for RH values. The model was able to predict moisture change in the soil accurately: from saturation state at the beginning, the growing media goes through a drying process until the continuous rain happened and get saturated again. The heat flux profile are plotted in Figure 47 and 48. HAMFit-GR accurately predicts heat fluxes in both compared points: under the growing media and ceilings.

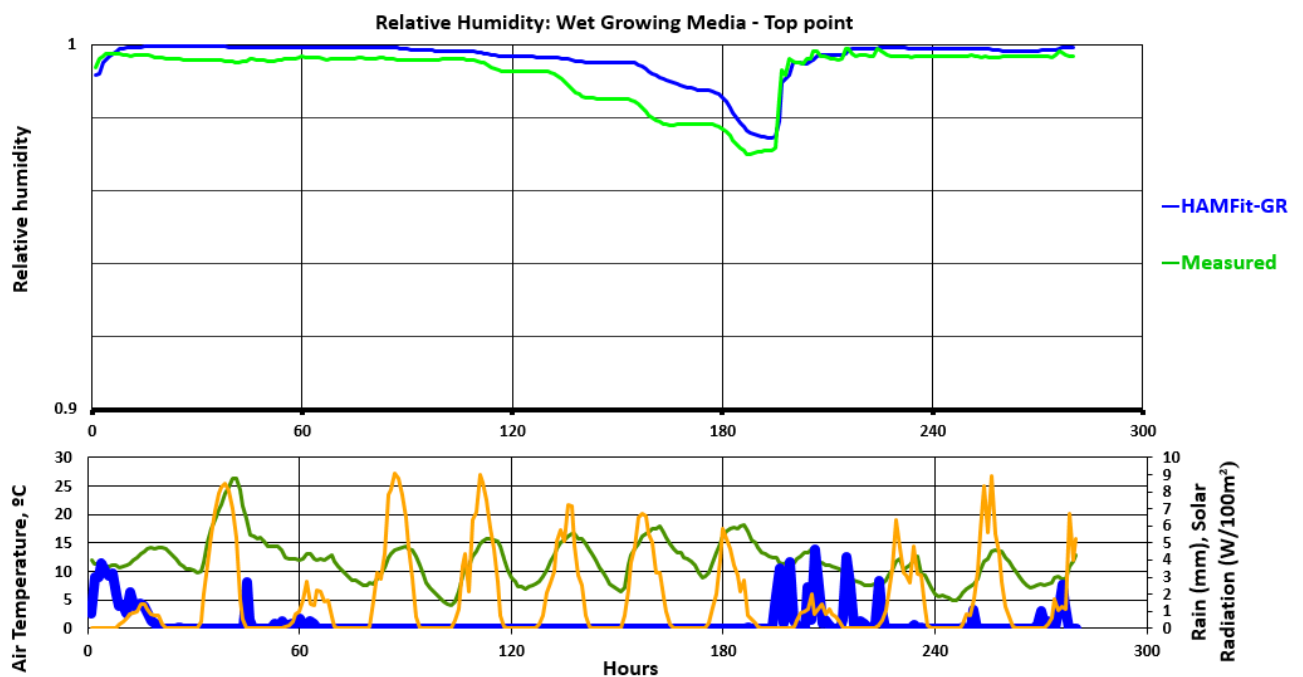


Figure 41. Case 2 - Relative Humidity – ½” below the upper surface.

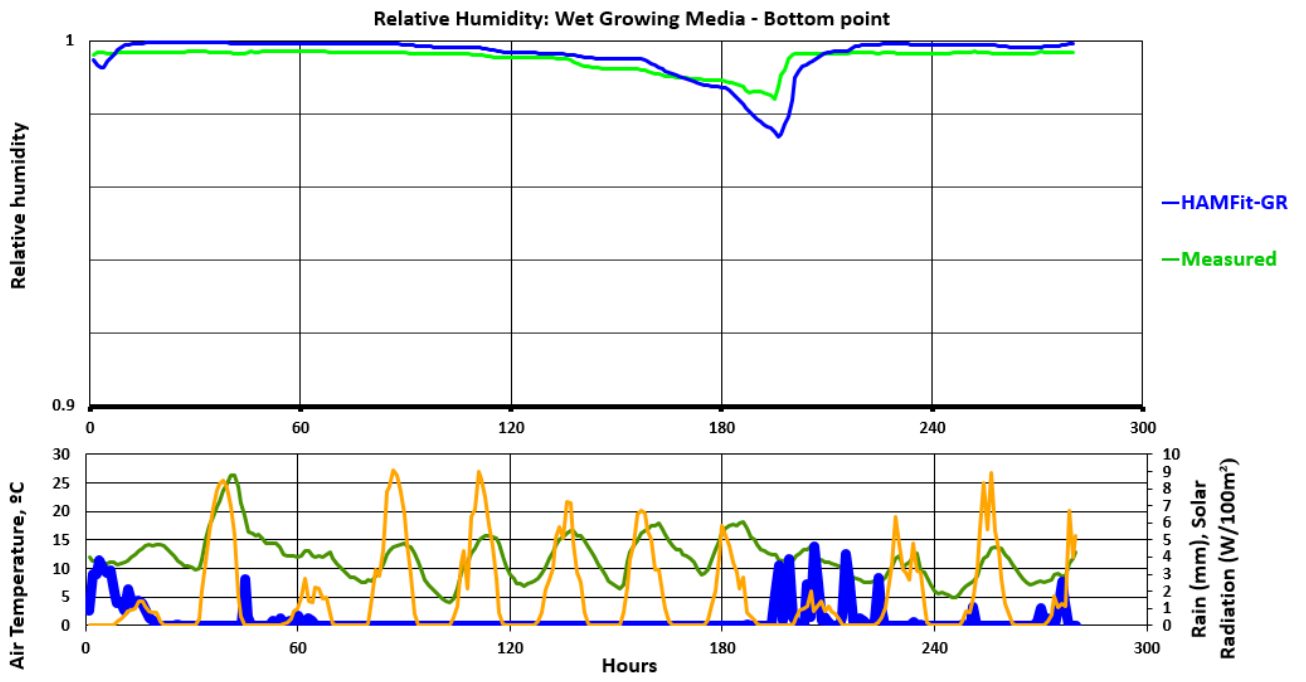


Figure 42. Case 2- Relative Humidity – ½” above the bottom surface.

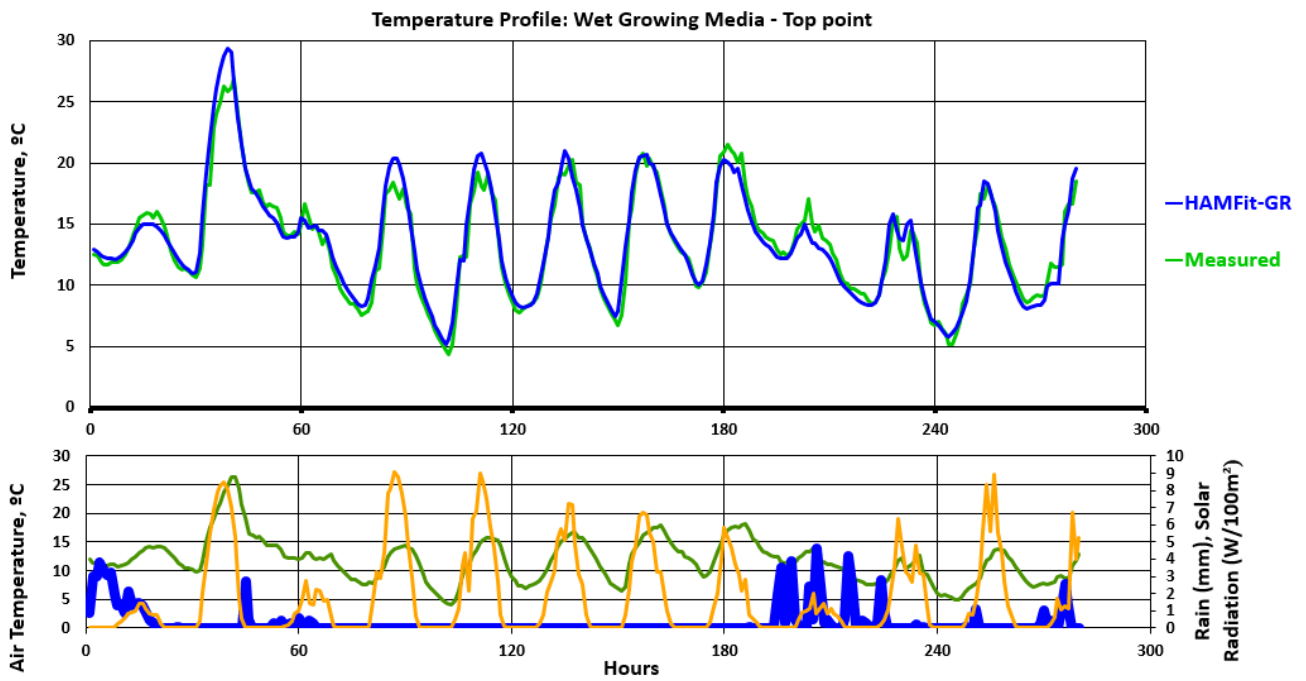


Figure 43. Case 2 – Temperature – ½” below the upper surface.

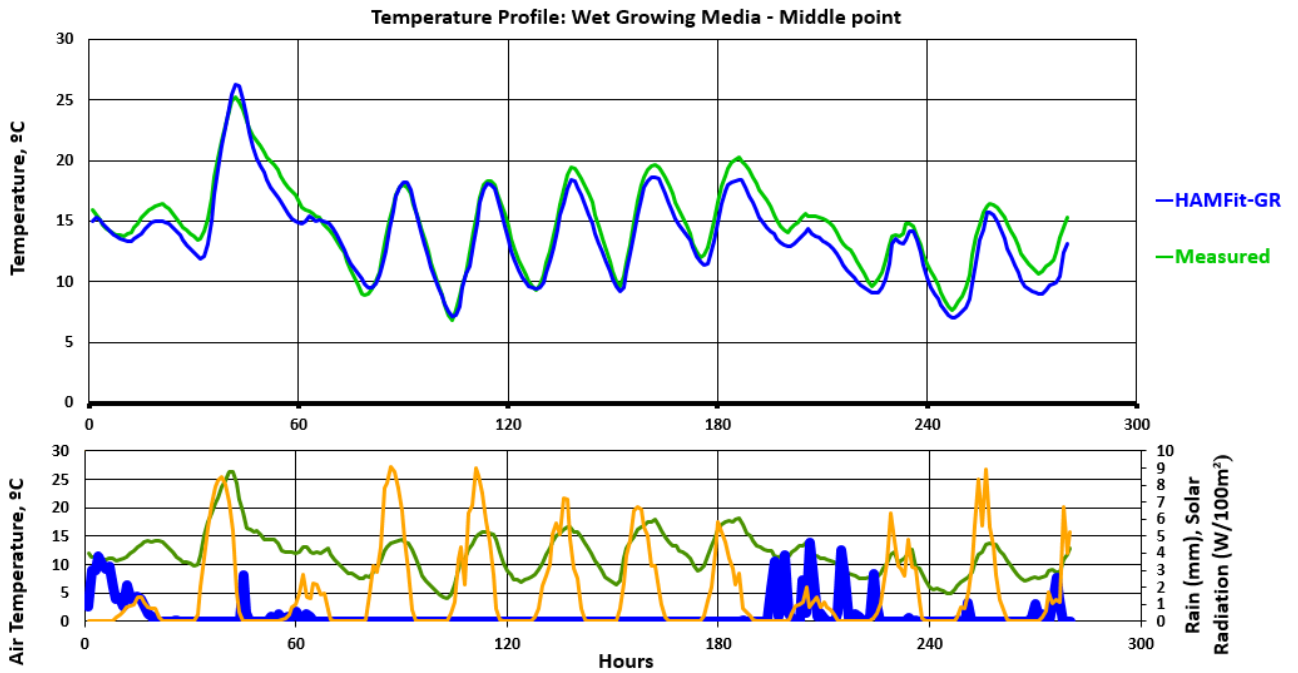


Figure 44. Case 2 -Temperature –in the middle of the growing media layer.

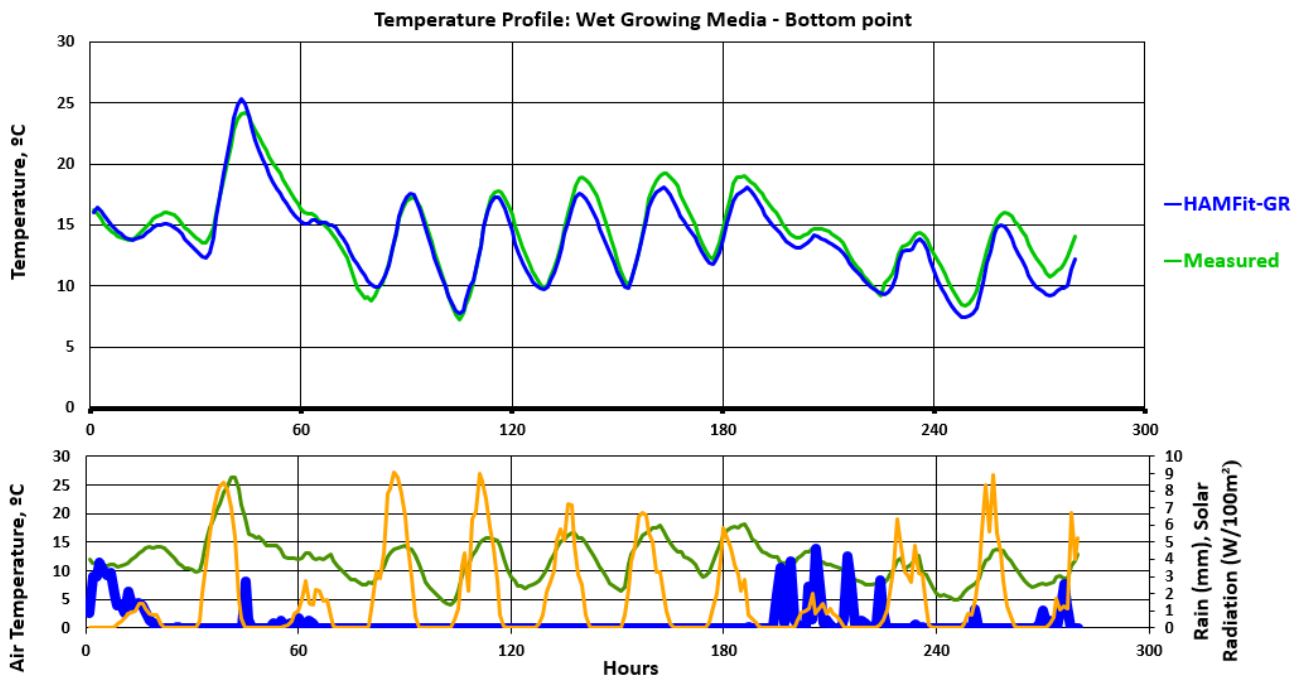


Figure 45. Case 2 - Temperature – 1/2" above the bottom surface.

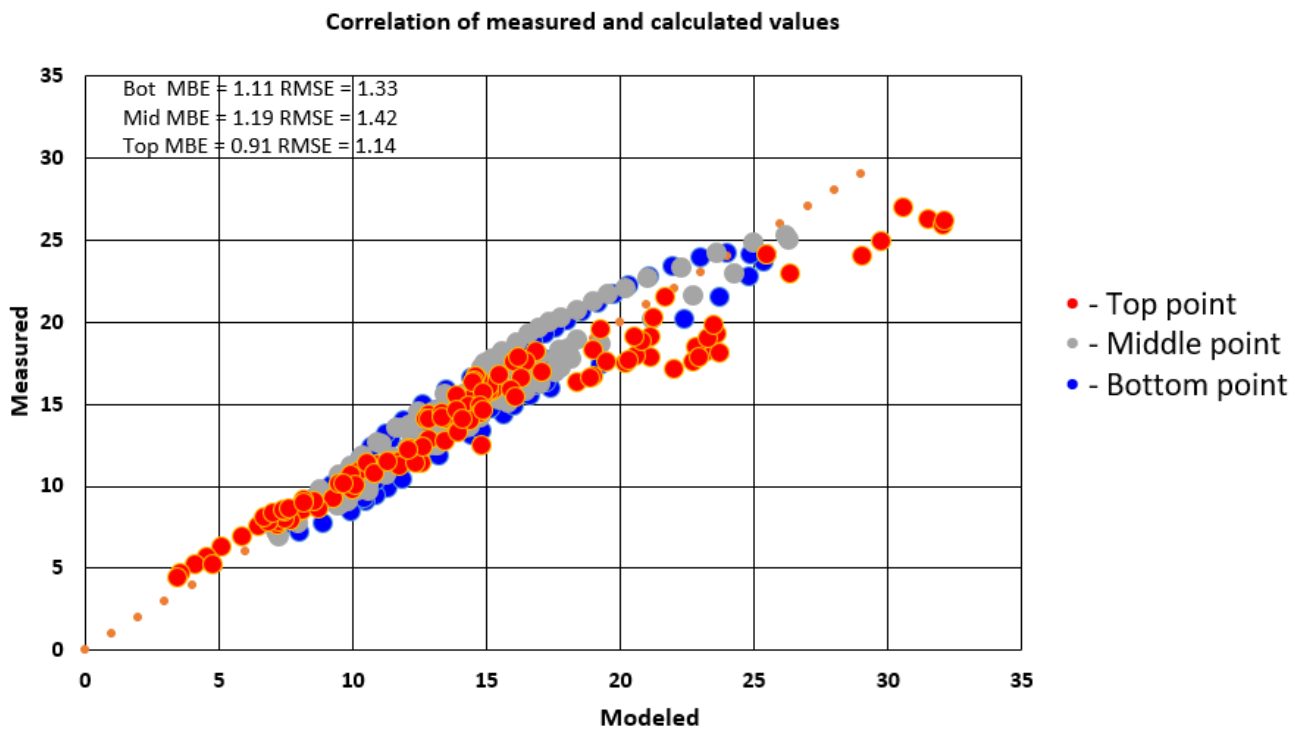


Figure 46. Case 2- Correlation of measured and calculated values.

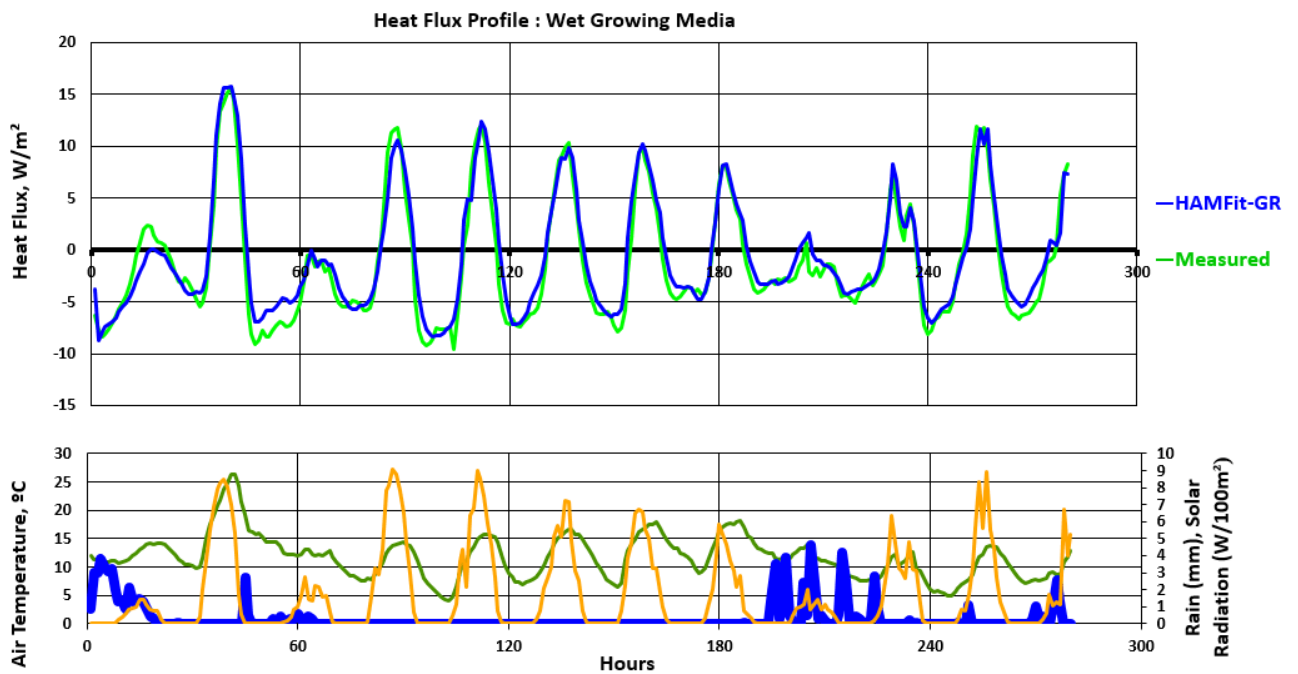


Figure 47. Case 2 - Heat Flux - growing media bottom.

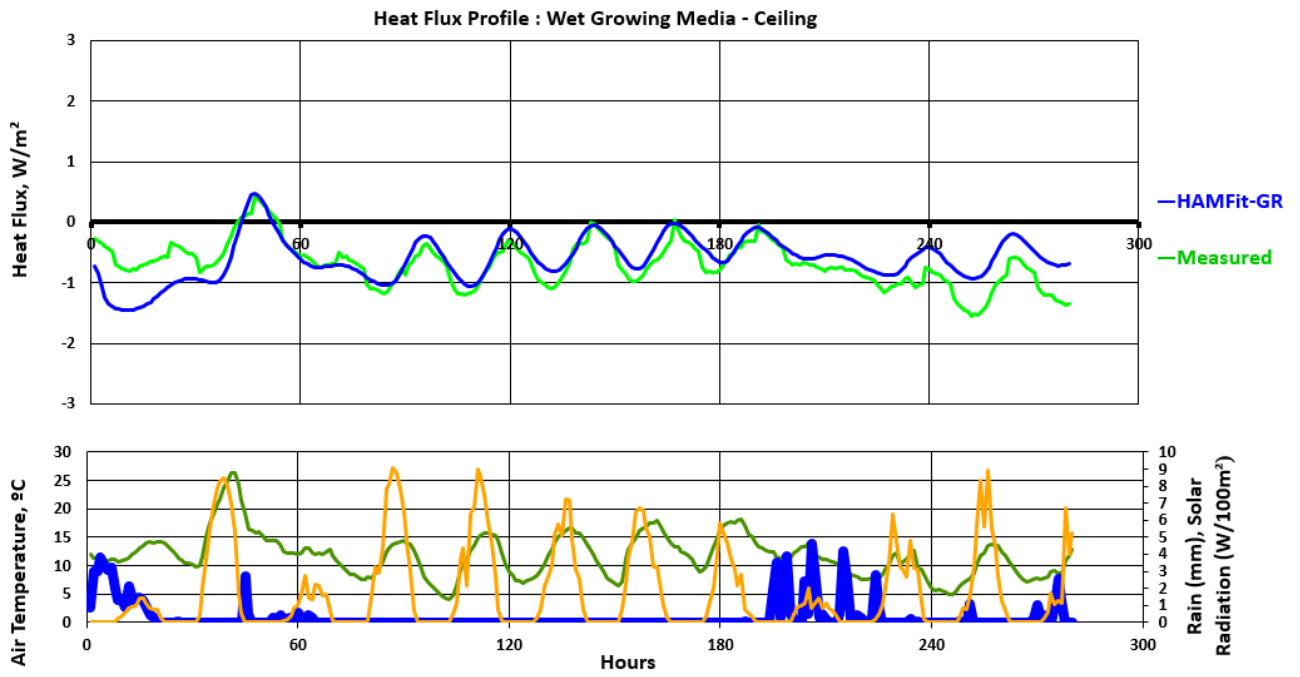


Figure 48. Case 2 - Heat Flux - Ceiling.

7.3 Vegetative Model Validation

7.3.1 Leaves temperature

As discussed in the previous section, thermocouples are installed to measure leaves and ground surface temperatures. In this validation case, measured ground temperatures were used as a known variable to separately validate the vegetation model by comparing calculated and experimental temperatures of leaves. The period from June 30 to July 15 is selected with daily active sun and temperature range of 10-30°C. Figures 49 and 50 demonstrate foliage temperature profile and correlation. In this case, the separated vegetative model has been validated with MBE equals to 1.83 and RMSE equals to 2.15

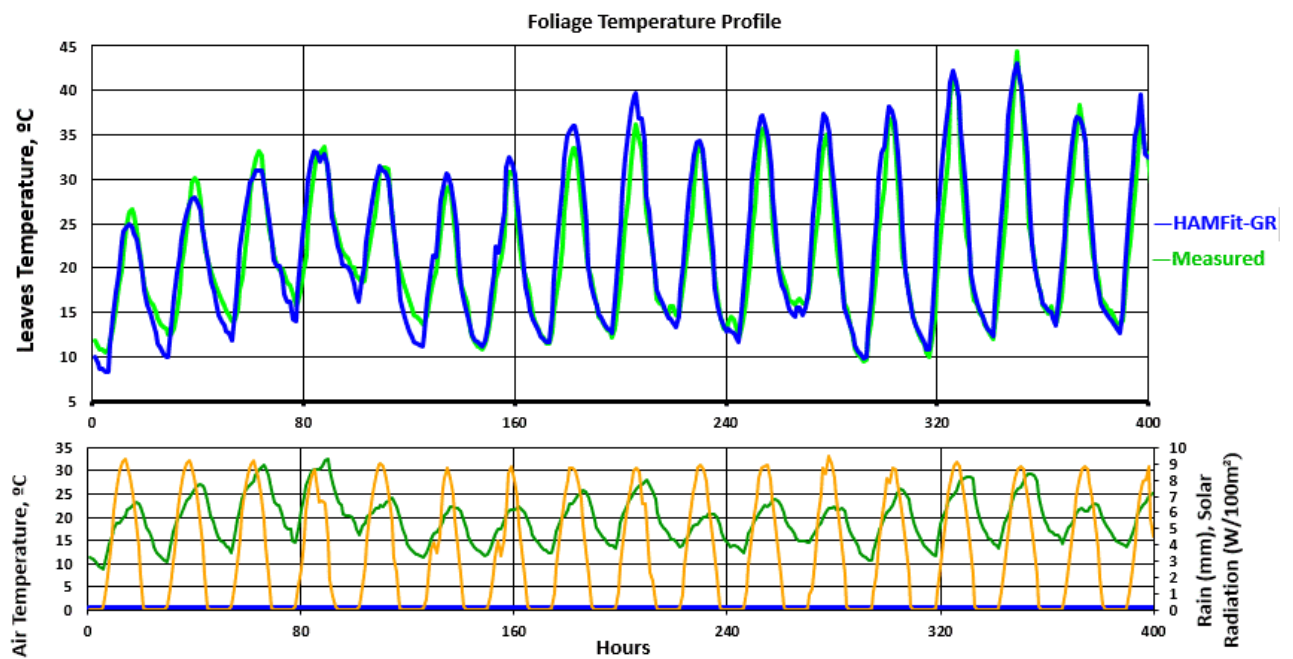


Figure 49. Measured and Modeled Temperatures.

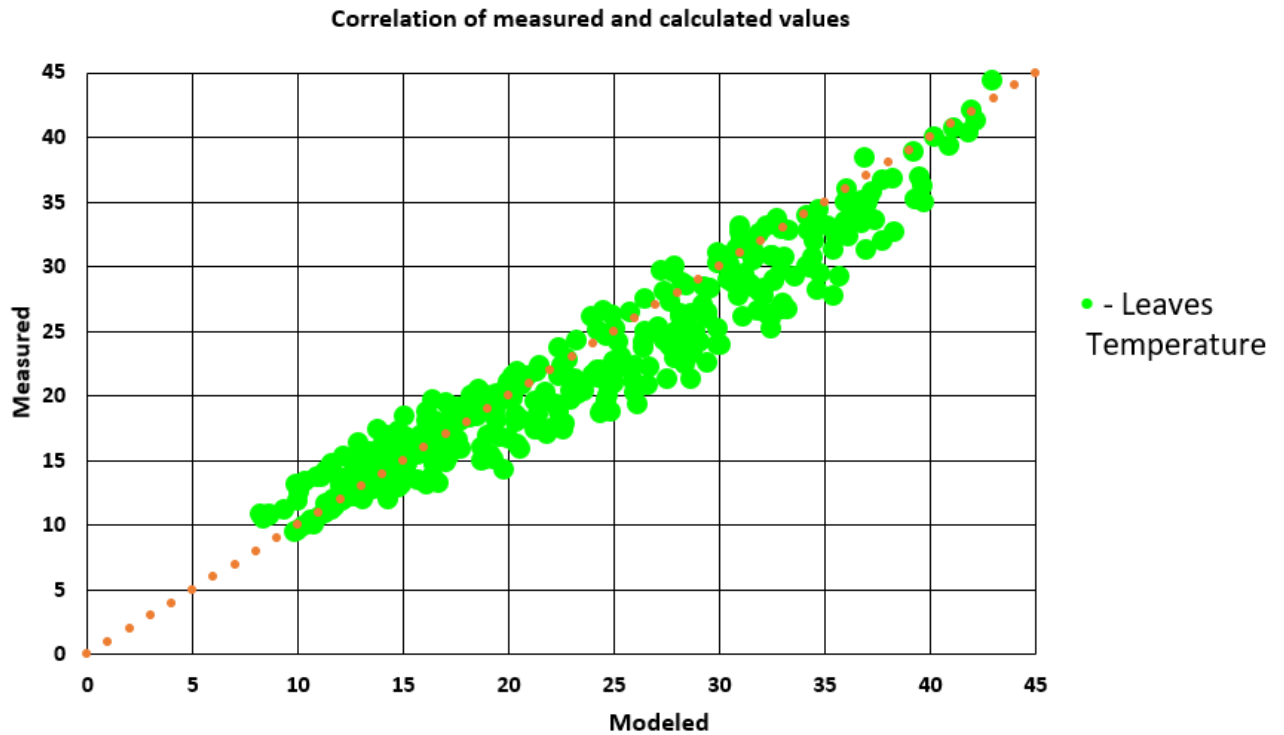


Figure 50. Case 3- Correlation of measured and calculated values.

7.4 HAMFit-GR Model Validation: A case with Vegetation

7.4.1 Vegetated roof in the dry period

Since the vegetative, as well as heat and moisture model, are validated separately using experimental data, the next validation exercise focus on validating the full HAMFit-GR model, coupled vegetative and HM model, using experimental data. For this case, the same dry period as in the first case is used but a test roof with vegetation. Figures 51 to 59 compares temperature, relative humidity and heat flux profiles. In addition to temperature and relative humidity values within the growing media, leaf temperature is plotted and compared. Here, two methods of model validations, comparison with experimental data and results from another available green roof model – WUFI, are used to benchmark HAMFit-GR, All the inputs, such as indoor and outdoor boundary conditions, heat transfer coefficients, material properties are the same. As can be seen from the graphs, both WUFI

and HAMFit-GR are able to predict the moisture content in the soil at both top and bottom points reasonably well however, WUFI model incorrectly estimates the upper soil surface temperature, while HAMFit-GR model predicts the temperatures more accurately. Figure 57 shows the correlation of the measured and simulated temperature results (HAMFit-GR). HAMFit-GR model MBE is 0.8°C and RMSE is 1.02°C for internal growing media temperature points, MBE - 1.9 °C and 2.2 °C for the growing media surface, and 1.9°C and 2.3°C for vegetation temperatures. Relative Humidity MBE is 0.029 and RMSE is 0.031.

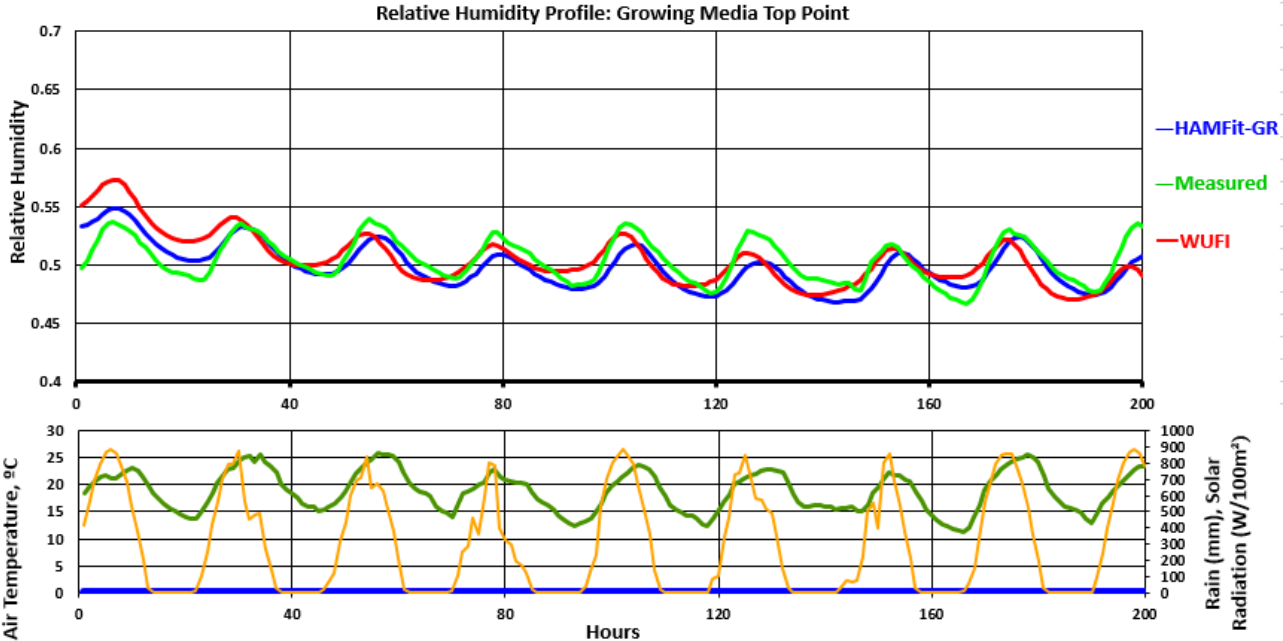


Figure 51. Relative Humidity – ½” below the upper surface.

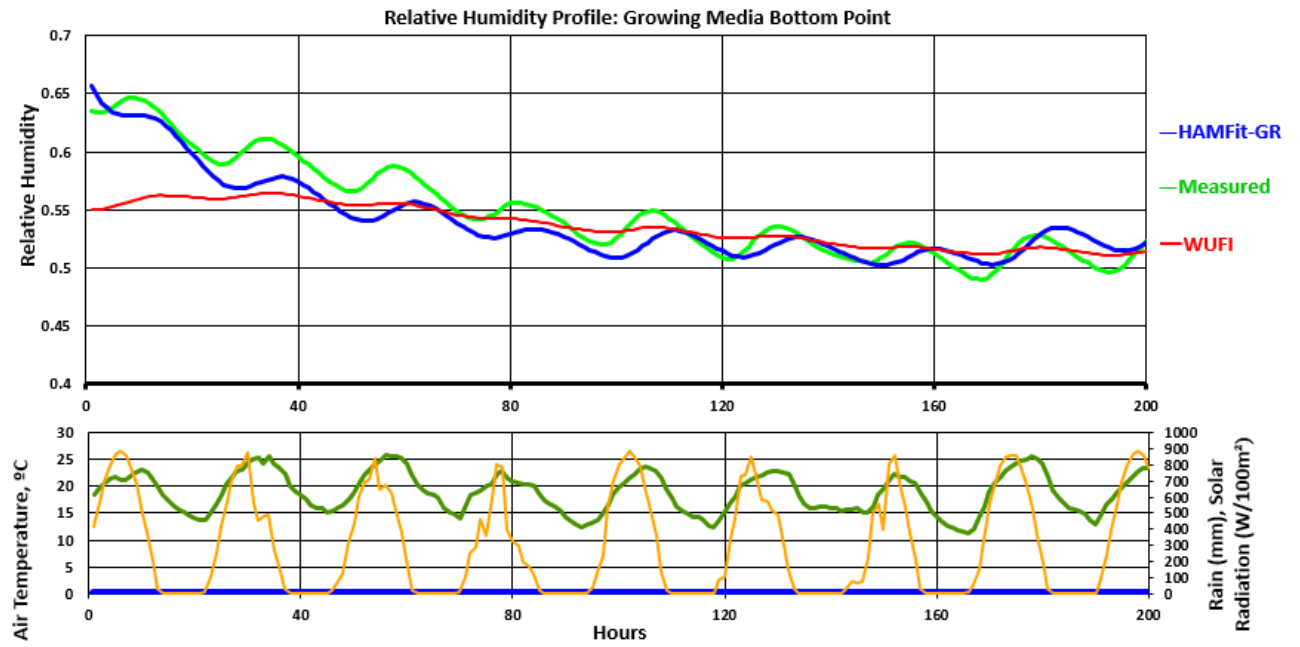


Figure 52. Relative Humidity – 1/2” above the bottom surface.

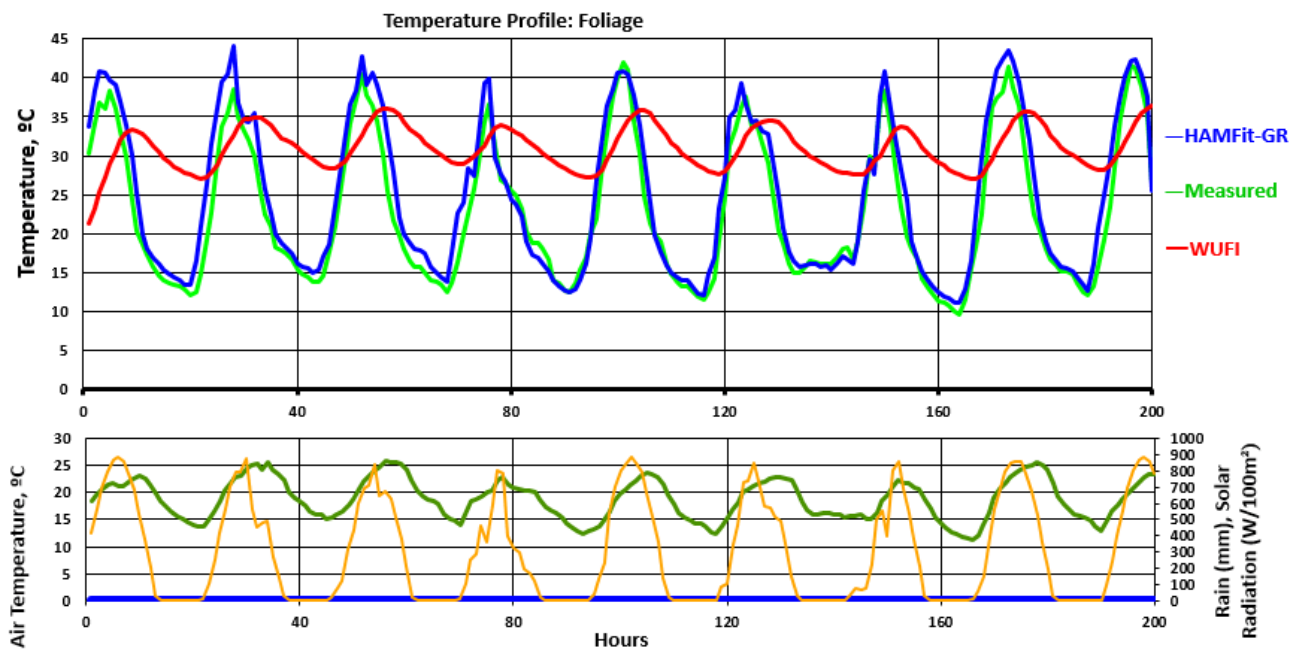


Figure 53. Case 4 – Foliage Temperatures.

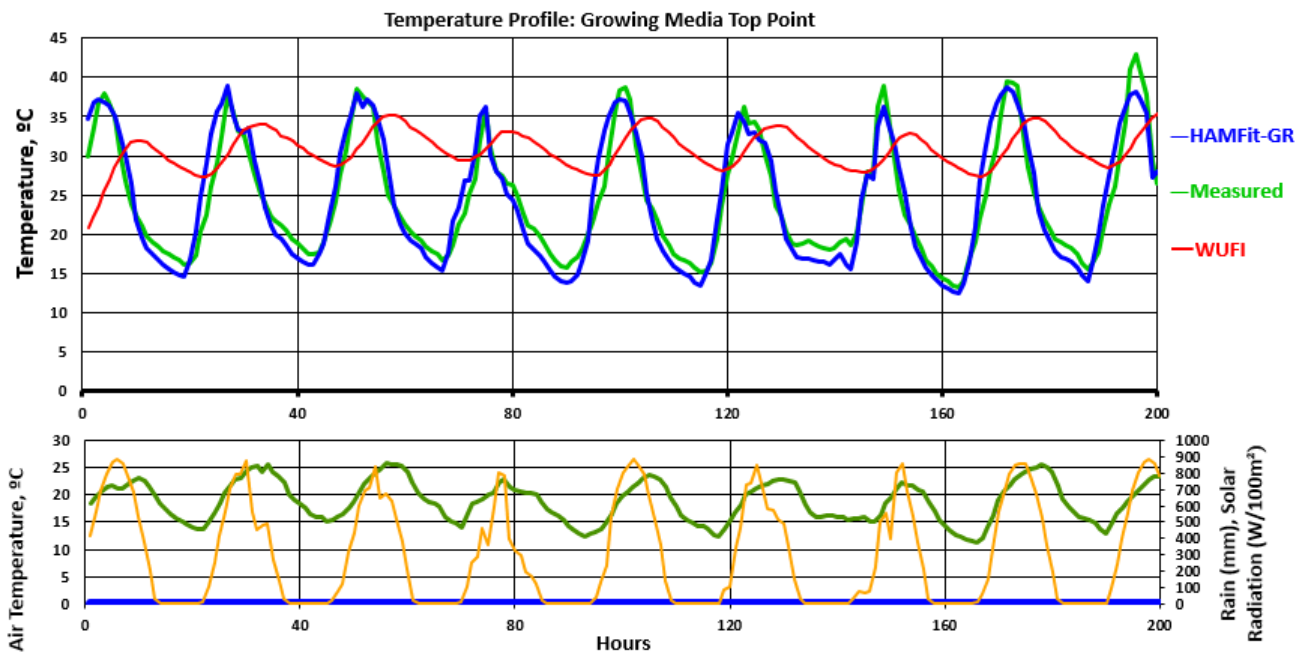


Figure 54. Case 4 – Temperature – Soil Surface.

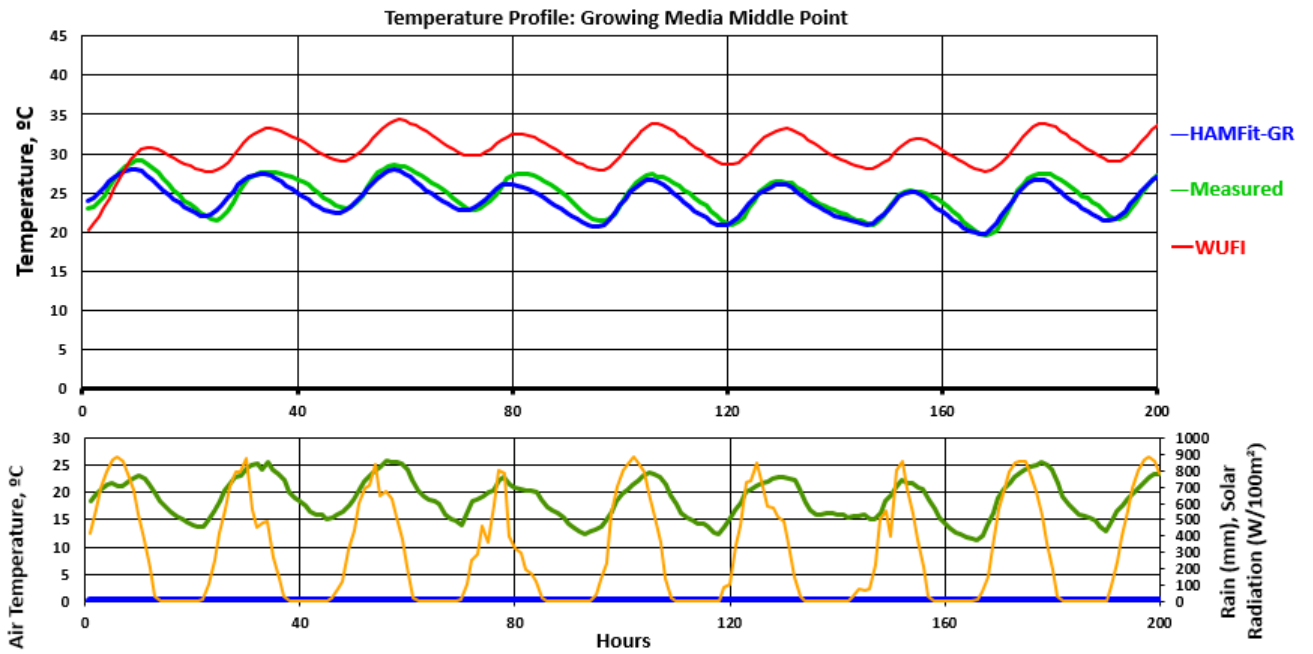


Figure 55. Case 4 – Temperature – in the middle of the soil layer.

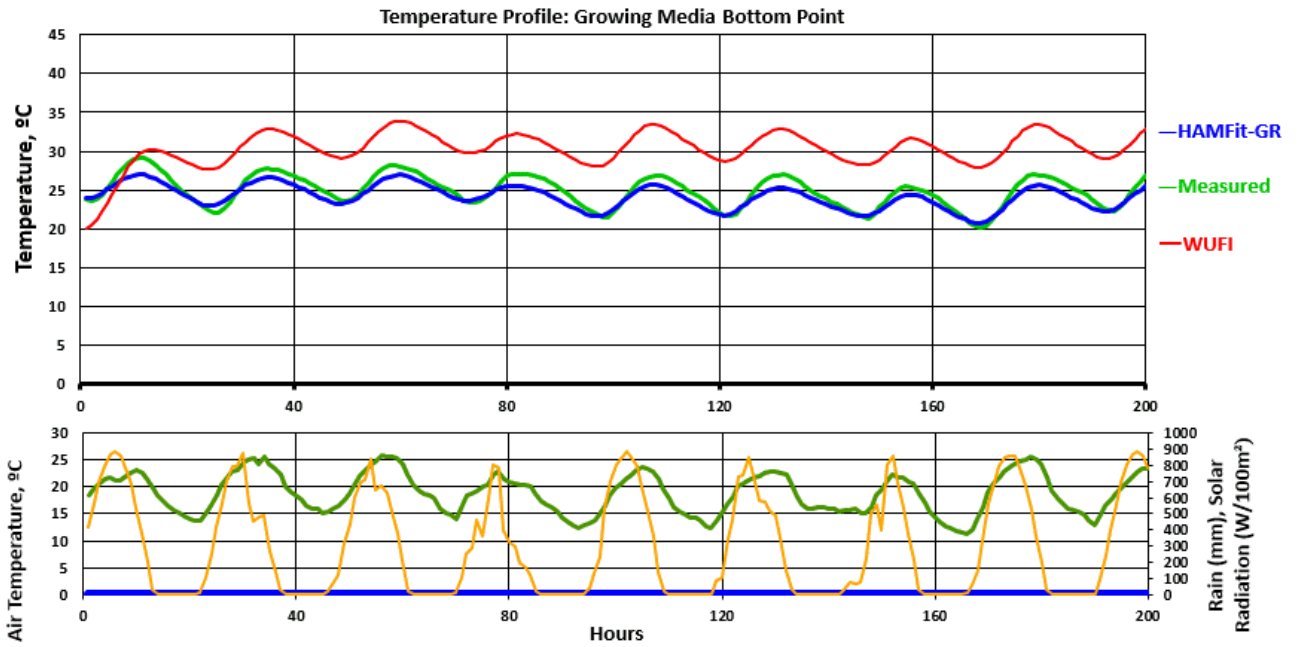


Figure 56. Case 4- Temperature- 1/2" above the bottom surface.

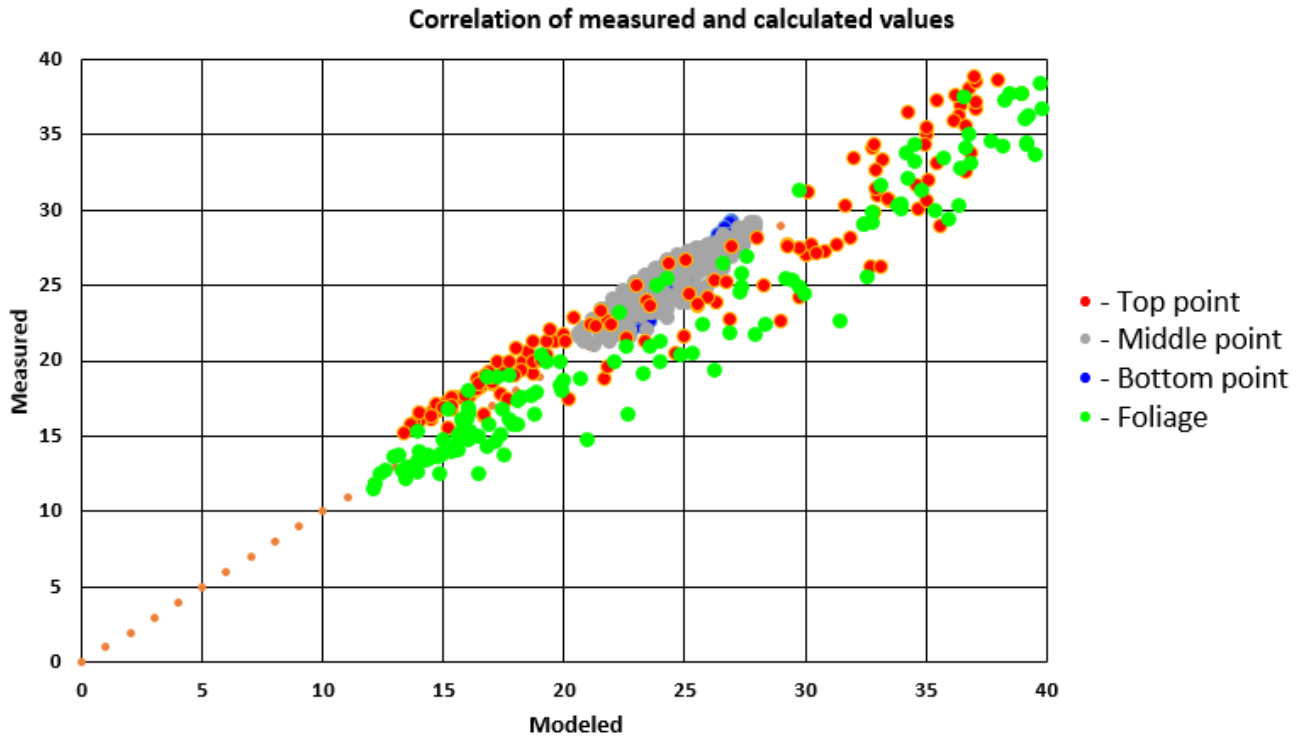


Figure 57. Case 4 – Correlation of measured and calculated values.

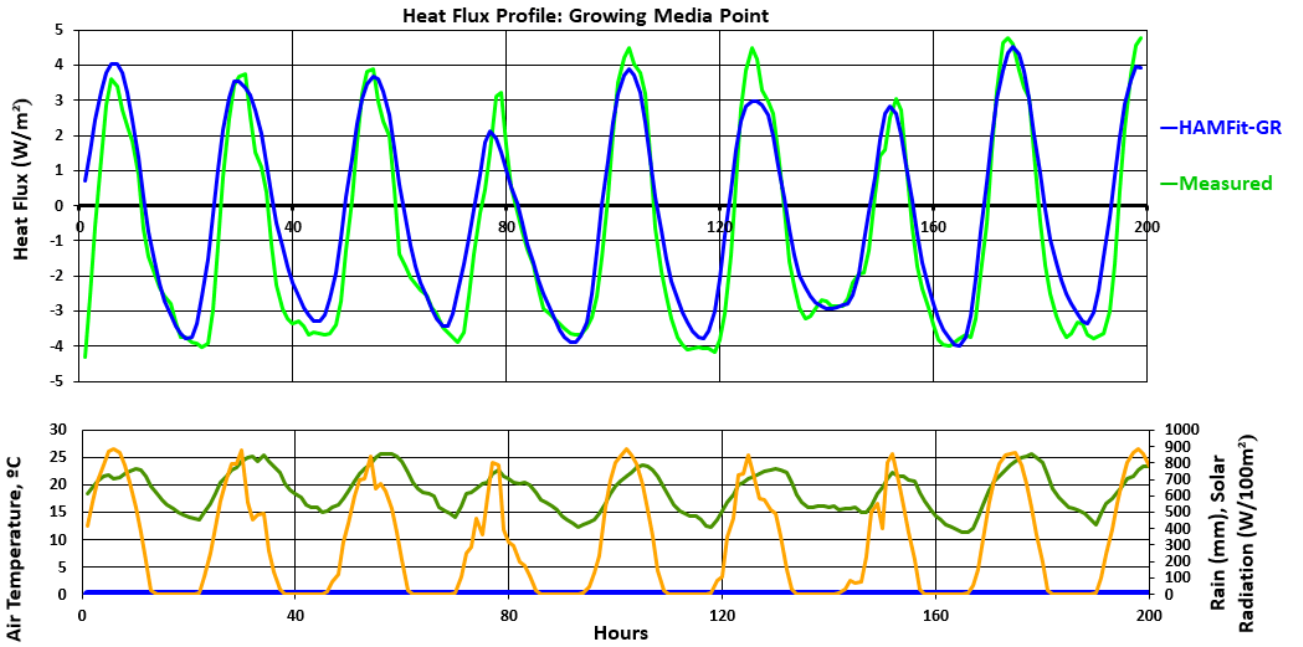


Figure 58. Case 4 - Heat Flux - Growing media.

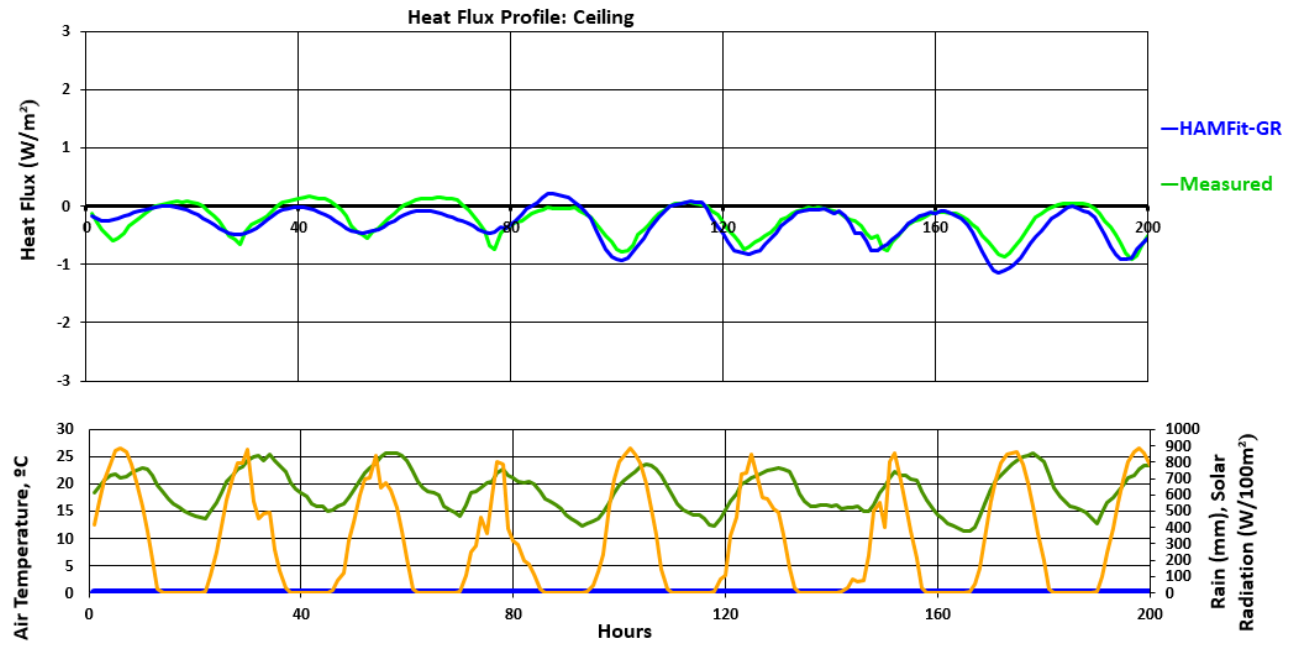


Figure 59. Case 4 - Heat Flux - Ceiling.

7.4.2 Vegetated roof in the rainy period

Following the same logic, the fifth validation case uses experimental results of the same green roof system during a timeframe with rain events. The period is characterized by stable air temperatures between 15 to 25°C, sunny days and two rain events. In this case, the soil stays near saturation condition for most of the period. In Figures 60 to 68, the simulation results of HAMFit-GR and WUFI models and the measured soil temperature and moisture content (represented in relative humidity) are presented. As it can be seen, both models accurately calculate then moisture content in the soil. Regarding temperature, HAMFit-GR results are in a good agreement with experimental temperature in all four cases (plants, soil surface, middle point, bottom point), while WUFI results are correct only at middle and bottom points, as shown in Figures 60-61. Figure 66 illustrates the correlation between the measured and HAMFit-GR temperature simulation results. The simulation results at the top, middle and bottom points have a combined MBE of 0.55°C, and RMSE of 0.67°C; for foliage MBE is 1.28°C, and RMSE is 1.67°C. Relative humidity MBE is 0.012 and RMSE is 0.013. In addition to RH and Temperature profiles, heat flux prediction of HAMFit-GR is compared with experimental data on Figures 67 and 68.

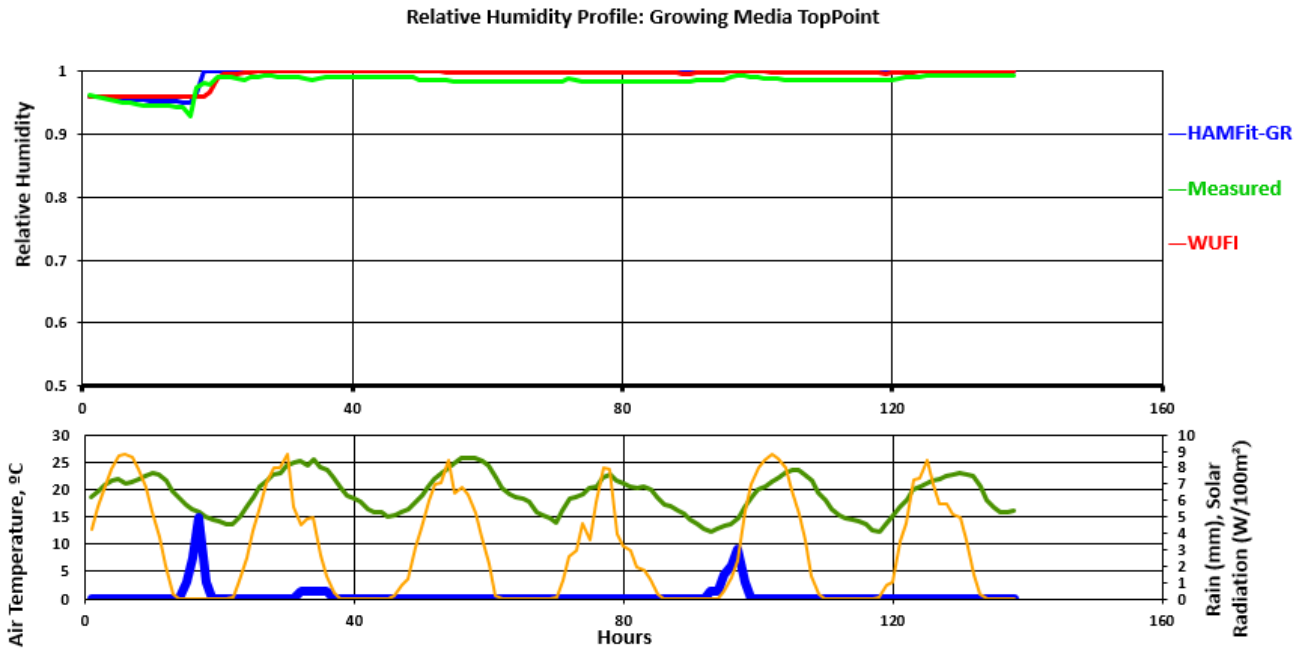


Figure 60. Case 5- Relative Humidity – 1/2” above the bottom surface.

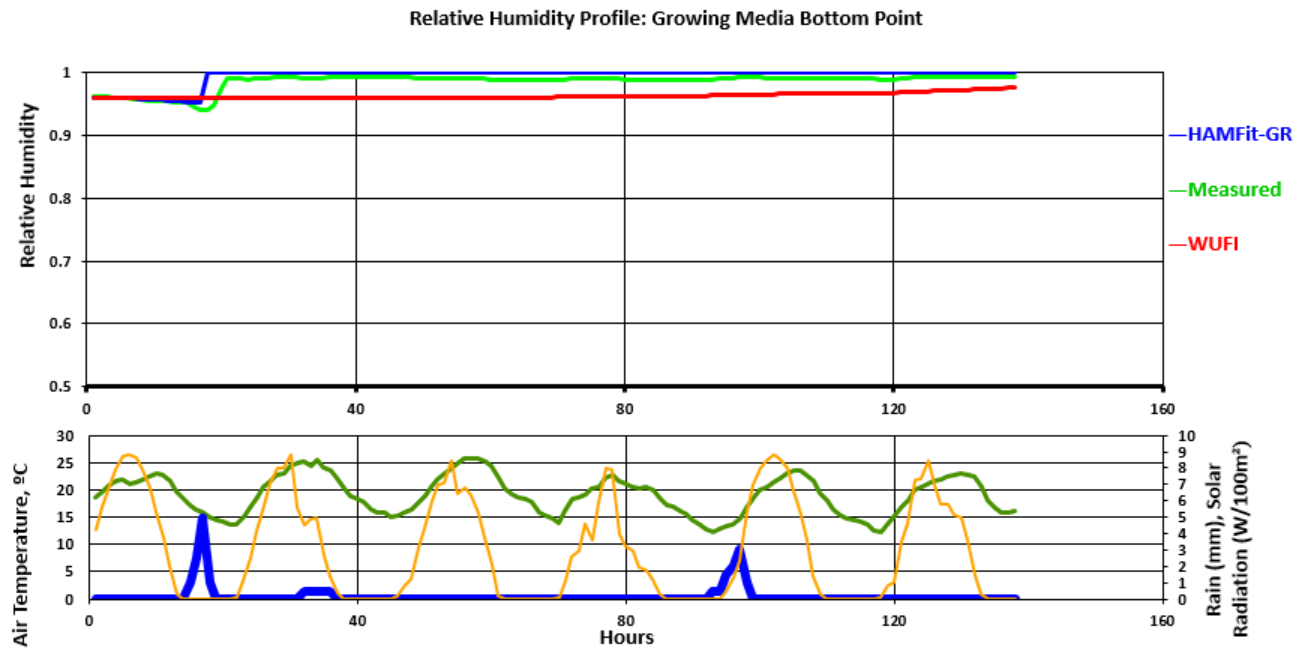


Figure 61. Case 5- Relative Humidity – 1/2” above the bottom surface.

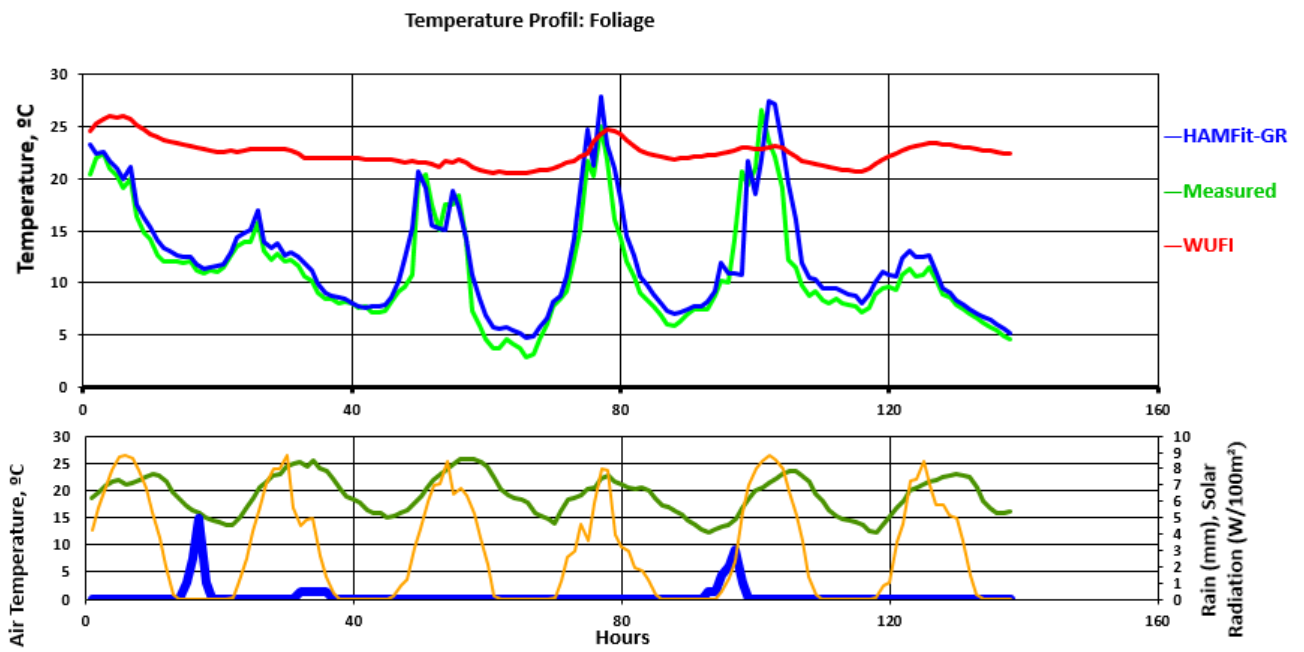


Figure 62. Case 5 – Foliage Temperature.

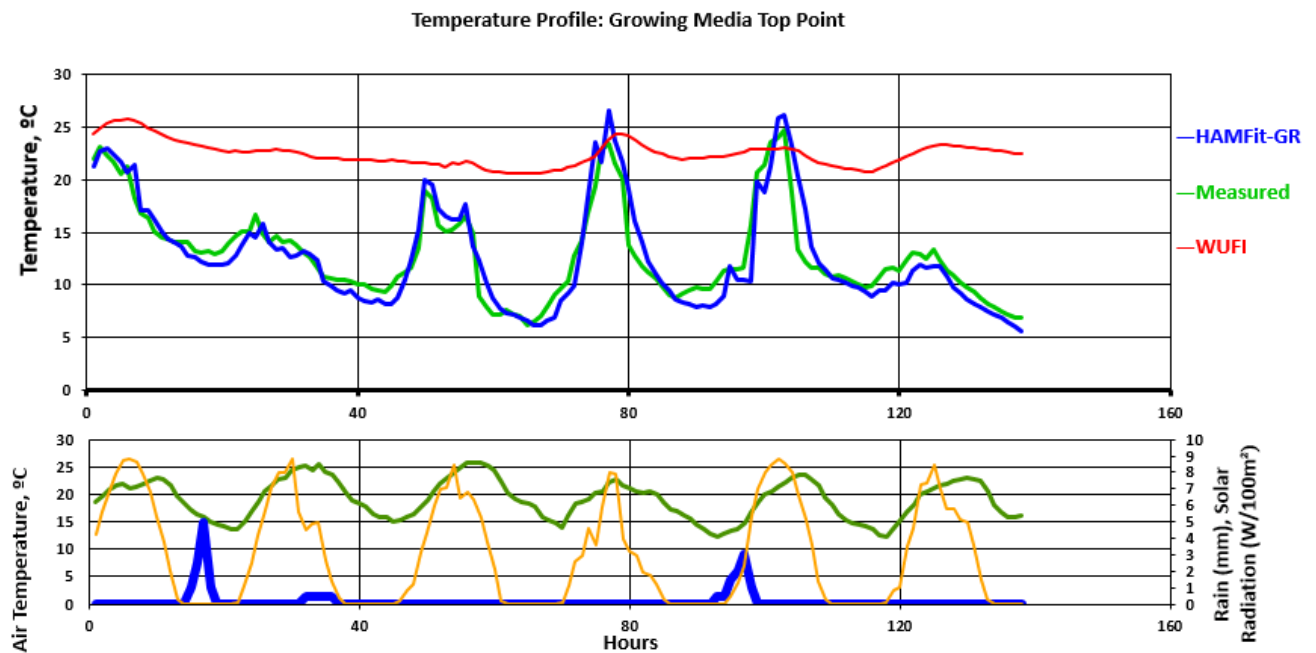


Figure 63. Case 5 – Soil Surface Temperature.

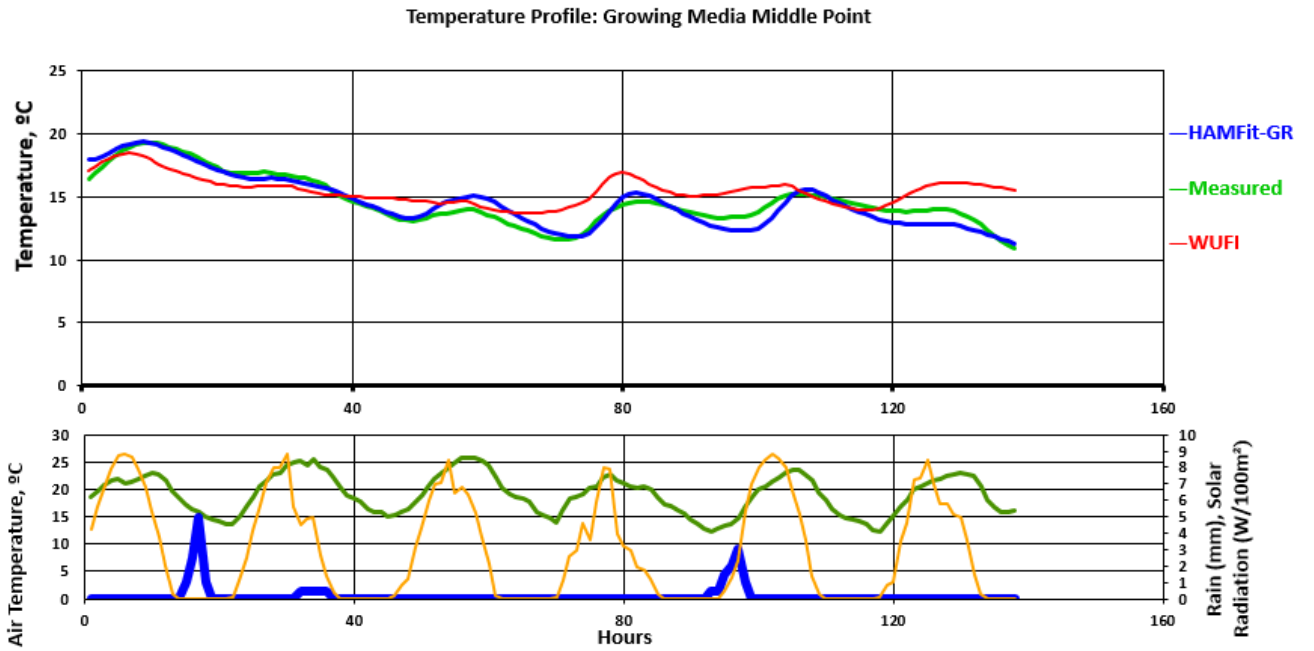


Figure 64. Case 5 – Soil Middle Point Temperature.

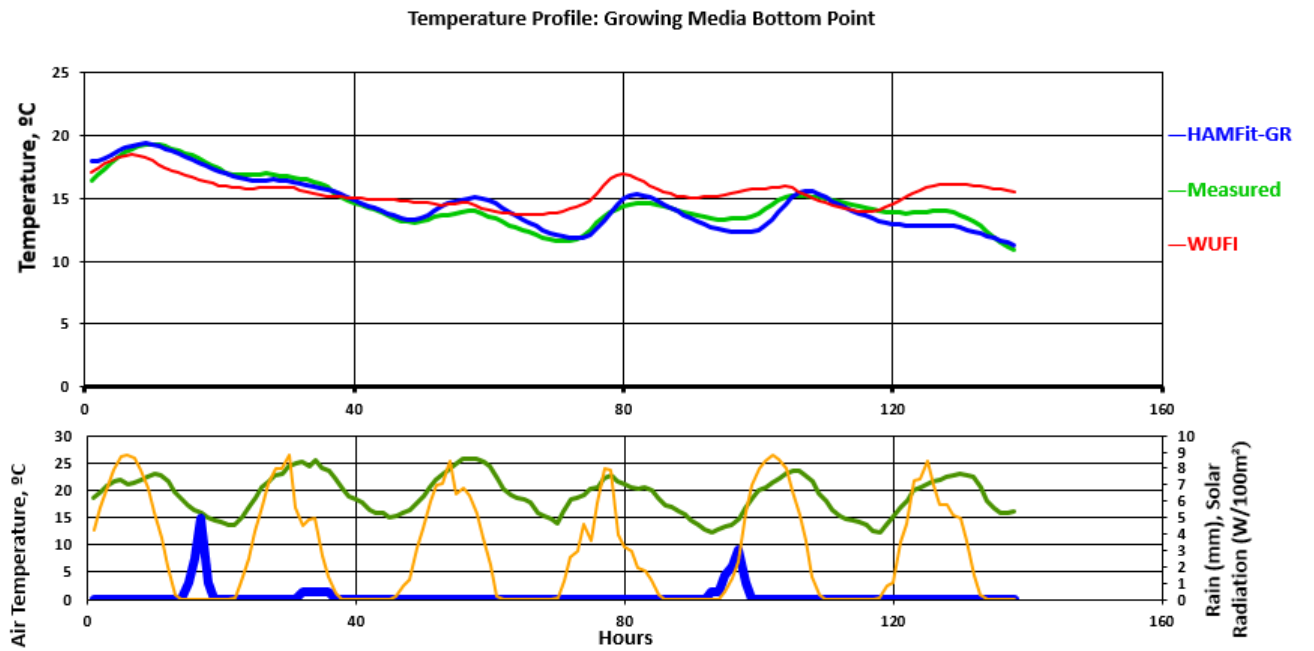


Figure 65. Case 5 – Soil Bottom Point Temperature.

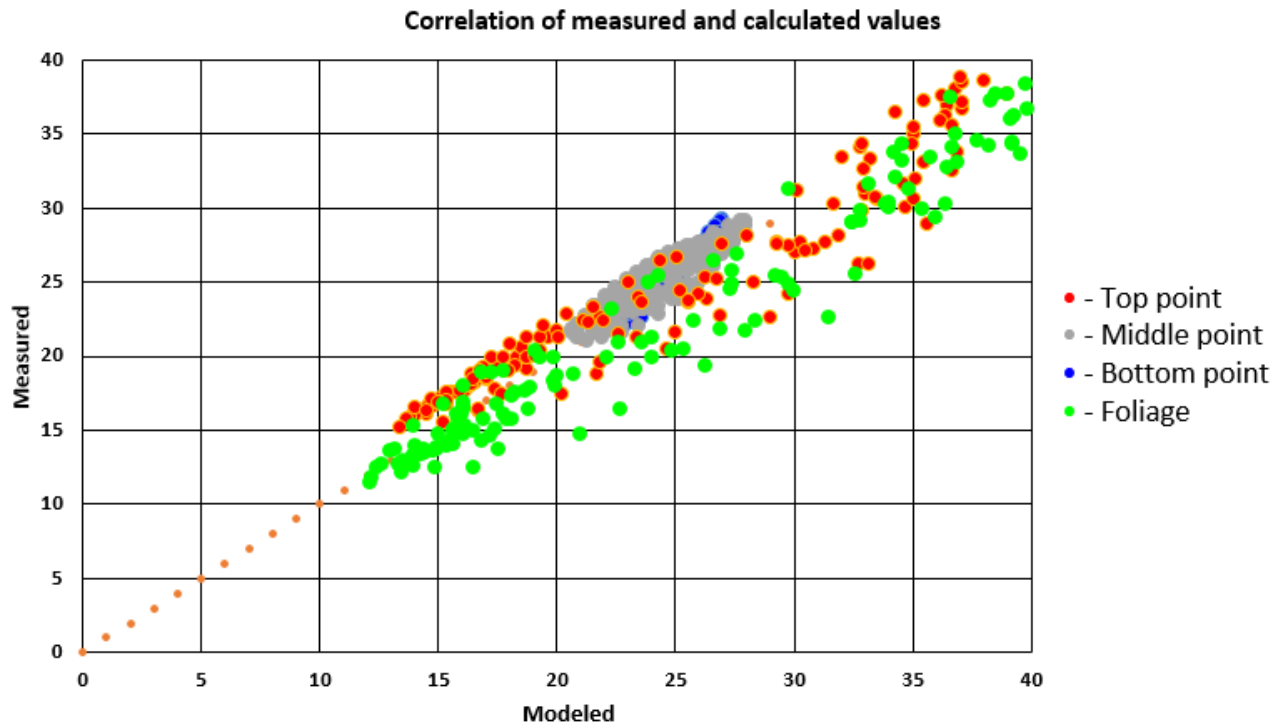


Figure 66. Case 5 – Temperature values distribution.

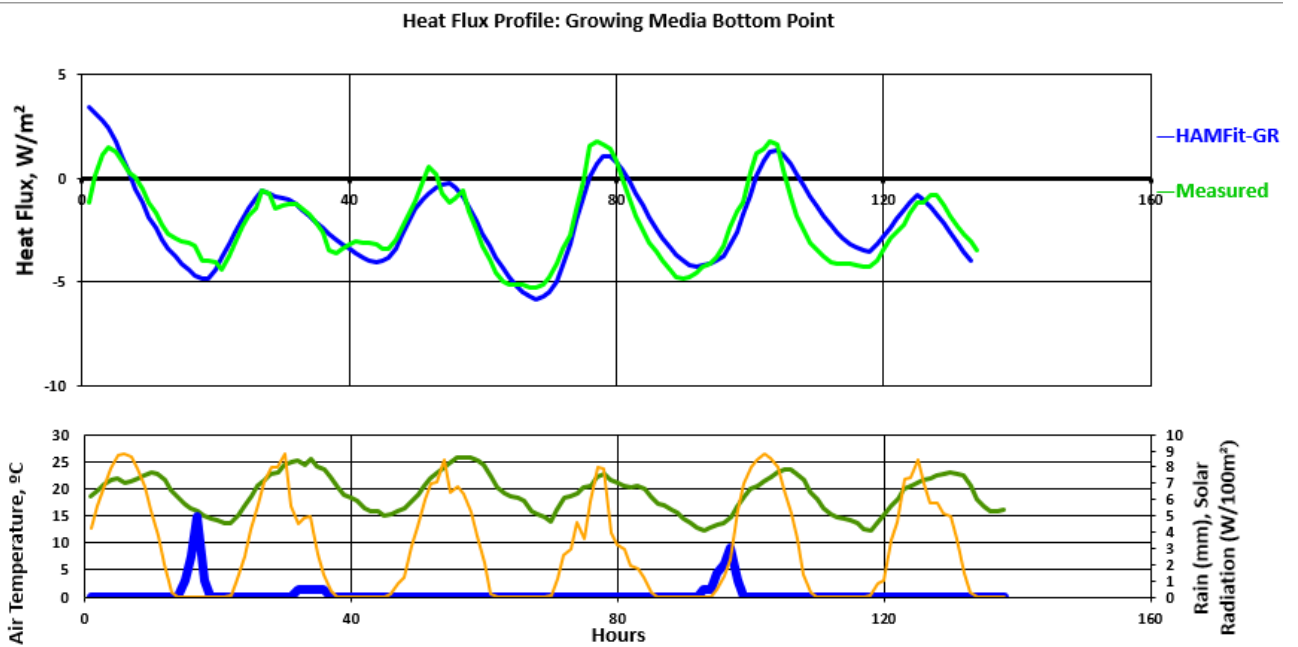


Figure 67. Case 5 – Heat Flux model vs measured.

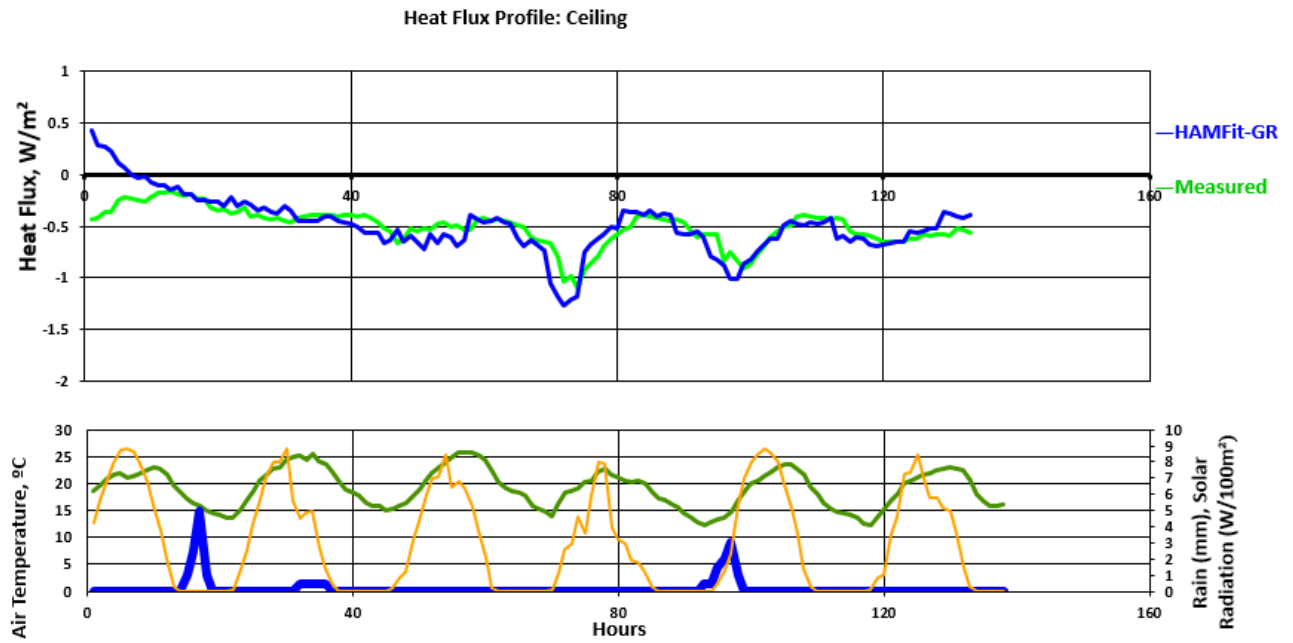


Figure 68. Case 6 – Heat Flux model vs measured.

7.5 Sensitivity analysis

In order to investigate the importance of input parameters, the HAMFit-GR model sensitivity study is prepared by setting input parameters to its minimal and maximum values. The time period is selected to be the same as the validation case #3 – ten days representing the summertime in Vancouver. The list of study variables is following: coverage ratio; leaf area index; root depth and a fraction; minimal stomatal resistance; plants height; growing media density and heat capacity; moisture content and runoff water convective heat calculation.

7.5.1 Coverage ratio

The coverage ratio is a percentage of area covered by plants leaves and stems per the same unit area. In the HAMFit-GR model, coverage ratio is described by minimum and maximum values, that are basically reflects seasonal values. In green roof modelling, those numbers vary from 0.25 to 0.5 and from 0.5 to 0.95 for minimum and maximum coverage respectively. The coverage ratio is

responsible for heat and moisture transfers between foliage and soil. In Figures 69 and 70, the soil bottom point temperature and ceiling heat flux profiles, respectively, are plotted. The higher coverage ratio case demonstrates its ability to keep heat inside the growing media and cut heat flow from and to a living space. This behaviour is explained by lower soil surface area exposed to the negative heat flow due to radiation, evaporation and convection. In the same time, coverage ratio determines the amount of solar coming to the system (shading), this effect can be seen in the periods of high solar activity when a gap between the temperature lines becomes lower.

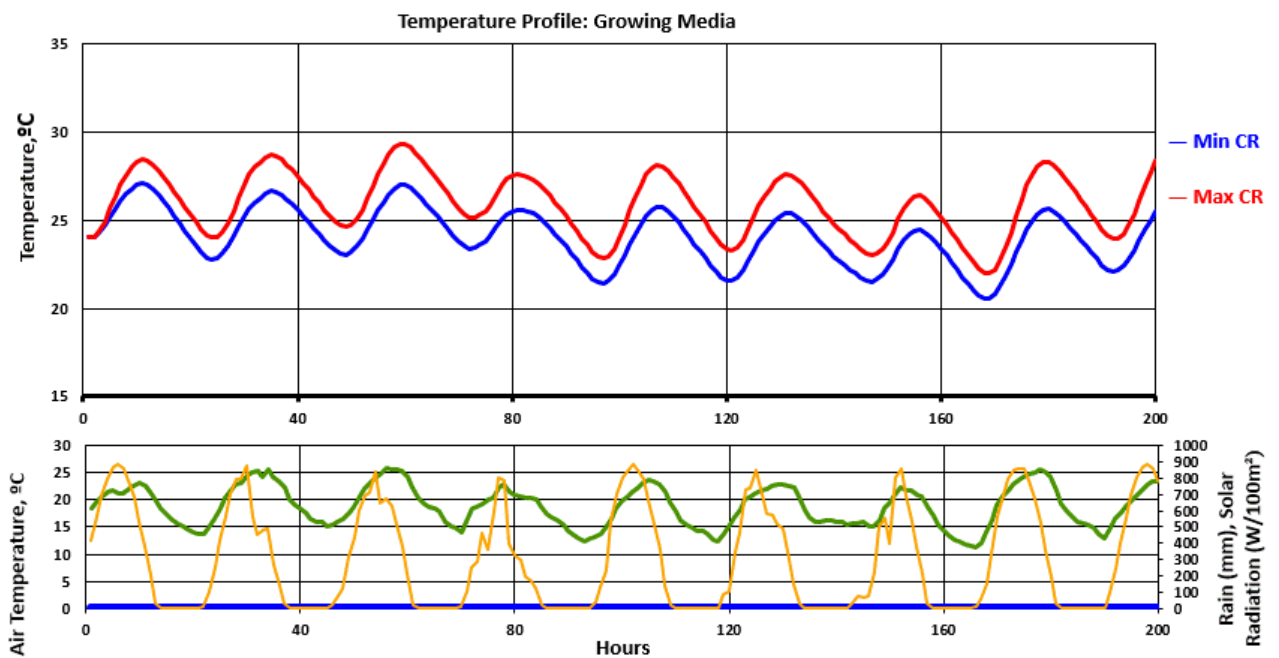


Figure 69. Coverage ratio impact on the growing media temperature.

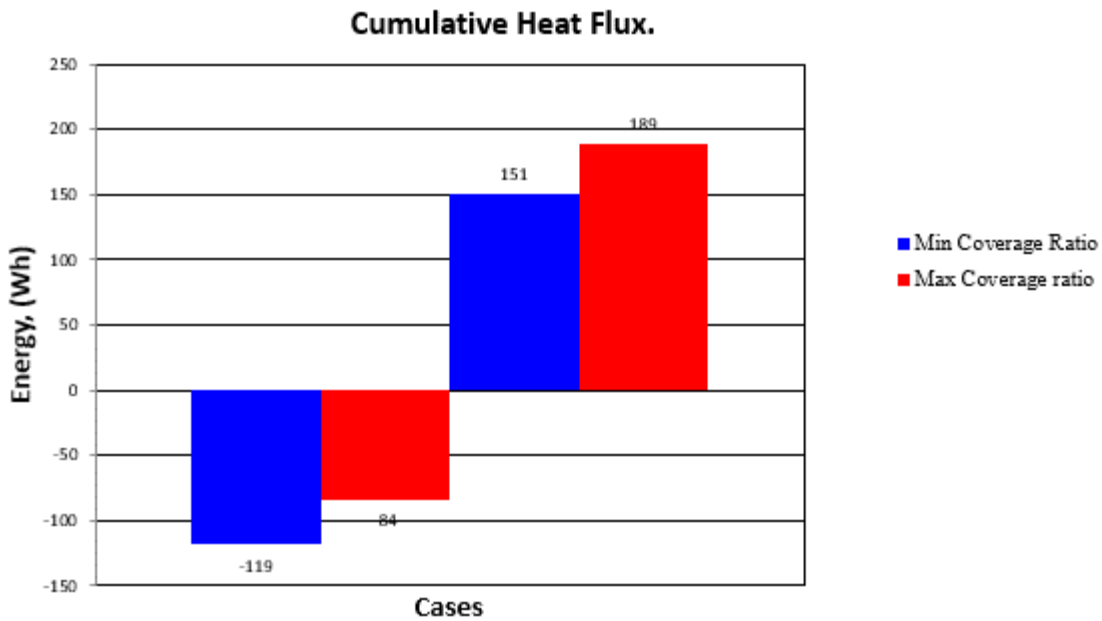


Figure 70. Coverage ratio impact on heat flux.

7.5.2 Leaf Area Index

Leaf Area Index (LAI) is defined as the one-sided green leaf area per unit ground surface area. LAI is a key parameter in evapotranspiration calculation (latent heat flux). LAI also influences sensible heat flow in the foliage energy balance. In order to study how sensitive model to LAI variations, minimum (0.5-2) and maximum (0.5-6) options are compared. Bottom soil temperature and heat flux on ceiling profiles are plotted in Figures 71 and 72. The model calculated that temperature in the growing media bottom point fluctuates daily, but the temperature under higher LAI green roof stays about 5°C cooler than under the lower LAI roof. Since the simulation period is summer when the leaf area index is at its maximum, temperature and heat flux profiles significantly differ from each other. Higher LAI value increases heat losses due to evapotranspiration. When LAI is multiplied by a factor of three, the energy loss decreased by 2.1 times. Thus, the model is sensitive to LAI value.

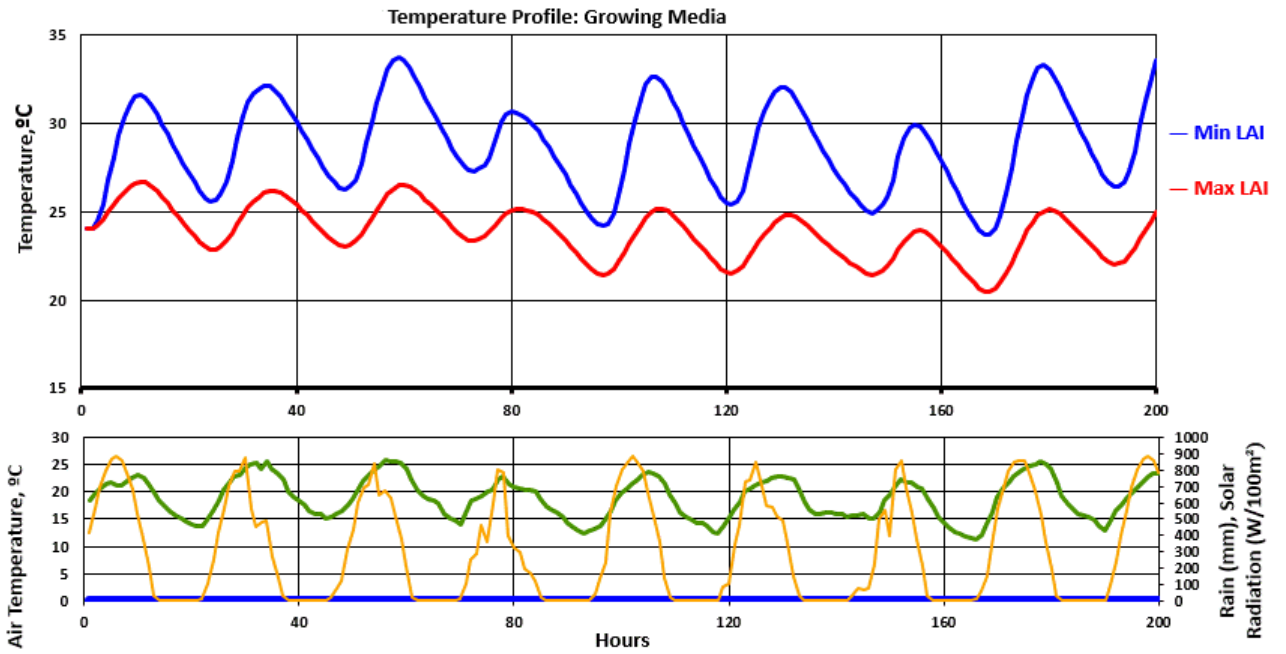


Figure 71. Leaf Area Index impact on the growing media temperature.

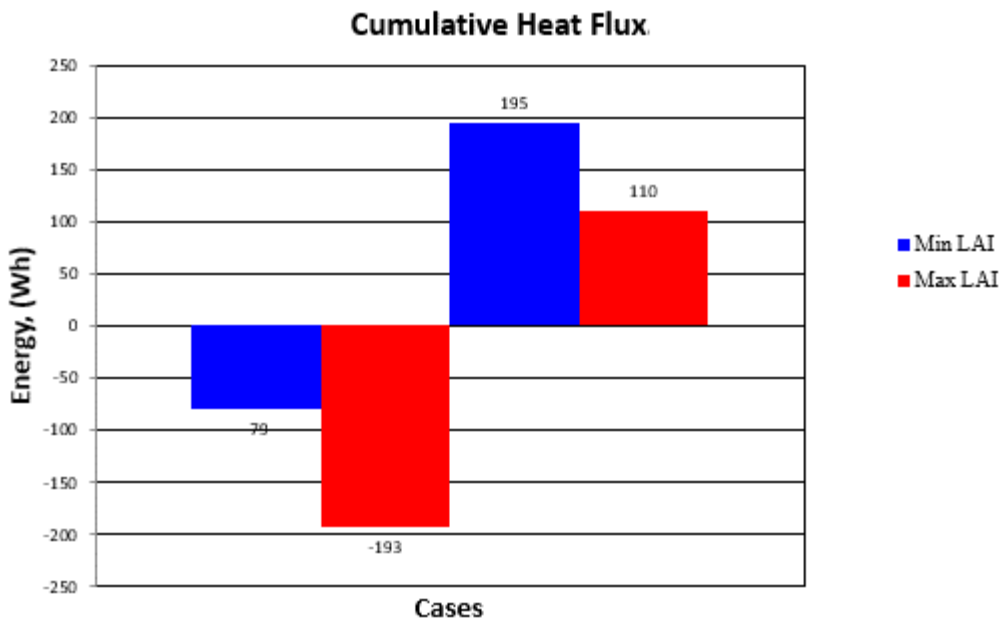


Figure 72. Leaf Area Index impact on heat flux.

7.5.3 Coverage ratio and leaf area index

After coverage ratio and leaf area index impact is studied separately in the ten days period, the influence of vegetation properties throughout a year is the next focus of this thesis. Plants do not have any significant thermal mass to affect the heat flow, but vegetation can change the green roof thermal performance through evapotranspiration (latent heat), sensible heat flow and radiative heat exchange influenced by leaves shading and different radiative properties. In the model, the amount of shaded area is characterized by coverage ratio that defines the proportions of heat and moisture flow to/from soil or vegetation layers. Another value – Leaf Area Index is mainly responsible for the amount of water and heat transfer by evapotranspiration and convection. With the aim to analyze those parameters, three cases reflecting low, normal, and high vegetation density for each climate are prepared. The only differences in those cases are the maximum values of coverage ratio (Low – 0.7, Normal – 0.8, High – 0.9) and corresponding Leaf Area Index (Low – 3.5, Normal – 4.3, High – 6).

The heat fluxes in the concrete roof with R33 XPS insulation, 10 cm growing media, and different coverage ratio are for Vancouver, Winnipeg and Toronto are included in Appendix A because the difference between cases is not noticeable at the high scale.

Firstly, heat fluxes in February, like a month representing winter in Vancouver, is plotted on Figures 73 and 74. Air temperature in that period in Vancouver is relatively warm and fluctuate within the range of 2-15 °C, which means the model assumes that plants are alive with corresponding heat transfer process. In the analyzed period, heat losses are lower for high covered scenario because plants reduce long wave radiation exchange with a colder sky. However, during the sunny days, the difference in heat losses between cases become lower due to higher evapotranspiration rate and shading from incoming solar radiation (ex. Feb 7, 8). The amount of heat left the room has a variation around 2% between the cases.

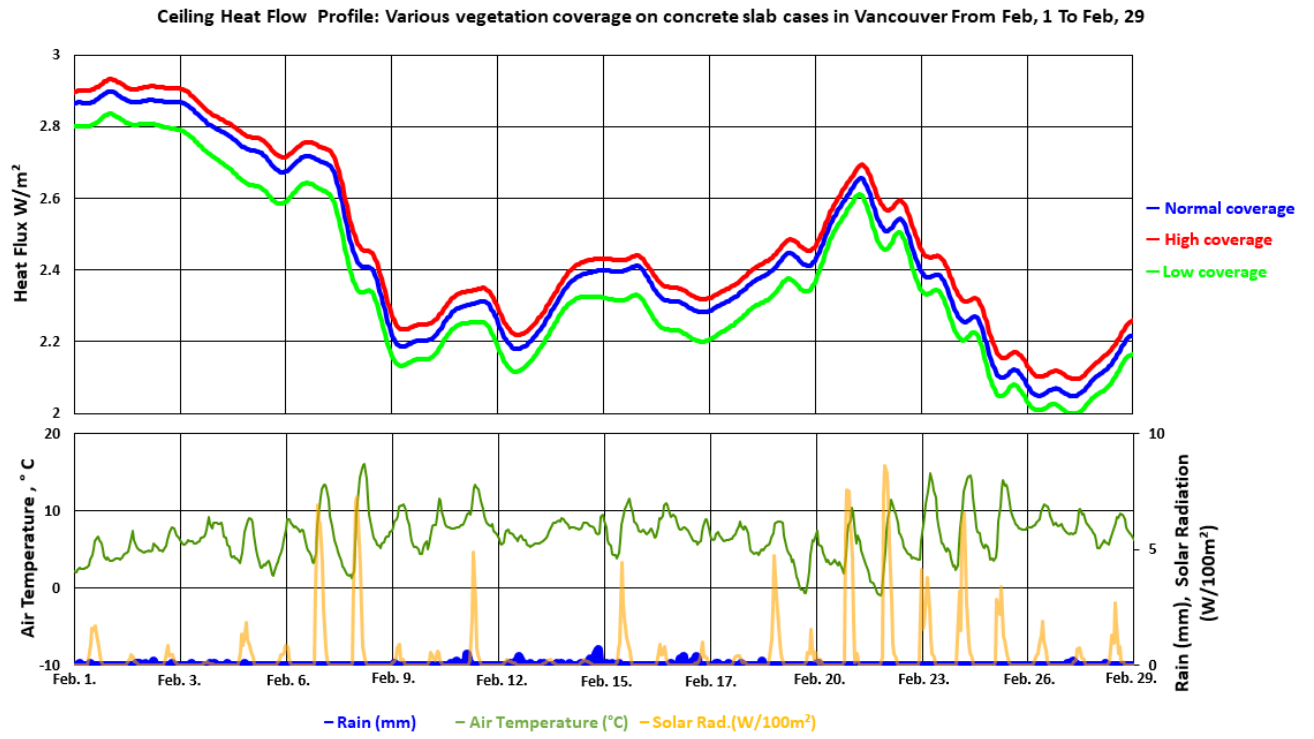


Figure 73. Heat flux through Low, Normal, and High covered green roofs in February in Vancouver.

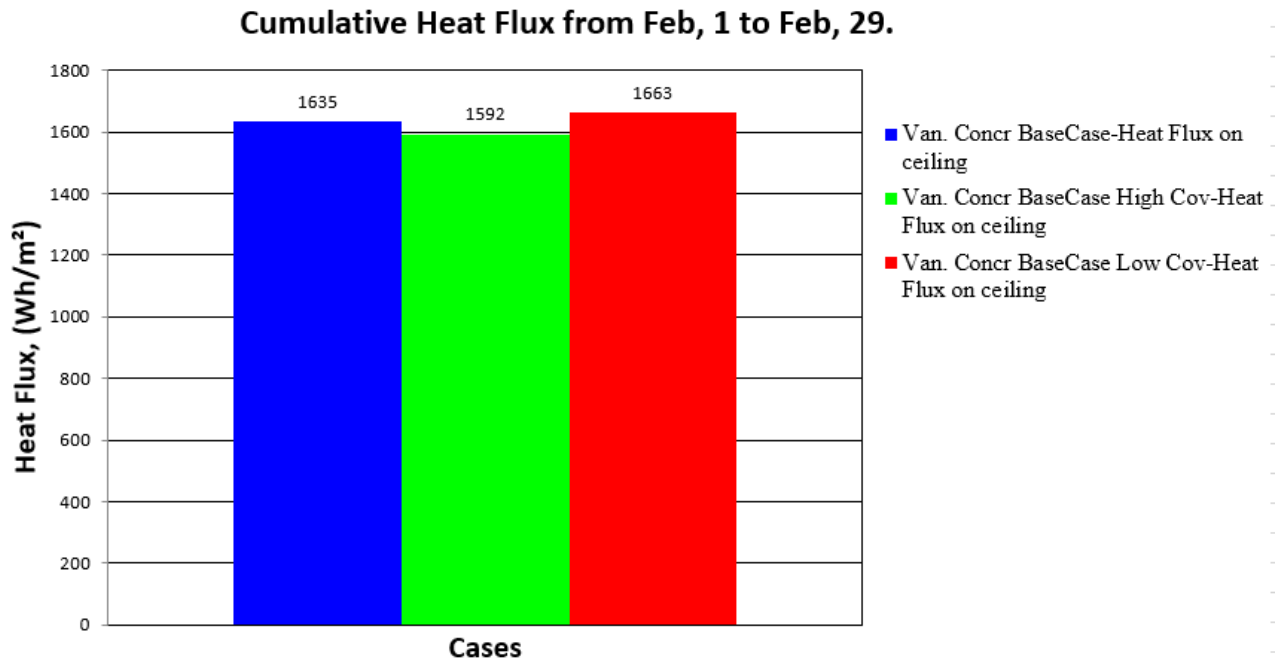


Figure 74. Overall heat losses through Low, Normal, and High covered green roofs in February Vancouver.

August is selected to represent summer month in Vancouver. Heat flow results are plotted in Figures 75 and 76. During the whole period, all three lines fluctuate near zero, indicating that green roof with all three vegetation options is efficient. High covered roof shows lower night time losses slightly because evapotranspiration is highly reduced at nights, but plants still cut longwave radiation exchange.

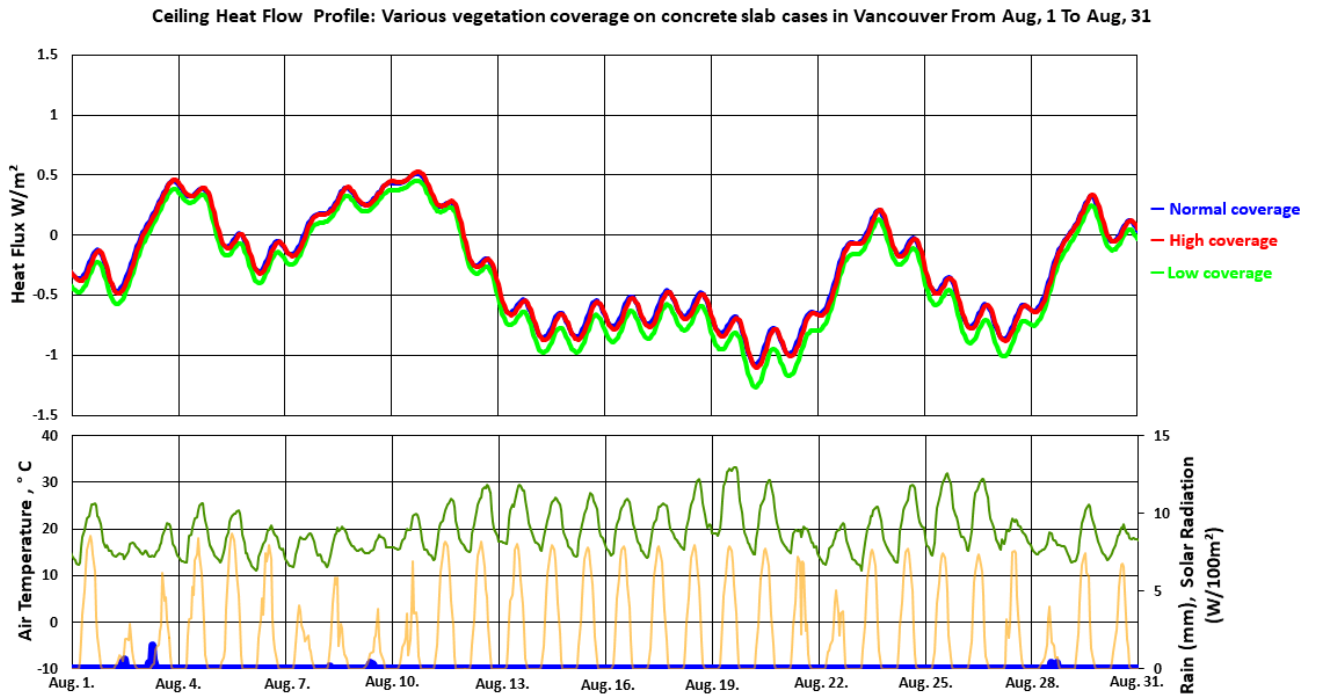


Figure 75. Heat flux through Low, Normal, and High covered green roofs in August in Vancouver.

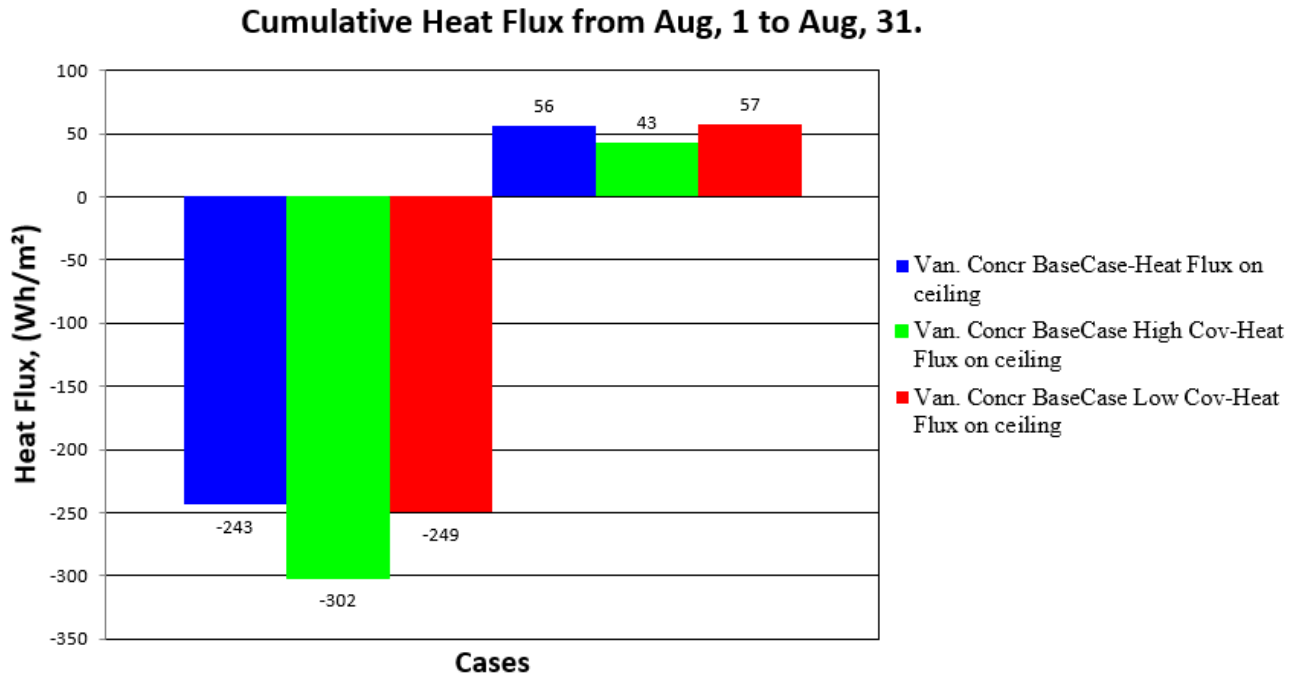


Figure 76. Overall heat losses through Low, Normal, and High covered green roofs in August in Vancouver.

7.5.4 Root depth and root fraction.

In HAMFit-GR, root depth and fraction values are used to determine the area where moisture is available for plants to transpire. To assess the importance of this parameter, two simulations with root depth 5, $a_{\text{root}} 5.558$, $b_{\text{root}} 1.627$ and root depth 30 mm $a_{\text{root}} 10.739$, $b_{\text{root}} 2.614$ are simulated. Figures 77 and 78 present the results. As it can be seen, there is no significant influence on energy flow by root depth and a fraction. Therefore, any reasonable values can be used.

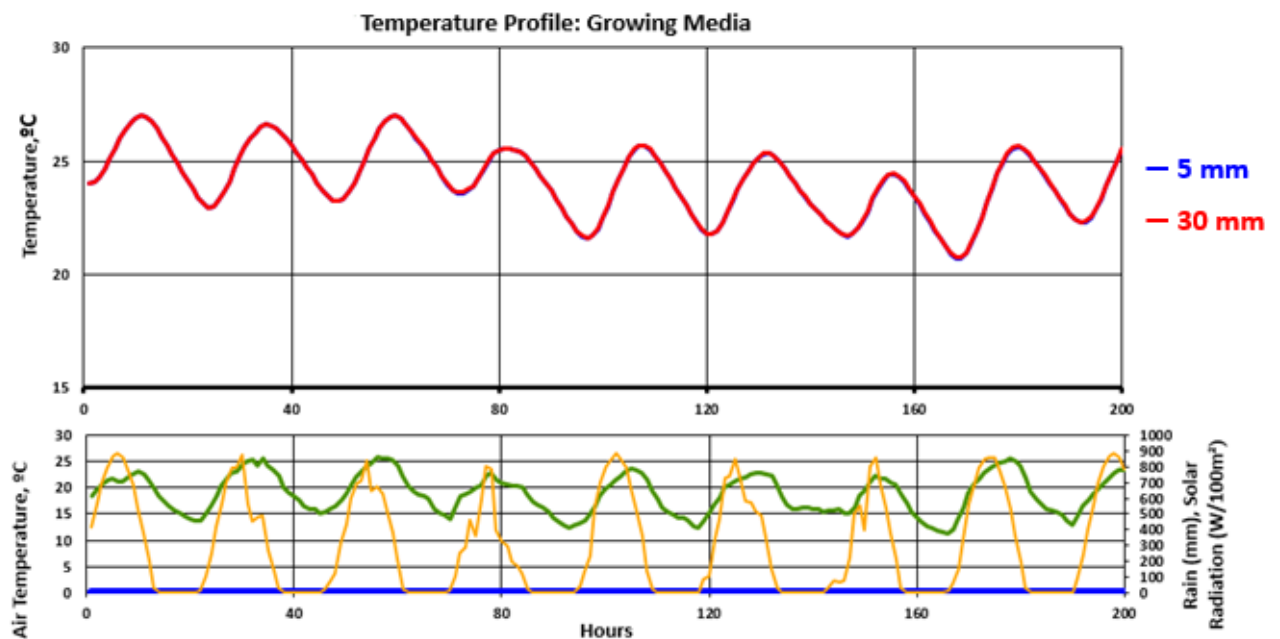


Figure 77. Root distribution impact on the growing media temperature.

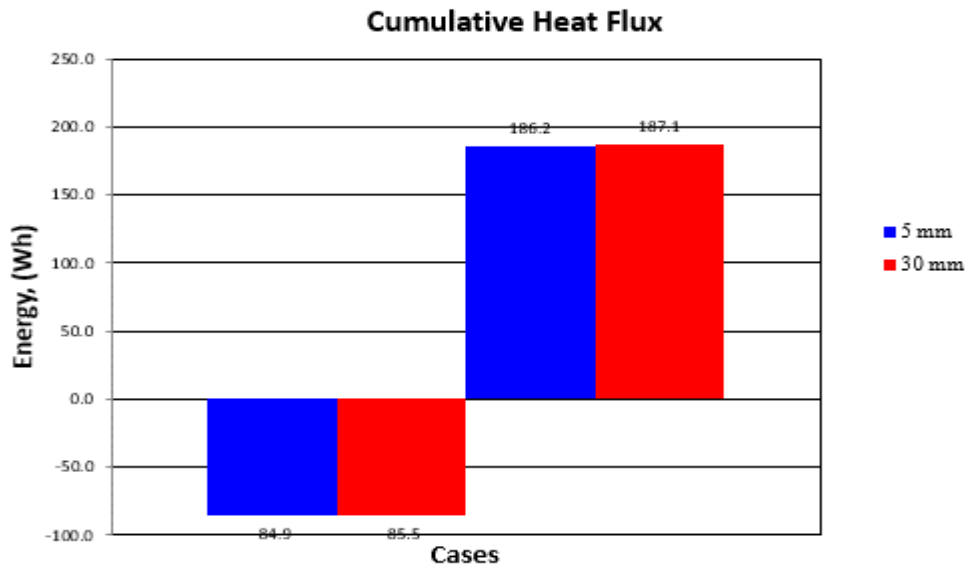


Figure 78. Root distribution impact on heat flux.

7.5.5 Minimal stomatal resistance

Evapotranspiration rate and latent heat in the HAMFit-GR model are determined from the stomatal resistance value that in its turn is a function from soil moisture availability, amount of sun radiation, soil temperature and minimal stomatal resistance. Minimal stomatal resistance is a constant value characterizes the ability of plants to pass water through stems and leaves. In case of sedums, this value could vary from 120 s/m to 900 s/m. Two cases with minimum and maximum possible options are investigated. To study an insolation of minimum stomatal resistance, ideal conditions are set, such as high solar radiation and originally fully saturated soil. As shown in Figures 79 and 80 there is no significant difference in the temperature profile; however, plants with lower stomatal resistance have cooling ability 2% higher due to higher evapotranspiration.

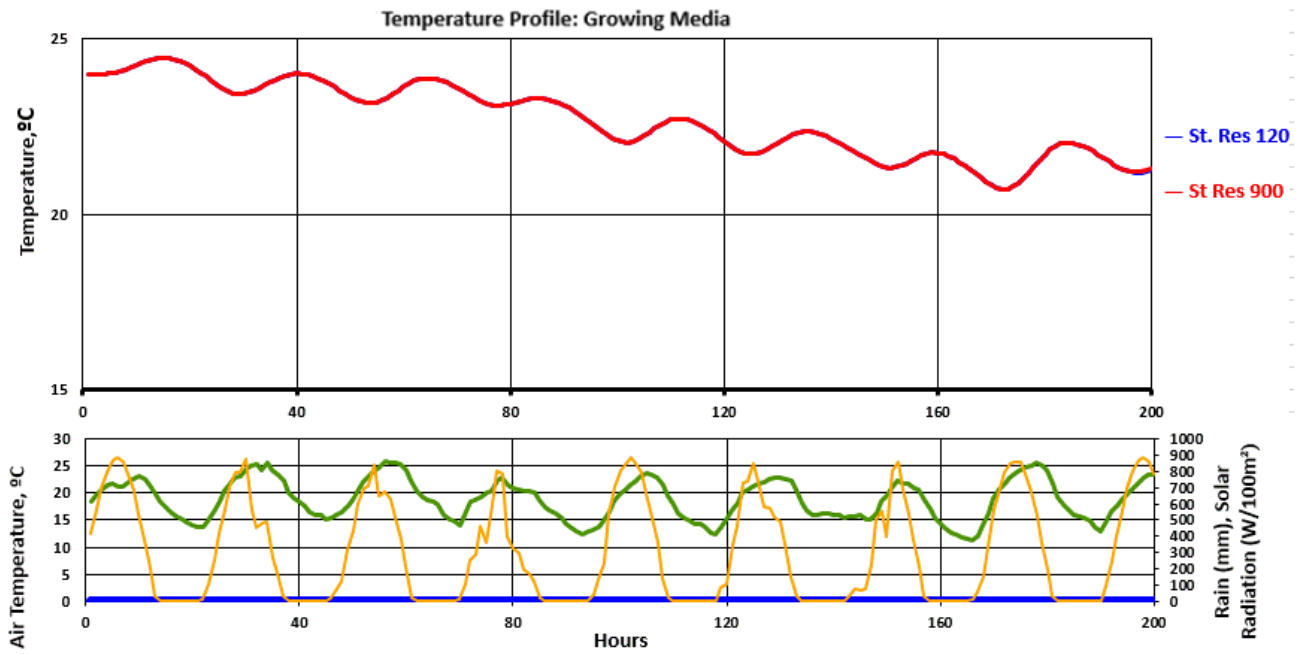


Figure 79. Minimal stomatal resistance impact on the growing media temperature.

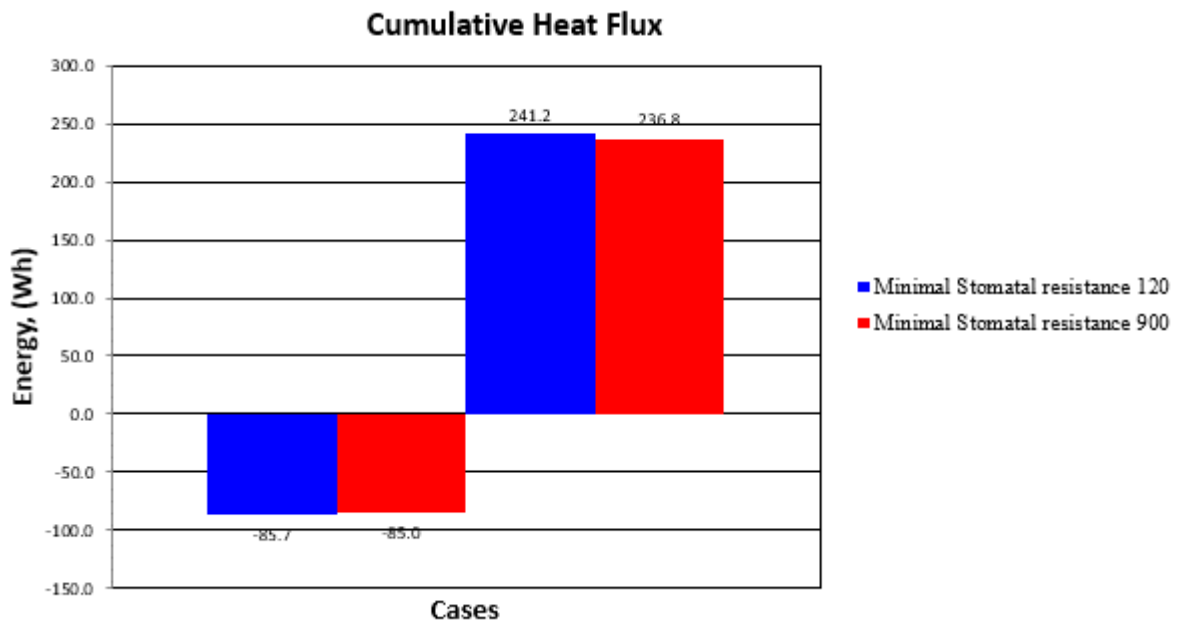


Figure 80. Minimal stomatal resistance impact on heat flux.

In addition to short-term simulation, another yearlong scenario is prepared, focusing on the impact of plants' evapotranspiration. The major variable responsible for evapotranspiration is stomatal resistance. Sedum's that are mostly used as a vegetation type in green roof systems could have this value varies from 120 to 900 s/m. Therefore, two cases of 200 and 700 s/m minimum stomatal resistance are provided and shown in Figure 81. The difference between those cases appears when plants have the conditions for evapotranspiration (solar radiation, wet soil, warm air temperature) and the rate of heat flow by evapotranspiration is mostly defined by minimum stomatal resistance. When some of the above-listed conditions do not exist, stomatal resistance becomes high, evapotranspiration rate is significantly lowered, and there is no noticeable difference in heat flux on the graph.

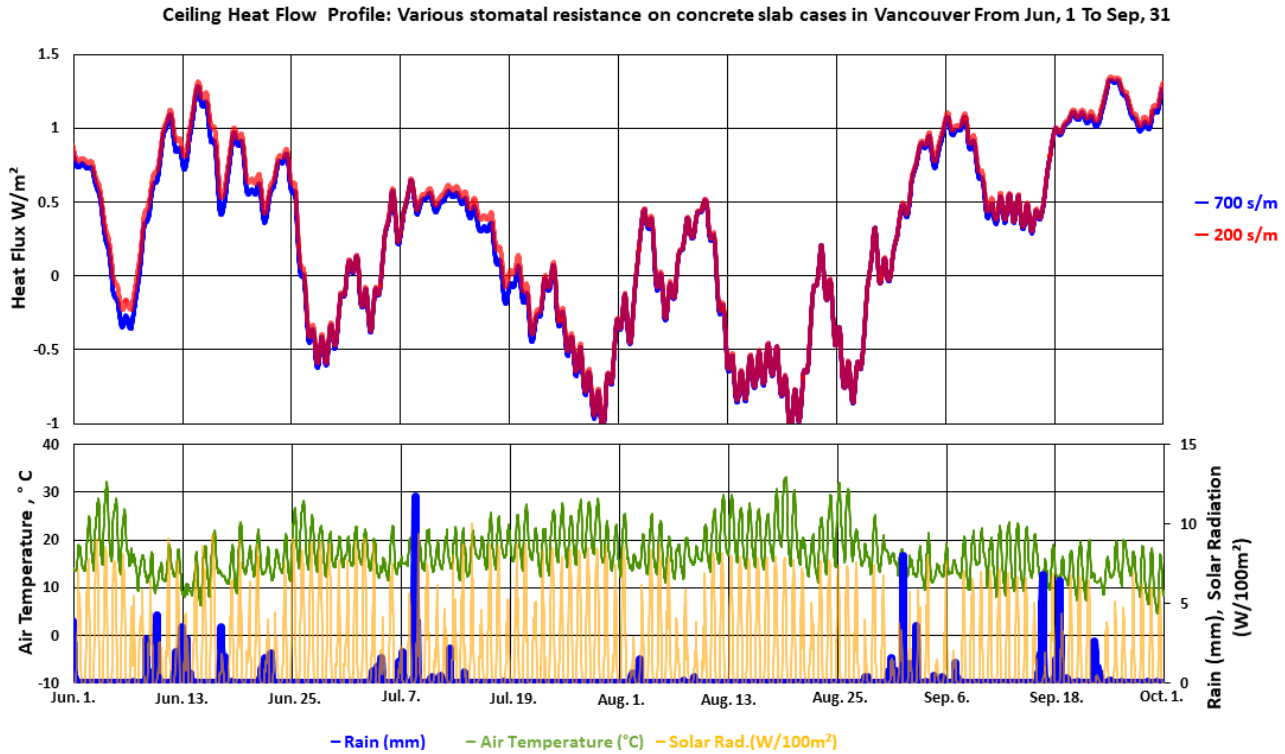


Figure 81. Heat flux through 200 and 700 minimum stomatal resistance sedums planted green roofs in summer in Vancouver.

7.5.6 Plants height

Plants height is an essential variable in sensible and latent heat calculation. With regard to sensible heat, height is a base to determine the resistance of foliage to wind flow and following sensible heat transfer. In latent heat determination, plants height is one of the parameters that is required to calculate atmospheric resistance to vapour flow and evapotranspiration rate. The simulation results for plant heights of 2 cm to 15 cm are plotted in Figures 82 and 83. In the case of plants with higher height, the temperature at the bottom of the soil is relatively lower, and the corresponding heat flow is higher due to the higher sensible and latent heat flows.

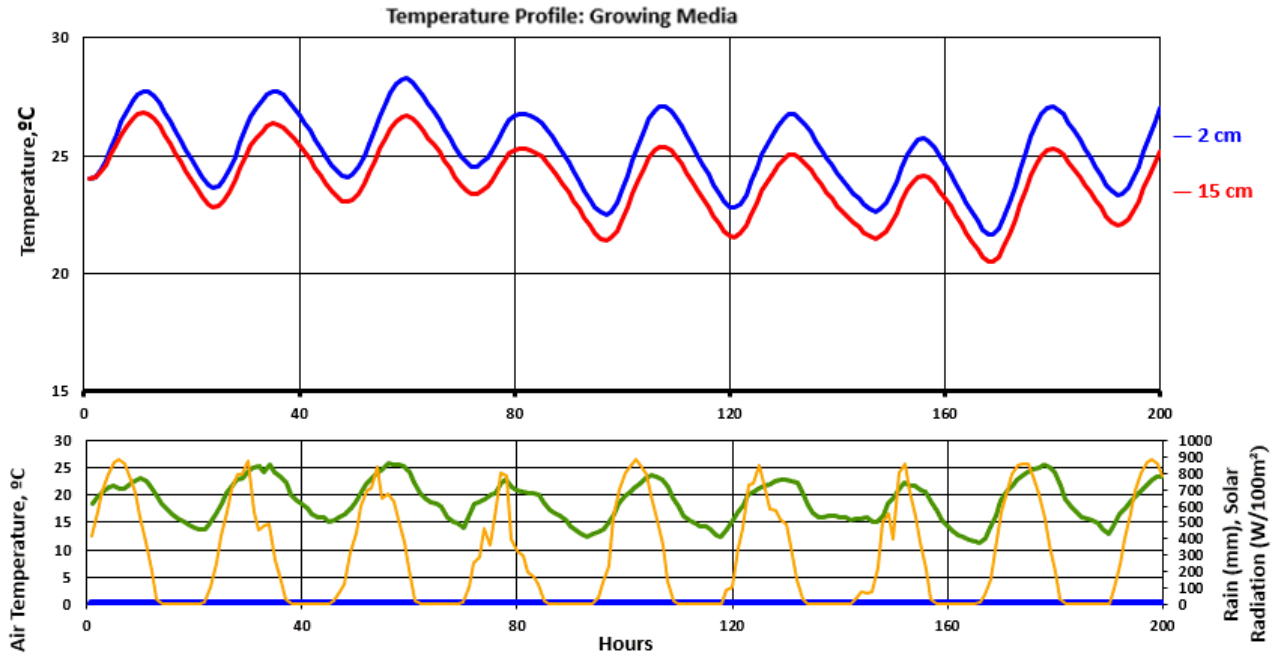


Figure 82. Plants height impact on the growing media temperature.

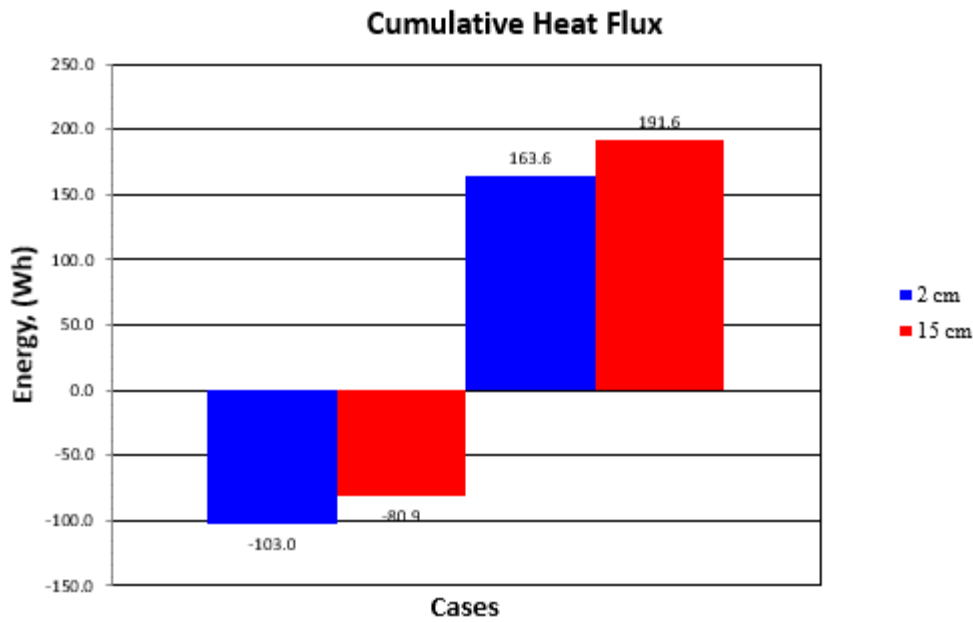


Figure 83. Plant height impact on heat flux.

7.5.7 Density and heat capacity

Density and heat capacity are used in the HAMFit-GR model to estimate thermal mass. The density and heat capacity of growing media mixtures that are used in the green roof design vary from 600 kg/m³ to 1500 kg/m³ and 1000 J/kgK to 1800 J/kgK, respectively. Therefore, two runs are prepared with minimum density and heat capacity as well as maximum density and heat capacity. Figures 84 and 85 compare the growing media temperature and heat flux. Soil with high thermal mass absorbs and retain heat and decreases the amount of heat that can reach the bottom surface of the soil by 6%.

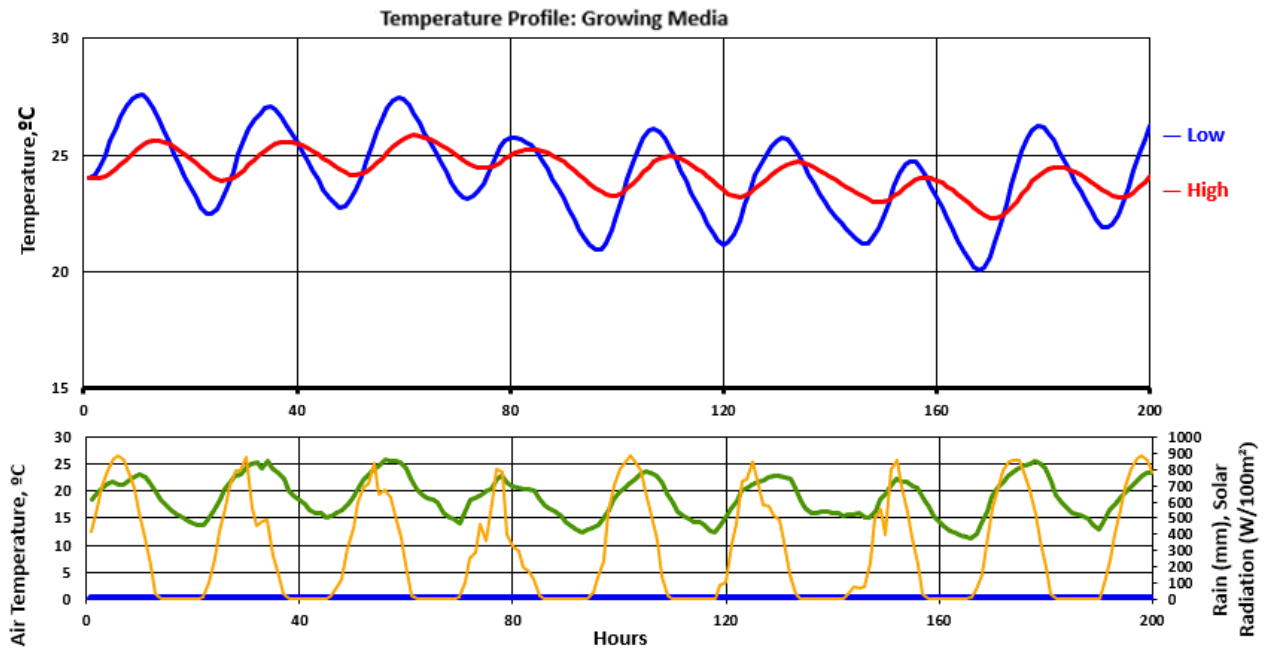


Figure 84. Thermal mass impact on the growing media temperature.

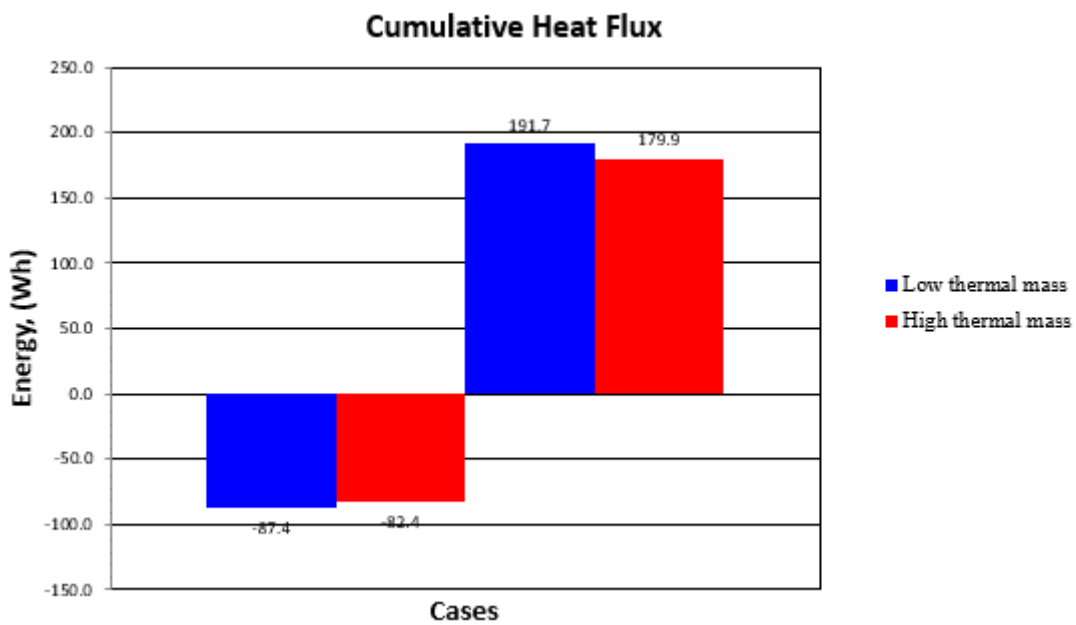


Figure 85. Thermal mass impact on heat flux.

7.5.8 Moisture content

In some models, the moisture content within the growing media is assumed to be constant (near saturation) or lumped. To study the importance of the accurate moisture modelling in a green roof, three cases with a moisture content of 0, 100% and HAMFit-GR approach are studied. Figure 86 illustrates temperature profile in the soil bottom point, and Figure 87 illustrates heat flow at the ceiling surface. In a case of the fully saturated growing media, the temperature stays stable, oppositely, in the dry case, temperature line highly fluctuates between 20 and 28°C. HAMFit-GR approach allows to properly model growing media properties and adjust heat fluxes and temperature profiles. High thermal mass due to water in the growing media reduces heat flow through the soil and keeps the temperature more stable. Therefore, it is essential to estimate water balance accurately. HAMFit-GR calculates soil properties based on moisture content in each point of the growing media layer. For example, 10 cm soil model includes 320 points and for each of them such properties as heat capacity, thermal, liquid and vapour conductivity are calculated.

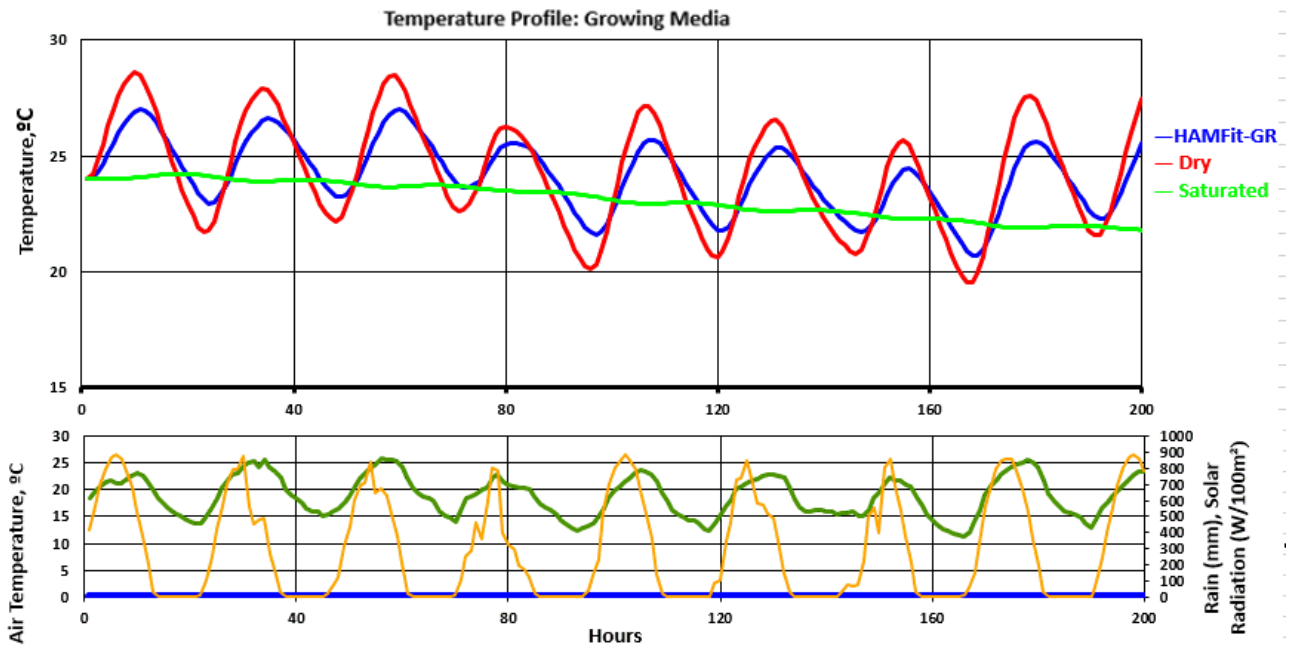


Figure 86. Moisture content impact on the growing media temperature.

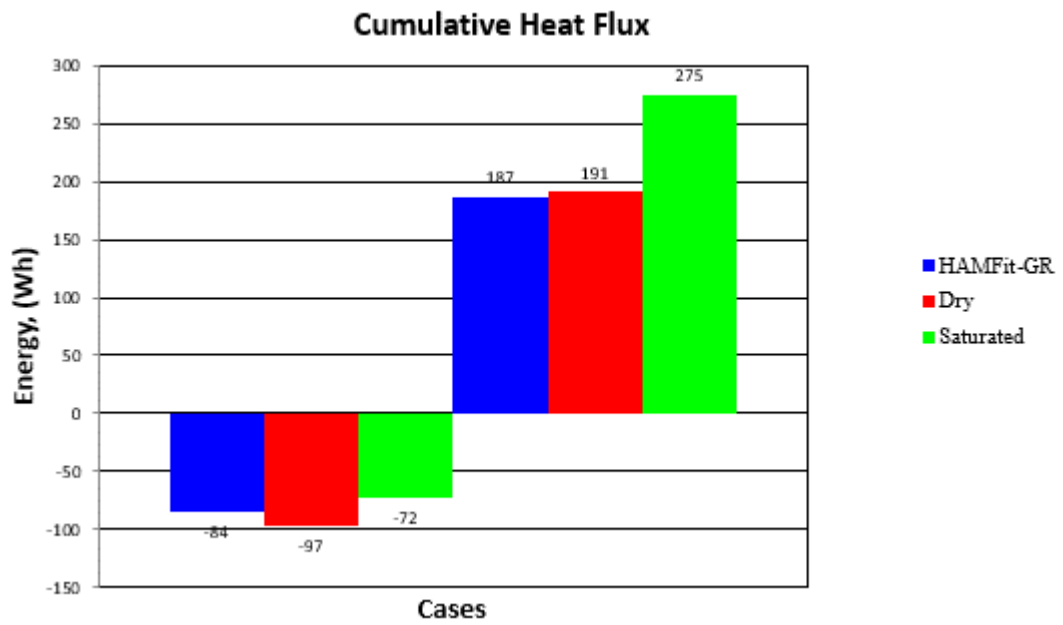


Figure 87. Moisture content impact on heat flux.

7.5.9 Runoff convection

One of the improvements that are made in the HAMFit-GR is the ability to account convective heat transfer associated with water flow through the green roof system during rain events. In the current green roof models, runoff convective heat flow is usually assumed to be negligible; however, in climates with high precipitation amount and periods, it could have an impact on overall model accuracy. With the aim of investigating the impact of convective heat flow, two cases with 0 mm/hr and constant 10 mm/hr rain cases are simulated. As Figure 88 shows, the temperature difference between the two cases at the bottom of the soil is about 0.25°C and heat flux difference of 4%. The low-temperature difference can be associated with the high insulation level of the roof (R-48), where the roof surface is expected to be low due to reduced upward heat flow. In the cases of roofs with lower insulation values, the effect can be higher.

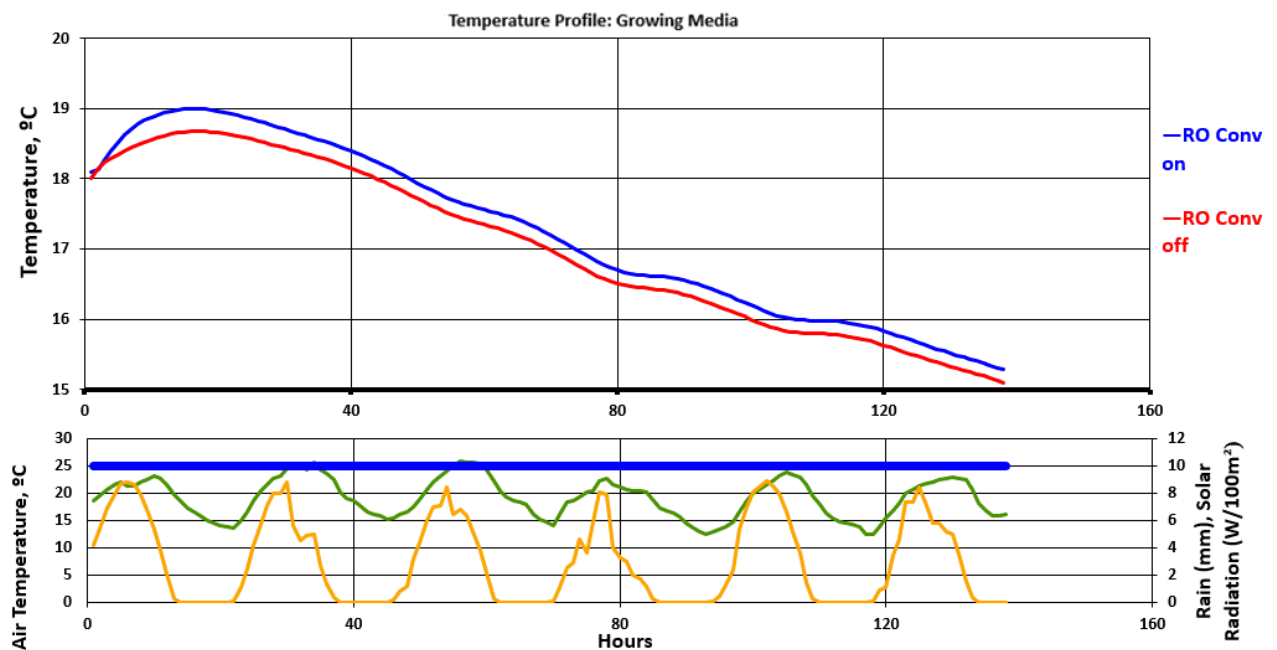


Figure 88. Convective heat flow impact on the growing media temperature.

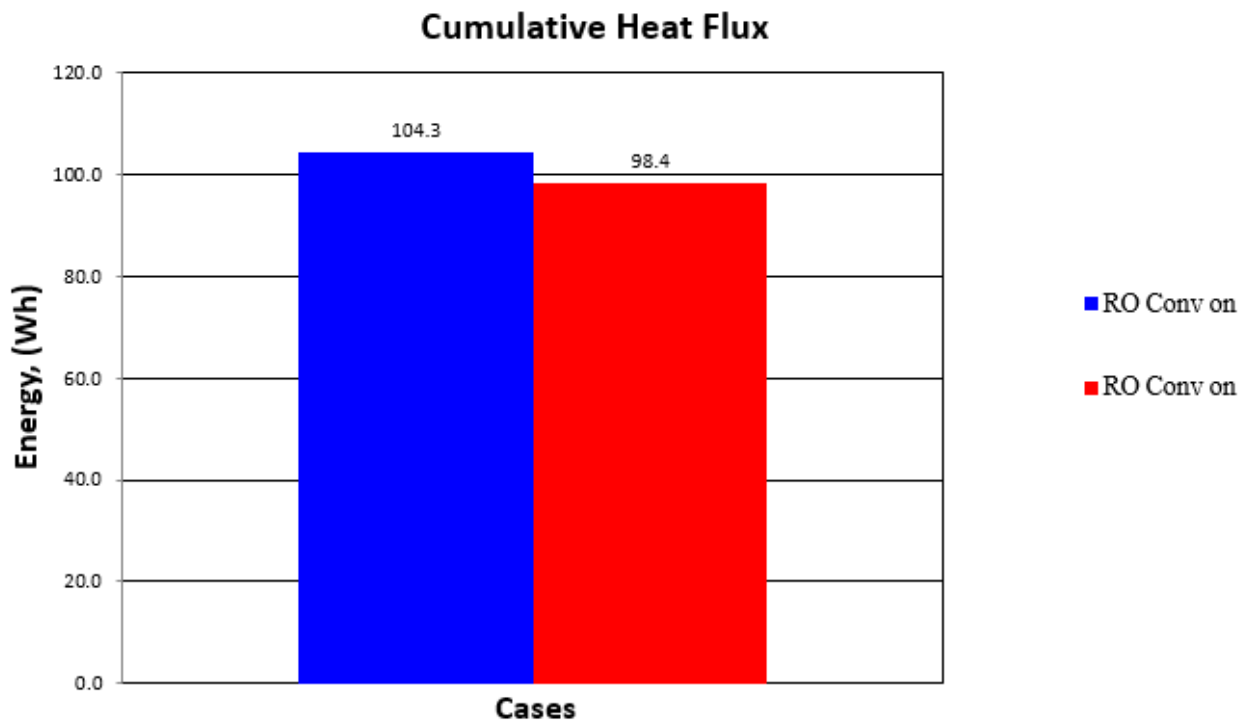


Figure 89. Runoff convection impact on heat flux.

8 MODEL APPLICATION

Since the model is developed and validated, the next step is the application of the model to understand and investigate selected green roof parameters based on whole year simulations. The parameters that are considered for the study include climate, insulation level of the roof deck, type of roof deck and the thickness of growing media. For each parameter, two or three options are considered:

- Roof: With and without a green roof
- Climate: Vancouver; Toronto; Winnipeg.
- Impact of insulation: Non-insulated (low insulated); medium –R33; High –R60.
- Impact of roof system: lightweight and mass roof systems
- Soil thickness: 10 cm; 15 cm; 20 cm.

8.1 Comparison of conventional and green roof systems (Energy)

Green roofs are often proposed as an option to improve the energy performance of a building. In this section simulation cases with and without a green roof are compared to various seasons, climates and insulation amounts.

8.1.1 Green roof performance in mild temperature and wet climate: Vancouver

The base case is assumed to be 6" (15 cm) concrete roof with 6" (15 cm) XPS insulation covered by asphalt shingles or by a green roof system. The first question to answer is how a green roof influences the energy flow in a roof in different seasons and its impact on the system yearly energy performance. As the reference year, 2016 is selected for all three climates. Figure 90 shows a comparison of heat leaving the room from January to December. Green roof damps the heat flux line due to the additional thermal mass of soil and water held in it. Figures 91 and 92 illustrate, the time series and monthly

total heat fluxes in the conventional roof and the roof with vegetation in Vancouver in February as a reference winter month. As a result of the added green roof, heat losses are reduced by 11% in Vancouver.

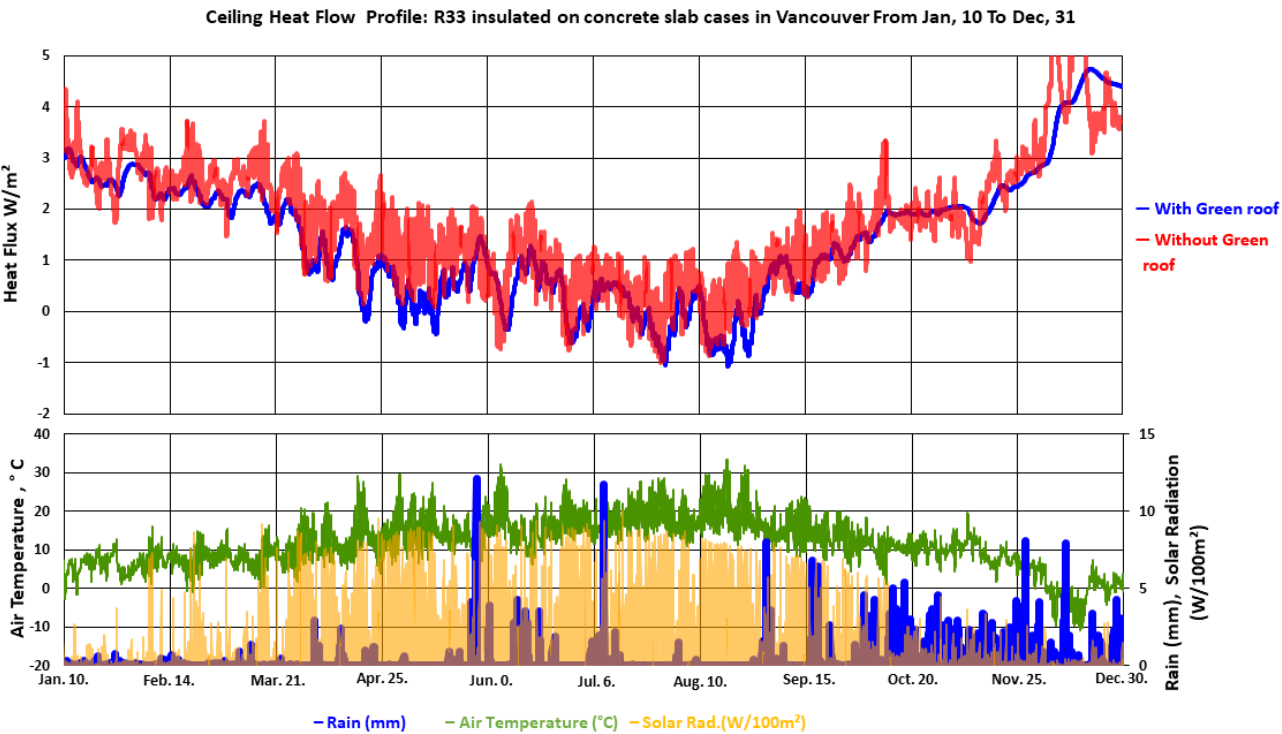


Figure 90. Heat flux through the R33 insulated roof in Vancouver.

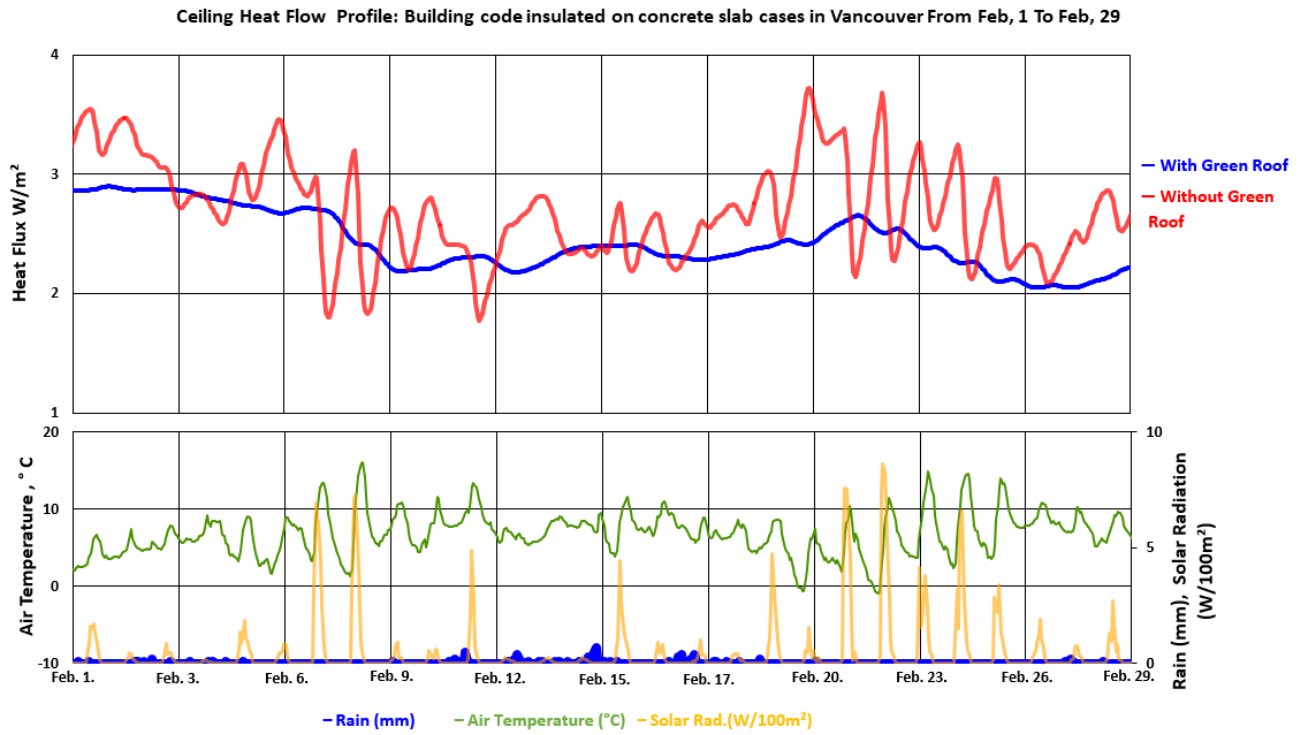


Figure 91. Heat flux through the R33 insulated roof in Vancouver in February.

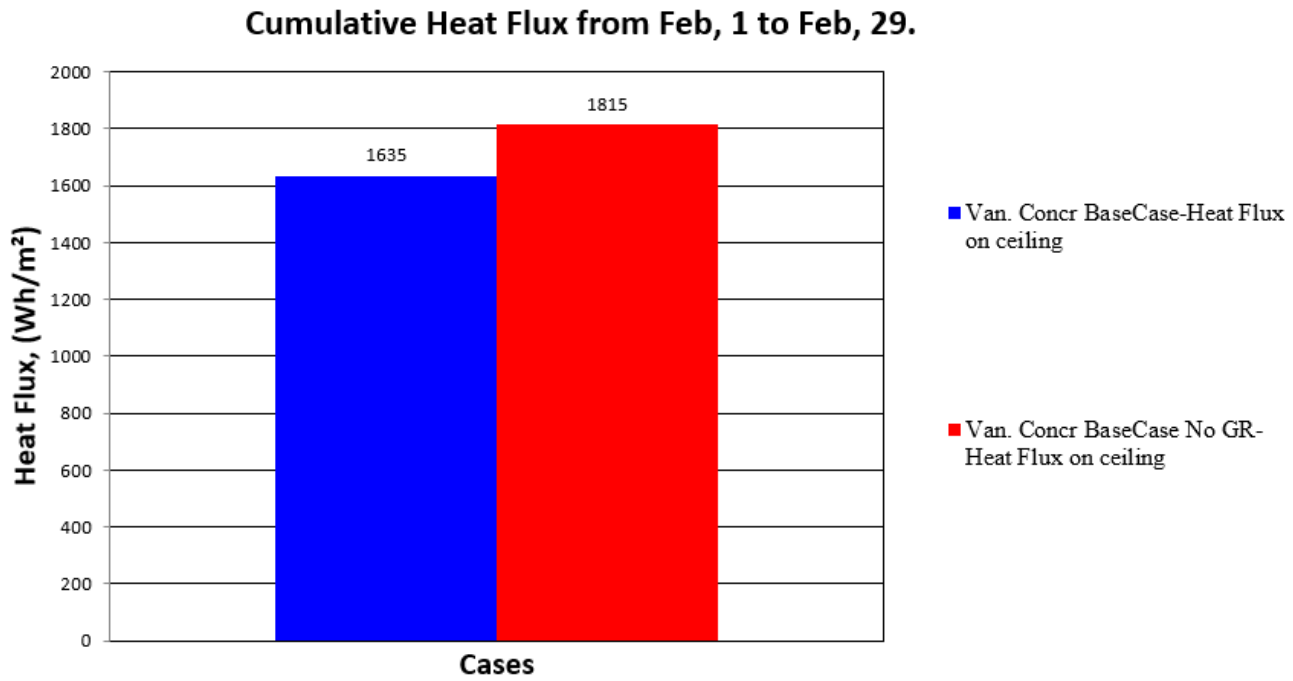


Figure 92. Energy consumption in Vancouver in February – R33-insulated concrete roof.

The green roof presence in the summertime similarly has “dumping” effect on the heat flow line as shown in Figures 93 and 94. In the mild Vancouver climate where summer temperatures are around 20°C and the indoor temperature is assumed to be maintained at 22°C, heat flow lines fluctuate near zero-line and savings due to a green roof are only noticeable during nights because of additional insulation and thermal mass green roof effects. During the whole summer, the green roof reduces heating load from 1243 Wh/m² to 572 Wh/m² and cooling load from 438 Wh/m² to 155 Wh/m² (Table TT).

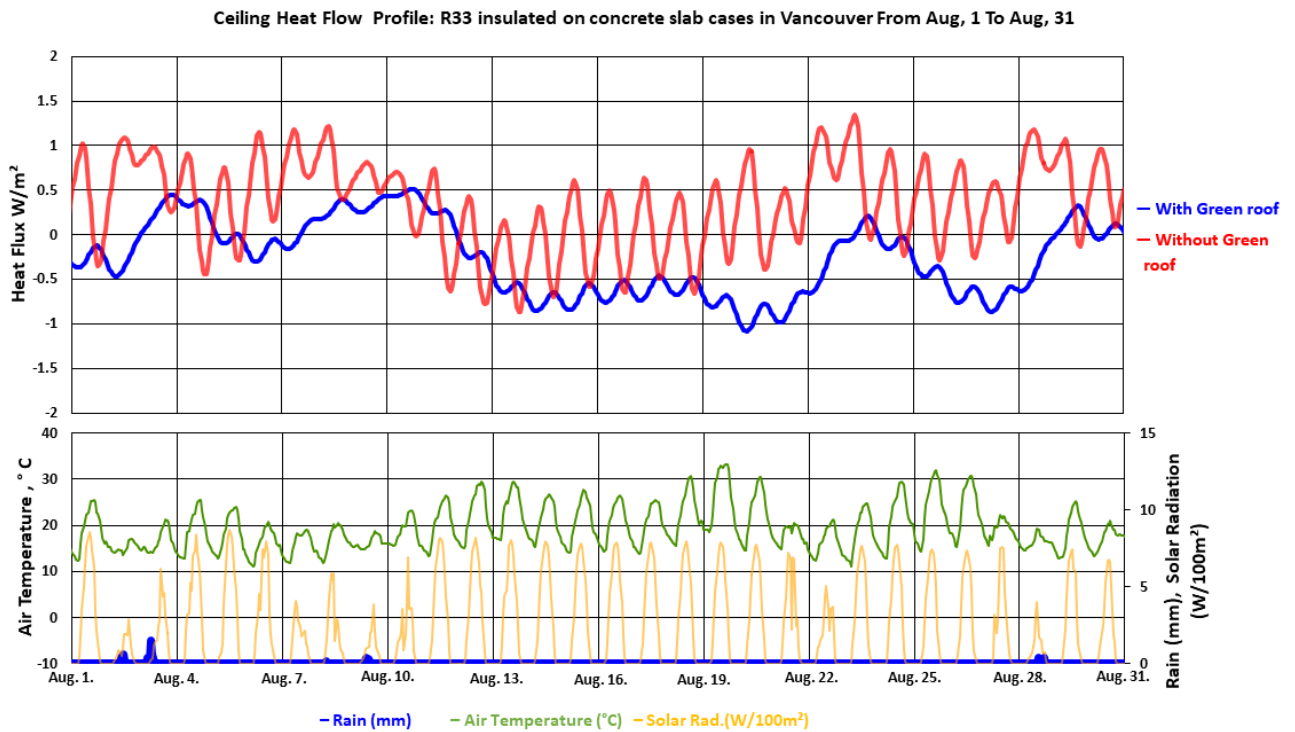


Figure 93. Heat flux through building code insulated roof in Vancouver in August.

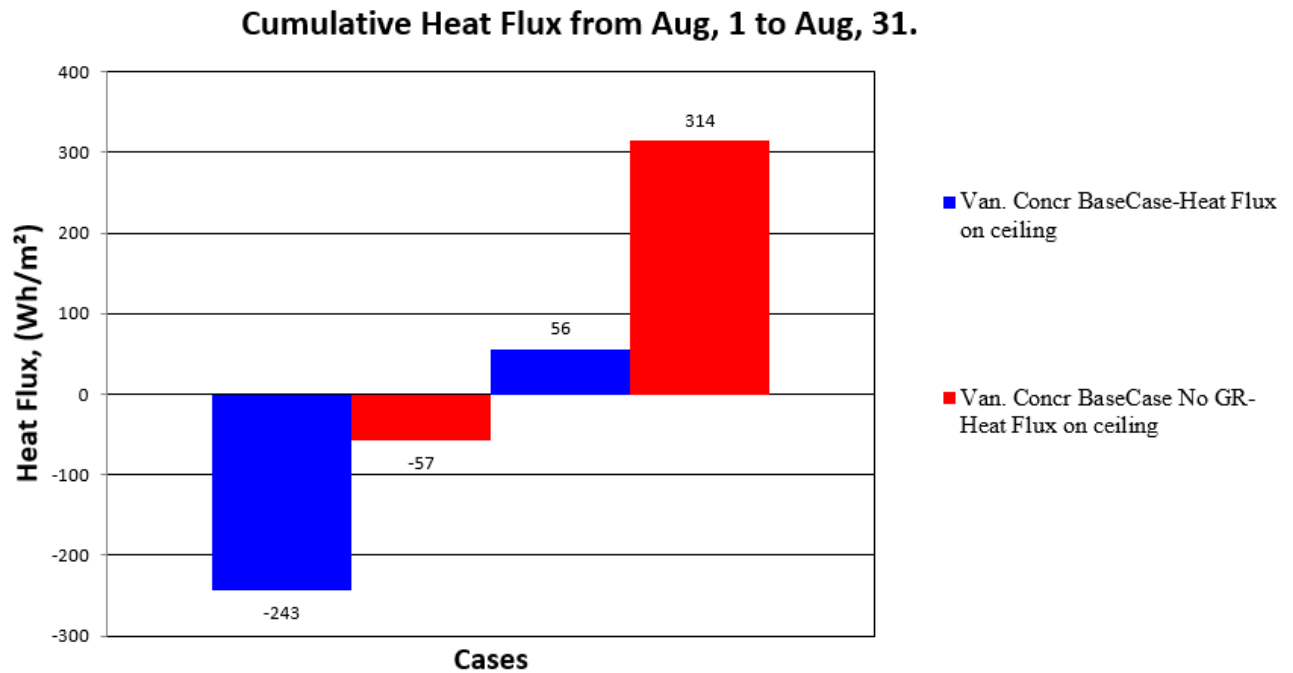


Figure 94. Energy consumption in Vancouver in August– R33-insulated concrete roof.

8.1.2 Green roof performance in cold and hot summer climates: Toronto

Besides Vancouver climate, the energy performance of the same roof in Toronto and Winnipeg climates are performed. The runs include non-insulated, R33 and R60 insulated roofs with and without a green roof; simulation results are summarized in Tables 7 and 8. Figure 95 shows heat flux through the roof throughout the year in Toronto. The general effect of green roof installation remains the same as in Vancouver: additional thermal mass and extra insulation on the top of the roof dumps the heat flux line allowing to save heat in the winter and middle seasons as well as avoid excessive heat gain in summer. Figure 96 compares cases with and without a green roof in Toronto respectively. In February in Toronto, green roof installation reduces heat losses by up to 14%. In summertime in Toronto, by evapotranspiration, radiative properties of a green roof excessive heat gain decreased by 38 %.

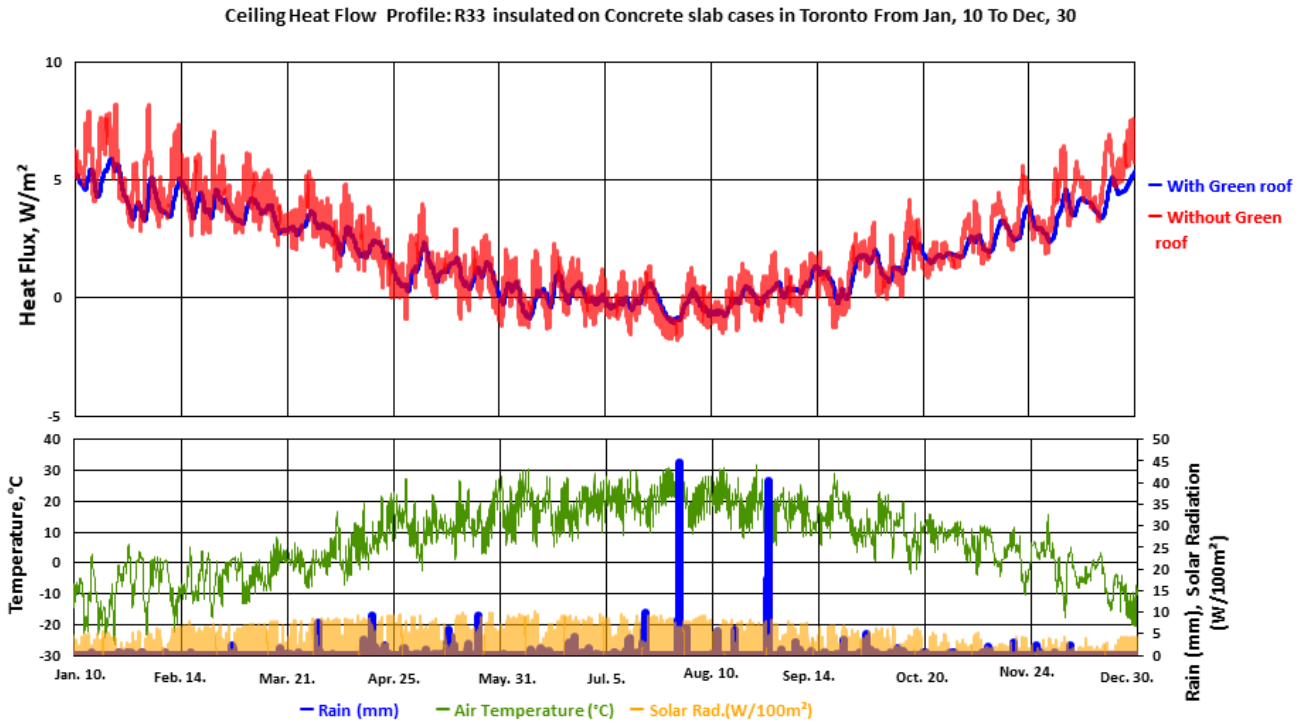


Figure 95. Heat flux through the R33 insulated roof in Toronto.

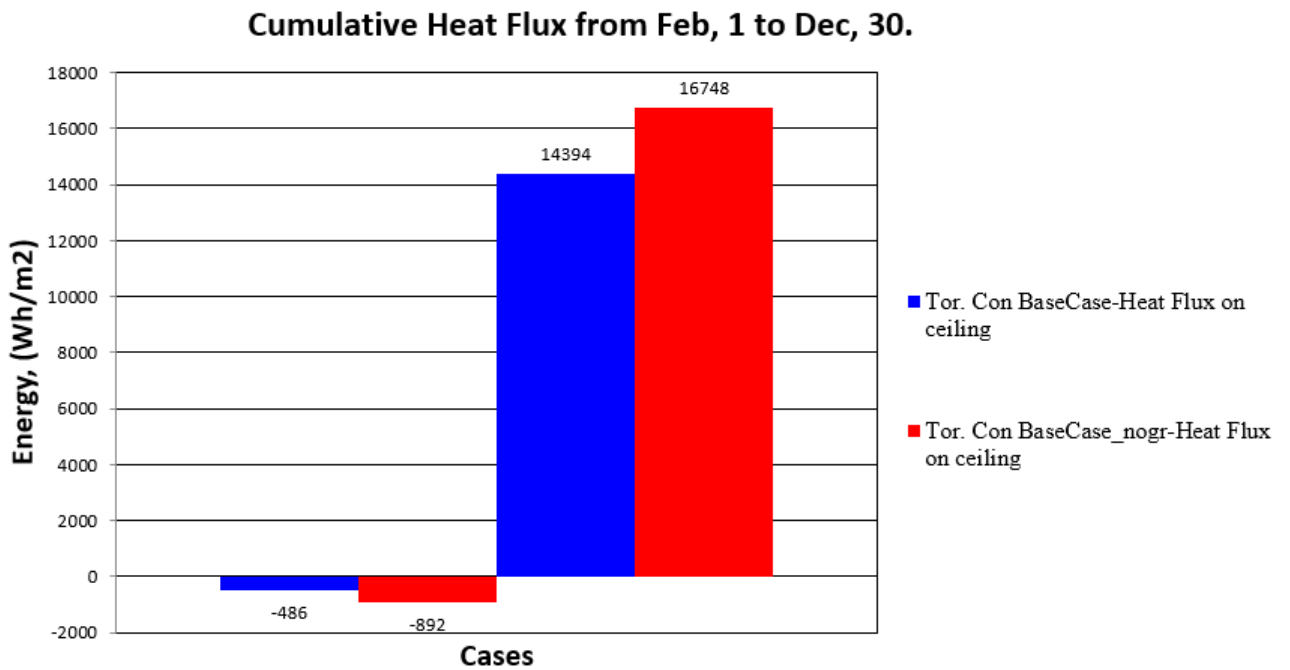


Figure 96. Energy consumption in Toronto – R33 insulated concrete roof.

8.1.3 Green roof performance in non-insulated and high-insulated roofs

Besides new construction, a green roof system could be applied to an existing building. To evaluate a retrofit green roof application a case comparing 6" (15 cm) concrete roof covered by asphalt shingles and with a green roof is calculated. Figure 97 shows heat flux on the ceiling. As it is expected, the heat flow in the uninsulated roof is significantly higher than the reference roof, and the effect of thermal insulation and mass of the green roof is more noticeable. Bar charts showing overall heat through the roof is plotted in Figure 98. Therefore, green roofs might be an applicable option during building renovation. Moreover, a case called high-insulated with doubled XPS layer (R60) is simulated, and results are shown in Figures 99 and 100. Generally, a green roof works as an additional layer of insulation in the all three cases: non-insulated, R33 and R60 insulated, with the more significant thermal performance improvement on the less original insulated case. In Vancouver, adding a green roof above non-insulated concrete roof drops energy consumption by 85% in both heating and cooling load; however, in a case of R60 insulated roof, energy consumption can be reduced by 23% (Table 7).

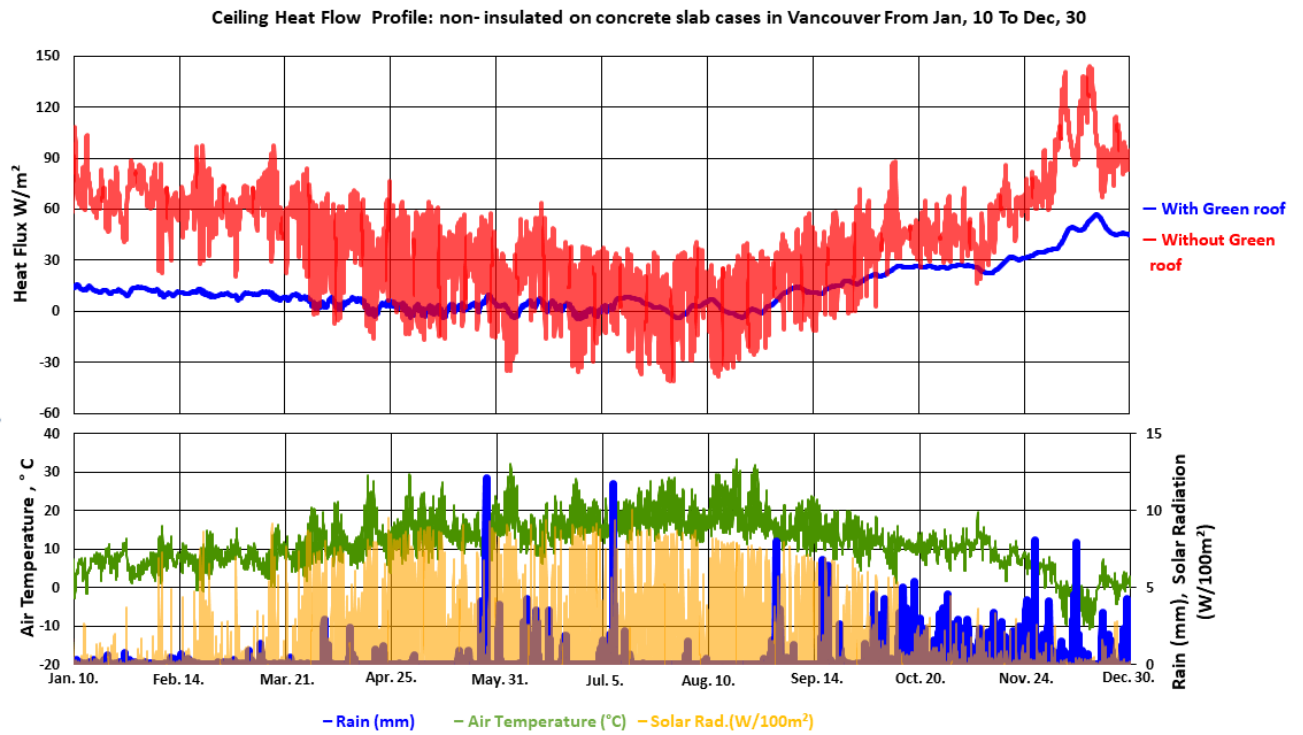


Figure 97. Heat flux through the non-insulated roof in Vancouver in 2016.

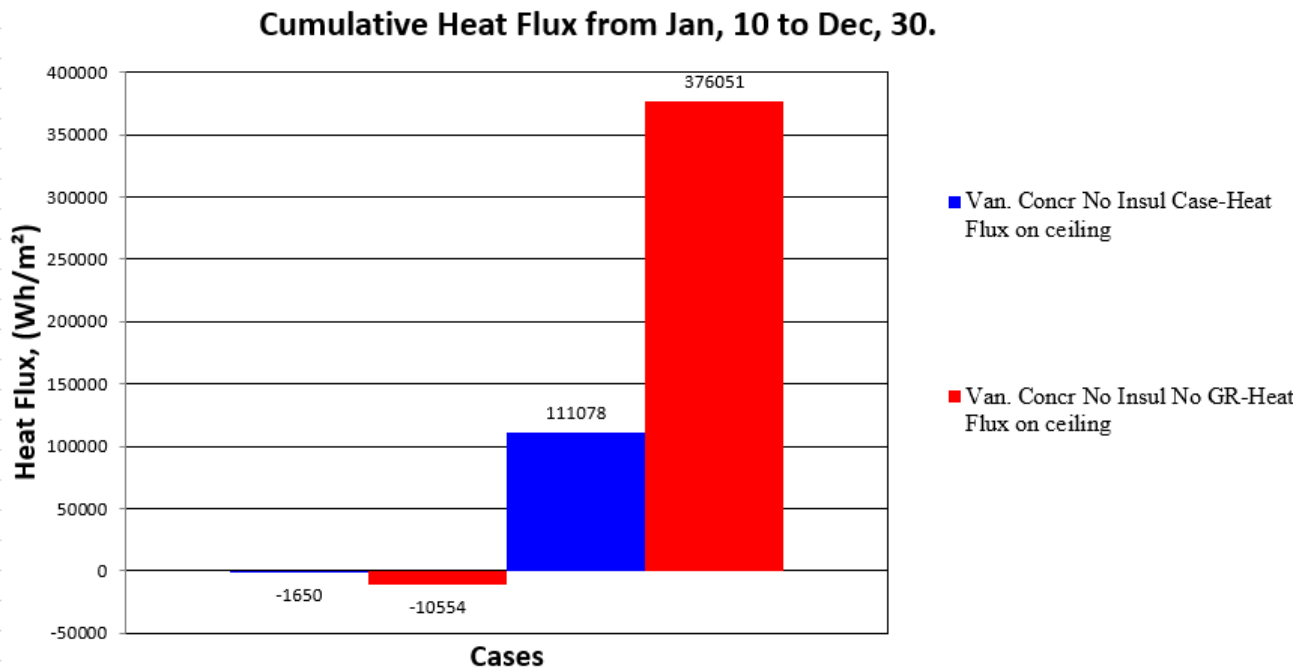


Figure 98. Energy consumption in Vancouver – non-insulated concrete roof.

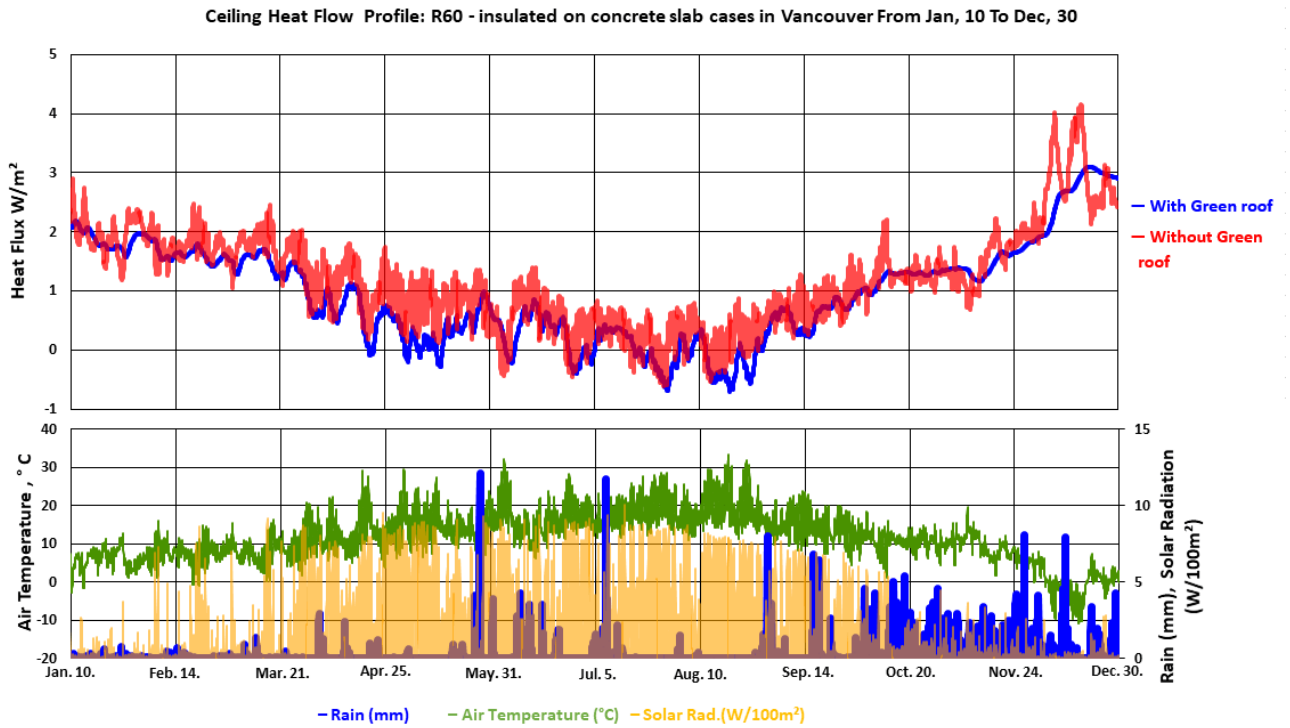


Figure 99. Heat flux through the R60-insulated roof in Vancouver.

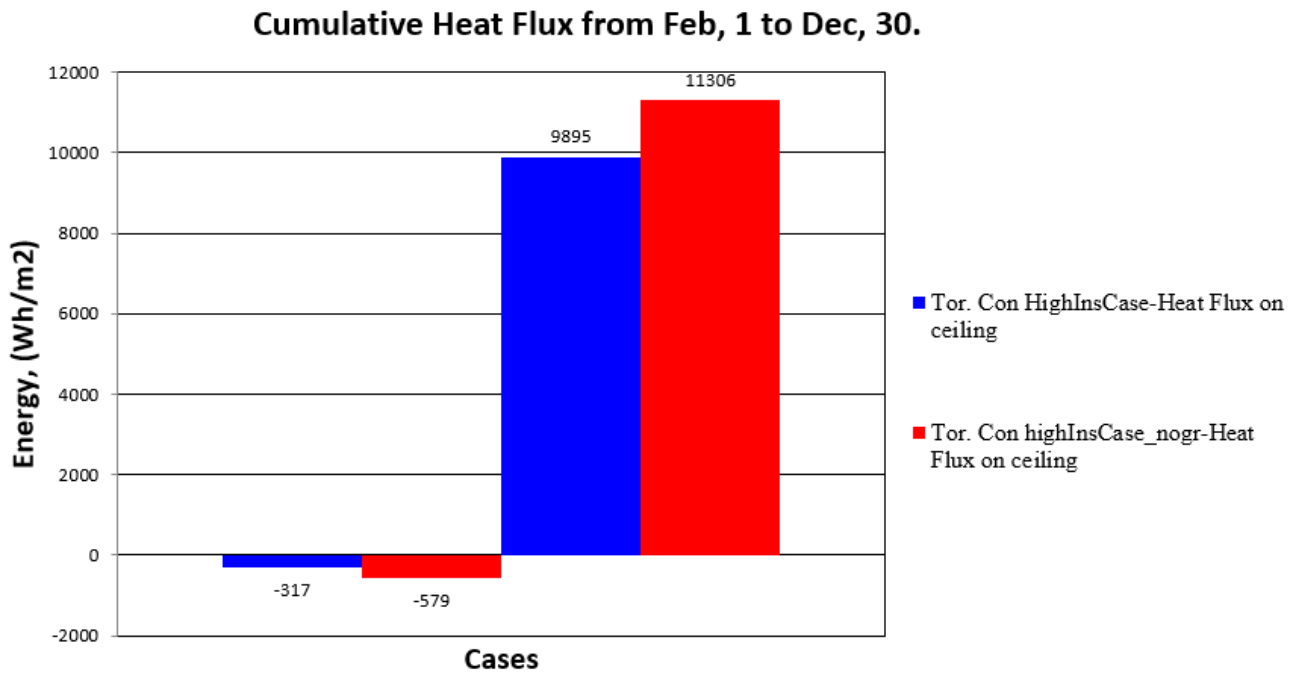


Figure 100. Energy consumption in Vancouver – R60-insulated concrete roof.

8.1.4 Green Roof performance in lightweight roof system: wood-frame roof

Wood-frame roof cases are modelled for non-insulated, R33 and R60 insulated roofs in Vancouver and Winnipeg climate similarly with shingles and a green roof system. Figures 101-104 illustrate heat flux through the roofs and overall energy consumptions. In this case, the thermal mass of a roof itself is less because a concrete slab is substituted by wood and heat flux daily fluctuations are higher in both cases with and without a green roof. However, a structure with green roof shows similar to the earlier case behaviour of additional thermal mass and insulation in throughout the year and evapotranspiration phenomena in the summertime. Cases combining different climates, insulation and frames are included in Appendix A.

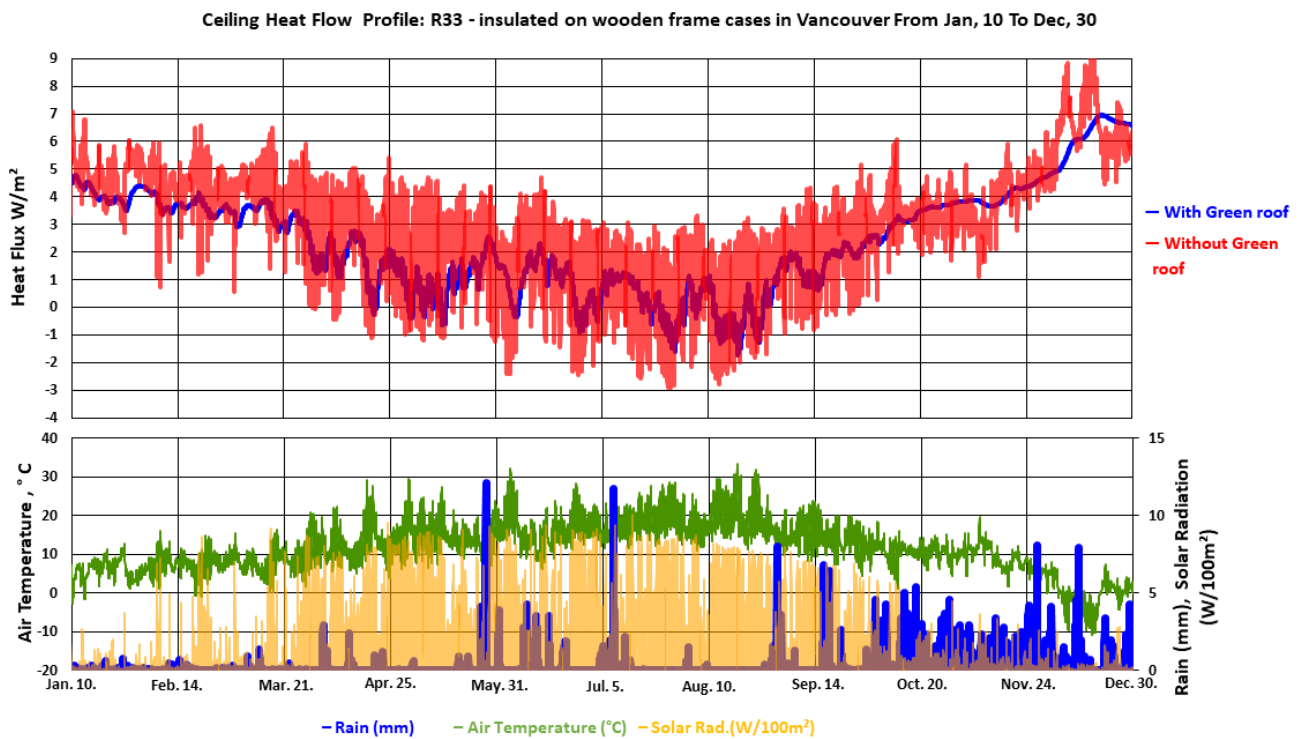


Figure 101. Heat flux through the R33 insulated roof in Vancouver.

Cumulative Heat Flux from Jan, 10 to Dec, 30.

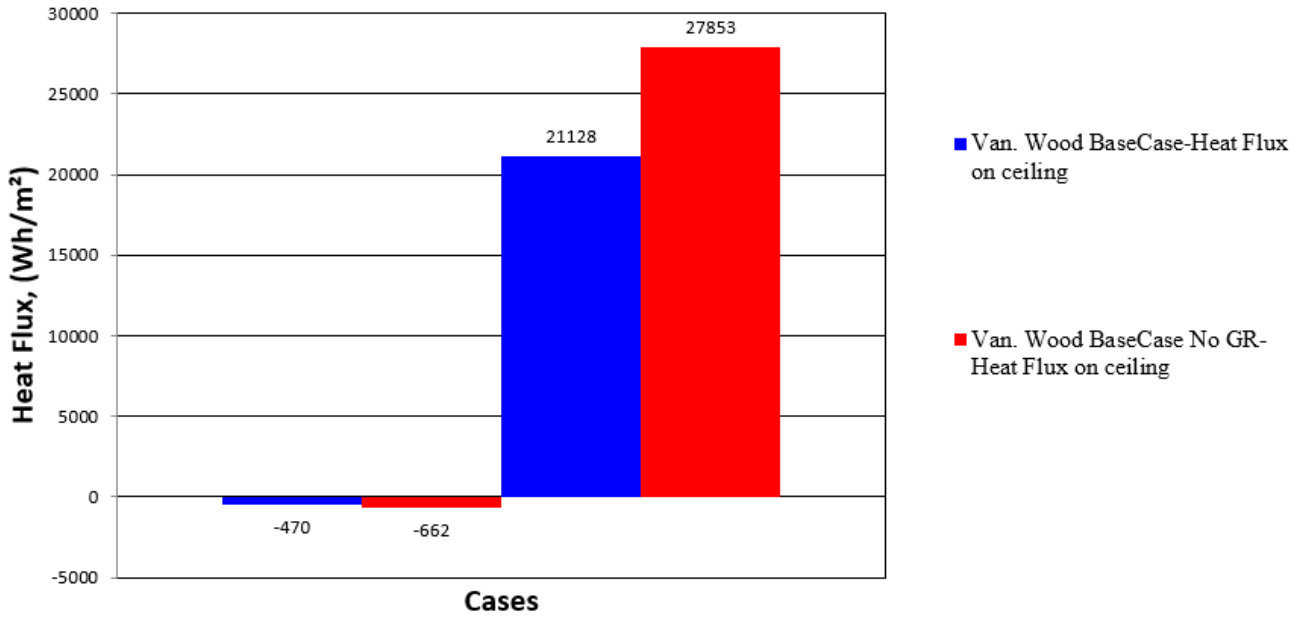


Figure 102. Energy consumption in Vancouver – R33-insulated wood frame roof.

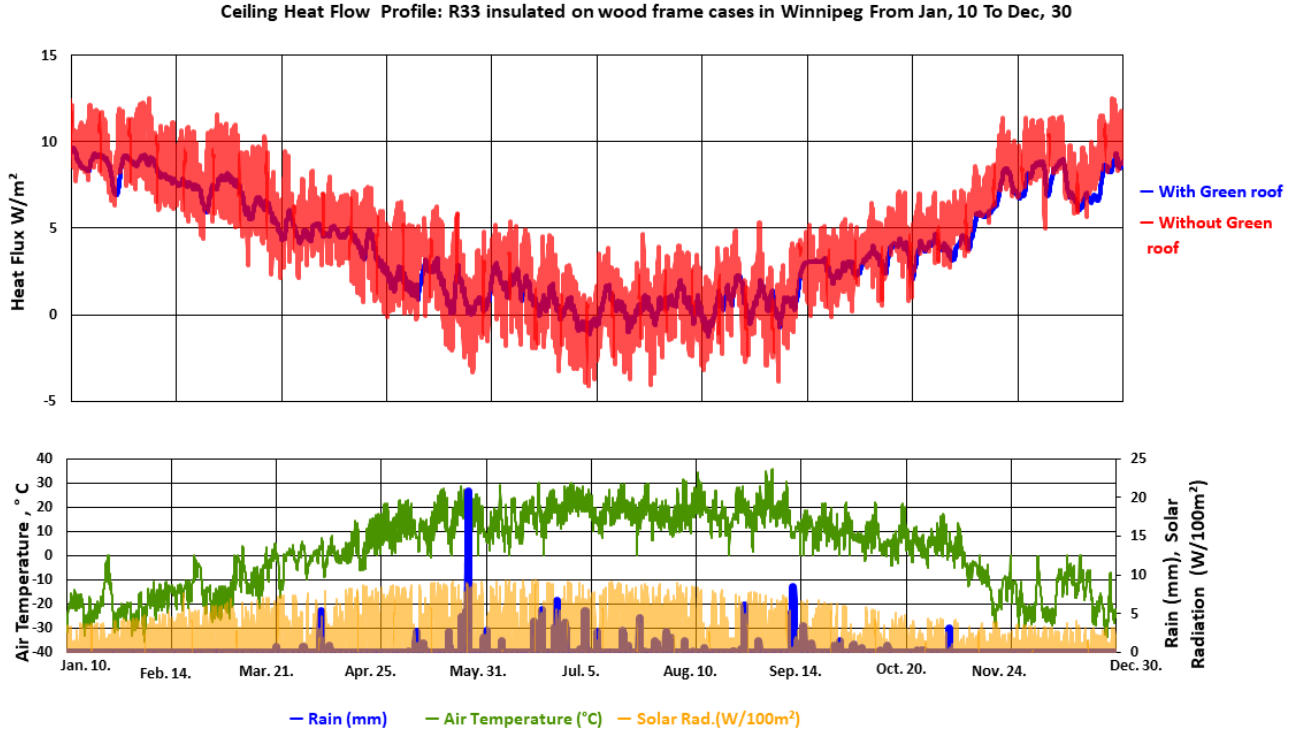


Figure 103. Heat flux through the R33 insulated roof in Winnipeg.

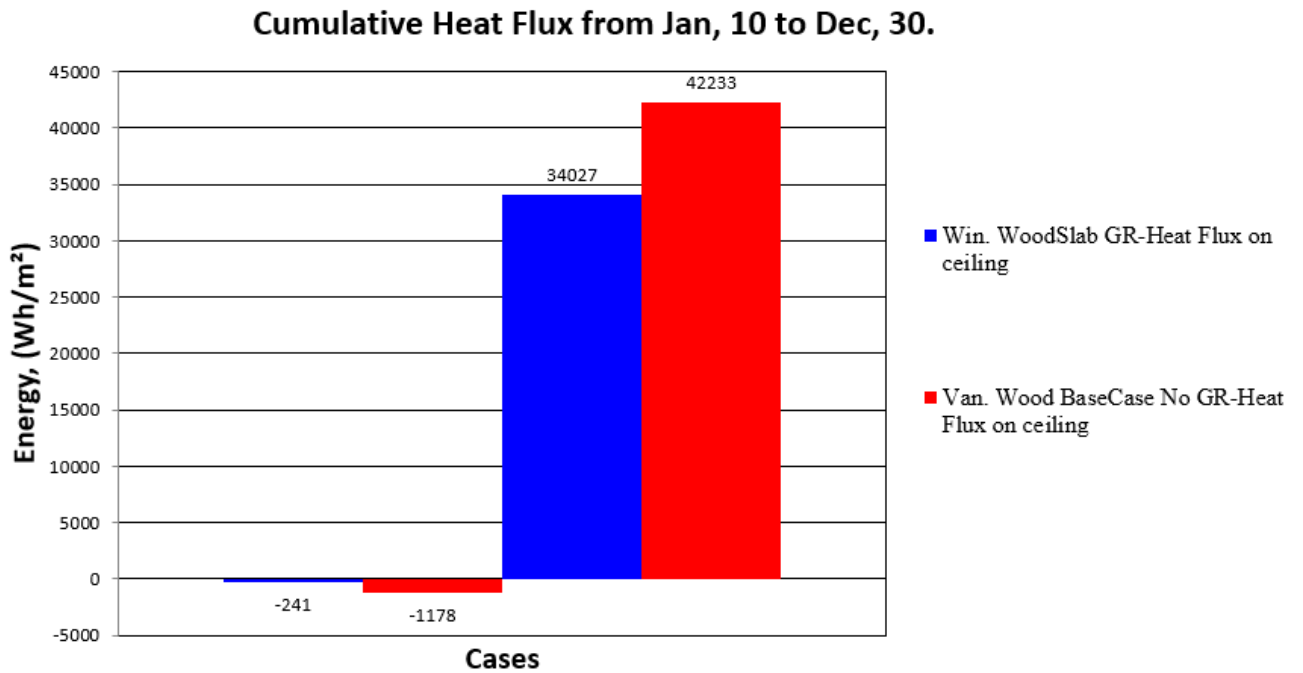


Figure 104. Energy consumption in Winnipeg in 2016.

8.1.5 Comparison of conventional and green roof systems summary

The simulation results are summarized in Tables 7 and 8. Tables are divided into heating and cooling loads by months representing seasons which are winter (February 1 to March 1), spring (April 1 to May 1) and summer (July 1 to August 1). Green roofs reduce heating loads in all climates and insulation levels; however, additional savings due to a green roof reduce with higher insulation: from 80% heating load reduction for concrete non-insulated roof during winter months in Vancouver to 7% for R60 insulated roof and from 83% to 12% in Toronto. It is also found that green roof is efficient as an insulator during spring periods in all three climates because the growing media layer is not frozen and work as additional thermal mass dumping heat fluxes.

Table 7. Energy consumption summary – concrete frame.

#	Base case Compared case	Heating						Cooling				Total (Jan 10- Dec 31)			
		Winter (Feb)		Spring (Apr)		Summer (Jul)		Spring (Apr)		Summer (Jul)		Heating		Cooling	
		Energy	%	Energy	%	Energy	%	Energy	%	Energy	%	Energy	%	Energy	%
1	Vancouver Non-insulated w/o green roof	45266		27156		9125		196		3297		376051		10554	
	Vancouver Non-insulated with green roof	7614	83.18	2749	89.88	2505	72.55	76	61.22	169	94.87	111078	70.19	1650	84.37
2	Vancouver R33-insulated w/o green roof	1882		1110		310		0		104		15426		466	
	Vancouver R33-insulated with green roof	1689	10.26	642	42.16	140	54.84	0		60	42.31	12622	18.17	155	66.81
3	Vancouver R60-insulated w/o green roof	1274		751		208		0		36		10369		311	
	Vancouver R60-insulated with green roof	1163	8.71	445	40.75	95	54.33	0		38	-5.56	8569	17.36	91	70.74
4	Toronto Non-insulated w/o green roof	76435		37160		3985		0		10826		403221		32798	
	Toronto Non-insulated with green roof	12661	83.44	6506	82.49	352	91.17	0		1107	89.77	67381	83.28	2824	91.39
5	Toronto R33-insulated w/o green roof	3319		1560		98		0		342		16748		892	
	Toronto R33-insulated with green roof	2845	14.28	1354	13.21	51	47.96	0		190	44.44	14394	14.06	486	45.52
6	Toronto R60-insulated w/o green roof	2244		1059		62		0		223		11036		579	
	Toronto R60-insulated with green roof	1955	12.88 ²	1005	5.1	34	45.16	0		125	43.94	9895	12.46	317	43.44

Table 8. Energy consumption summary – wooden frame.

#	Base case Compared case	Heating						Cooling				Total (Jan 10- Dec 31)			
		Winter (Feb)		Spring (Apr)		Summer (Jul)		Spring (Apr)		Summer (Jul)		Heating		Cooling	
		Energy	%	Energy	%	Energy	%								
1	Vancouver R20-insulated w/o green roof	7459		4707		1860		74		661		36461		2167	
	Vancouver R20-insulated with green roof	4595	38.4	1792	61.93	487	73.82	22	70.27	303	54.16	17267	52.64	1308	39.64
2	Vancouver R33-insulated w/o green roof	3303		2083		908				205		16084		645	
	Vancouver R33-insulated with green roof	1889	42.81	1149	44.84	360	60.35			106	48.29	11373	29.29	469	27.29
3	Vancouver R60-insulated w/o green roof	1869		1277		607				56		9779		151	
	Vancouver R60-insulated with green roof	1755	6.1	976	23.57	441	27.35			30	46.43	7460	23.71	137	9.27
4	Winnipeg R20-insulated w/o green roof	15498		7849		1311				1312		63416		2909	
	Winnipeg R20-insulated with green roof	9911	36.05	4803	38.81	670	48.89			343	73.86	39442	37.8	696	76.07
5	Winnipeg R33-insulated w/o green roof	6306		3354		645				431		24924		1066	
	Winnipeg R33-insulated with green roof	5462	13.38	2800	16.52	285	55.81			121	71.93	20116	19.29	229	78.52
6	Winnipeg R60-insulated w/o green roof	3529		1965		430				141		14425		310	
	Winnipeg R60-insulated with green roof	3353	4.99	1856	5.55	275	36.05			39	72.34	13099	9.19	51	83.55

8.2 Impact of growing media thickness in green roof performance

After the impacts of a green roof in differ roof systems types are studied, the next question is how the growing media thickness influences on heat flow through the modelled roof. With this aim simulation with various growing media thicknesses (10 cm, 15 cm, 20 cm), climates (Vancouver, Toronto, Winnipeg) and frame types (Concrete, Wood) have been prepared. Figure 105 shows heat flux through the ceiling over the whole year in Vancouver. Generally, thicker soil dumps the heat flux due to higher overall thermal resistance and thermal mass. Thicker growing media layer absorbs a greater amount of water and increases its thermal mass what allows to absorb and release heat from or to the atmosphere with daily fluctuations, what can be seen in Figure 105 during fall and winter season when high rainfalls occur. Therefore, the growing media layer in the green roof structure works as an additional damper which prevents energy exchange with building itself.

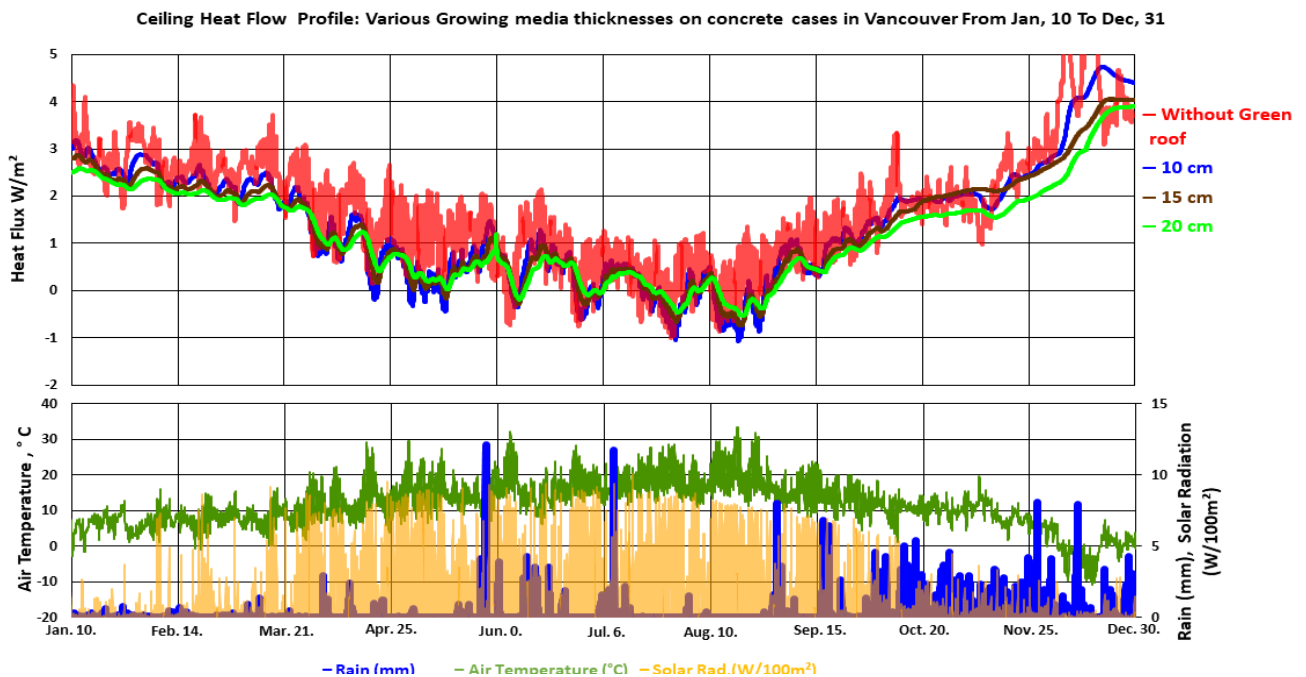


Figure 105. Heat flux through 10, 15, 20 cm green roofs in Vancouver in 2016.

Figures 106 and 107 show heat flow from the internal space through the roof in February in Vancouver. Heat exchange rate decreases with higher soil thickness. Extra 5 cm and 10 cm of soil give 6.5% and 11.8% heat loss reduction, respectively. The heat flux lines are relatively dumped due to the high moisture content within winter – the wet period in Vancouver and high heat capacity (soil and water in the soil). Therefore, thicker soil and corresponding high amount of water in it could absorb and accumulate a more considerable amount of energy. During the whole winter period, heat flux stays negative and varies between 2 and 3 W/m². The same effects can be seen if a green roof is built on a wooden frame (Appendix A). Soil thicknesses increasing results in 9% drop in heat losses; doubling soil thicknesses reduce 17% of heat losses. However, the possibility of 20 cm green roof implementation on wooden frame might be restricted by green roof weight.

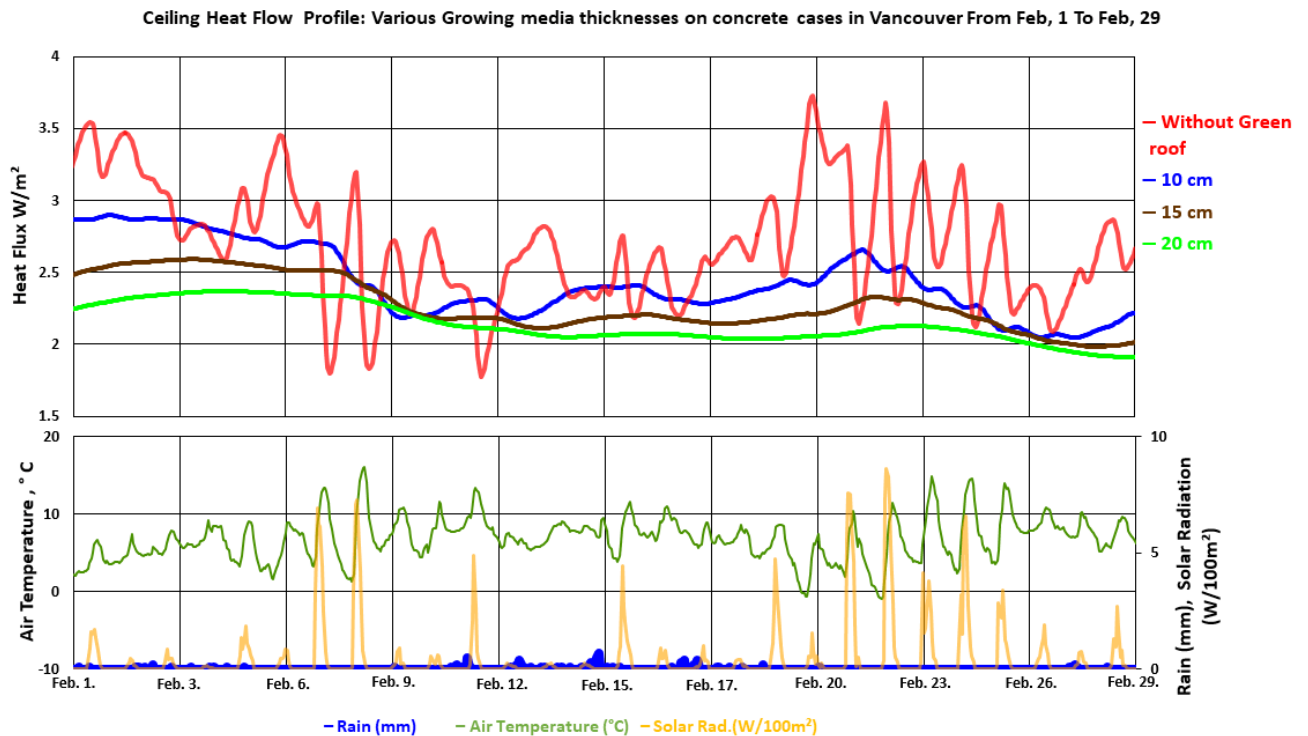


Figure 106. Heat flux through 10, 15, 20 cm green roofs in Vancouver in February.

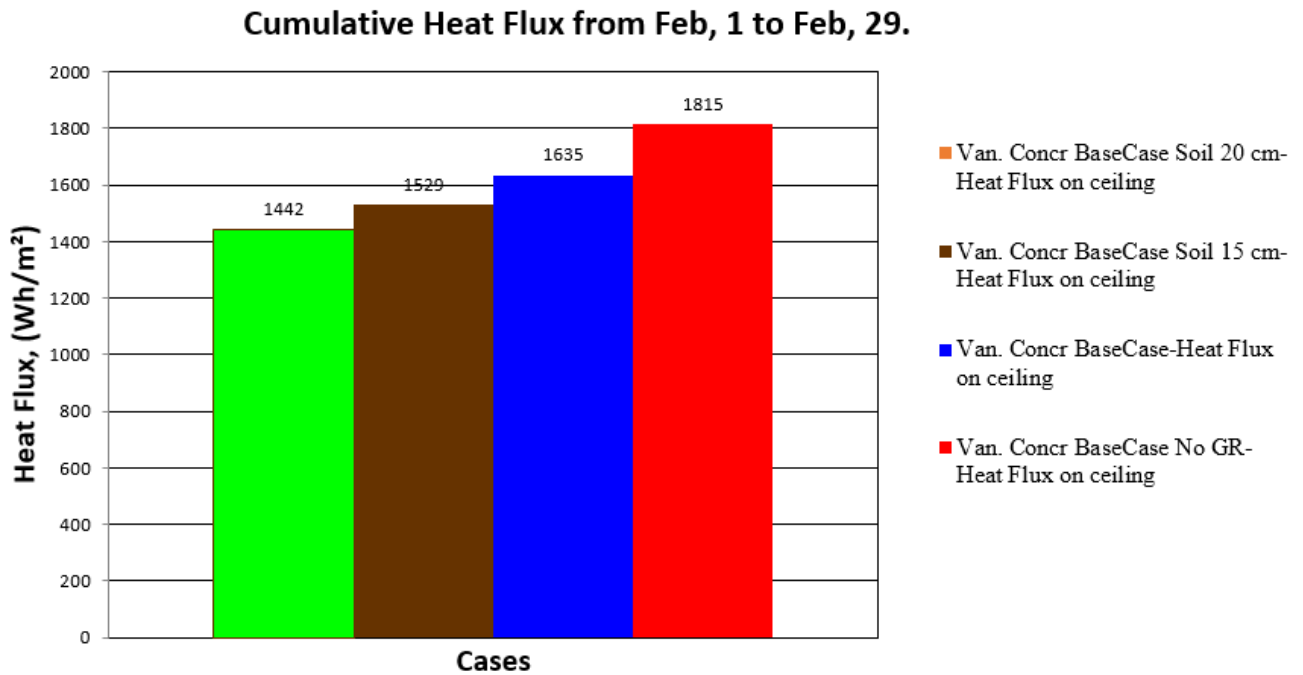


Figure 107. Overall heat left through 10, 15, 20 cm green roofs in Vancouver in February.

May is chosen to represent middle spring season. Figure 108 shows heat flow during this period. 20 cm thick soil layer damps heat flux line on both wooden and concrete cases (wood case is in Appendix A). As a thicker soil as damper a line, because of soil works as additional insulation. Thicker soil layer reduces heat losses during “cold” periods; however, when it is relatively warm outside, thicker growing media layer increases upward heat flux due to higher thermal mass with the lower temperature on the top of a roof slab. Thicker soil layer reduces potential cooling effect in "hot" days. Overall thermal performance during the middle season is affected by soil (insulation thickness). Heat losses were 5% less for 15 cm roof and 7.5% less for 20 cm roof on the wooden frame. Extra 5 cm of the growing media reduces by 7% and extra 10 cm by 12.7%. The dependence is not linear.

After a significant rain event on May 27, heat losses of 10 cm soil case were much higher (black circle on Figure 109). Evapotranspiration phenomenon might explain this effect. On the top

surface of any soil thickness evapotranspiration heat flow is relatively equal, but green the roof dumping effect on heat flow is less due to smaller growing media thickness.

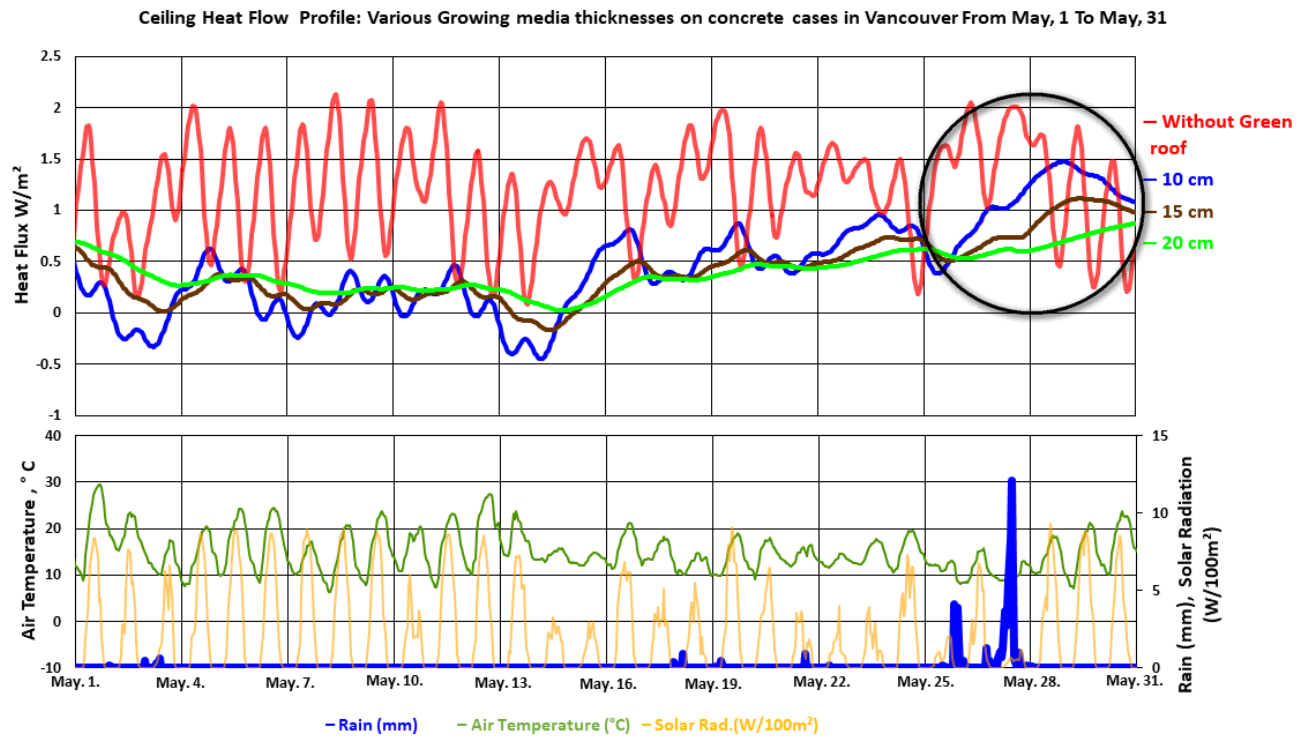


Figure 108. Heat flux through 10, 15, 20 cm green roofs in Vancouver in May.

In July, 20 cm soil line is dumped. Figure 109 and 110 illustrate various dimensions of a roof energy performance in the summertime. All types of green roofs have the cooling effect or reduce incoming heat; therefore, green roof implied on a building in Vancouver can keep heat flow through the roof near zero. In Vancouver, the second part of 2016 summer is characterized as dry period, and the model shows that cooling ability of green roof through evapotranspiration is reduced.

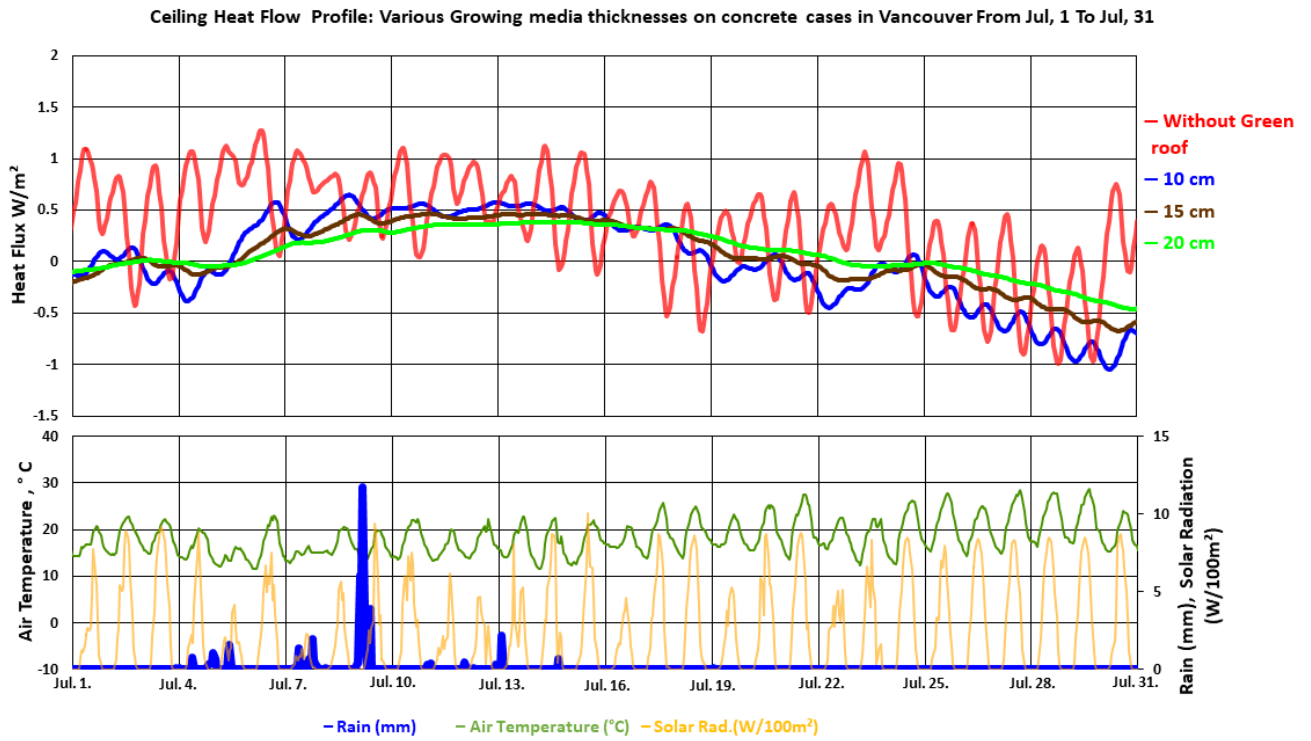


Figure 109. Heat flux through 10, 15, 20 cm green roofs in Vancouver in July.

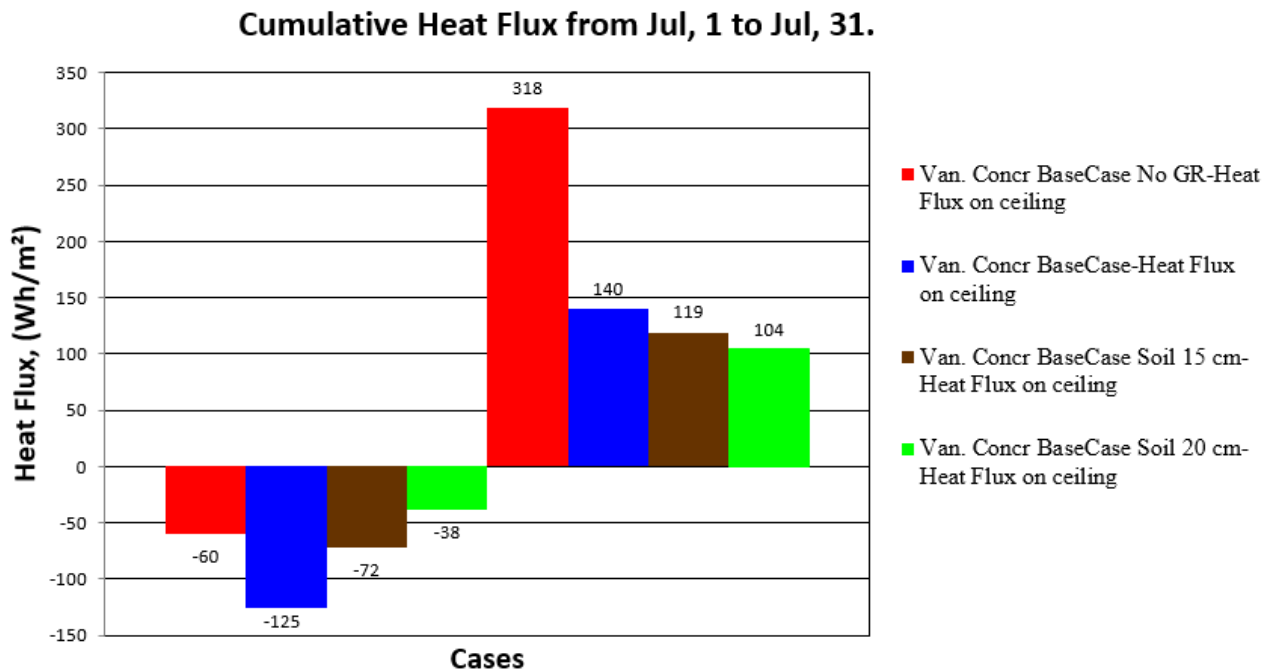


Figure 110. Overall heat through 10, 15, 20 cm green roofs in Vancouver in July.

Additionally, to Vancouver, a case with Winnipeg climate, the same three thicknesses on a wooden frame is analyzed and presented in Figure 111 and 112. In Winnipeg, the winter period is characterized by cold, much below zero temperatures. Plants during a cold winter, apparently, don't play any significant role in heat and moisture transfer. It is assumed that initial relative humidity level in soil was 0.95 as it is a reasonable value under the green roof. Therefore, soil simply works as additional insulation layer with its thermal mass with heat flux reduction by 9 and 17 % respectively on each type of frame.

During the middle season on both concrete and wood frame roofs as well as in previous cases, thicker soil layer damps the heat flux line. In the second part of the season, when outdoor condition allowed plants to grow, it can be seen that on 10 cm growing media evapotranspiration effect is higher. In Winnipeg during the summer season, with relatively frequent rain event, green roof keeps the flux lines near zero, and cumulative heat flux stays negative, that proves the cooling ability of a green roof in Winnipeg climate. Thick soil stabilizes the heat flux line and compensates outdoor boundary conditions fluctuation. Similarly to Winnipeg in Toronto, the evapotranspiration effect occurs when moisture is within the soil. Results are shown in Figure 113 and 114. The thicker soil could hold the more significant amount of water and provide long-term moisture availability for plants and corresponding evapotranspiration.

In summary, a thicker growing media layer provides better energy performance in all simulated climates in both cold and warm periods of a year; therefore, it is recommended to use as thick growing media as possible regarding the roof ability of supporting a green roof weight and the green roof cost increasing due to higher amount of growing media.

Ceiling Heat Flow Profile: Varios growing media thicknesses on wood frame cases in Winnipeg From Jan, 10 To Dec, 30

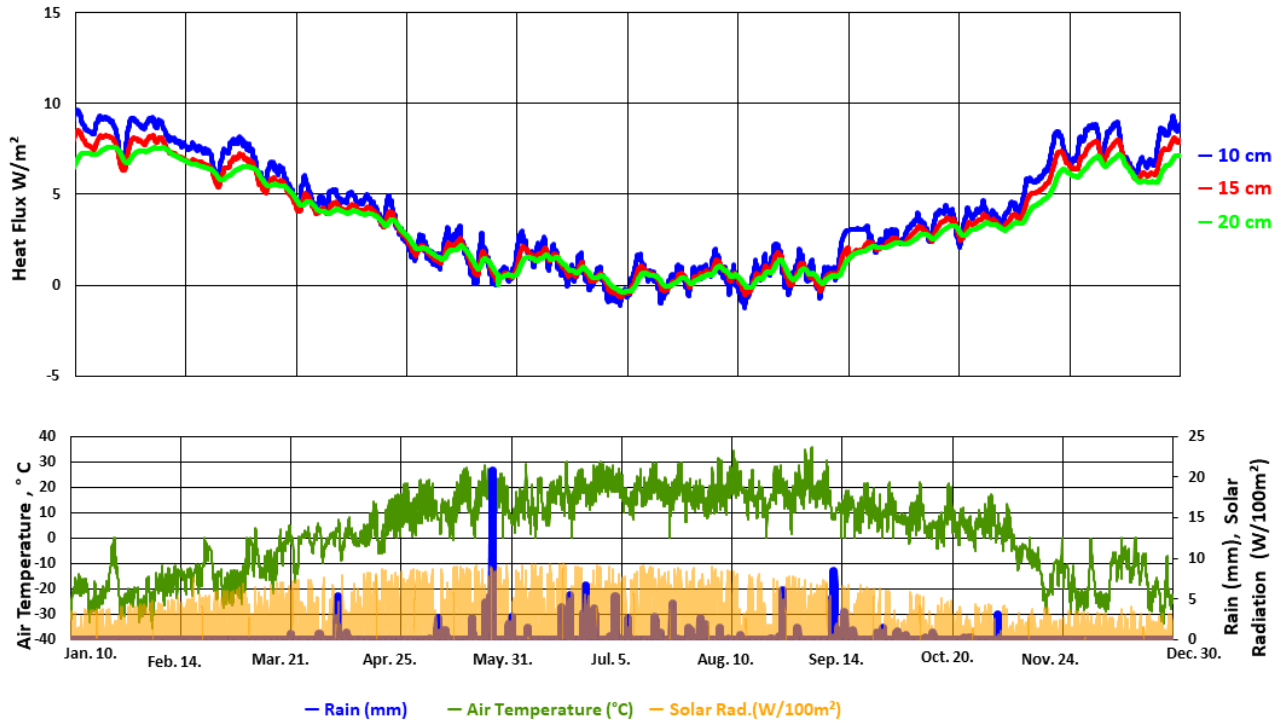


Figure 111. Heat flux through 10, 15, 20 cm green roofs in Winnipeg.

Cumulative Heat Flux from Jan, 10 to Dec, 30.

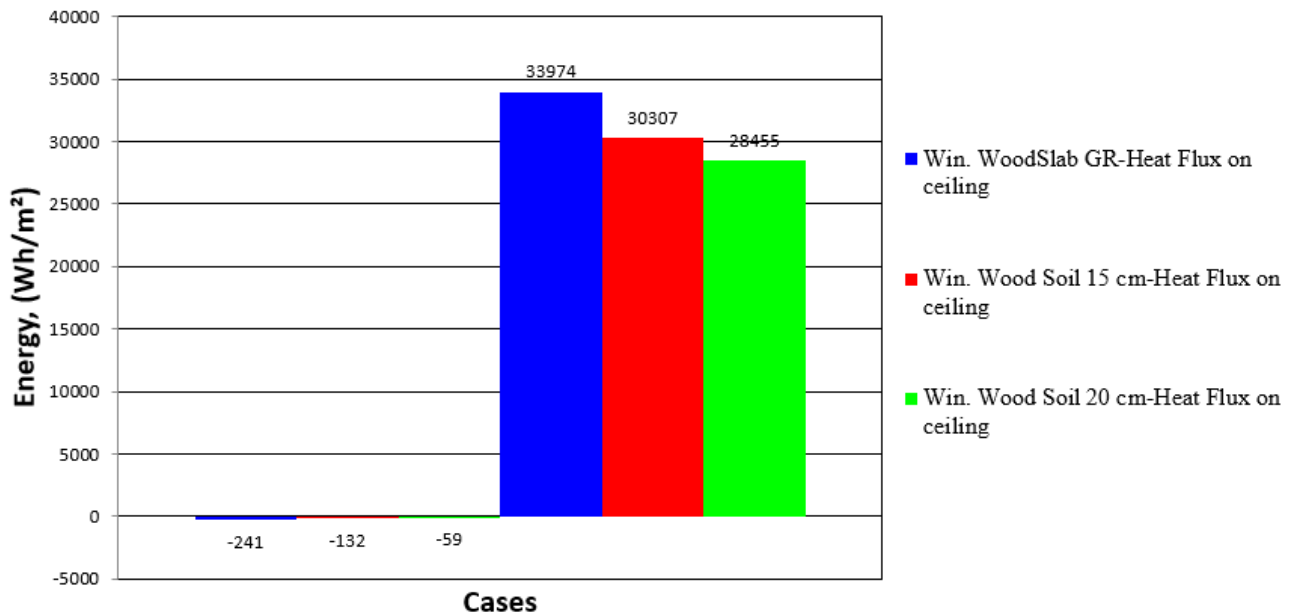


Figure 112. Overall heat through 10, 15, 20 cm green roofs in Winnipeg.

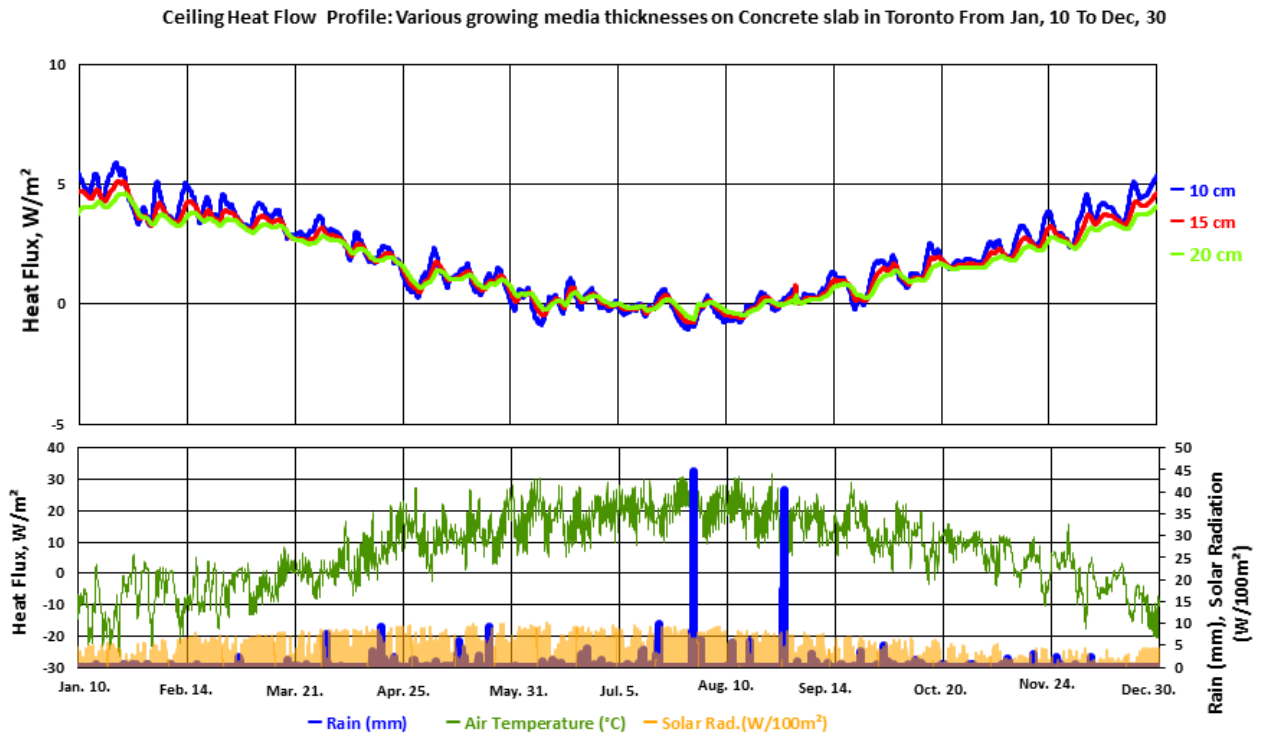


Figure 113. Heat flux through 10, 15, 20 cm green roofs in Toronto.

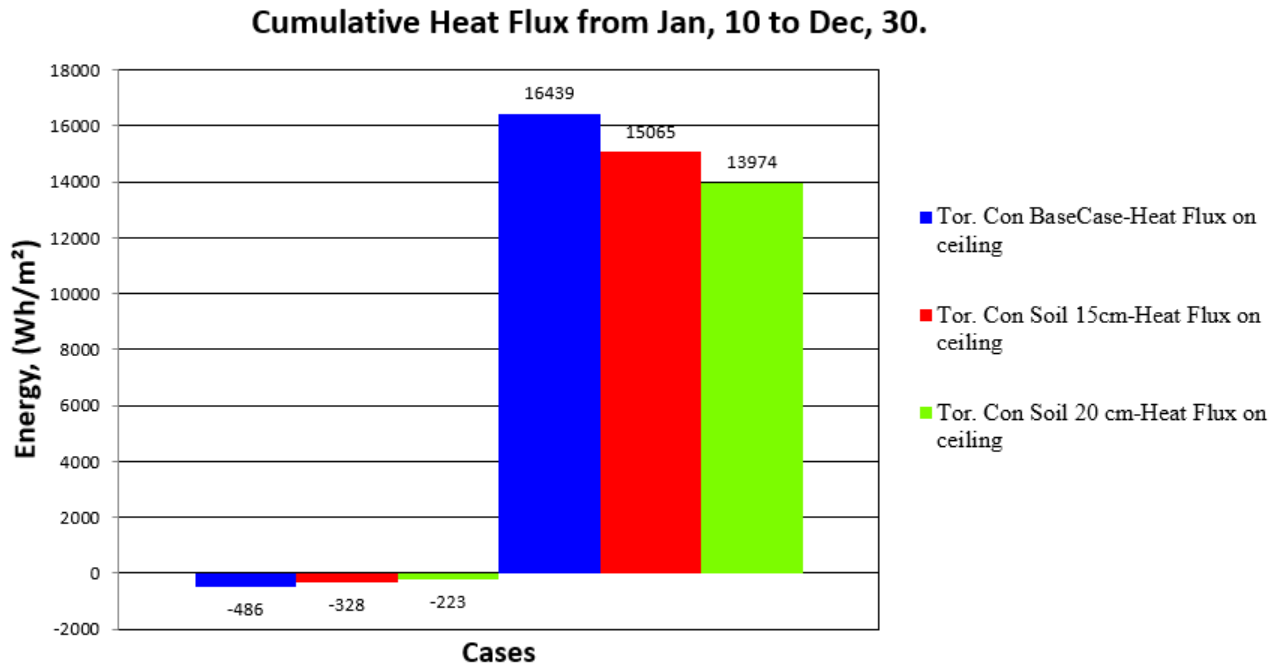


Figure 114. Overall heat through 10, 15, 20 cm green roofs in Toronto.

8.3 Impact of Green roof parameters on membrane and plywood temperatures

The membrane is the weakest part of a green roof system due to thermal expansion and contraction. Constantly repetitive change in membrane structure can cause failure near weak regions, such as connections between layers, edges or neat fasteners. Green roofs are designed to hold the great amount of water in its growing media; moreover, green roof layers above roof deck obstruct water vapour evaporation. Therefore, in a case of membrane failure, water would penetrate into the structure, bringing concomitant damage to a building. Membrane temperature in all the simulation presented in pervious sections cases are reviewed, but only cases with different growing media thicknesses have some observed variations. Figure 115 shows membrane temperature in Vancouver over the simulated year; the rest of profiles are included in Appendix B. Generally, green roof presence stabilizes membrane temperature by eliminating picks. Thicker soil gives stronger stabilization, such as 10 cm soil maintains membrane temperature within the range of 5-25°C; 20 cm soil in the range of 7-22°C degrees. In the last month, 15 and 20 cm soil cases, the membrane from getting frozen while outdoor temperature was as low as -10°C. The similar effect is observed in Toronto cases that are plotted in Figure 116. In Toronto, membrane temperature stays up to 10°C lower in summertime and up to 15°C higher in wintertime.

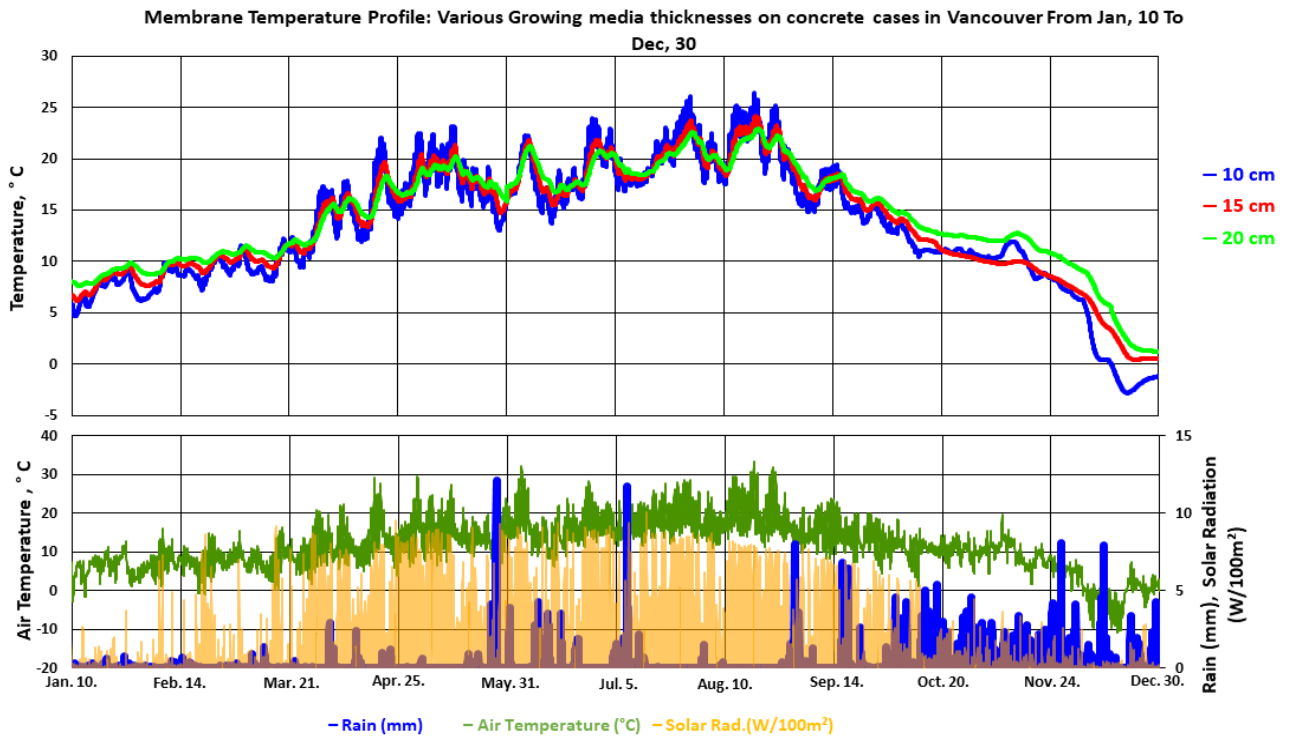


Figure 115. Membrane temperature under 10, 15, 20 cm green roof in Vancouver.

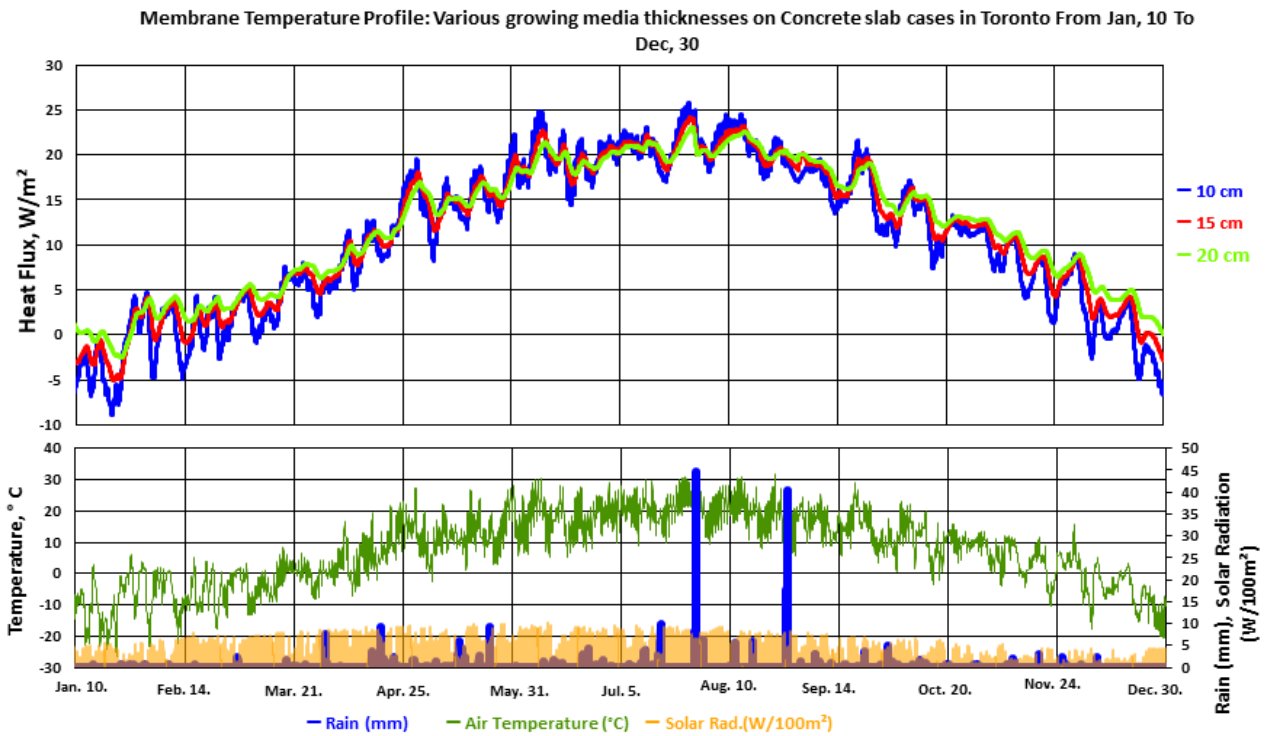


Figure 116. Membrane temperature under 10, 15, 20 cm green roof in Toronto.

In the case of Winnipeg, the simulation is performed for a wood frame building with a membrane located above plywood and insulation. Figure 117 compares membrane temperature under the growing media of 10, 15, 20 cm and a conventional roof. Green roof prevents the membrane from thermal expansion and contraction that occurs in the conventional roof system, where daily temperature fluctuations reach 60°C with summer picks up to 100°C and winter -30°C. The membrane that is protected by a green roof stays up to 20°C warmer in the wintertime and 10°C colder in the summertime. Additionally to the potential membrane damage, plywood temperature that is close to membrane temperature stays warmer in the wintertime and middle season; therefore, in a case of air penetration from the inside, condensation risk is lower. Comparing growing media thicknesses, thicker growing media damps the temperature line.

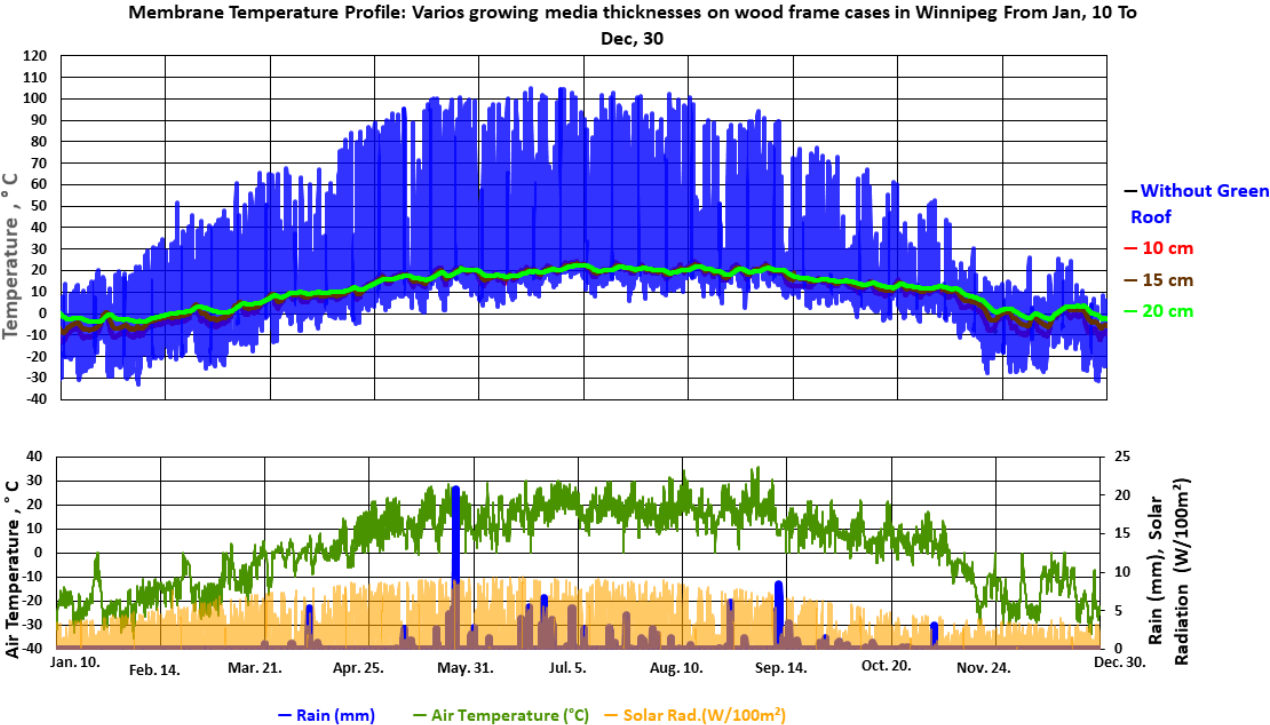


Figure 117. Plywood temperature under 10, 15, 20 cm green roof in Winnipeg.

8.4 Impact of green roofs on rainwater retention

Green roofs are able to hold rainwater for some time in its structure. It is believed that green roof can store up to 70-80% of all incoming water and help a city drainage system to deal with rainwater flows. In Figure 118, the drainage amounts in growing media of different thickness are provided. The simulation results show that green roofs can hold up to 60% rain. If rain is not strong enough to saturate the soil layer, the moisture is absorbed and then evaporates. Otherwise, if rain is heavy, it quickly saturates the growing media regardless its thickness. On the other hand, thicker soil can hold the more significant amount of water, and it takes a longer time to release it through evapotranspiration. However, the difference is not significant – 3% per extra 5 cm. Graphs showing drainage amounts for Winnipeg and Toronto are in Appendix C.

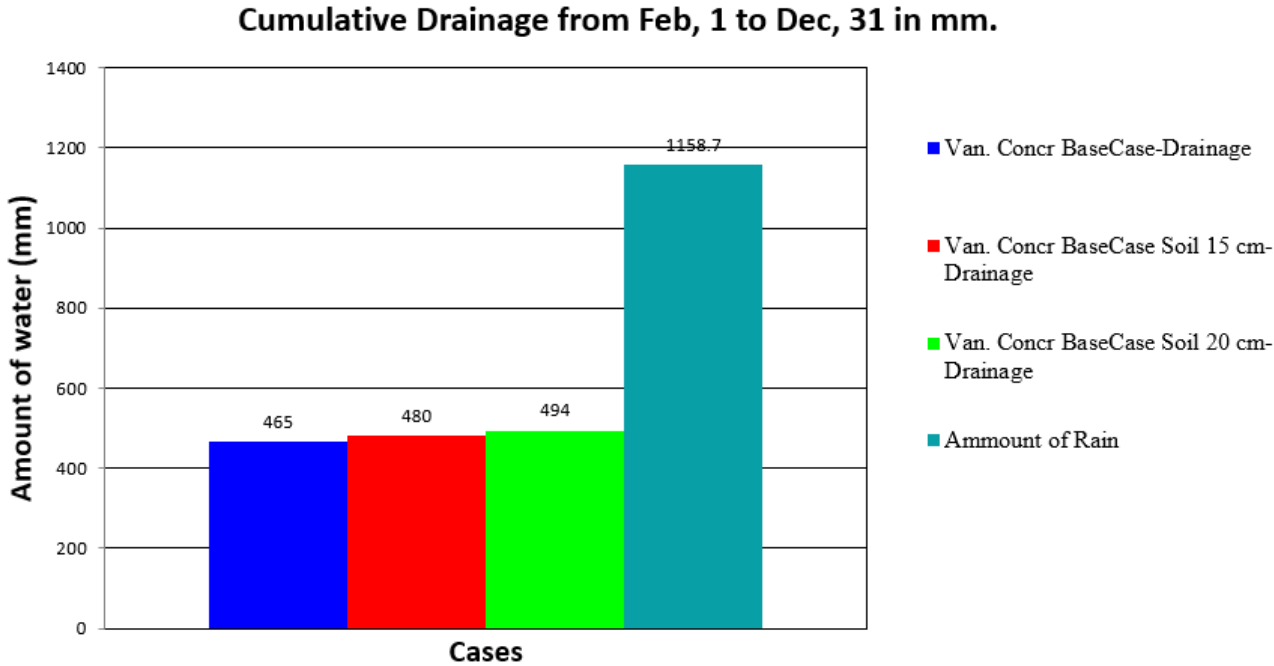


Figure 118. Drainage via 10, 15, 20 cm of soil in Vancouver.

Vegetation parameters are believed to be essential parameters in water flow. Figure 119 compares drainage amount through low, average and high dense, covered green roofs. Coverage ratio reduces the amount of water that can penetrate to the soil layer and then leaves the system by drainage. Moreover, leaf area index is a crucial parameter in evapotranspiration mass transfer calculation. Highly dense vegetation reduces the overall amount of water leaving the system by additional 7%. A comparison of water drainage through the system in the case of low stomatal resistance is plotted in Figure 120. Lower minimum stomatal resistance sedums slightly faster transpire water to the air. This faster transpiration reduces drainage amount by 0.8%. The rest of cases are in Appendix C

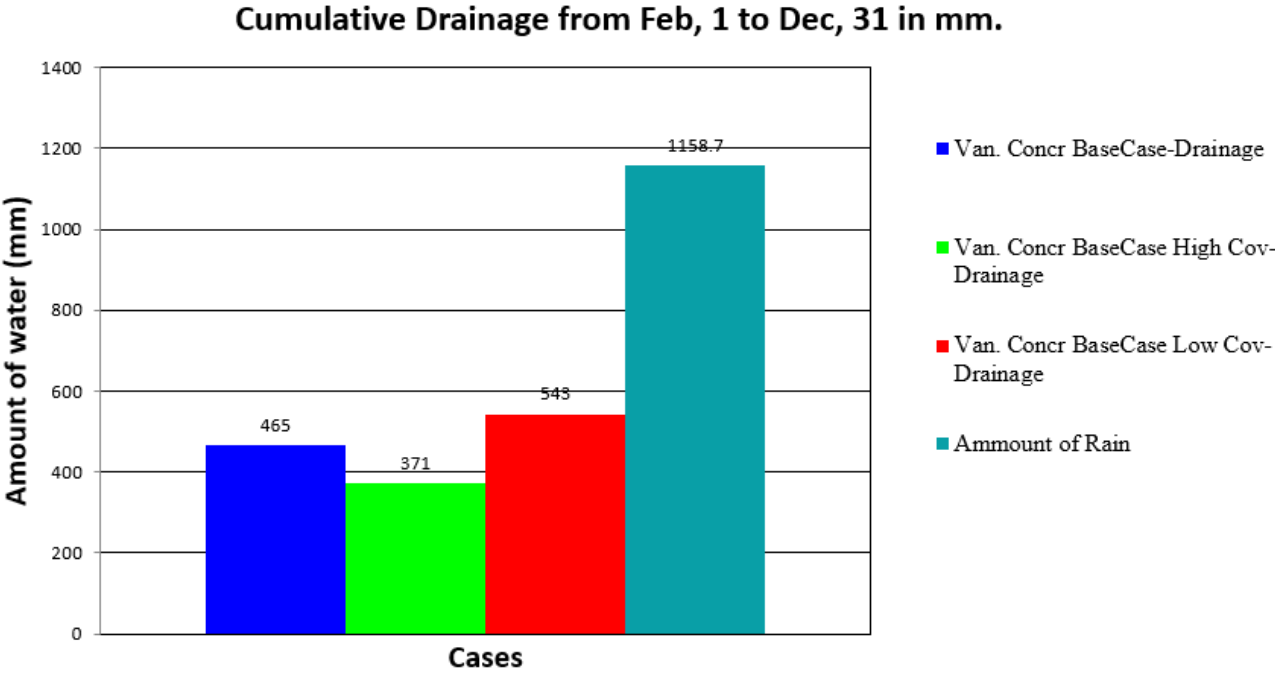


Figure 119. Drainage via low, standard, high dense covered green roof in Vancouver.

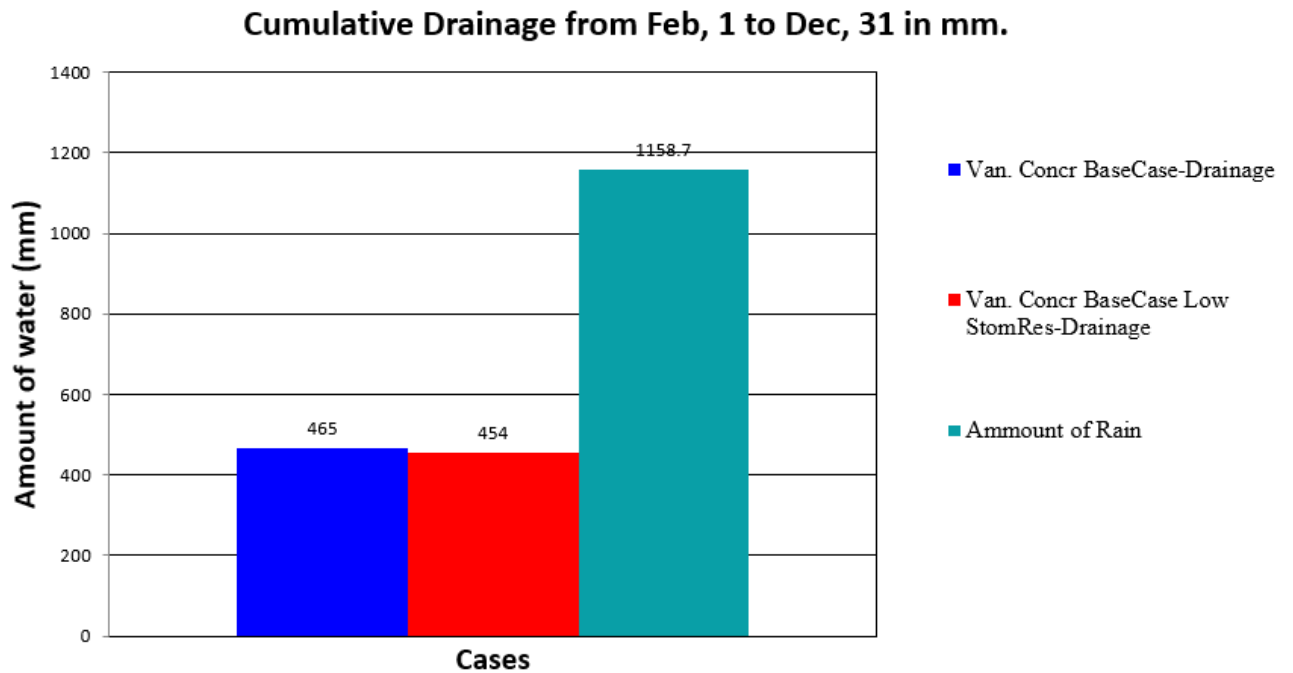


Figure 120. Drainage via low and high minimum stomatal resistance green roof in Vancouver.

8.5 Green roof recommendations

Fifty-four yearly studies combining various climates, types of roof decks, insulation levels, growing media thicknesses and plants parameters are prepared and analyzed. It is found that green roofs are most beneficial with poorly insulated roofs. This is explained by additional thermal resistance and mass of green roofs. Regarding energy performance, thicker growing media layers have more significant effect on higher mass. It is also found that green roofs are most effective in periods when the soil is unfrozen, and a green roof absorbs and releases heat from and to the environment. Therefore, green roofs are recommended in climates with medium temperatures and available moisture or in designs that have green roofs with primary aims different from thermal performance improvement.

CONCLUSIONS

The thesis presents development, validation and application of the new green roof model named HAMFit-GR. The model is a combination based on Heat – Air – Moisture (HAMFit) as a base model and Fast All-Season Soil Strength as a vegetative model base. The model is designed to be fully coupled regarding heat and moisture transfer as well as vegetative and soil models interruption. It is possible to apply the model changing any structural, growing media or plants parameter. A newly developed drainage model is introduced to green roof modelling. Drainage calculation includes the amount of water leaving and convective heat flow associated with the leaving water.

The model is fully validated by comparing estimated and measured temperatures, heat flow and moisture content values within the growing media and foliage surface. There are several cases involved in the validation process including vegetated and bare soil roofs as well as dry and wet periods of time. As a part of the validation process, some of the green roof parameters have been measured by field and laboratory experiments and then applied to the model. Visualization technique is developed and applied to get accurate values of the coverage ratio and leaf area index from digital pictures of the vegetation.

The sensitivity analysis of the HAMFit-GR model is prepared to analyze possible influence of green roofs components and parameters. It has been found that regarding green roof vegetation, the most critical parameters are coverage ratio and leaf area index. Minimal stomatal resistance slightly affects evapotranspiration and associated latent heat, while such variables as root depth and fraction do not have any noticeable influence. Density heat capacity and porosity are key soil parameters to define the thermal mass that is the most significant contribution of a green roof system in the building energy performance.

The model is used to simulate 54 different yearly cases with regards to climate, soil thickness, vegetation coverage, stomatal resistance and insulation amount. Simulations show that green roofs have the biggest impact on the thermal performance by its additional thermal mass of the growing media and water held in the growing media. Moreover, increasing the growing media layer, overall thermal resistance is increased as well; thus, a thicker growing media layers show the better performance in heating dominated countries like Canada. Vegetation amount influences on the flow through the roof mainly by shading effect reducing longwave radiation exchange with the sky and covering from the direct sunbeams. Vegetation coverage and stomatal resistance cases illustrate that evapotranspiration is not a significant source of cooling and only occurs when all the necessary conditions, such as solar radiation and moisture availability affecting a roof. The results show that green roofs improve the thermal performance of any insulated roof, but the bigger impact is observed on less insulated roofs.

FUTURE WORK

Future work regarding model mathematics can be applied to vegetative properties and temperature determination. Firstly, coverage ratio and leaf area index are currently based on the ground temperature; however, those variables reflect plants development, which is a biological process and depends on a season, available moisture content and plants characteristic. Second, the region that is referred in the thesis air-foliage with its own temperature and mixing ratio can be divided into two sections: one is air within foliage and second is air above the foliage. Therefore, the foliage energy balance can be rewritten as foliage interaction with both above and within vegetation environments.

The model also can be involved in a long-term study including season changes, climates different from Vancouver. In this thesis, the green roof was modelled without including the rest of a building envelope; therefore, a study analyzing green roofs impact on a whole building can be conducted.

REFERENCES

1. Allen, Richard G, L.S. Pereira, D. Raes and Smith, M. "Crop evapotranspiration: Guidelines for computing crop requirements No 56". Irrigation and Drainage Paper No. 56, FAO. (1998): 1-56.
2. Ambrosini, Dario, Giorgio Galli, Biagio Mancini, Iole Nardi and Stefano Sfarra. "Evaluating mitigation effects of urban heat islands in a small historical center with the ENVI-Met climate model." Sustainability (Switzerland) 6 (2014): 7013-7029.
3. Arkar, Ciril, Suzana Domjan, Darja Majkovi, Jure Šumi and Sašo Medved. "Lightweight Green Roofs' Thermal Response under Freezing Conditions". 6th International Building Physics Conference, IBPC 2015 78 (2015): 1189-1194.
4. ASTM International. "Standard Practice for Thin-Walled Tube Sampling of Soils for Geotechnical Purposes." D1587-8. (2008):1-4.
5. ASTM International. "Standard Test Method for Determination of Thermal Conductivity of Soil and Soft Rock by Thermal Needle Probe Procedure 1". Annual Book of ASTM Standards, (2011): 6-13.
6. ASTM International. "Standard Test Method for Hygroscopic Sorption Isotherms of Building Materials" (2016):2-5.
7. ASTM International. "Standard Test Method for Specific Heat of Rock and Soil." (2016):1-5.
8. ASTM International. "Standard Test Methods for Laboratory Determination of Density (Unit Weight) of Soil Specimens." ASTM. (2009): D7263-9, 1-7.
9. ASTM International. "Standard Test Methods for Laboratory Determination of Water (Moisture) Content of Soil and Rock by Mass." ASTM D2216-10. (2010): 1-7.
10. ASTM International. "Standard Test Methods for Water Vapor Transmission of Materials" (2002): 1-10.

11. Ayata, Tahir, Paulo Cesar Tabares-Velasco and Jelena Srebric. "An investigation of sensible heat fluxes at a green roof in a laboratory setup." *Building and Environment* 9 (46) 2011: 1851-1861.
12. Berardi, Umberto. "The outdoor microclimate benefits and energy saving resulting from green roofs retrofits." *Energy and Building* 121 (2016): 217-229.
13. Bianchini, Fabricio and Kasun Hewage. "How "green" are the green roofs? Lifecycle analysis of green roof materials". *Building and Environment* 48 (2012): 57-65.
14. Coutts, Andrew M., Edoardo Daly, Jason Beringer and Nigel J. Tapper. "Assessing practical measures to reduce urban heat: Green and cool roofs." *Building and Environment* 70 (2013): 266-276.
15. Connelly, M. and M. Hodgson. "Experimental investigation of the sound absorption characteristics of vegetated roofs". *Building and Environment* 92 (2015): 335-346.
16. Conservation Technology Inc. "Green Roof Handbook". (2008). 1-25.
17. Deardorff, J. W. "Efficient Prediction of Ground Surface Temperature and Moisture , With Inclusion of a Layer of Vegetation." 83(7). (1978).
18. Dickinson, R. E., Henderson-Sellers, A., Kennedy, P. J., & Wilson, M. F. Biosphere-atmosphere transfer scheme (BATS) for the NCAR Community Climate Model." *Journal of Climate*, (1986), 72.
19. Dickinson, R. E., & Henderson-Sellers, A. "Modeling Tropical Deforestation - a Study of Gcm Land Surface Parametrizations." *Quarterly Journal of the Royal Meteorological Society*, 114(480), (1988): 439–462.
20. Djedjig, Rabah, Salah-Eddine Ouldboukhitine, Rafik Belarbi and Emmanuel Bozonnet. "Development and validation of a coupled heat and mass transfer model for green roofs." *International Communications in Heat and Mass Transfer* 21 (2012):752-761.
21. Djedjig, Rabah, Emmanuel Bozonnet and Rafik Belarbi. "Integration of a green envelope model in a transient building simulation program and experimental comparison." *Proceedings of BS 2013: 13th Conference of the International Building Performance Simulation Association* (2013): 47-53.

22. Epa, U S. "Reducing Urban Heat Islands: Compendium of Strategies". Heat Island Reduction Activities. (2008): 1-23.
23. Erhorn, Hans and Heike Erhorn-Kluttig. "Terms and definitions for high performance buildings". Concerted action: energy performance of buildings. (2011): 1-8.
24. European Federation of Green Roof Associations. "Environmental Advantages". (2016):8-10.
25. Frankenstein, S and G. Koenig. "FASST Vegetation models". US Army Corps of Engineers. Engineer Research and Development Center (2004): 1-57.
26. Gagliano, A., M. Detommaso, F. Nocera, F. Patania and S. Aneli. "The retrofit of existing buildings through the exploitation of the green roofs - A simulation study". Energy Procedia 62 (2014): 52-61.
27. Gargari, Caterina, Carlo Bibbiani, Fabio Fantozzi and Carlo Alberto Campiotti. "Simulation of the thermal behavior of a building retrofitted with a green roof: optimization of energy efficiency with reference to Italian climatic zones." Agriculture and Agricultural Science Procedia 8 (2016): 628 – 636.
28. Gettera, Kristin L., D. Bradley Rowea, Jeff A. Andresenb and Indrek S. Wichman. "Seasonal heat flux properties of an extensive green roof in a Midwestern U.S. climate". Energy and Buildings 43 (2011): 3548-3557.
29. Goodrich, L. E. "Efficient numerical technique for one-dimensional thermal problems with phase change". International Journal of Heat and Mass Transfer 21 (1978): 615-621.
30. Hagos, S. "Thermal and Moisture Transfer in Green Roof System: An Experimental Field Study". MASc Thesis (2018).
31. He, Hongming and C.Y. Jim. "Simulation of thermodynamic transmission in the green roof ecosystem". Ecological Modelling 24 (2010): 2949-2958.

32. Heidarinejad, Ghassem and Arash Esmaili. "Numerical simulation of the dual effect of green roof thermal performance." *Energy Conversion and Management*. 106 (2015): 1418-1425.
33. International Organization for Standardization. "ISO 15927-1. Hygrothermal performance of buildings — Calculation and presentation of climatic data – Part 1: Monthly means of single meteorological elements". (2003): 1-34.
34. Jim, C.Y. and Hongming He Department "Coupling heat flux dynamics with meteorological conditions in the green roof ecosystem." *Ecological Engineering* 36 (2014): 1052-1063.
35. Jim, C.Y. and S.W. Tsang. "Modeling the heat diffusion process in the abiotic layers of green roofs". *Energy and Buildings* 43 (2011): 1341-1350.
36. Jones, A., Jones, E and Jones, P. "Developing a one-dimensional heat and mass transfer algorithm for describing the effect of green roofs on the built environment: Comparison with experimental results." *Building and Environment* 42 (2007): 2835 – 2849.
37. Jordan, R. A. "One-Dimensional Temperature Model for a Snow Cover: Technical Documentation for SNTHERM.89." U.S.Army Corps of Engineers, Cold Regions Research & Engineering Laboratory, (Special Report 91-16), 49. (1991).
38. Karagiannis, N., Karoglou, M., Bakolas, A., & Moropoulou, A. "New Approaches to Building Pathology and Durability." 6. (2016).
39. Keiner, Marco. "The future of sustainability". *The Future of Sustainability* January (2006):1-257.
40. Kotsirisa,G., A. Androutsopoulosb, E. Polychronib and P.A. Nektarios. "Dynamic U-value estimation and energy simulation for green roofs." *Energy and Buildings* 45 (2012): 240-249.
41. Lazzarin, Renato M., Francesco Castellotti and Filippo Busato. "Experimental measurements and numerical modelling of a green roof." *Energy and Buildings* 37 (2005): 1260-1267.
42. Lin, Weibin, Bin Chen, Shichao Luo and Li Liang. "Energy Consumption" (2015): 45-49.

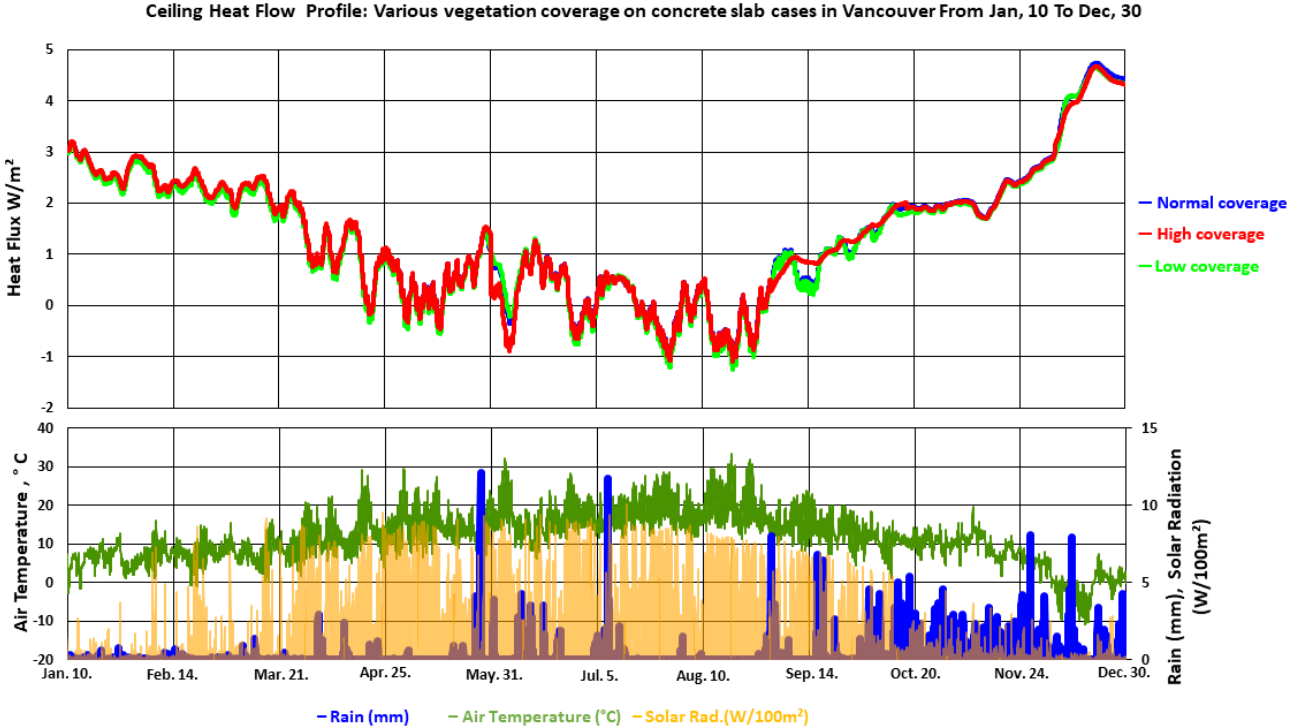
43. Louis, J. F. "A parametric model of vertical eddy fluxes in the atmosphere." *Boundary-Layer Meteorology*, 17(2), (1979):187–202.
44. Marasco, Daniel E., Patricia J. Culligana and Wade R. McGillisb. "Evaluation of common evapotranspiration models based on measurements from two extensive green roofs in New York City." *Ecological Engineering* 84 (2015): 451 – 462.
45. Moody, Seth S. and David J. Sailor. "Development and application of a building energy performance metric for green roof systems". *Energy and Buildings* 60 (2013): 262-269.
46. Ouldboukhitea, Salah-Eddine, Graig Spolekb and Rafik Belarbi. "Impact of plants transpiration, grey and clean water irrigation on the thermal resistance of green roofs." *Ecological Engineering* 67 (2014): 60-66.
47. Ouldboukhite, Salah-Eddine and Rafik Belarbi. "Experimental Characterization of Green Roof Components". *Energy Procedia* 78 (2015): 1183-1188.
48. Ouldboukhite, Salah-Eddine, Rafik Belarbi, Issa Jaffal and Abdelkrim Trabelsi. "Assessment of green roof thermal behavior: A coupled heat and mass transfer model." *Building and Environment* 46 (2011): 2624-2631.
49. Ouldboukhite, Salah-Eddine, Rafik Belarbi and Rabah Djedjig. "Characterization of green roof components: Measurements of thermal and hydrological properties." *Building and Environment* 56 (2012): 78-85.
50. Pereira, Luis S., Richard G. Allenb, Martin Smithc and Dirk Raes. "Crop evapotranspiration estimation with FAO56: Past and future". *Agricultural Water Management* 147 (2015): 4-20.
51. Qin, Menghao, Rafik Belarbi, Abdelkarim Aït-Mokhtar and Francis Allard. "Simulation of coupled heat and moisture transfer in air-conditioned buildings." *Automation in Construction* 18 (2009): 624-631.

52. Qina, Hua-peng, Yue-nuan Penga, Qiao-ling Tanga and Shaw-Lei Yu. "A HYDRUS model for irrigation management of green roofs with a water storage layer". *Energy and Buildings* 95 (2016): 399-408.
53. Ramírez, J. A., & Senarath, S. "A statistical-dynamical parameterization of interception and land surface-atmosphere interactions." *Journal of Climate*, 13(22), (2000): 4050–4063.
54. Rayner, John P., Claire Farrell, Kirsten J. Raynor, Susan M. Murphy and Nicholas S.G. Williams "Plant establishment on a green roof under extreme hot and dry conditions: The importance of leaf succulence in plant selection". *Urban Forestry and Urban Greening* 15 (2016): 6-14.
55. Sailor David J. "A green roof model for building energy simulation programs." *Energy and Buildings* 40 (2008): 1466-1478.
56. Sailor, David J, Timothy B. Elley and Max Gibson. "Exploring the building energy impacts of green roof design decisions - a modeling study of buildings in four distinct climates" *Journal of Building Physics* 4 (35) 2012: 372-391.
57. Sandoval1, V., F. Suárez, S. Vera, C. Pinto, F. Victorero, C. Bonilla, J. Gironás, W. Bustamante, V. Rojas and P. Pastén. "Impact of the properties of a green roof substrate on its hydraulic and thermal behavior." 6th International Building Physics Conference, IBPC 2015 *Energy Procedia* 78 (2015): 1177 – 1182.
58. Stovin, Virginia, Simon Poë and Christian Berretta Department. "A modelling study of long term green roof retention performance." *Journal of Environmental Management* 131 (2013): 206-215.
59. Sun, Ting, Elie Bou-Zeid, Zhi-Hua Wang, Eileen Zerba and Guang-Heng Ni. "Hydrometeorological determinants of green roof performance via a vertically-resolved model for heat and water transport." *Building and Environment* 60 (2013): 211-224.
60. Tabares-Velasco, Paulo Cesar and Jelena Srebric "A heat transfer model for assessment of plant based roofing systems in summer conditions". *Building and Environment* 49 (2012): 1052-1063.

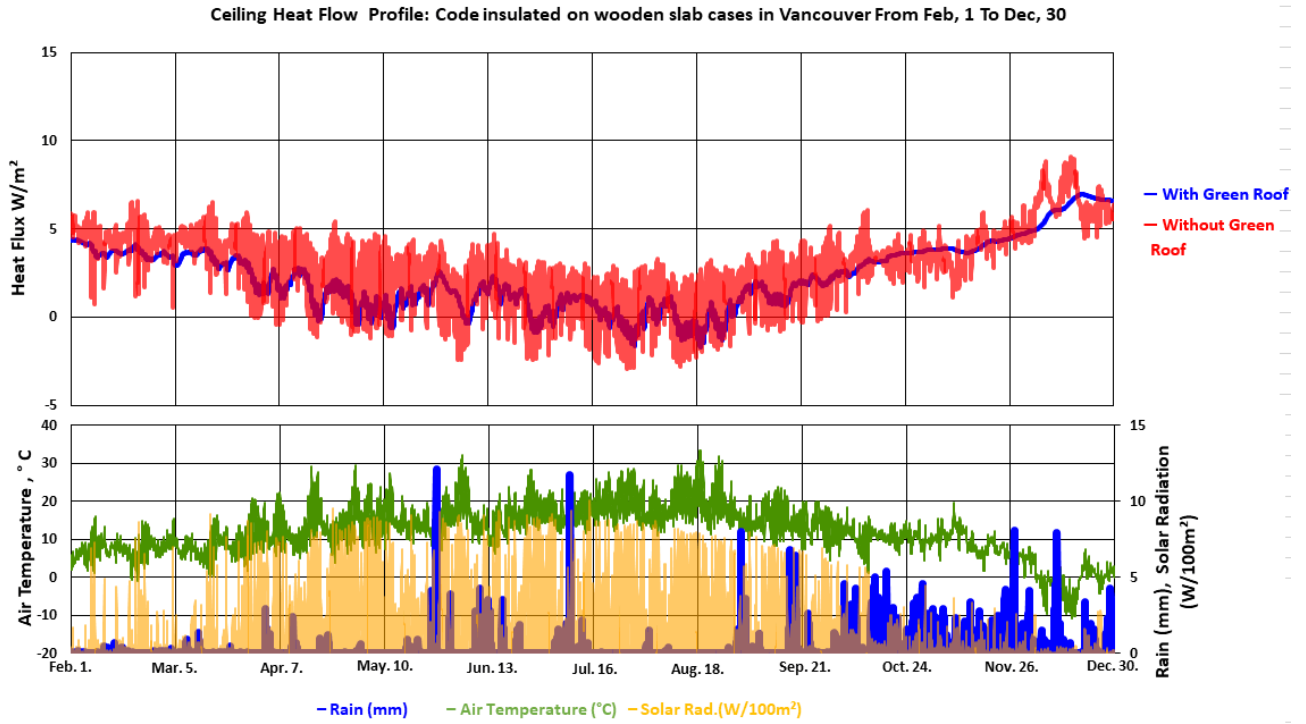
61. Tabares-Velasco, Paulo Cesar, Mingjie Zhao, Nicole Peterson, Jelena Srebric and Robert Berghage. "Validation of predictive heat and mass transfer green roof model with extensive green roof field data". *Ecological Engineering* 47 (2012): 165-173.
62. Tang, Xin and Ming Qu. "Phase change and thermal performance analysis for green roofs in cold climates". *Energy and Buildings* 121 (2016): 165-175.
63. Tariku, F. "Whole building heat and moisture analysis". (2008): 1-374.
64. US Department of Energy. "EnergyPlus Engineering Reference: The Reference to EnergyPlus Calculations". (2010): 1-847.
65. Yaghoobian, Neda and Jelena Srebric. "Influence of plant coverage on the total green roof energy balance and building energy consumption". *Energy and Buildings* 103 (2015): 1-13.
66. Yang, Jiachuan, Zhi-Hua Wang. "Physical parameterization and sensitivity of urban hydrological models: Application to green roof systems" *Building and Environment* 75 (2014): 250-263.
67. Zhao, Mingjie, Paulo Cesar Tabares-Velasco, Jelena Srebric, Sridhar Komarneni and Robert Berghage. "Effects of plant and substrate selection on thermal performance of green roofs during the summer" *Building and Environment* 78 (2014): 199-211.

APPENDIX A. HEAT FLUX ON CEILING

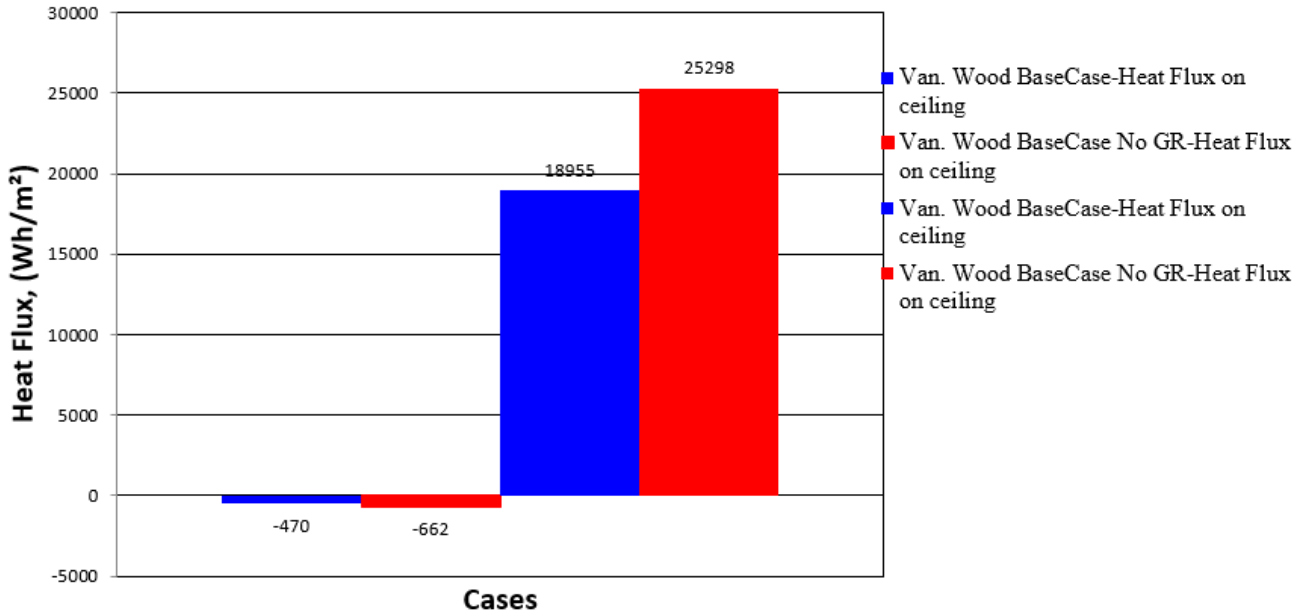
Heat flux through Low, Normal, and High covered green roofs in Vancouver.



Vancouver. Code insulated on Wood slab.

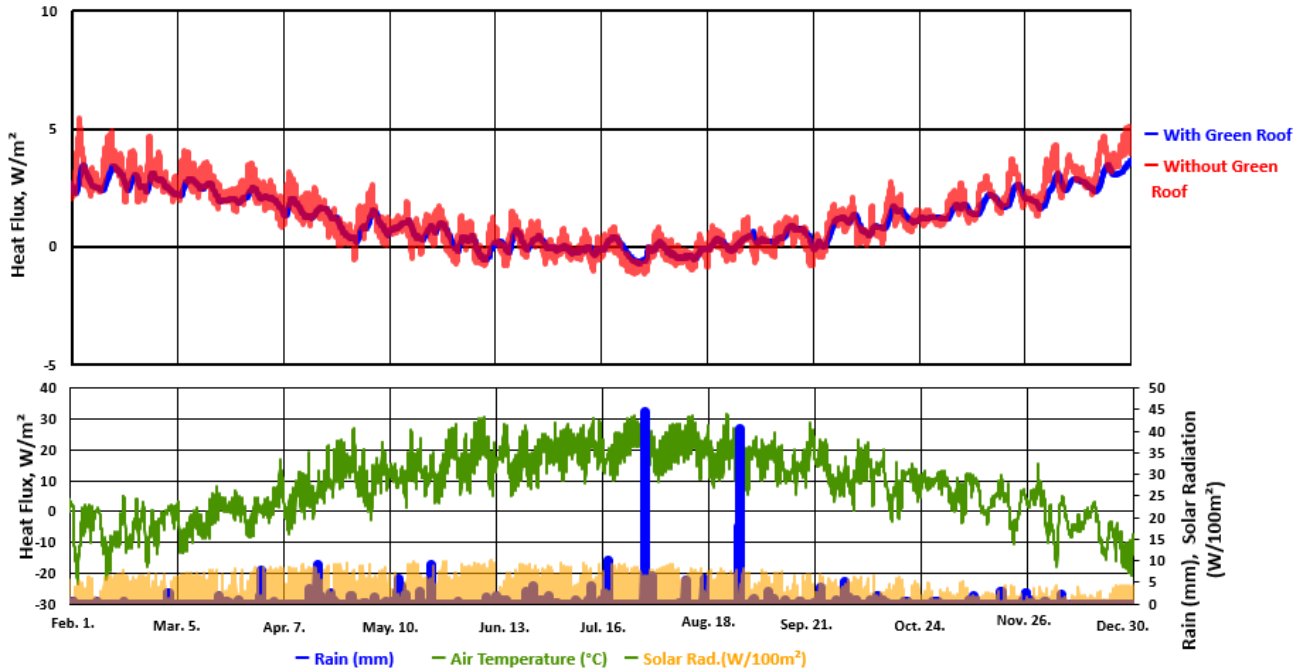


Cumulative Heat Flux from Feb, 1 to Dec, 30.

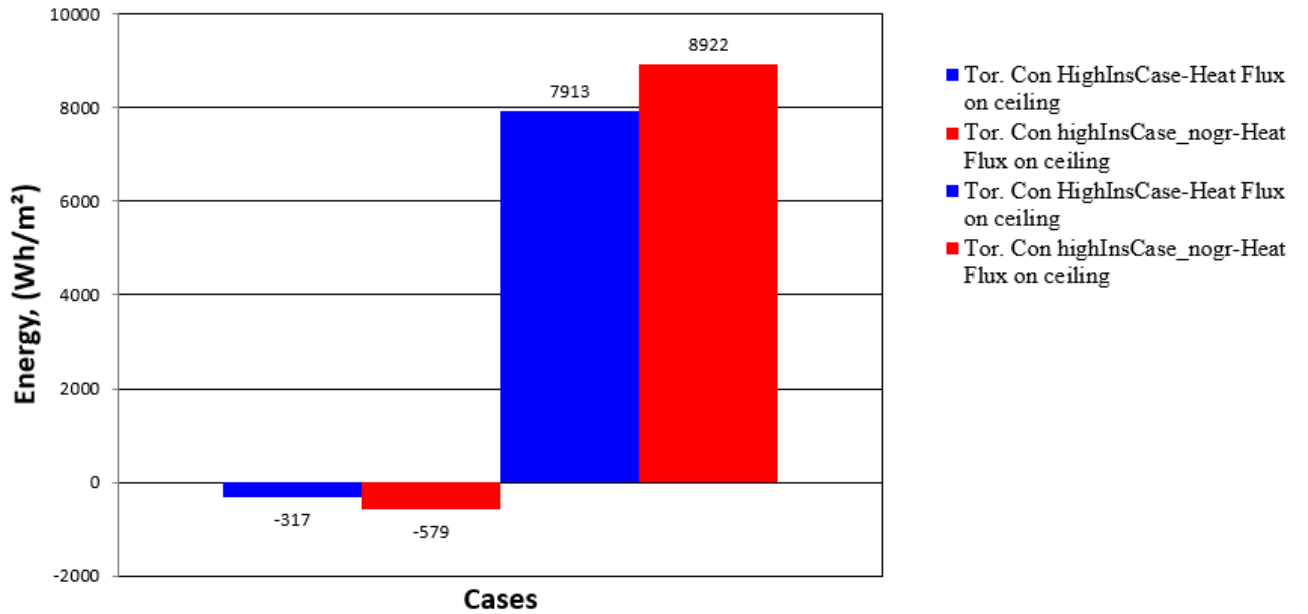


Toronto. High- Insulated scenario.

Ceiling Heat Flow Profile: High insulated on Concrete slab cases in Toronto From Feb, 1 To Dec, 30

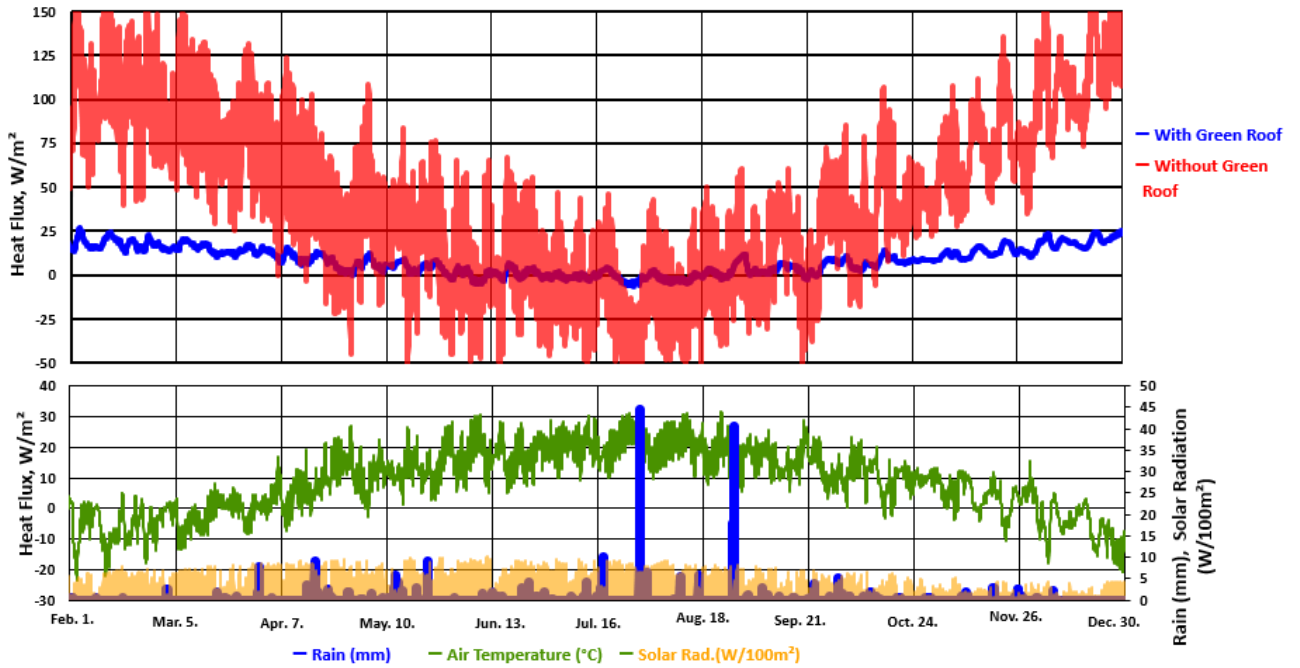


Cumulative Heat Flux from Feb, 1 to Dec, 30.

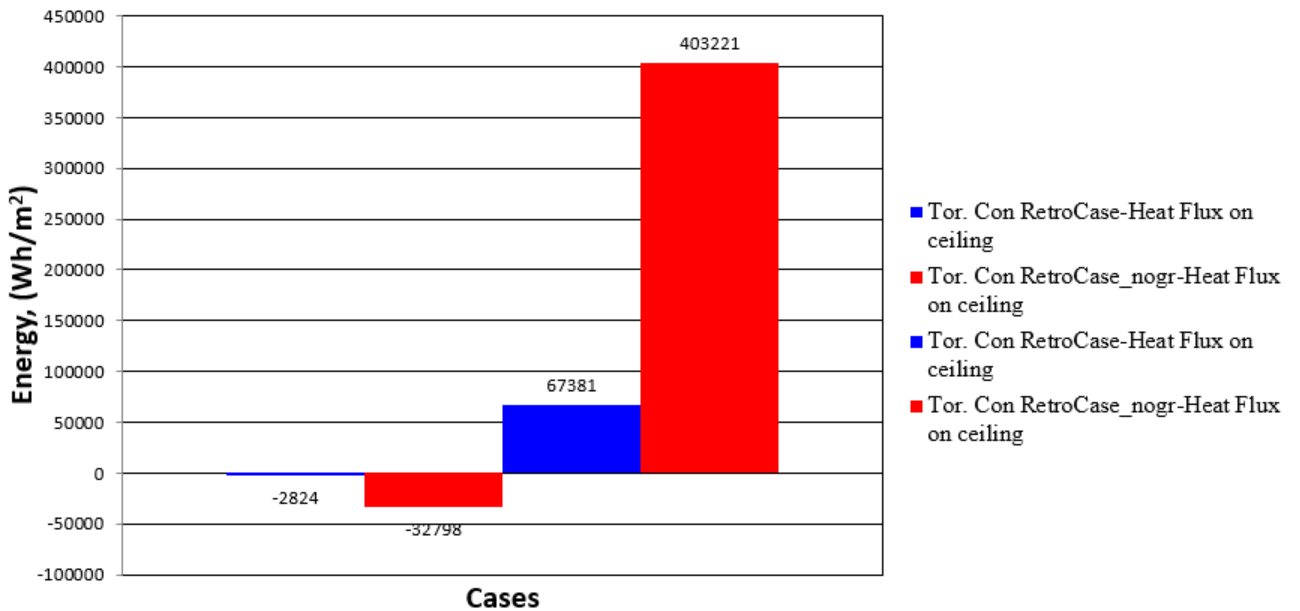


Toronto. Retro insulated scenario.

Ceiling Heat Flow Profile: Non insulated on Concrete slab cases in Toronto From Feb, 1 To Dec, 30

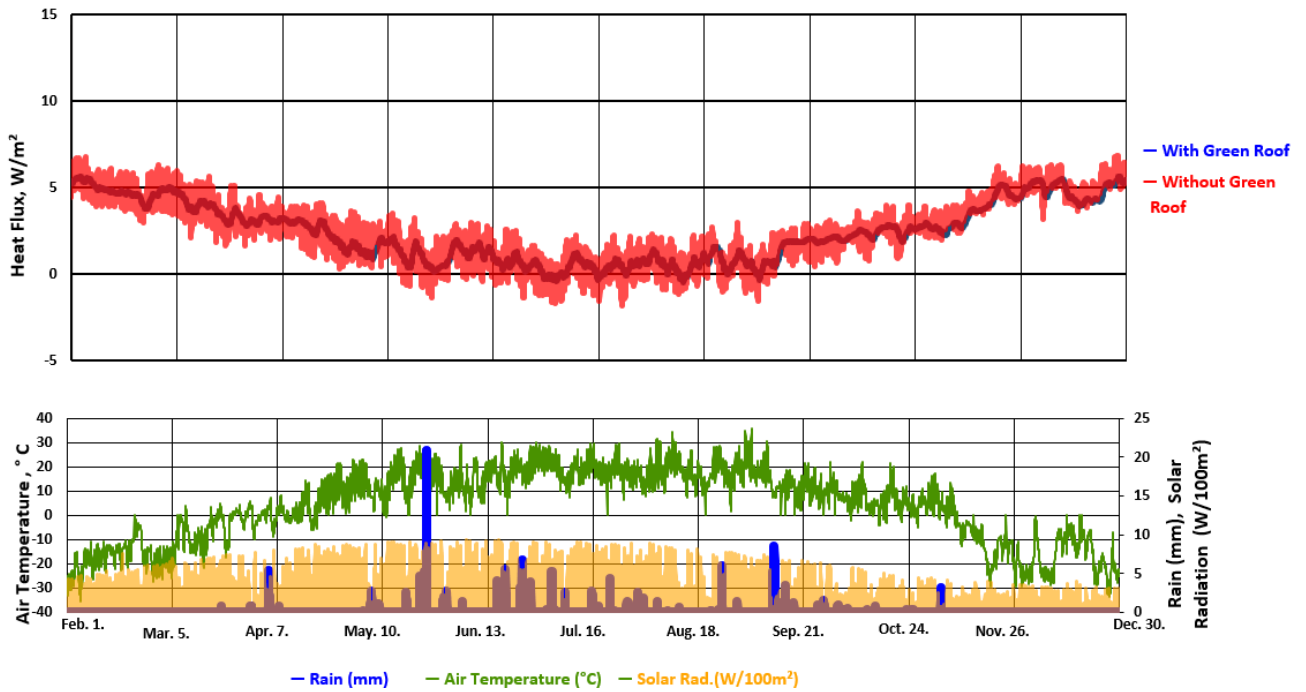


Cumulative Heat Flux from Feb, 1 to Dec, 30.

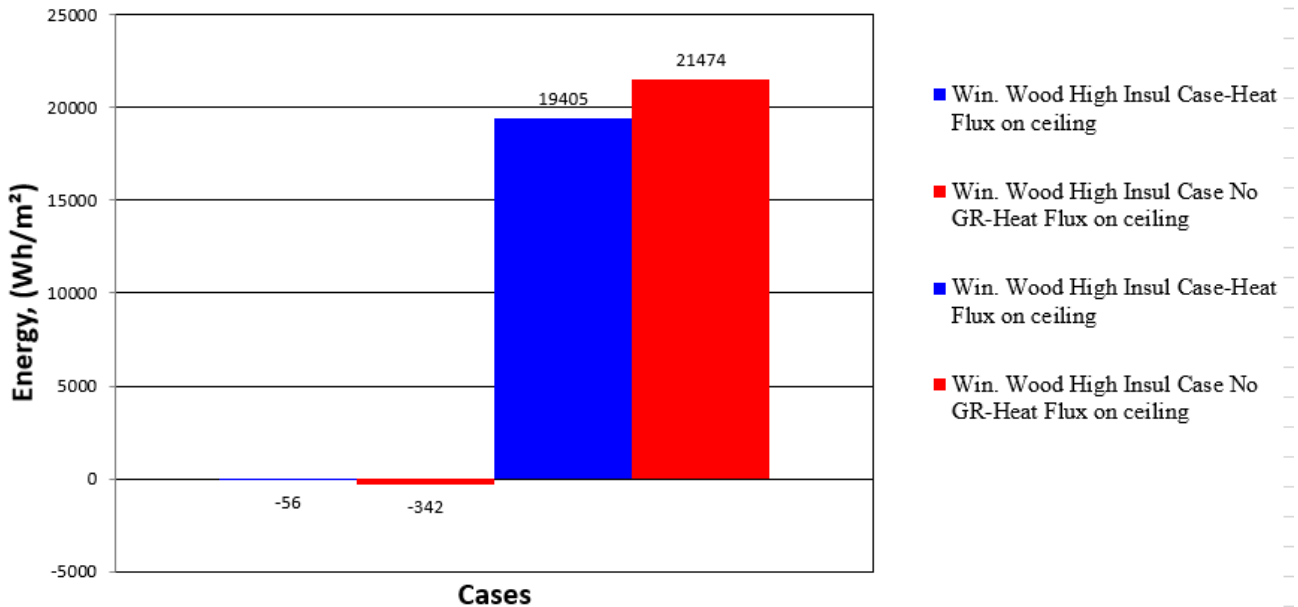


Winnipeg High-Insulated Scenario

Ceiling Heat Flow Profile: Green Roof High Insulated on Wooden slab cases in Winnipeg From Feb, 1 To Dec, 30

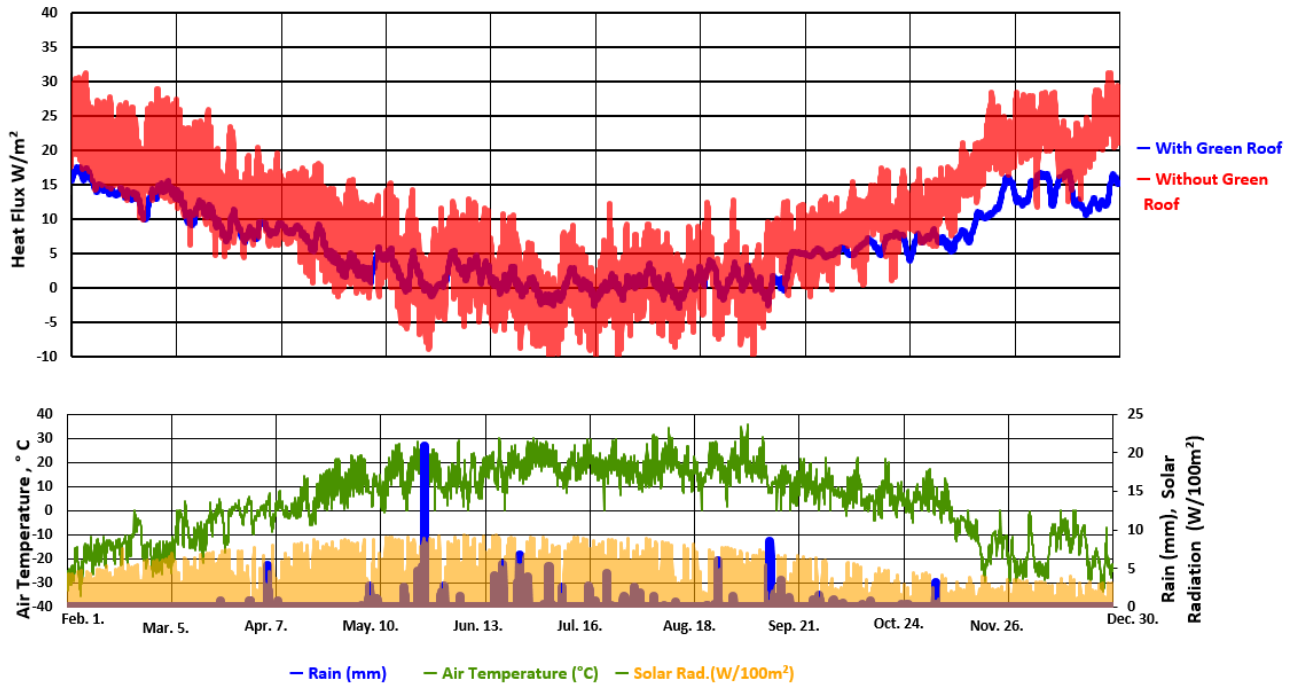


Cumulative Heat Flux from Feb, 1 to Dec, 30.

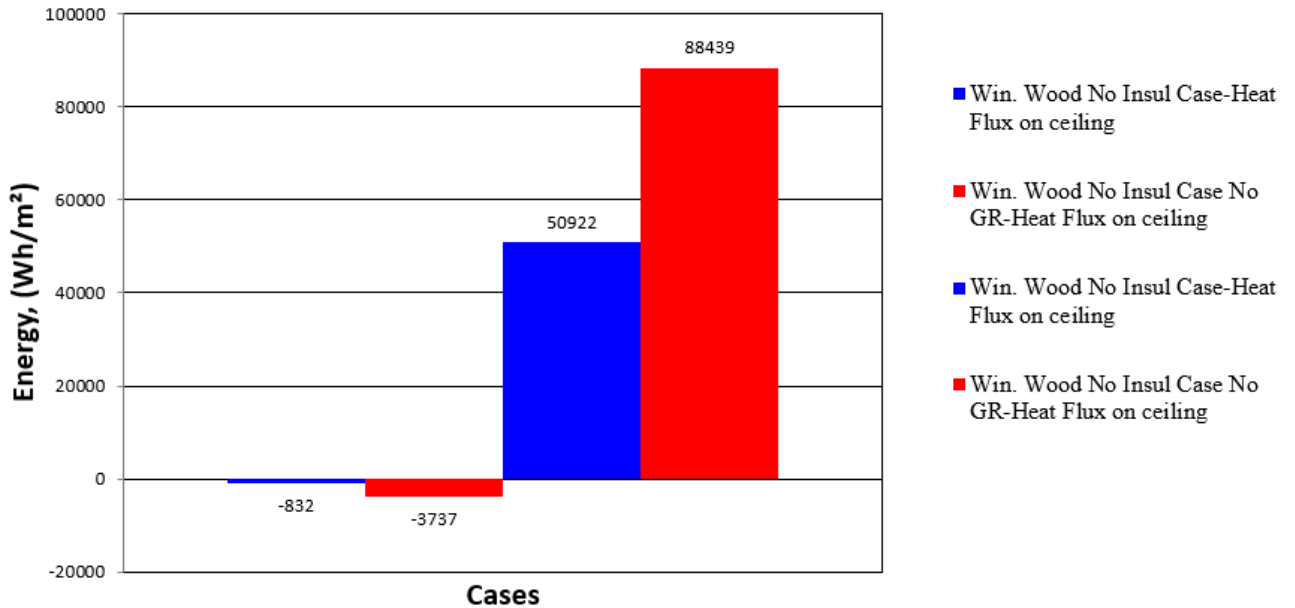


Winnipeg Retro-Insulated scenario

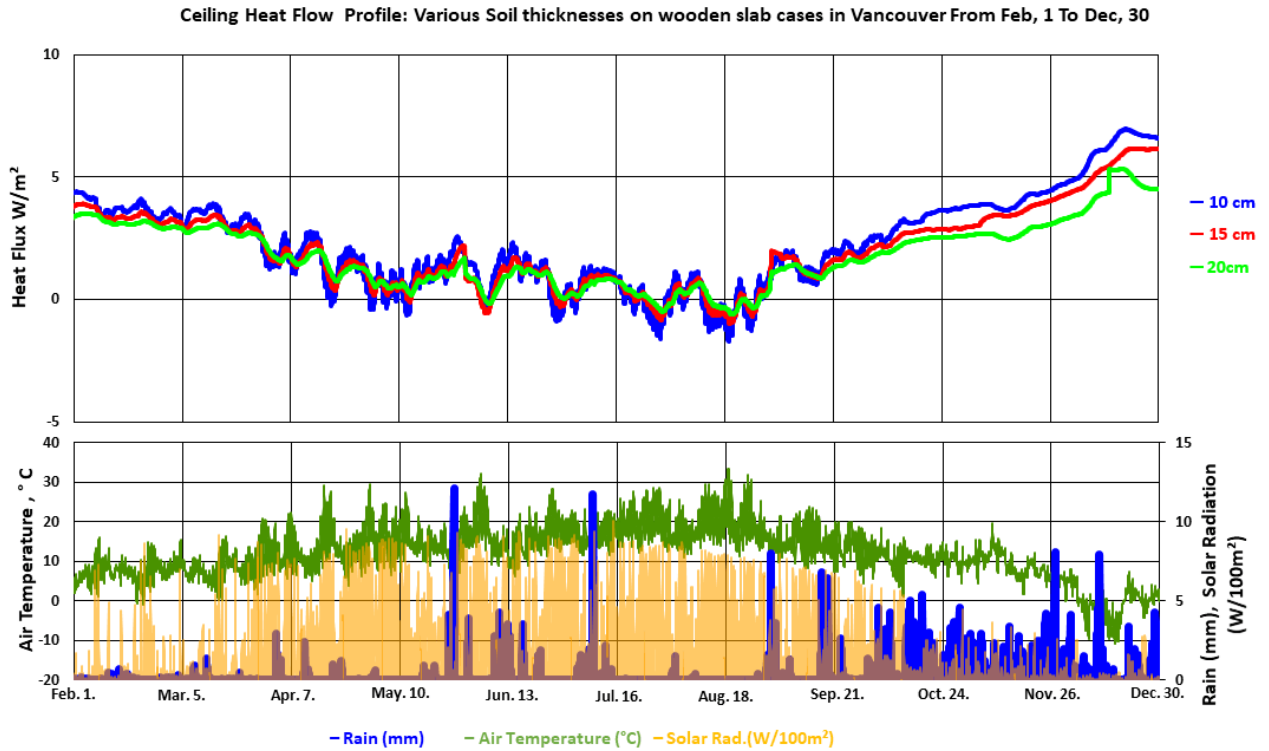
Ceiling Heat Flow Profile: Green Roof Non Insulated on Wooden slab cases in Winnipeg From Feb, 1 To Dec, 30



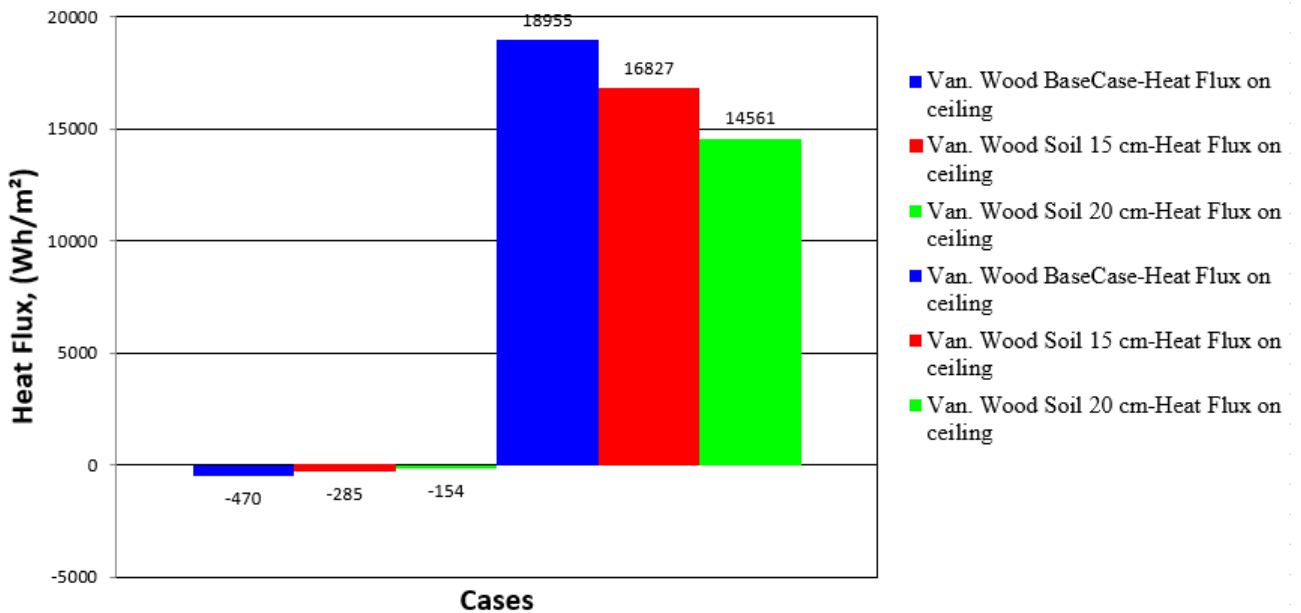
Cumulative Heat Flux from Feb, 1 to Dec, 30.



Vancouver. Various soil thicknesses on a wooden slab

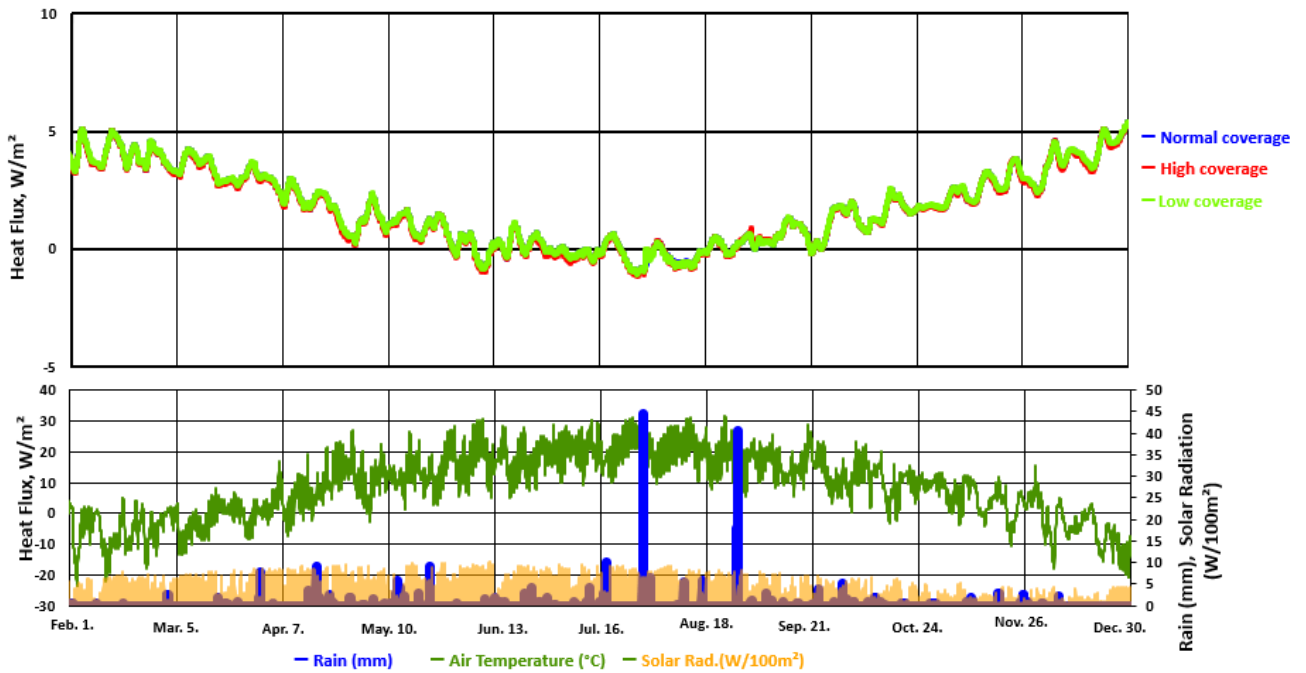


Cumulative Heat Flux from Feb, 1 to Dec, 30.

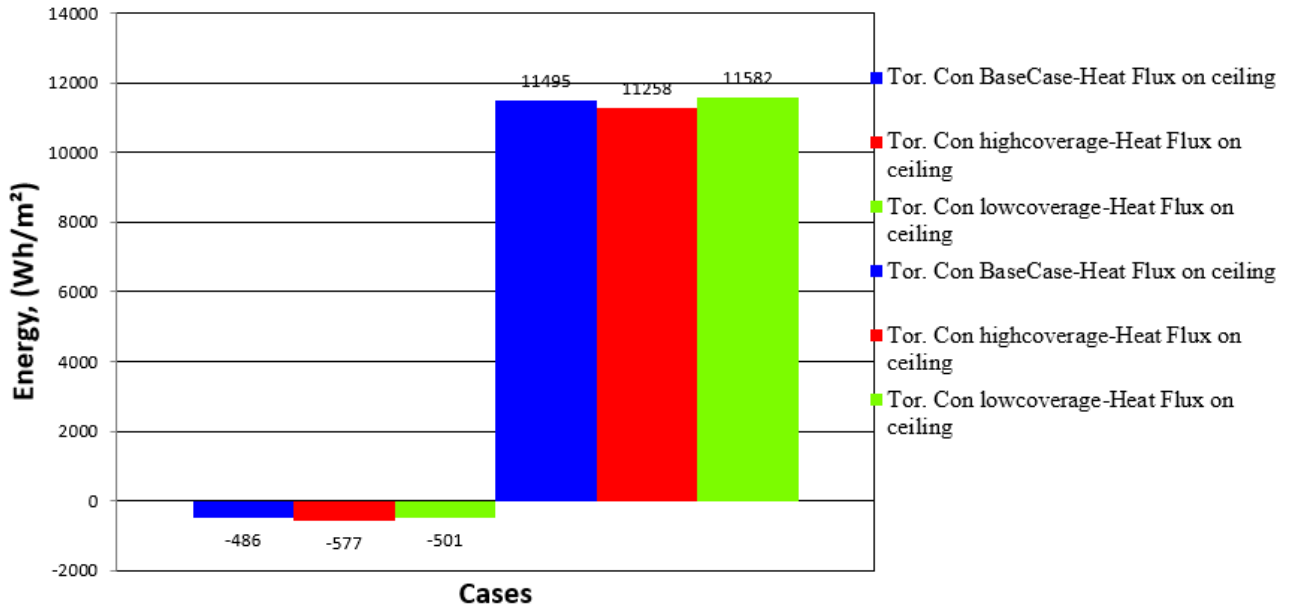


Toronto. Various vegetation coverage

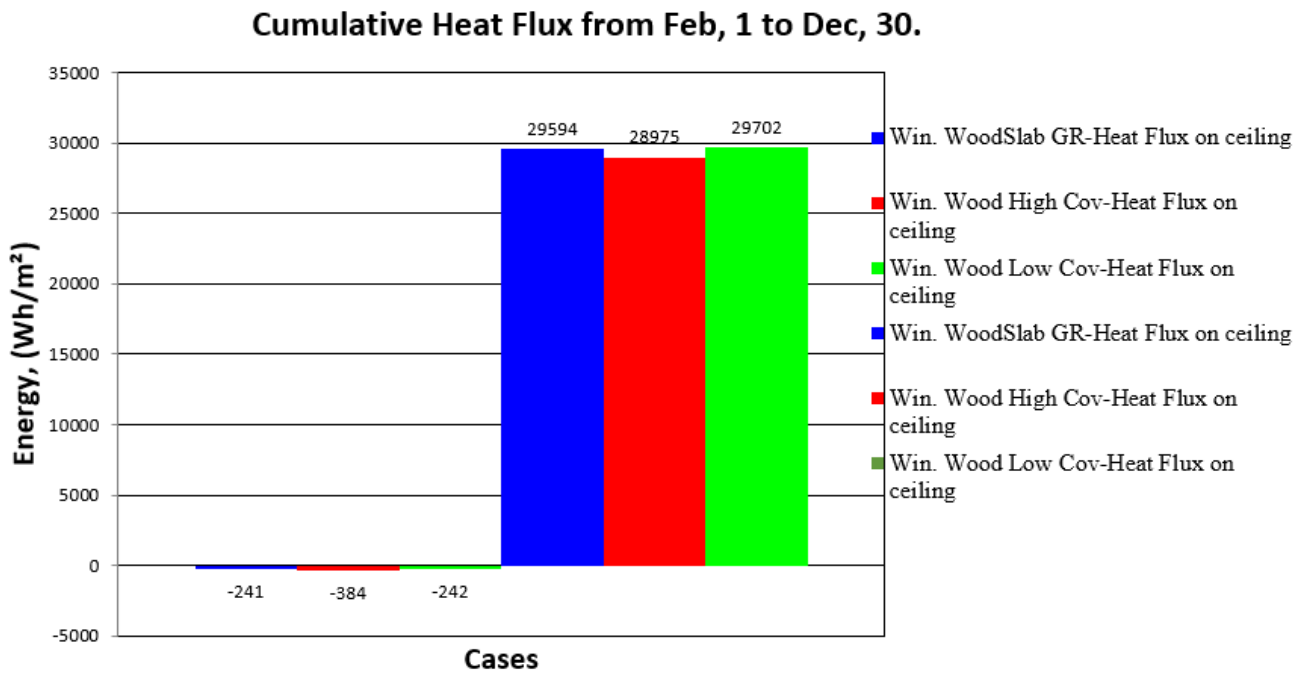
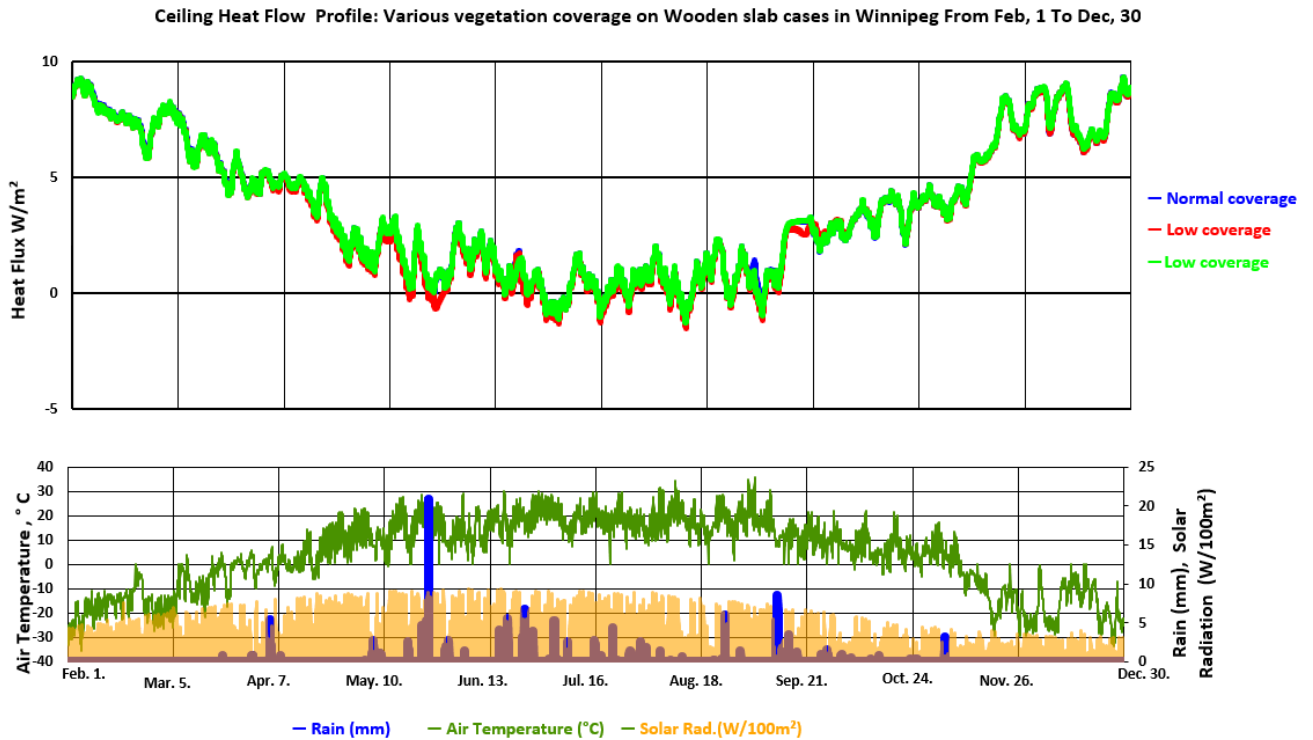
Ceiling Heat Flow Profile: Various stomatal resistance on Concrete slab cases in Toronto From Feb, 1 To Dec, 30



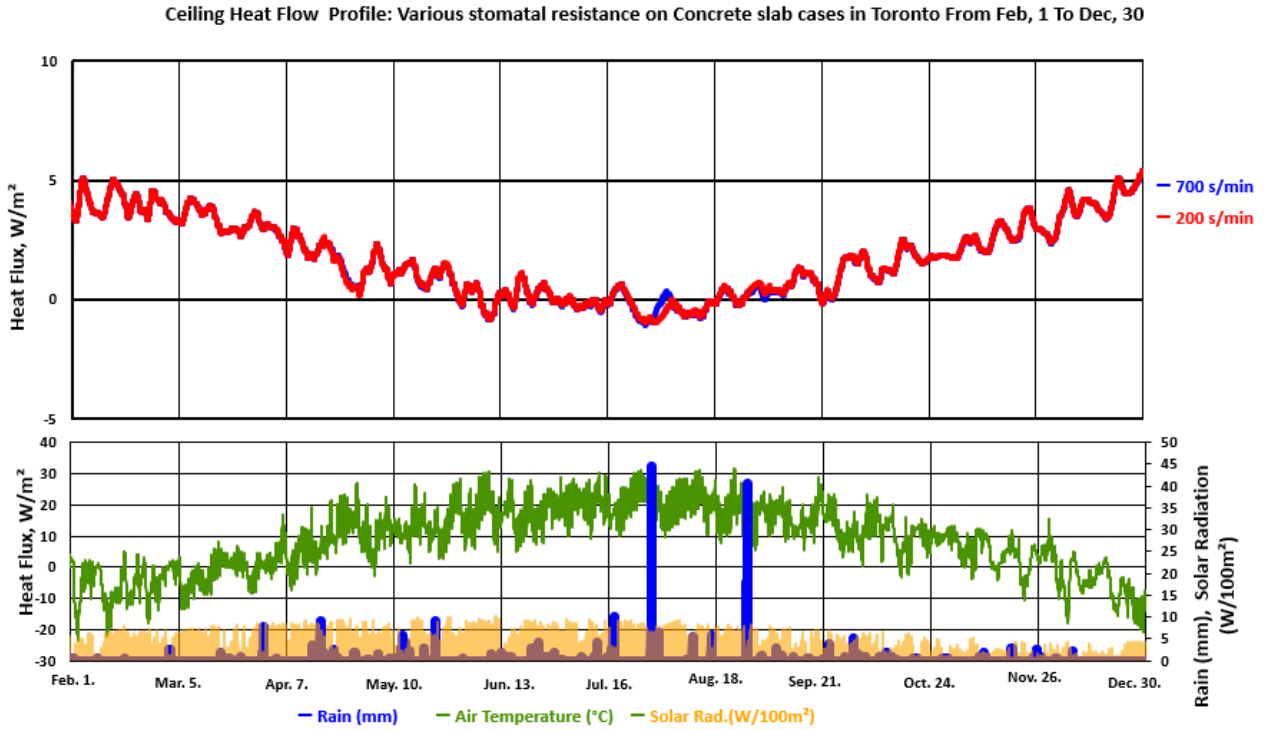
Cumulative Heat Flux from Feb, 1 to Dec, 30.



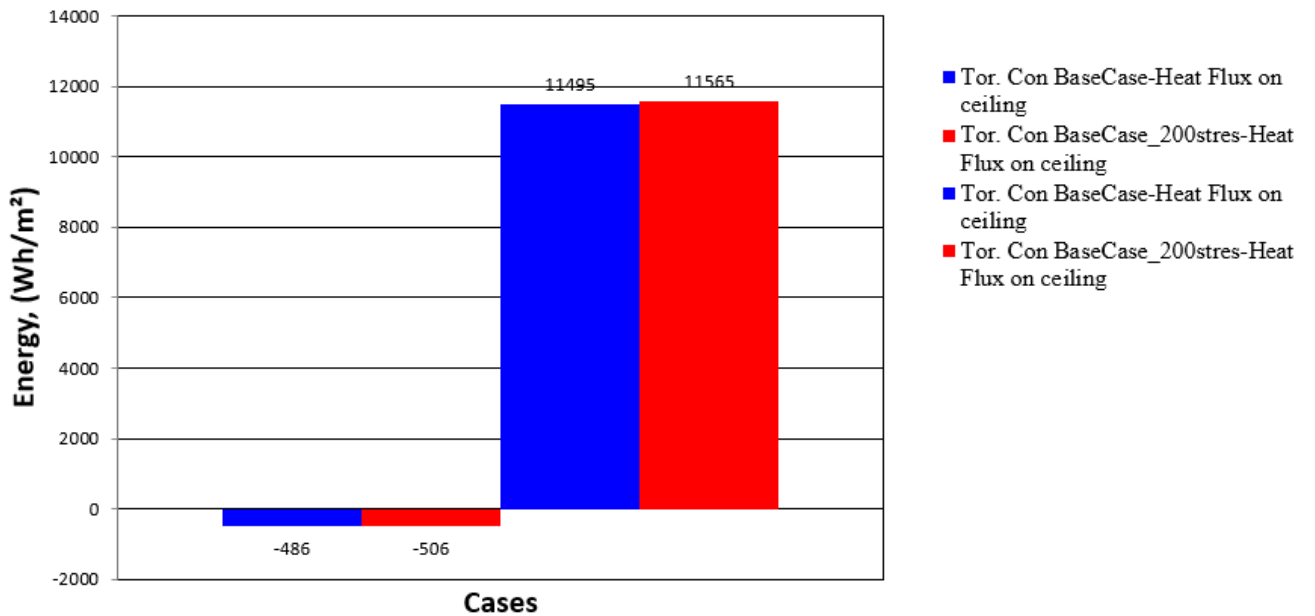
Winnipeg. Various vegetation coverage.



Toronto. Minimum stomatal resistance scenario

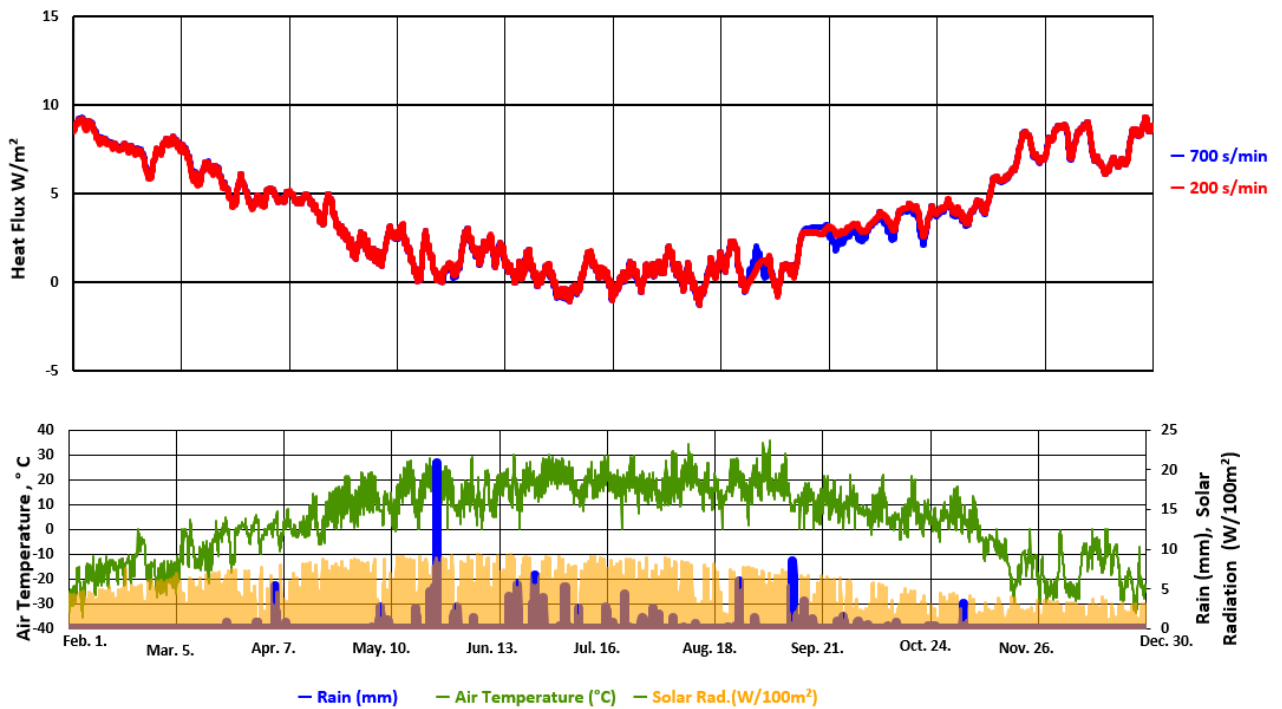


Cumulative Heat Flux from Feb, 1 to Dec, 30.

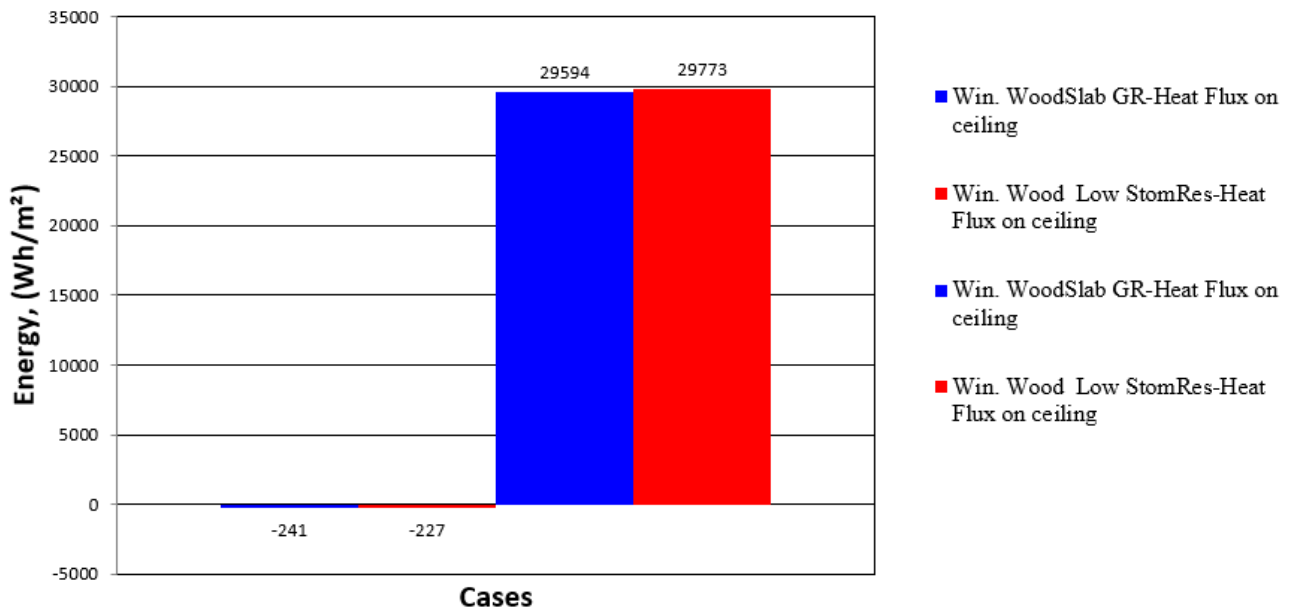


Winnipeg. Minimum stomatal resistance scenario.

Ceiling Heat Flow Profile: Various stomatal resistance on Wooden slab cases in Winnipeg From Feb, 1 To Dec, 30

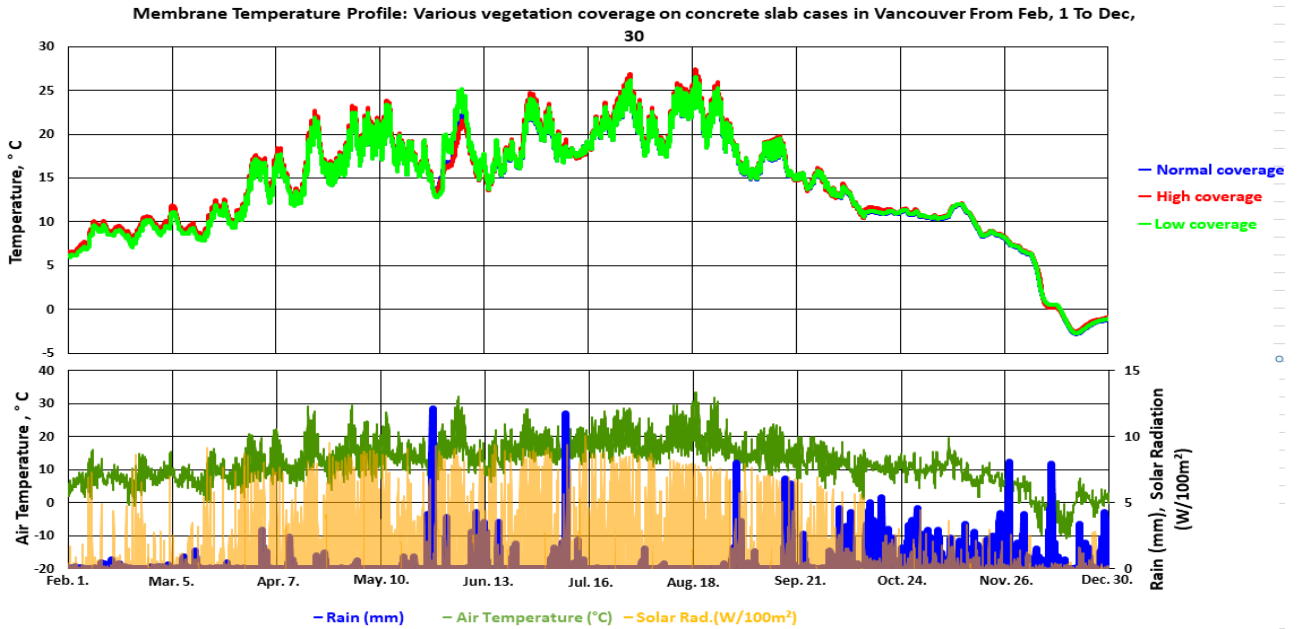


Cumulative Heat Flux from Feb, 1 to Dec, 30.

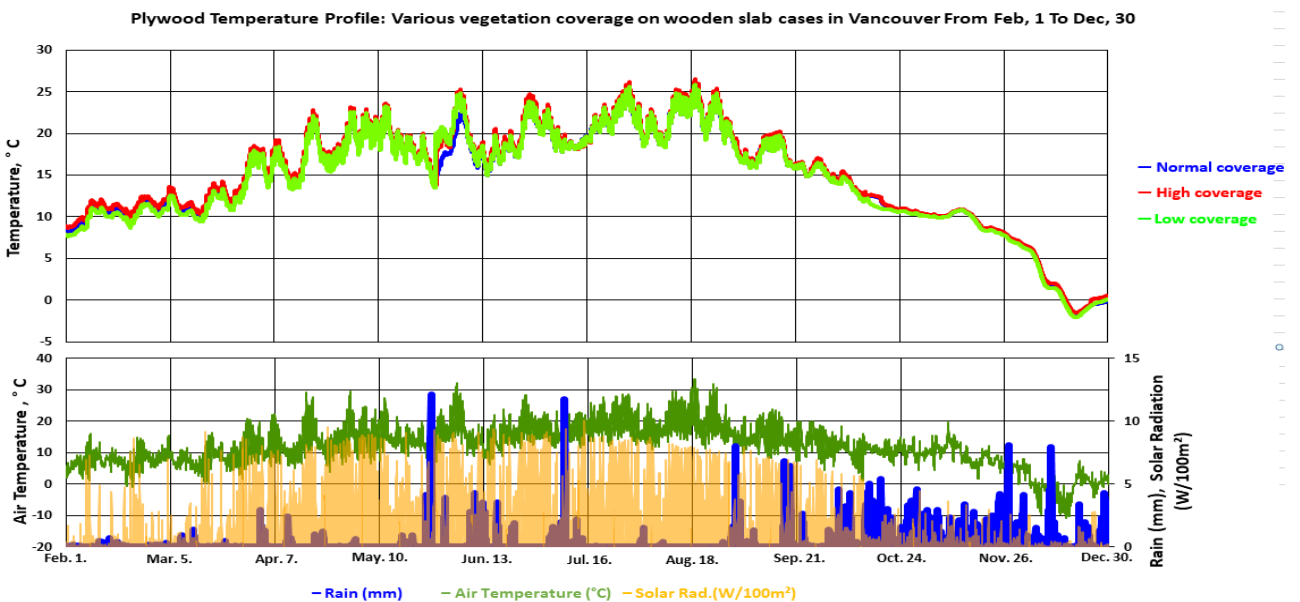


APPENDIX B. MEMBRANE AND PLYWOOD TEMPERATURES

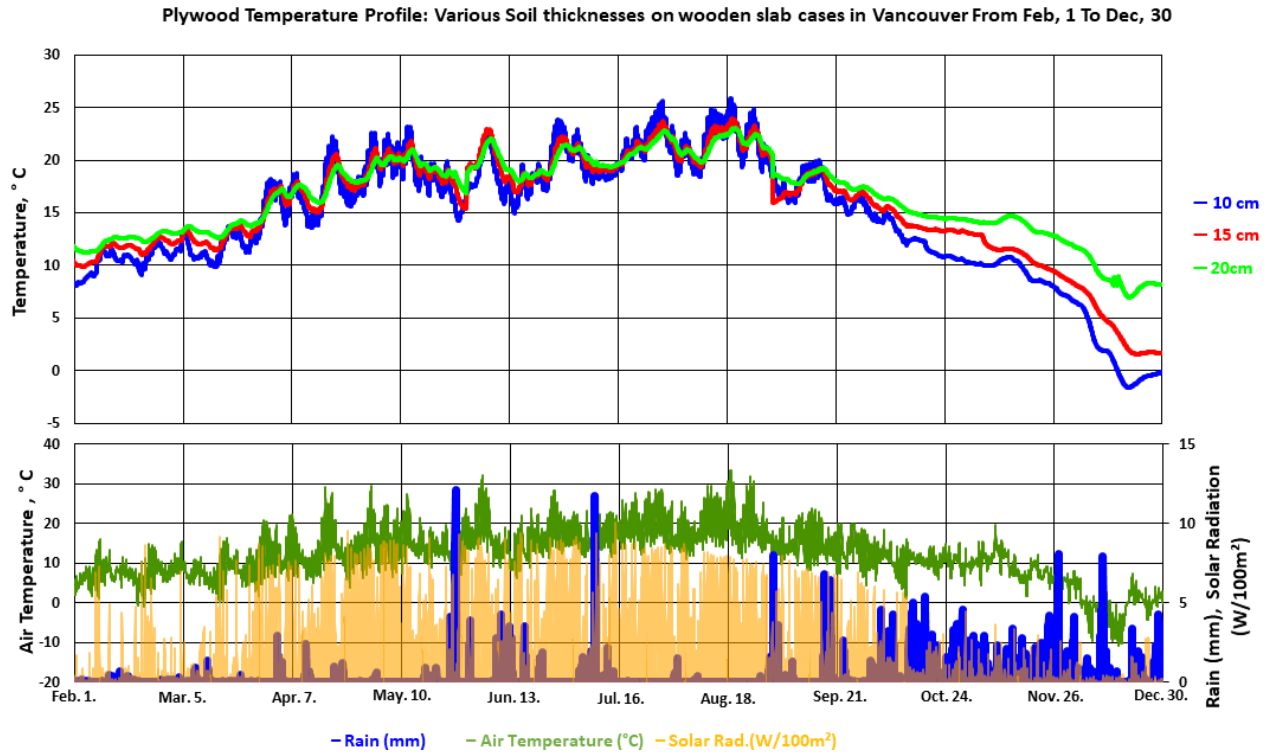
Vancouver. Various vegetation coverage on a concrete slab.



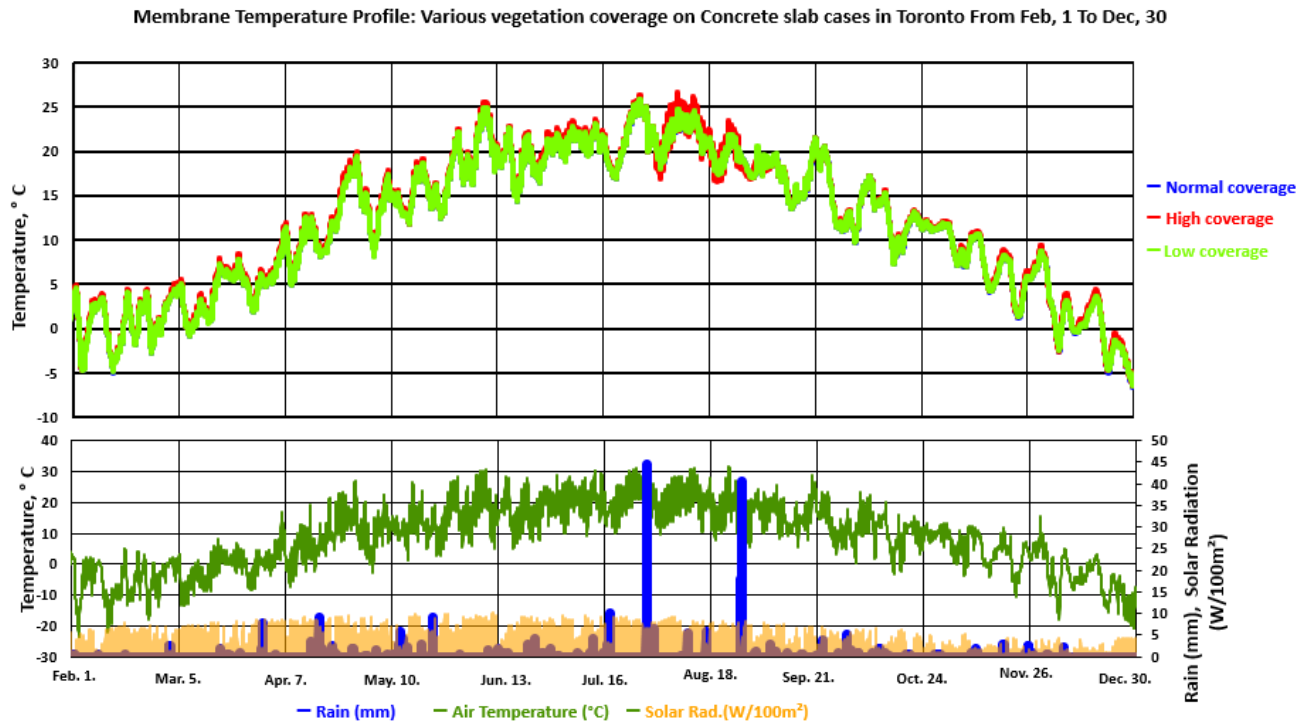
2. Vancouver. Various vegetation coverage on a wooden slab.



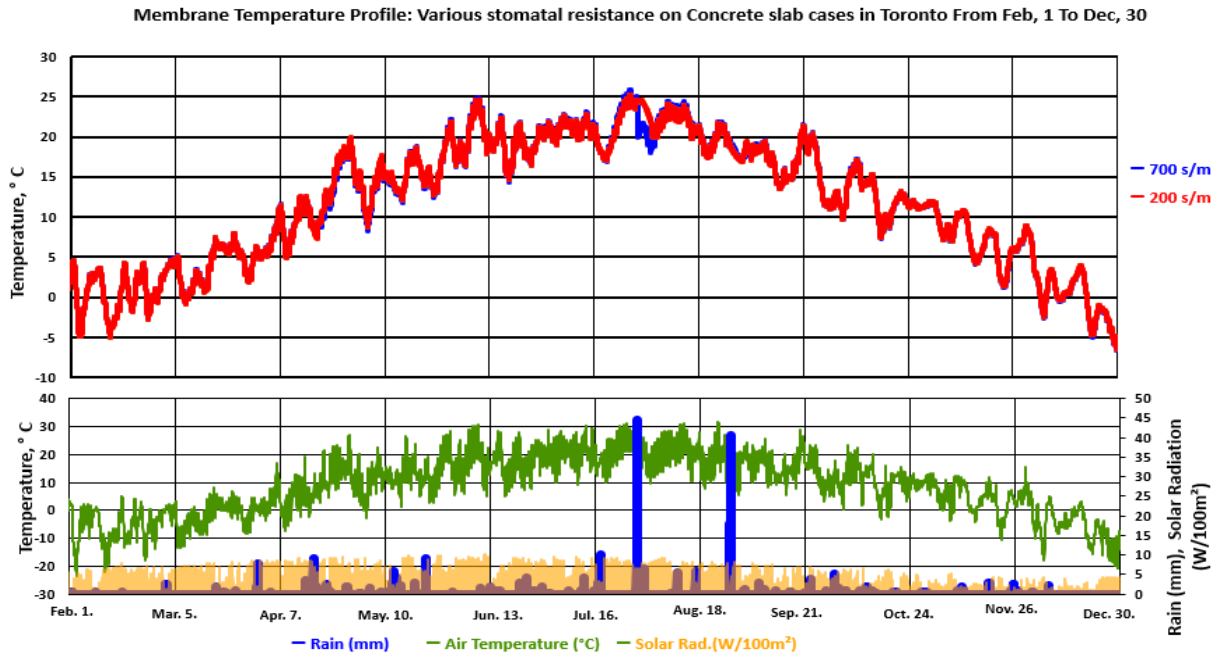
Vancouver. Various soil thicknesses on a wooden slab



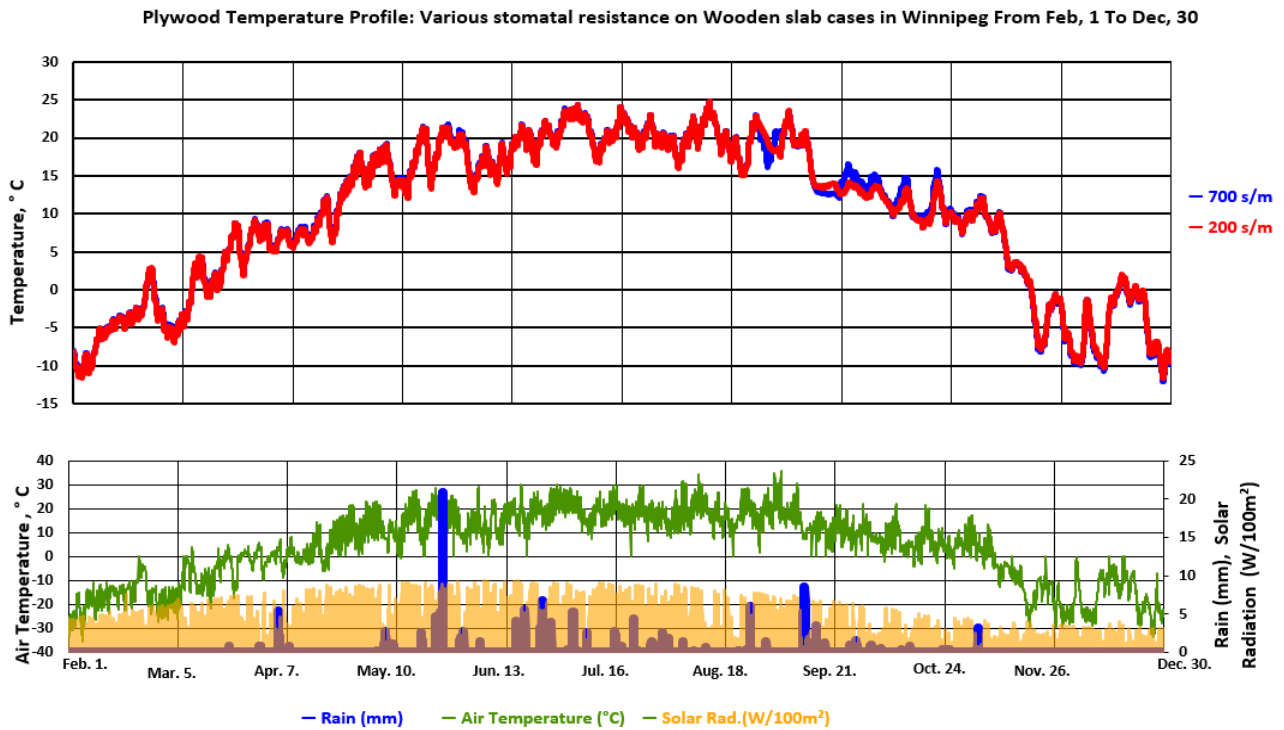
Toronto. Various vegetation coverage.



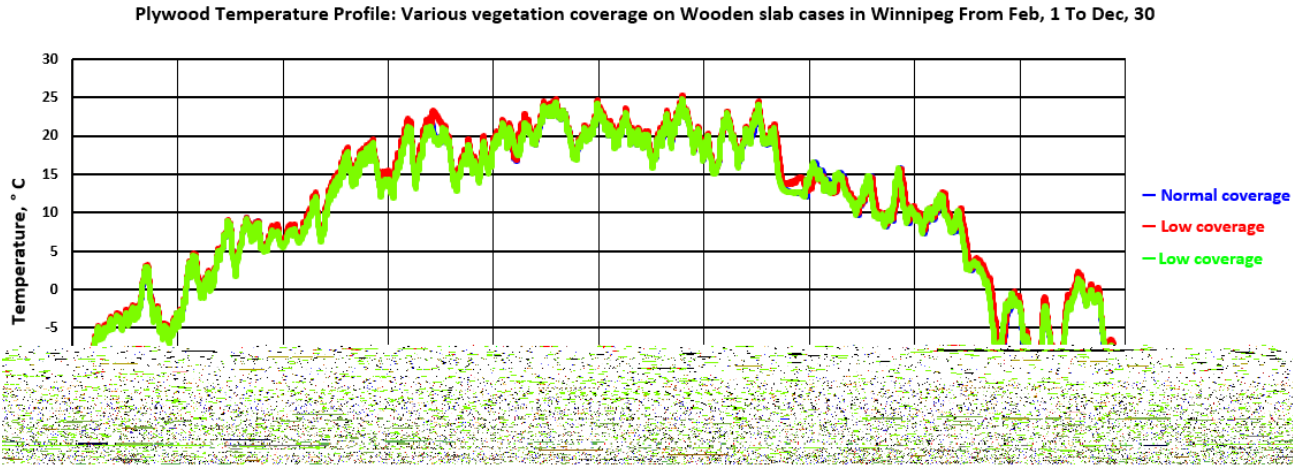
Toronto. Various stomatal resistance.



Winnipeg. Various stomatal resistance.

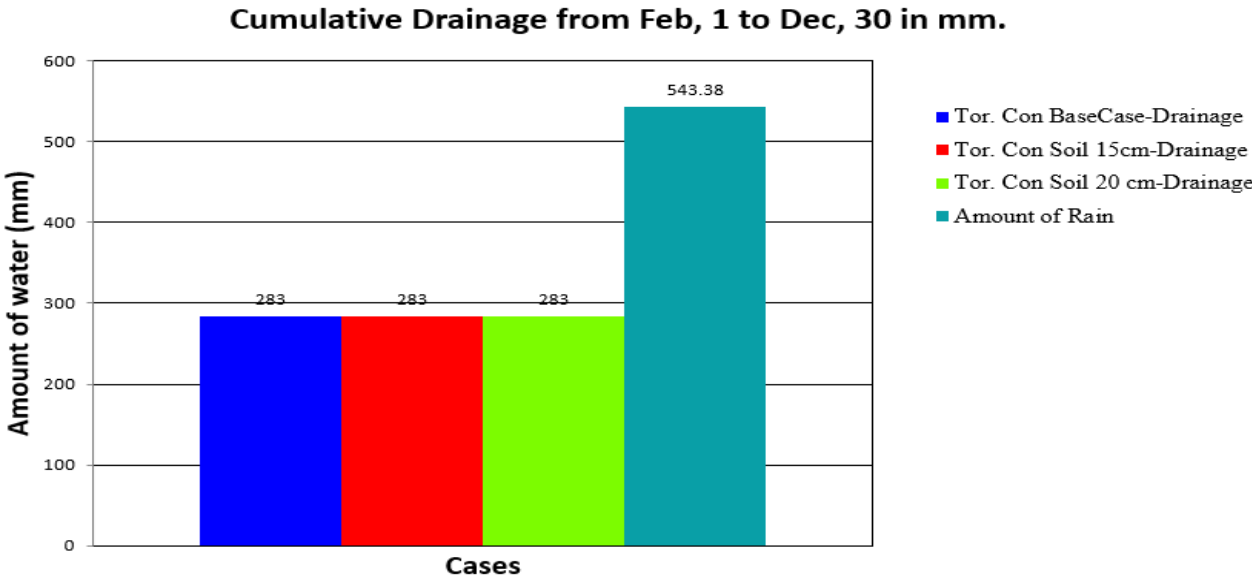


Winnipeg. Various vegetation coverage.

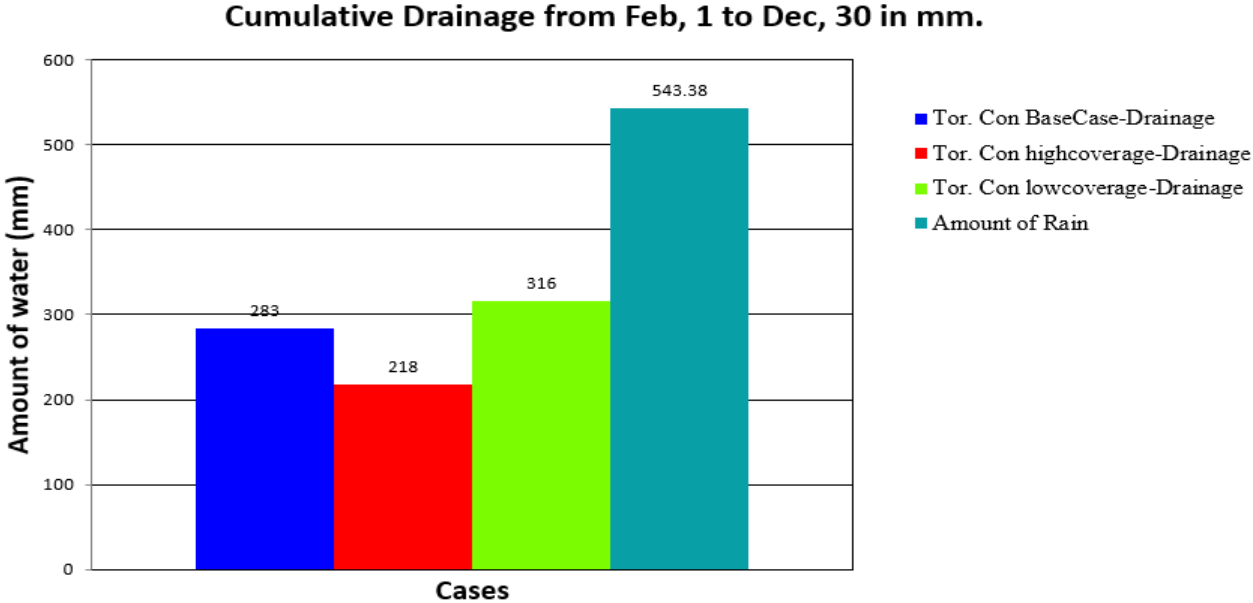


APPENDIX C. DRAINAGE

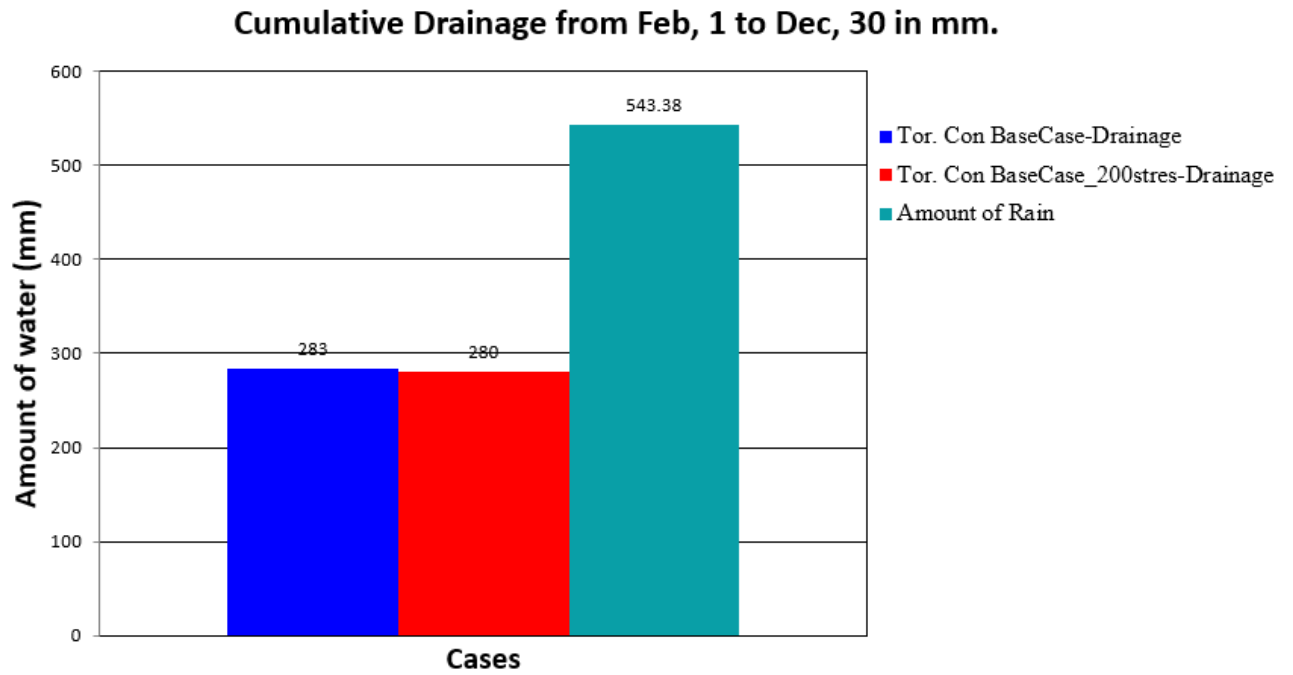
Toronto. Various soil thicknesses.



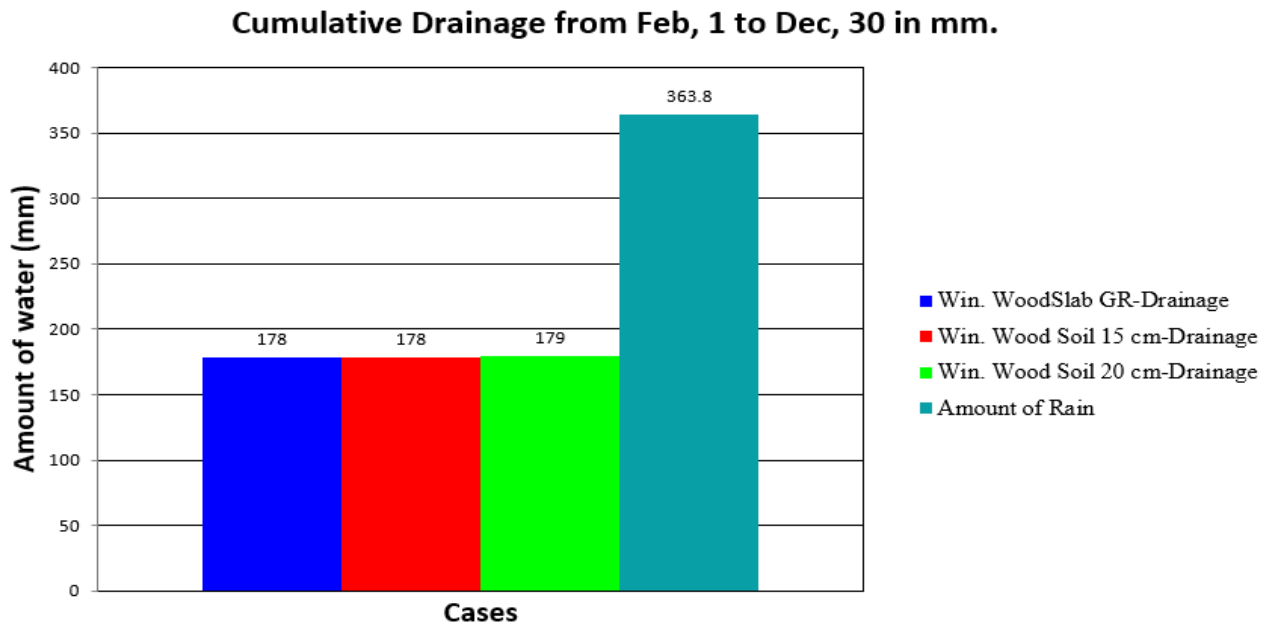
Toronto. Various vegetation coverage.



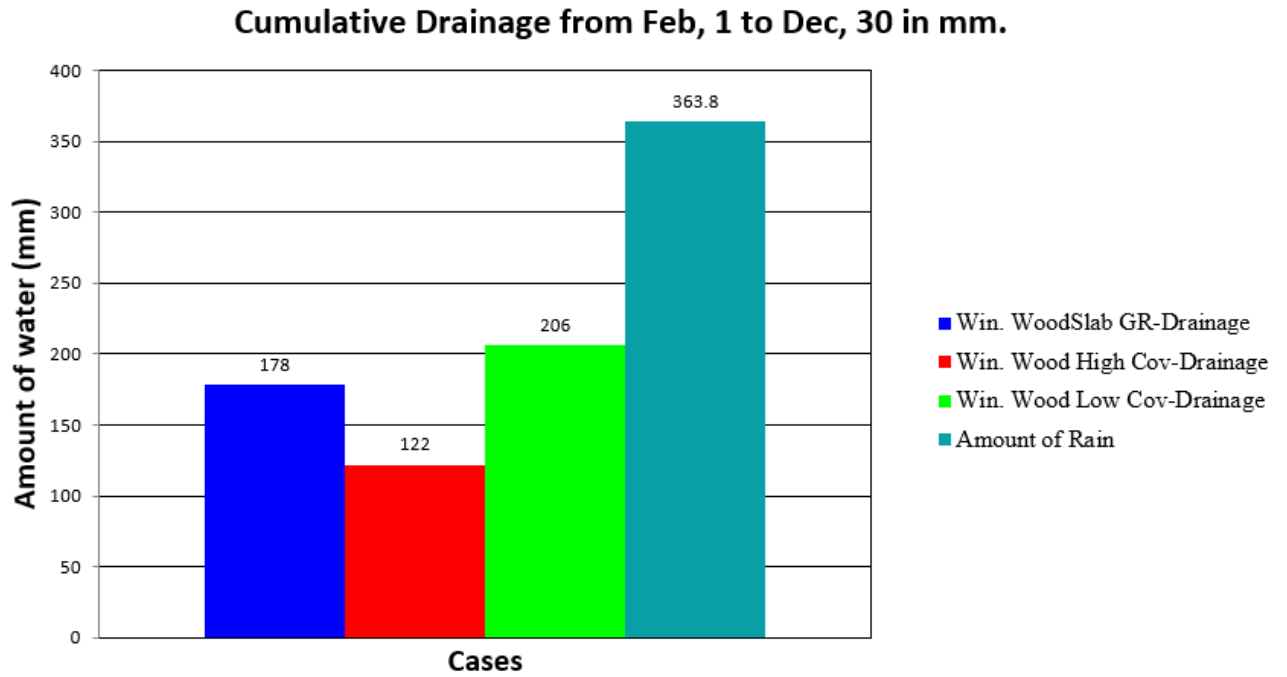
Toronto. Various stomatal resistance.



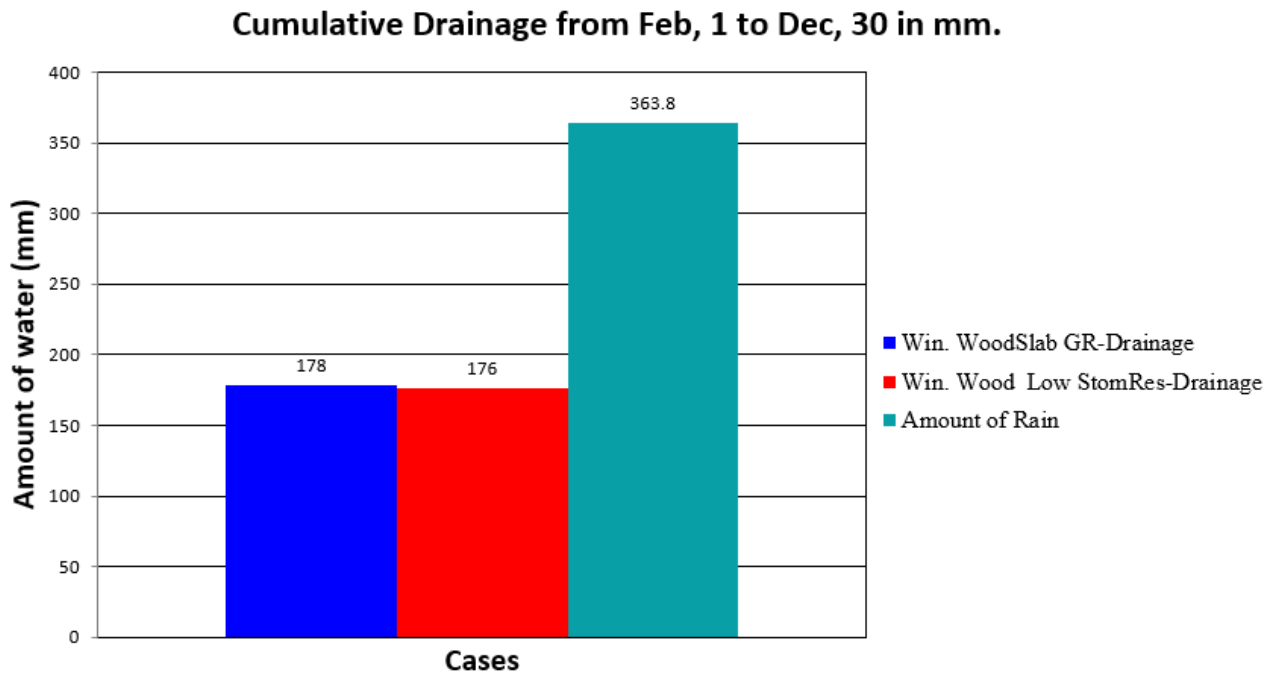
Winnipeg. Various soil thicknesses.



Winnipeg. Various vegetation coverage.



Winnipeg. Various stomatal resistance.



APPENDIX D. VEGETATION PARAMETERS VISUALIZATION

MATLAB SCRIPTS

```
function [CV]=LAI(image,nColors,cN);
%image - image variable in matlab workspace, need to be read before
%script start by (imread('name.jpg'))
%nColors - approximate number of colours on image, 6 works for green rood
%cN - a number of color that needs to be analyzed
fabric=image;
load regioncoordinates;
%L*a*b* image analyzing
sample_regions = false([size(fabric,1) size(fabric,2) nColors]);

for count = 1:nColors
    sample_regions(:, :, count) = roipoly(fabric,region_coordinates(:,1,count),...
        region_coordinates(:,2,count));
end

lab_fabric = rgb2lab(fabric);
a = lab_fabric(:, :, 2);
b = lab_fabric(:, :, 3);
color_markers = zeros([nColors, 2]);

for count = 1:nColors
    color_markers(count,1) = mean2(a(sample_regions(:, :, count)));
    color_markers(count,2) = mean2(b(sample_regions(:, :, count)));
end
fprintf(['%0.3f,%0.3f] \n',color_markers(2,1),color_markers(2,2));
color_labels = 0:nColors-1;
a = double(a);
b = double(b);
distance = zeros([size(a), nColors]);
for count = 1:nColors
    distance(:, :, count) = ( (a - color_markers(count,1)).^2 + ...
        (b - color_markers(count,2)).^2 ).^0.5;
end

[~, label] = min(distance, [], 3);
label = color_labels(label);
clear distance;rgb_label = repmat(label,[1 1 3]);
segmented_images = zeros([size(fabric), nColors], 'uint8');

for count = 1:nColors
    color = fabric;
    color(rgb_label ~= color_labels(count)) = 0;
    segmented_images(:, :, :, count) = color;
end

imshow(segmented_images(:, :, :, cN)), title('Objects');
imwrite(segmented_images(:, :, :, cN), 'image_temp.jpg');
rgbImage =imread('image_temp.jpg') ;
% Split the original image into color bands.
redBand = rgbImage(:, :, 1);
greenBand = rgbImage(:, :, 2);
```

```
blueBand = rgbImage(:,:, 3);
%find dark zones
redMask = (redBand < 30);
greenMask = (greenBand < 30);
blueMask = (blueBand < 30);
blackObjectsMask = uint8(redMask & greenMask & blueMask);
%find number of black dots
GreenDots=sum(sum(blackObjectsMask));
numOfRows = size(blackObjectsMask, 1);
numOfCols = size(blackObjectsMask, 2);
CV=GreenDots/(numOfRows*numOfCols);
disp(CV)
S1=50*50;
S2=(5*25.4)^2;
n=100;
LAI=(1-CV)*S1*n/S2;
disp(LAI)
```